# PHARMACOKINETIC CHARACTERIZATION AND OPTIMIZATION OF POLY (LACTIDE-CO-GLYCOLIDE) NANOPARTICLES *IN VIVO*

A Thesis Submitted to the College of

Graduate Studies and Research

In Partial Fulfillment of the Requirements

For the Degree of Doctor of Philosophy

In the College of Pharmacy and Nutrition

University of Saskatchewan

Saskatoon

By

PEDRAM RAFIEI

# PERMISSION TO USE

In presenting this thesis in partial fulfillment of the requirements for a Postgraduate degree from the University of Saskatchewan, I agree that the Libraries of this University may make it freely available for inspection. I further agree that permission for copying of this thesis in any manner, in whole or in part, for scholarly purposes may be granted by the professor or professors who supervised my thesis work or, in their absence, by the Head of the Department or the Dean of the College in which my thesis work was done. It is also understood that any copying or publication or use of this thesis or parts thereof for financial gain shall not be allowed without my written permission. It is also understood that due recognition shall be given to me and to the University of Saskatchewan in any scholarly use which may be made of any material in my thesis.

Requests for permission to copy or to make other use of material in this thesis in whole or part should be addressed to:

Dean of the College of Pharmacy and Nutrition

University of Saskatchewan

Saskatoon, Saskatchewan S7N 2Z4

Canada

OR

Dean of the College of Graduate Studies and Research

University of Saskatchewan

Saskatoon, Saskatchewan S7N 5A2

Canada

# ABSTRACT

To date, nanotechnology is used to modify drug delivery and confer desirable pharmacokinetics to drugs and improve pharmacodynamics. Polymeric nanoparticles of Poly (lactide-co-glycolide) (PLGA) are proposed as suitable vehicles that desirably modify pharmacokinetics. The variability in PLGA and nanoparticle fabrication techniques results in nanoparticles with variable characteristics. It is important to identify factors that significantly influence particle characteristics during nanoparticle preparation to fabricate nanoparticles with the desired properties. Factors like size, zeta potential, and drug loading ability influence fate of nanoparticle and loaded drug in the body.

An experimental factorial design based on the Taguchi robust model was used to evaluate the influence of preparation variables on nanoparticle characteristics. Docetaxel, an anticancer agent, was used in the design. Factors affecting nanoparticle properties with statistical significance were identified and models were built to predict particle characteristics. An optimized fabrication method was identified and used to prepare docetaxel-loaded PLGA nanoparticles and docetaxel-loaded PEGylated PLGA nanoparticles. Surface-modification with Poly (ethylene glycol) (PEG) conferred long-circulating properties to PLGA nanoparticles. A mass spectrometric analysis method was developed and partially validated for detection and quantification of docetaxel in biologic/non-biologic samples.

Size, zeta potential, Poly-dispersity index, drug release, and cytotoxicity of un-modified and surface-modified nanoparticles were determined. Pharmacokinetics and bio-distribution of docetaxel loaded in nanoparticles and in free solution were evaluated in mice and compared. PLGA and PLGA-PEG nanoparticles had average diameters of around 120 and 180 nm, respectively, with negative zeta potential. They demonstrated a biphasic release profile and were cytotoxic to Hela cells. Nanoparticles modified docetaxel's bio-distribution by increasing docetaxel's area under the curve, half-life, and mean residence time in blood

while decreasing systemic clearance and apparent volume of distribution. Particle size and surface characteristics likely caused the modifications in docetaxel's pharmacokinetics.

In summary, nanoparticles modified docetaxel's pharmacokinetics and bio-distribution. The relationship between nanoparticle properties and pharmacokinetic modifications can be established and used to design nanoparticles with intended characteristics that could intentionally change docetaxel's pharmacokinetics. Models built from the Taguchi design offer suitable means to prepare nanoparticles with predicted characteristics.

# ACKNOWLEDGEMENTS

I would like to express my sincere gratitude to my supervisor, Dr. Azita Haddadi, for her continuous support during the program. I am thankful for her guidance, motivation, patience, and help without which I would not have been able to conduct this research.

I would like to thank my committee members, Dr. Jane Alcorn, Dr. Ildiko Badea, Dr. Anas El-Aneed, and Dr. Troy Harkness, for spending their time reading my thesis. Their valuable and insightful comments and criticism have improved my research and incented me to widen my knowledge from various perspectives. I would like to express thanks to my advisory committee chair, Dr. Ed. Krol, for his guidance and help. I also acknowledge the time and consideration of Dr. David Blackburn for chairing my defence meeting.

Several people offered invaluable support and training during my experiments. Dr. Mehran Yarahmadi offered kind and valuable assistance during my animal experiments. Ms. Deborah Michel taught me to use the mass spectrometer. Mrs. Dorota Rogowski gave me significant support and training in the lab. Dr. Ayman El-Sayed trained me in tissue culture techniques. The staff of the College of Pharmacy and Nutrition also provided me with significant support. I am sincerely grateful to these people, without whom my research would not have been possible.

I gratefully acknowledge the financial support that I received from the College of Graduate Studies and Research, College of Pharmacy and Nutrition, and my supervisor. I would also like to thank my fellow lab mates for their friendship and support.

Finally, I would like to express my deep gratitude to my parents and my wife for their unlimited love and support during my academic pursuit. I also thank my brother for his care and support.

# TABLE OF CONTENTS

**CHAPTER 5**

**Experimental Section on Mass spectrometry Method for Quantification of Docetaxel**

# LIST OF TABLES

Table Page

# LIST OF FIGURES

Figure Page

# LIST OF ABBREVIATIONS

| | |
|---|---|
| ADME | Absorption, Distribution, Metabolism, and Excretion |
| ANOVA | Analysis of variance |
| AUC | Area under the curve |
| AUMC | Area under the moment curve |
| CAD | Collisionally activated dissociation |
| $C_0$ | Concentration at time zero |
| Cl | Clearance |
| CMC | Critical micelle concentration |
| COOH | Carboxylic acid |
| CRP | Cryoprotectant |
| CYP450 | Cytochrome P450 |
| CV% | Coefficient of variation |
| °C | Degree celsius |
| Da | Dalton |
| DMAB | Didodecyl dimethyl ammonium bromide |
| DMEM | Dulbecco's modified Eagle's medium |
| DP | De-clustering potential |
| dl/g | Deciliters per gram |
| +ESI | Positive electrospray ionization |
| FBS | Fetal bovine serum |
| FD | Freeze-drying |
| FDA | Food and Drug Administration |
| GA | Glycolic acid |
| HQC | High quality control |

| | |
|---|---|
| HUVEC | Human umbilical vein endothelial cells |
| IS | Internal standard |
| IV | Intravenous |
| kDa | Kilo Dalton |
| LUV | Large uni-lamellar vesicles |
| LA | Lactic acid |
| LASU | Lab Animal Services Unit |
| LOD | Limit of Detection |
| LOQ | Limit of quantitation |
| LQC | Low quality control |
| Ln | Natural logarithm |
| MLV | Multi-lamellar vesicles |
| Mw | Molecular weight |
| MPS | Mononuclear phagocytic system |
| mV | Millivolts |
| MRT | Mean residence time |
| mg/ml | Milligrams per millilitre |
| mg | Milligrams |
| mBar | Millibar |
| MRM | Multiple reaction monitoring |
| ml | Millilitres |
| m/z | Mass-to-charge ratio |
| µg/ml | Micrograms per milliliter |

| | |
|---|---|
| MQC | Middle quality control |
| nm | Nanometers |
| NDDS | Novel drug delivery systems |
| NLC | Nanostructured lipid carrier |
| OH | Hydroxyl |
| O/W | Oil in water |
| P-gp | P-glycoprotein |
| PLGA | Poly (lactide-co-glycolide) |
| PK | Pharmacokinetics |
| PD | Pharmacodynamics |
| PDI | Poly-dispersity index |
| PLA | Poly (lactic acid) |
| PGA | Poly (glycolic acid) |
| PVA | Polyvinyl alcohol |
| PEG | Poly (ethylene glycol) |
| PBS | Phosphate buffered saline |
| PET | Poly (ethylene terephthalate) |
| PRINT® | Particle replication in non-wetting templates |
| PLGA-PEG | Poly (lactide-co-glycolide) - co - Poly (ethylene glycol) |
| RES | Reticuloendothelial system |
| RPM | Revolutions per minute |
| $R^2$ | Coefficient of determination |
| SUV | Small uni-lamellar vesicles |
| SLN | Solid lipid nanoparticles |
| SDS | Sodium dodecyl sulfate |

| | |
|---|---|
| S/N | Signal-to-noise ratio |
| $T_{1/2}$ | Half-life |
| TBME | Tert-butyl methyl ether |
| $V_d$ | Volume of distribution |
| W/O/W | Water in oil in water |
| W/V | Weight per volume |

# CHAPTER 1*

## Literature Review

*This chapter has been published as a 'Review Article' in '*Pharmaceutical Nanotechnology*':
Pedram Rafiei, Azita Haddadi. Pharmacokinetic Consequences of PLGA Nanoparticles in Docetaxel Drug Delivery. *Pharmaceutical Nanotechnology,* 2017, Volume 5, Issue 1, Pages 1-29.

### 1.1.Background

Cancer in one of the leading causes of morbidity and mortality in Canada and around the world. Conventionally, chemotherapy has been the chief therapeutic technique to treat cancer. However, chemotherapy suffers disadvantages such as anticancer agents' lack of water solubility, their non-selectivity, and their unfavorable pharmacokinetics. For example, docetaxel, a chemotherapeutic agent used to treat a variety of cancer types, is poorly water soluble. Therefore, co-solvents (ethanol and polysorbate 80) have been used in drug's commercial formulation to make it soluble. Docetaxel has a high volume of distribution and binds to a wide range of tissues. The drug does not discriminate between normal and cancer cells and therefore acts non-selective. This results in a wide range of side effects.

The idea of applying nanotechnology and nanoparticles as drug delivery platforms to address disadvantages of conventional chemotherapy has led to the development of cancer nanomedicine. Accordingly, cancer nanomedicine represents as one of the most promising approaches to cancer treatment. Over the past decades, extensive research into cancer nanomedicine has significantly advanced scientists' understanding of the contribution that nanomedicine could have to cancer treatment. Several nanoparticulate drug delivery platforms have been introduced to the field, offering various benefits and drawbacks. One of

these platforms, polymeric nanoparticles prepared from poly (lactide-co-glycolide) (PLGA), has been extensively used to deliver a wide-spectrum of drugs, including chemotherapeutic agents.

PLGA polymer has a variable physicochemical nature. In addition, various techniques have been used to fabricate PLGA nanoparticles. The variability of PLGA polymer and the variabilities in nanoparticle preparation methods result in nanoparticles with distinctly different properties. In other words, PLGA polymer properties and the nanoparticle preparation technique used determine nanoparticle characteristics. After administration, nanoparticle characteristics influence the fate of the nanoparticle and the loaded drug in the body (bio-fate). Thus, the relationship between PLGA polymer properties, nanoparticle preparation technique, and PLGA nanoparticle characteristics must be established because the nanoparticle's characteristics affect the bio-fate of both the loaded drug and nanoparticle.

PLGA nanoparticles are believed to modify the pharmacokinetics and biodistribution of various drugs, including chemotherapeutic agents. These modifications can potentially change the drug's systemic concentration and the drug's effectiveness in various organs. However, mode of changes made to the loaded drug's pharmacokinetics and biodistribution mainly depends on the nanoparticles' properties such as size, surface characteristics, and shape. PLGA nanoparticles are believed to help elevate blood concentration and residence time of drugs in systemic circulation, which secondarily increases tumor exposure. By establishing a relationship between PLGA nanoparticle characteristics and the mode of changes made to drugs' pharmacokinetics and biodistribution profile, it would be possible to design nanoparticles with intended pharmacokinetic consequence.

PLGA nanoparticles offer the possibility of surface-modification as well. The attachment of poly (ethylene glycol) (PEG) to the surface of PLGA nanoparticles has been shown to improve blood residence time of nanoparticles and the loaded drugs.

## 1.2.Cancer

Medically known as malignant neoplasm, cancer includes a wide spectrum of diseases that generally involve a circumstance of unregulated cell growth [1]. Cancer cells proliferate uncontrollably and potentially affect nearby organs, resulting in disorders. Although new diagnostic and therapeutic approaches have improved therapy's success and patients' quality of life, cancer is still a leading cause of death in Canada [2].

Currently applied and well-established treatments for cancer (e.g., chemotherapy, radiotherapy, surgery) are variably effective depending on the type of cancer [3]. For example, primary solid tumours localized in the body can usually be removed by surgical interventions or subjected to radiation therapy to shrink the cancer tissue. However, cases with spreading features and tumour metastasis require extensive chemotherapy [4]. Chemotherapy uses highly cytotoxic agents that interfere with normal cell activities, like cell division and growth, upon entering the body and might also activate cell death pathways, promoting tumour shrinkage.

After administration, most anticancer agents demonstrate wide-spread distribution throughout the body and can easily reach non-tumour tissues. Furthermore, most chemotherapeutic agents possess a fairly rapid elimination rate after administration to the body. The wide-spread distribution of chemotherapeutic agents along with their fast elimination from the body results in pronounced drop in systemic concentration of anticancer agents. Therefore, to reach the required systemic therapeutic levels in the body, anticancer agents are required to be administered at high and frequent doses.

Most types of anticancer agents do not discriminate between normal cells and cancer cells. Anticancer agents' non-specific activity and their wide-spread distribution in the body lead to systemic toxicity and adverse effects [5]. A delicate balance must be maintained

between the therapeutic effectiveness and toxicity of anticancer agents: reducing the dose diminishes therapeutic outcomes and increasing the dose can give immoderate toxicity. Toxicity can cause extreme patient discomfort, contributing to delays, the reduction of doses, and the cessation of chemotherapy [6].

Anticancer agents often have variable physicochemical characteristics such as variable water solubility. Incorporating such active agents into formulations suitable for administration to the body requires the use of non-active ingredients (i.e., excipients) such as co-solvents or vehicles in the formulation. These excipients can cause serious side effects on their own (e.g., hypersensitivity reaction, nephrotoxicity, neurotoxicity) to a level that would also contribute to the cessation of chemotherapy [7-10]. Therefore, the development of strategies that can modify cancer chemotherapy by intervening in the mechanisms that lead to toxicity would help patients tolerate the adverse effects, comply with their cancer treatment regimens, and ultimately have better qualities of life.

To date, one of the strategies that show great promise to overcome the drawbacks of cancer chemotherapy is the application of 'novel drug delivery systems' (NDDS) [11-13]. The general idea behind NDDS is to modify the fate of drugs in the body after administration in a way that enhances therapeutic outcomes and at the same time undermines adverse effects, ultimately to increase patients' compliance of drug-therapy. Because of the many adverse effects associated with chemotherapy, chemotherapeutic agents make suitable candidates to be involved with NDDS.

Docetaxel has long been considered to be one of the most important and efficient anticancer agents being widely used in the chemotherapy of various cancer types. However, the clinical application of the drug is not without limitations due to docetaxel's poor water solubility, non-selective bio-distribution, fast elimination, and hypersensitivity reactions. The chemotherapeutic agent can result in toxicity and a variety of side effects. Due to its dose-

limiting toxicities, docetaxel's application in cancer-patients has long been accompanied with matters of concern [6, 14, 15]. The application of new drug delivery systems to help overcome such limitations could ultimately result in more successful clinical outcomes.

### 1.3.Docetaxel

Docetaxel (figure 1-1) is a member of taxan family of antineoplastic agents that exert their cytotoxic effects on microtubules [16]. Docetaxel is derived semi-synthetically from 10-deacetyl-baccatin III that is isolated from trees of Taxus family (e.g., Taxus baccata, Taxus brevifolia) [17]. Docetaxel inhibits the proliferation of cells by inducing a sustained block at the metaphase–anaphase boundary by disrupting the microtubular network necessary for mitotic cellular function [17, 18]. It inhibits the disassembly of tubulin leading to inhibited cell division and to cell death [19].

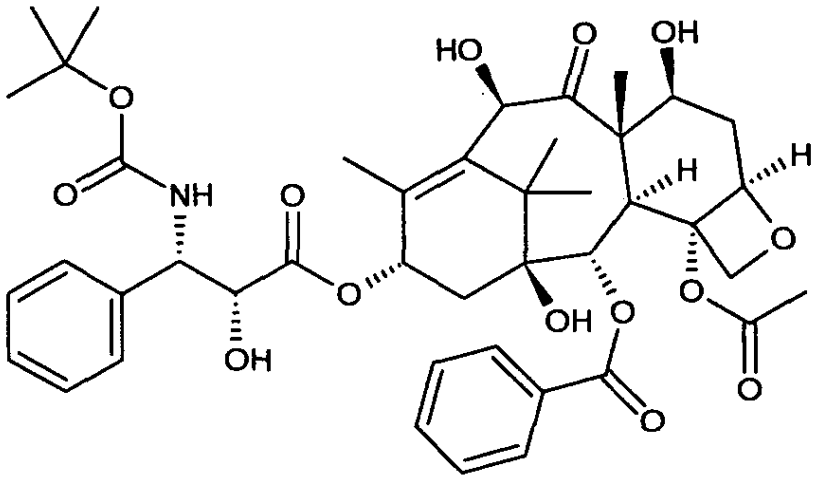


Figure 1-1. Docetaxel molecular structure

Docetaxel has demonstrated antitumor activity in patients with recurrent ovarian cancer, non-small cell lung cancer, metastatic and adjuvant breast cancer, squamous cell head and neck cancer, and gastric cancer [18]. In addition, docetaxel has demonstrated activity in previously treated patients with carcinomas of endometrial cancer, esophageal cancer,

bladder cancer, prostate cancer, small cell lung cancer, lymphomas, and other neoplasms [19]. Commonly, docetaxel is administered every three weeks at a doses-range of 60-100 $mg/m^2$ being infused in one hour. Dose of 75 $mg/m^2$ is the recommended dose when the drug is given either as a single agent or in combination with another antineoplastic [18]. At higher doses, docetaxel may be less well-tolerated, especially by patients who have received extensive previous bone marrow suppressive therapies. A weekly schedule of docetaxel administration at lower doses (25-40 $mg/m^2$) has been recommended and has had response rates similar to that of triweekly schedules with reduced myelosuppression [20]. Low-dose weekly infusion of docetaxel was investigated in patient groups such as elderly people, people with poor performance status, and those with a refractory disease [21].

Upon intravenous administration, docetaxel is rapidly distributed to body tissues [17, 22] and binds to plasma proteins (>90%) [23]. It has a relatively large volume of distribution accompanied with its binding to a wide range of tissues [18]. Its peak plasma concentrations generally exceeds levels required to induce relevant biologic effects [19]. However, the data about the bio-distribution of docetaxel in humans is limited. Immediately after treatment, the concentration is highest in the liver, bile, and intestines. Traces can also be found in the stomach, spleen, bone marrow, myocardium, and pancreas [19]. With the majority of excretion occurring in the first 48 hours, docetaxel gets eliminated predominantly through hepatic and biliary route and to a lesser extent by urinary excretion [18, 19, 21]. Plasma concentration profiles of docetaxel are determined by its elimination kinetics with an elimination half-life ranging from 11-19 hours [18].

Neutropenia, anaemia, and skin reactions are most common dose-limiting side effects of docetaxel [14]. Taking the extent of any existing myelosuppression (from previous therapy) into consideration as an important determinant, the blood counts are believed to reach lowest after 8-9 days of docetaxel treatment and recover by days 15-21 [18, 19].

Between 50% and 75% of patients receiving docetaxel develop skin toxicity. Skin reactions can include a pruritic maculopapular rash appearing on the forearms, hands, or feet, and less commonly, desquamation of the palms or the soles of the feet (palmar-plantar erythrodysesthesia) [18, 21]. Alopecia is also extremely common. Other cutaneous effects include onychodystrophy, onycholysis, soreness, and brittleness of the fingernails. Other possible toxicity is fluid retention, characterized by edema, weight gain, pleural effusion and ascites, which may be attributed to increased capillary permeability caused by docetaxel [18, 19, 21].

Because of docetaxel's poor water solubility (3 µg/ml), in the commercial formulation, the drug is dissolved in 50 % polysorbate 80 (Tween™ 80) (a non-ionic surfactant) and 50 % ethanol [24]. Administration of docetaxel has been associated with hypersensitivity reactions such as pruritus and systemic anaphylaxis [25-27]. Evidence suggests that these allergic reactions are in part due to polysorbate 80 [10]. Polysorbate 80 is considered responsible for fluid retention/edema by increasing membrane permeability [28] and decreasing plasma colloid osmotic pressure [29, 30]. It has also been shown to influence protein binding of docetaxel at clinically relevant concentrations [31]. However, the mechanistic basis for this is not clear. Docetaxel is subjected to metabolic conversion and inactivation in the liver by the cytochrome P450 (CYP450) isoenzymes [22]. Elimination of docetaxel is also dependent on transporters, particularly P-glycoproteins (P-gp), that exist at the bile canalicular membrane. It is believed that polysorbate 80 or its metabolites can inhibit CYP450 [32, 33] and/or P-gp mediated elimination of docetaxel and consequently affect docetaxel clearance from the body.

Other allergic reactions, such as dyspnea, bronchospasm, and hypotention, can happen within minutes after starting the infusion during the initial courses of docetaxel therapy; these reactions are attributed to the vehicle, solvent, or to the drug itself [18, 19, 21]. Docetaxel

also exerts adverse effects on other organs of the body such as the eyes (epiphoria), gastrointestinal tract (ischaemic colitis), heart (heart failure), and musculoskeletal system (arthralgia) [21].

### 1.4.Nanoparticle Drug Carrier Systems

To date, different types of nanoparticles and strategies based on nanotechnology have been developed to deliver various drugs (including anti-cancer agents) to the body [34-38]. Using nanoparticles as means of drug delivery is usually done to improve the pharmacokinetic characteristics of an active agent [39] by changing the drug formulation to create a more desirable absorption, distribution, metabolism, and excretion (ADME) profile. For example nanoparticles as drug delivery vehicles can i) protect drugs from degradation, ii) enhance drug absorption, iii) modify the drug's distribution profile, and iv) modify the drug's elimination rate/profile. [36]. Regardless of the mode of intervention made by nanoparticulate drug carrier systems, the consequence, which is the improvement in pharmacokinetic characteristics, secondarily improves the drug's pharmacodynamic characteristics.

Successful nanoparticle drug carriers must be able to contribute desirable modifications in their cargo's pharmacokinetic profile. In addition, ideal nano-carriers are expected to i) be biocompatible/biodegradable (i.e., be non-toxic to the human body), ii) have suitable drug loading capacities, iii) have physicochemical characteristics suitable for delivery purposes (e.g., targeted, non-targeted, systemic, and local drug delivery), and iv) have predictable and even controlled release profiles [35]. Nanoparticle drug carriers are categorized into various classes based on the component(s) used in their fabrication. The major categories of nanoparticulate drug carriers include lipid-based and polymer-based nanoparticles, which are briefly discussed below.

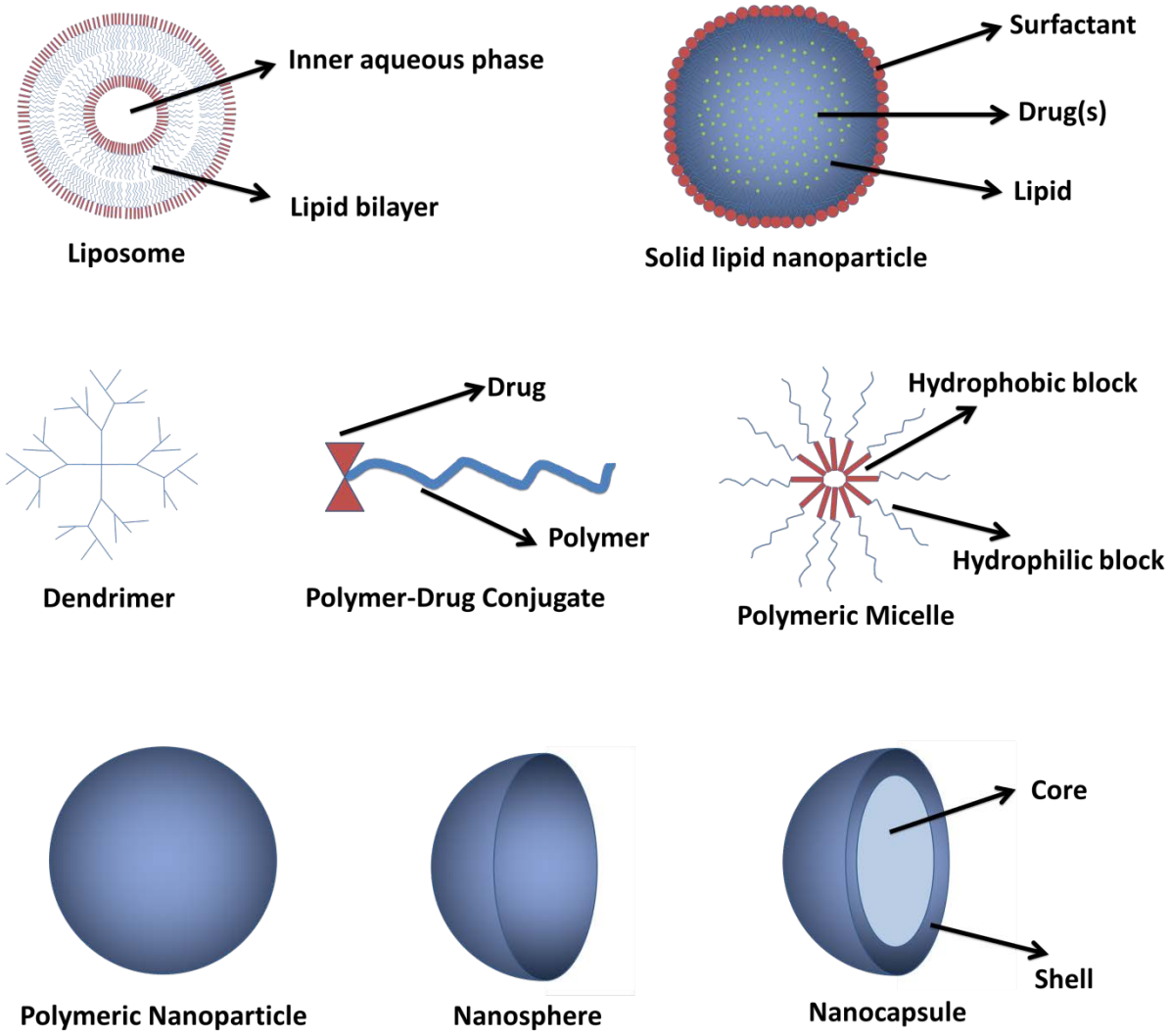


Figure 1-2. Various types of nanoparticles used in drug delivery.

### 1.4.1. Lipid-Based Nanoparticle Drug Carriers

#### 1.4.1.1.Liposomes

Liposomes are spherical vesicles comprising one or more bilayers of phospholipids that are arranged concentrically around one or more aqueous compartments and one central aqueous core (figure 1-2) [40, 41]. According to particle size and the number of phospholipid bilayers, liposomes are classified as large uni-lamellar vesicles (LUV), multi-lamellar vesicles (MLV), or small uni-lamellar vesicles (SUV) [40]. Liposomes can accommodate both hydrophilic and hydrophobic drugs [42]. Lipid bilayer of liposome acts as a membrane

to separate the aqueous core from the surrounding outside media [43]. Hydrophilic drugs are mainly entrapped in the core of liposomes or aqueous compartments [44], while hydrophobic drugs are mainly adsorbed or inserted in the lipid bilayers [45]. Drugs with poor water solubility are initially solubilized in the hydrophobic material (phospholipid) that forms the liposome bilayer. These drugs have poor water solubility and therefore low affinity towards the aqueous core or surrounding media [46]. Once placed in the liposome bilayer, they tend to remain entrapped in the region.

Liposomes' capability to contain both hydrophilic and hydrophobic drugs confers better solubility and distribution to the encapsulated drug than free drugs [47]. In addition, like other nanoparticle drug carriers, liposomes can be modified on the surface to enhance their bio-distribution and therapeutic efficiency [48]. Although liposomes' physicochemical and biological stability have been a matter of concern, the formulation of anticancer agents in liposomes has been extensively investigated for drug delivery purposes [35, 37].

Several liposomal formulations of anticancer agents are in clinical trial phases or have been approved for clinical application. Vinorelbine (Alocrest), docetaxel (ATI-1123), topotecan (Brakiva), doxorubicin (MCC-465), and an analogue of cisplatin (Aroplatin) are a few examples of chemotherapeutic agents in liposomal drug delivery systems in phase I clinical trials [49]. Liposomal formulations of paclitaxel (EndoTAG-1/LEP-ETU), oxaliplatin (MBP-426), and lurtotecan (OSI-211) are in phase II clinical trials [49]. Examples of liposomal formulation of anticancer agents in phase III trials include cisplatin (Lipoplatin), irinotecan (MM-398), and doxorubicin (Thermodox) [49]. Liposomal formulations of doxorubicin (Doxil/Myocet), daunorubicin (DaunoXome), vincristine (Marqibo), and cytarabine (DepoCyt) have been approved for treatment of various cancer types.

Liposomes as nanoparticle drug delivery systems have several advantages [50, 51]:

i) Liposomes increase efficacy and therapeutic index of loaded drugs,

ii) Liposomes protect the encapsulated drug from degradation (increased stability),

iii) Liposomes reduce encapsulated agents' toxicity,

iv) Liposomes are suitable for systemic administration,

v) Liposomes are biocompatible and biodegradable drug delivery systems, and

vi) Liposomes can be surface-engineered for active targeting purposes.

However, liposomes are not without drawbacks, which include [50, 51]:

i) A short half-life,

ii) The possibility of oxidation and hydrolysis of some phospholipids in nanoparticle formulation,

iii) Low stability,

iv) The possibility of leakage of encapsulated drug from liposomes,

v) Low solubility, and

vi) A high cost of production.

#### 1.4.1.2.Solid Lipid Nanoparticles and Nanostructured Lipid Carriers

Solid lipid nanoparticles (SLNs) are spherical particles in the nanometer size range (figure 1-2) that are prepared from lipids that are in solid state both at room and body temperature [52, 53]. SLNs are usually prepared from triglycerides, a mixture of triglycerides, or even wax [54]. The incorporation of both lipophilic and hydrophilic drugs in SLNs is potentially feasible [55]. In SLNs, the drug is usually dispersed throughout the bulk of the lipid matrix forming the nanoparticle structure. A few advantages are offered by SLNs over other lipid-based nanoparticle formulations like liposomes such as flexibility in modulating the drug release profile, pronounced physical stability, and protection of loaded drug from chemical degradation [56]. However, SLNs' disadvantages include low drug loading and the possibility of drug expulsion during shelf-life (as a result of polymorphic

transition of lipid to thermodynamically more stable form) [57]. To solve such disadvantages, another generation of lipid nanoparticles called nanostructured lipid carriers (NLCs) were introduced [58] based on an application of a mixture of a solid and a liquid lipid [59, 60]. NLCs are prepared from lipid mixtures in a way to create a spherical nanoparticle in which the liquid lipid is encapsulated (i.e., particle core) by the solid lipid (i.e., particle shell). The simultaneous encapsulation of the dissolution of a drug (in a liquid lipid core) by a solid lipid shell gives NLCs a higher loading capacity and more controlled release [61, 62].

The important advantages attributed to solid lipid based nanoparticles include [63-66]:

i) Protection and improved of stability loaded drug,

ii) Increased non-toxicity (most lipids used in fabrication of solid lipid based nanoparticles are biocompatible),

iii) Possibility of large-scale fabrication,

iv) Avoidance of using organic solvents during preparation,

v) Possibility of incorporating hydrophobic and hydrophilic drugs, and

iv) Possibility of targeting.

Also, important drawbacks of solid lipid based nanoparticles include [65, 66]:

i) Poor capacity for drug loading,

ii) Drug leakage and expulsion during storage (SLN), and

iii) Particle growth.

### 1.4.2. Polymer-Based Nanoparticle Drug Carriers

#### 1.4.2.1.Polymer-Drug Conjugate

Polymer-drug conjugates are a type of nanoparticulate delivery system in which the drug and polymer are covalently attached to each other (Figure 1-2). This attachment creates a new molecule that predominantly demonstrates the polymer's physicochemical

characteristics [67]. Usually, a water-soluble polymer is used to improve the solubility of conjugated drug. The covalent link between the drug and polymer is maintained by a spacer moiety (e.g., peptidyl or ester), which needs to be degradable in the physiologic/pathologic condition of the body (e.g., pH of the tumour tissue) to release the drug after administration to the body [68]. Other than being water-soluble, ideally, the polymer must be non-immunogenic, non-toxic, and have an easy elimination pathway from the body. Wide spectrums of drugs have been formulated as polymer-drug conjugates, including anticancer agents [69, 70]. Several successful nanoparticle therapeutics in clinical cancer care are drug-conjugates [36]. Many polymer-drug conjugate products are in the market or in the clinical phase, and others are being researched [71]. Asparaginase attached to PEG (Oncaspar®) is a well-known marketed product used for acute lymphoblastic leukaemia [72]. Other examples include Interferon α-2b attached to PEG (Sylatron™) as adjuvant therapy for resected stage III melanoma, PEGylated Interferon α-2a to treat melanoma (Phase I clinical study) and chronic myelogenous leukemia (phase II clinical study) [73], and Poly glutamic acid – conjugated paclitaxel (Opaxio®) (phase III clinical study) to treat ovarian cancer [74]. Conjugation of polymer resulted in increased half-life and efficacy, and decreased administration frequency of the mentioned agents.

Several advantages have been attributed to polymer-drug conjugates as nanoparticle drug delivery systems [72, 75]:

i) Increased stability and protection of conjugated drug,

ii) Prolongation of drug release and action,

iii) Possibility of targeting of conjugated drug,

v) Ability to delivery hydrophobic and hydrophilic drugs, and

vi) Increased blood residence and circulation time.

However, polymer-drug conjugates have some drawbacks which include [72, 74, 76]:

i) Potential toxicity of polymers (due to frequency of administration),

ii) High cost of production, and

iii) Poor drug loading capacity.

### 1.4.2.2.Dendrimers

Dendrimers are spherical nanoparticles prepared from highly-branched polymers that form a macromolecular structure (figure 1-2) [77]. Dendrimers possess a unique three-dimensional feature in which the polymer is repeatedly/regularly branched giving rise to a structure with a core at the centre, branching units surrounding the core, and terminal functional groups available for possible interaction forming the exterior [78]. The exterior section is responsible for chemical behaviour of the dendrimer and can be subjected functionalization/modification to further determine the solubility, miscibility, and reactivity of the nanoparticle [79, 80]. The core and the internal section offer a suitable environment (nano-cavity) in which drug molecules can either be physically entrapped or chemically conjugated to the branched polymer structure [81]. Containing the drugs in the core helps protect drugs from degradation and contributes to their solubility. The functionality of dendrimers' exterior section allows for the complexation or conjugation of drugs to the surface of dendrimers as well [82-84]. Consequently, due to dendrimers' favourable characteristics, such as tuneable functionality, mono-dispersity, encapsulation ability, and water solubility, they have been extensively investigated for the delivery of a wide spectrum of drugs [85, 86], including chemotherapeutic agents [87-90]. For example, association with dendrimers improved the bioavailability of methotrexate [91] and increased the water solubility of 5-fluorouracil, doxorubicin, and paclitaxel [91, 92].

Advantages attributed to dendrimers in drug delivery include [93]:

i) Possibility of targeting due to the presence of multiple functional groups,

ii) Possibility of controlling nanoparticle characteristics through preparation methods,

iii) Possibility of delivering hydrophobic as well as hydrophilic drugs, and

iv) Possibility of large-scale production

Disadvantages attributed to dendrimers include [94-96]:

i) Easy renal excretion due to relatively small particle size range,

ii) Labour-intensive, multi-step fabrication process, and

iii) Possibility of toxicity due to polymer accumulation (for non-biocompatible polymers).

#### 1.4.2.3.Polymeric Micelles

Polymeric micelles are nanoparticles made from polymers with one hydrophilic end and one hydrophobic end (i.e., amphiphile molecules in water). Because of their dual physicochemical characteristics, amphiphilic polymers can interact with other polymers and water molecules. When the concentration of polymer in an aqueous environment is increased above a certain level known as critical micelle concentration (CMC), amphiphilic polymers self-assemble and form a micelle structure [97]. Structurally, hydrophobic segments of the polymer interact (by hydrophobic interactions) inside the micelle to form an internal zone (core) and hydrophilic segment of the polymers arrange at the surface to form a shell (figure 1-2) [98]. Hydrophobic drugs can be entrapped in the hydrophobic environment of the internal zone by chemical conjugation or by physical means, which enhance the drug's solubility [99, 100]. Entrapping the drug in the internal zone protects the associated drug from degradation or biological triggers and can modify the drug's bio-distribution as well [101]. Due to their delivery performances, micelles have been used for the delivery of various drugs [102, 103], including anticancer agents [104] such as paclitaxel (in phase III clinical

study), doxorubicin (in phase II clinical study), cisplatin (in phase III clinical study), oxaliplatin (in phase I clinical study), and epirubicin (in phase I clinical study) [105].

To summarize, several important advantages are attributed to polymeric micelles [100, 106, 107]:

i) Polymeric micelles are prepared relatively easy because they self-assemble,

ii) They allow for the possibility of surface-modification and targeting,

iii) They can solubilize drugs with poor water solubility, and

iv) They protect incorporated drug.

Disadvantages attributed to polymeric micelles include [100, 106, 108]:

i) A high level of polymer chemistry and synthesis is usually required,

ii) Scaling up preparation procedures is difficult,

iii) The number of polymers for preparation of micelles is limited.

#### 1.4.2.4.Polymeric Nanoparticles

Polymeric nanoparticles are solid colloidal drug carriers prepared from polymers (or macromolecules), and have a size range between 10 and 1000 nm [109]. Structurally, two types of nanoparticles are defined for polymeric nanoparticles—nanocapsule and nanosphere (figure 1-2)—which are obtained based on different methods of preparation [110]. Depending on its physicochemical characteristics, the drug or biologically active agent is usually associated to polymeric nanoparticles in one of three different forms: encapsulated (or entrapped), dissolved (or dispersed), or adsorbed (or attached) [111]. In nanospheres, the drug is uniformly (homogeneously) distributed throughout the matrix of polymer that forms the nanoparticle. In nanocapsules, the drug is encapsulated inside the core of nanoparticle and is confined by a shell of polymer (around the central cavity) [112].

The polymers typically used to fabricate polymeric nanoparticles can be categorized as either biodegradable or non-biodegradable. The accumulation of non-biodegradable polymers in the body may cause toxicity. Additionally, non-biodegradable polymeric nanoparticles' drug-release mechanism is dependent on drug characteristics, permeability, and diffusion [113]. Polymeric nanoparticles fabricated from biocompatible, biodegradable polymers are non-toxic and release the drug mainly as the polymer degrades in the body [114].

Another way to categorize polymers used in preparation of polymeric nanoparticles is whether their source is natural or synthetic [115]. As mentioned, synthetic polymers contribute to a controlled release profile of the drug or active agent over a long period, while polymeric nanoparticles prepared from natural polymers tend to release the drug in relatively shorter time-periods. During nanoparticle fabrication, natural polymers lack the need for organic solvents, while synthetic polymers usually require organic solvents and harsh preparation [116, 117]. However, both types of polymers are being widely used in preparation of polymeric nanoparticles. Poly(esters), poly(cyanoacrilates), and poly(anhydrides) are examples of synthetic polymers; chitosan, albumin, dextrans, and alginate are examples of natural polymers [112].

Because of the diversity in the type and characteristics of polymers and approaches used in fabrication of polymeric nanoparticles, nanoparticles have versatile features and characteristics [36]. This makes polymeric nanoparticles a unique and promising tool to deliver a wide-spectrum of drugs and active agents with different purposes. Polymeric nanoparticles offer many advantages as drug-delivery systems [34-37]. Generally, they have high stability and confer stability and protection from degradation to the loaded drug. They can incorporate both hydrophobic and hydrophilic drugs and active agents to increase solubility compared to a free drug. They can also sustain or control the drug's release from

the nanoparticle by masking the drug molecules and active agents from recognition in the body and therefore protecting the drug from rapid or premature elimination. In addition, they offer further structural modifications, particularly on the surface of nanoparticles, to enhance their therapeutic performance. These abilities help improve the drug's absorption/bioavailability, distribution, metabolism, and elimination in the body and thus provide a favourable impact on pharmacodynamic features [118].

To summarize, polymeric nanoparticles as drug delivery systems have the following advantages [117]:

i) They have high stability,

ii) They offer protection and increase the stability of loaded drugs,

iii) They can incorporate hydrophobic and hydrophilic drugs,

iv) They offer controlled and/or sustained release of loaded drug, and

v) They allow for surface-modification and targeting.

However, polymeric nanoparticles have some drawbacks [119, 120]:

i) Non-biodegradable/biocompatible polymers may accumulate and cause toxicity, and

ii) They may be cleared by the reticuloendothelial system (RES) (according to size).

Among the long list of synthetic, natural, biodegradable, and non-biodegradable polymers, Poly (lactide-co-glycolide) (PLGA) has attracted substantial interest from researchers for the fabrication of polymeric nanoparticles for drug delivery because of PLGA's unique features and characteristics.

### 1.4.3. PLGA Nanoparticles

#### 1.4.3.1. PLGA polymer

PLGA polymer has attracted considerable attention in the field of pharmaceutical and biomedical sciences [121, 122]. Owing to its variable nature, PLGA polymer demonstrates

variable physicochemical properties, such as tuneable mechanical characteristics and a wide range of degradation times. Furthermore, it has been approved by the United States Food and Drug Administration (FDA) for use in humans [123] because of its biocompatibility, biodegradability, and non-toxicity profiles [124, 125].

#### 1.4.3.1.1. Physicochemical characteristics

A thorough knowledge of PLGA's physicochemical properties is essential in designing drug-delivery systems. PLGA is a linear co-polymer composed of monomer units of lactic acid (LA) and glycolic acid (GA) (figure 1-3). LA possesses a chiral centre (α carbon) to where the side methyl group is attached, which contributes to LA having two forms of D, L, or a racemic mixture of DL-isomers. Accordingly, poly(lactic acid) (PLA) can be prepared from either the isomers (i.e, D or L) or the optically inactive racemic mixture [126]. In D, L-PLA two stereo-isomeric forms of LA irregularly distribute in polymer chain and contribute to non-crystallinity in the material. GA lacks the pendant methyl group, which makes poly (glycolic acid) (PGA) highly crystalline. Non-crystallinity is considered important in the application of polymer for drug-delivery purposes because it contributes to a more homogenous distribution of the drug in the polymer matrix and to higher rates of polymer hydration and hydrolysis [121]. Therefore, the crystallinity of PGA is reduced when co-polymerized with PLA. In addition, using D,L-LA racemic mixture for PLGA preparation gives PLGA co-polymers higher levels of non-crystallinity [127].

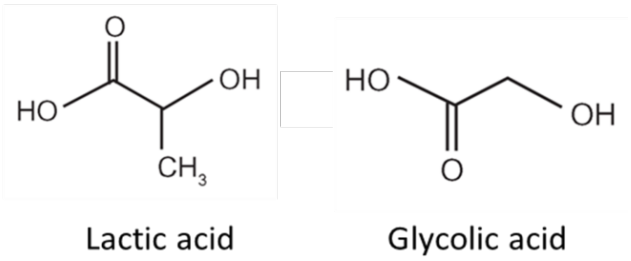


Figure 1-3. Monomers used in fabrication of PLGA.

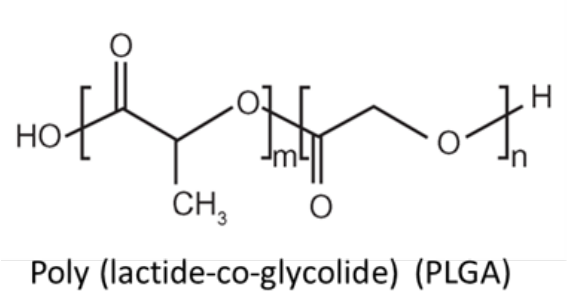


Figure 1-4. Molecular structure of PLGA.

PLGA (figure 1-4) is usually categorized based on different characteristics including the ratio between two monomers (i.e., LA:GA), the polymer molecular weight, and the type of terminal functional group. GA is more hydrophilic compared to LA because of the presence of methyl on α carbon atom of LA. Consequently, PLGA polymers with more LA monomers in the polymer structure exhibit fewer hydrophilic characteristics. PLGA polymers with more hydrophilic characteristics absorb more water and degrade faster [128, 129]. Ultimately, higher degradation rates accelerate drug release. An exception is the polymer with 50:50 monomer ratio, which also demonstrates a higher degradation rate. Therefore, the degradation rate tends to increase when the portion of GA monomers increases from 50 to 100 percent. Polymer molecular weight also influences the physicochemical characteristics of PLGA [129]. Polymers with lower molecular weight tend to degrade faster, which secondarily influences the rate of drug release from the polymeric delivery system. The

polymer degradation rate and drug release are also influenced by the type of polymer functional terminal group. Compared to ester-terminated PLGA polymers, free carboxyl end-group has the potential to attract water and catalyse the hydrolysis reaction between LA and GA and thus increase degradation and release rates [130].

#### 1.4.3.1.2. Polymer Degradation and Drug Release from PLGA

Upon contact with an aqueous environment, PLGA polymer undergoes hydrolytic degradation at the ester bond site where hydrolysis happens randomly [131]. Hydrolysis of the ester bonds throughout the polymer chain results in structures having COOH (carboxylic acid) and OH (hydroxyl) end-groups. Hydrolysis results in reduction of polymer molecular weight and creates fragments with higher water solubility. Further hydrolysis of these fragments creates LA and GA, which enter normal biochemical pathways of the body. It is believed that the produced acid environment catalyses the hydrolysis procedure (i.e., autocatalysis) and further contributes to degradation of PLGA polymer [123].

Various factors affect the degradation procedure of polymeric systems including PLGA (table 1-1). The important factors include polymer composition, polymer molecular weight, and the associated drug. Having a thorough understanding of these factors and the magnitude at which they affect the degradation procedure can help researchers design polymeric drug-delivery systems with desired characteristics: since release of the drug is a result of polymer degradation, when the degradation process is understood, release rates can be predicted.

Table 1-1. Factors affecting PLGA degradation and drug release from delivery systems.

| Factor | Effect |
|---|---|
| **Polymer composition** | PLGA polymers with higher content of glycolic acid degrade faster |
| **Polymer Molecular Weight** | PLGA polymers with higher molecular weight degrade slower |
| **Associated Drug** | The drug's chemistry determines interactions between the drug and polymer and affects polymer degradation rate |
| **Polymer Crystallinity** | Crystallinity of PLGA polymer can increase or decrease rate of degradation |
| **Polymer Terminal Group** | Ester-terminated PLGA degrades slower than acid-terminated polymers |
| **Delivery System Size** | Delivery systems with a smaller size (larger surface-area) have higher degradation rates |

The degradation process of PLGA is profoundly affected by the composition (i.e., the ratio between LA and GA) of the polymer. GA monomers in PLGA structure make the polymer more hydrophilic and thus accelerate the rate of degradation. This has been demonstrated by several research groups [132, 133]. For example, Wu and colleagues [130] used a set of PLGA polymers having similar molecular weight but different compositions (L:G ratio of 50:50, 65:35, 75:25, 85:15, 100:0) in a degradation experiment. They demonstrated that PLGA polymers with higher content of GA degrade faster. They attributed this relationship to the presence of the methyl group in LA, which hindered the approach of water molecules and the further hydrolysis of the ester bond. In another study, Lu et al. prepared foams from 85:15 and 50:50 L:G-ratio PLGA and conducted degradation tests [134]. The 85:15 polymer demonstrated little or no variation in water absorption, weight and other characteristics, while 50:50 polymer exhibited a marked increase and decrease respectively in water absorption and weight during the test period.

Molecular weight has been demonstrated to influence degradation rate of PLGA polymers. The degradation rate of polymers is directly related to the polymer chain size. Molecular weight of polymers increases parallel to chain size. Thus, polymers with lower molecular weight possess a higher degradation rate (i.e., require less time to break down)

compared to polymers with higher molecular weight [135-137]. For example, Xie et al.[138] studied the effect of molecular weight on degradation of polymer membranes prepared from PLGA 85:15 at two different molecular weights (i.e., 2.3 and 3.1 dl/g inherent viscosity). The PLGA with lower molecular weight demonstrated faster weight loss compared to the polymer with higher molecular weight. Also, Tracy and colleagues [139] used 50:50 PLGA with various molecular weights (i.e., 0.17, 0.19, 0.23, and 0.4 dl/g inherent viscosity) to evaluate factors affecting degradation rate of microspheres including polymer molecular weight. They observed a faster degradation with lower molecular weight polymer microspheres.

The chemical properties of the drug associated to the PLGA polymer can also affect the degradation rate [140]. Depending on the drug's hydrophilicity/hydrophobicity and the potential bonds that can form between PLGA structure and loaded drug, the degradation mechanism can shift from bulk erosion to surface erosion [141]. If interactions between the drug and polymer are strong, surface erosion is the predominant mechanism of the release. In the case of weak drug-polymer interactions, water molecules can more easily access the bulk of the matrix of the particles and contribute to bulk erosion. Therefore, the potential interactions that can happen between drug and PLGA polymer and their influence on polymer degradation and drug release should be considered before designing a polymeric drug delivery system [131].

Other factors can affect the degradation pace of PLGA polymer. There are conflicting reports on the effect of crystallinity on PLGA degradation rate [123, 131, 142, 143]. Various studies have suggested that polymer non-crystallinity contributes to faster PLGA polymer degradation [144]. However, a few have proposed otherwise [131].

The size and shape of the drug-delivery system are two of the factors affecting the rate of PLGA degradation due to the ratio of surface area to volume. Polymeric systems with

larger surface areas have larger amounts of the polymer matrix exposed to the surrounding media, which contributes to higher degradation rates [144, 145].

The type of terminal functional group on the PLGA polymer chain has been reported to influence polymer degradation time [146]. Ester-terminated PLGA polymer was reported to have delayed degradation time in comparison with acid-terminated (i.e., COOH) polymer of similar composition and molecular weight.

#### 1.4.3.1.3. Drug Release from PLGA Matrices

As noted, upon contact with an aqueous environment, PLGA undergoes hydrolysis. The degradation of polymer is commenced with the cleavage of the ester bond between monomers, which leads to formation of oligomers and ultimately monomers [143]. This process releases the associated drug into the surrounding media. Generally, the release of drugs from polymeric drug-delivery systems happens as a function of polymer degradation. Three mechanisms are considered responsible for drug-release [123, 147]: i) erosion of polymer at surface of drug-delivery systems that contributes to the release of the physically-entrapped drug (i.e., surface erosion (figure 1-5)), ii) erosion of polymer within the matrix of the drug-delivery system, which releases the drug by diffusion (i.e., bulk erosion (figure 1-5)), and iii) cleavage of bonding between the polymer and drug molecules (i.e., for example in the case of polymer-drug conjugates), which releases the drug by diffusion.

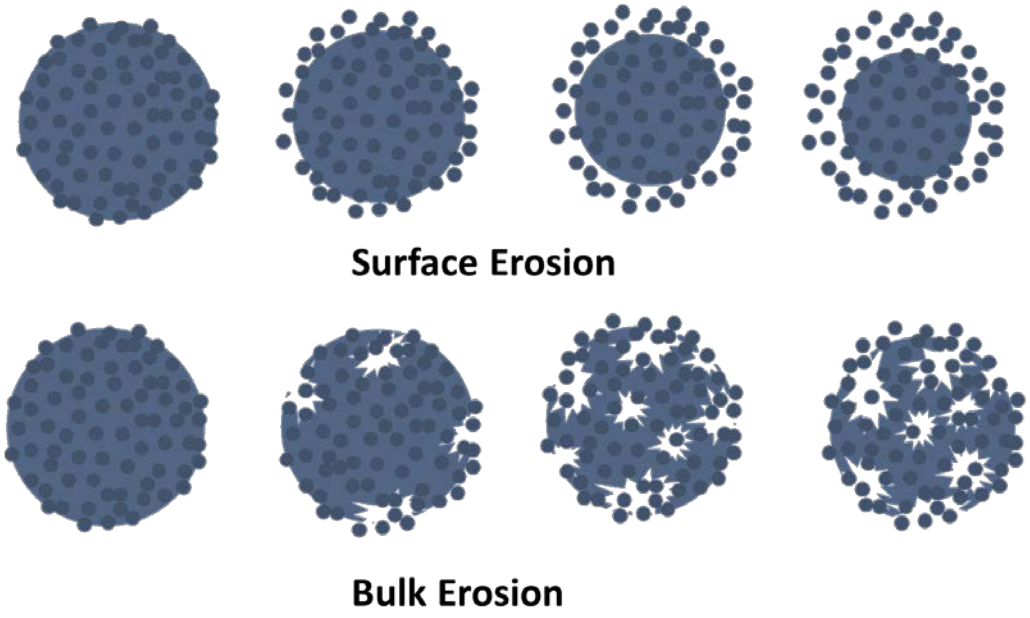


Figure 1-5. Polymeric nanoparticles erosion mechanisms that leads to eventual drug release.

Although surface erosion in part contributes to drug-release, bulk erosion is considered to be the main degradation mechanism of PLGA matrices and therefore is mainly responsible for the release of loaded drug [143]. In bulk erosion, the rate of hydrolysis of the PLGA polymer is less than the rate of water uptake into the matrix of the polymer [145]. As degradation propagates within the polymer matrix, degradation products become more water soluble. This attracts more water, which allows the degradation products and the loaded drug to diffuse out of the eroding matrix.

Degradation of PLGA polymer is a collective process of different mechanisms that can be affected by many factors, such as polymer composition, polymer molecular weight, the associated drug, and polymer crystallinity. Therefore, the rate and pattern of the release of the drug associated to the PLGA matrix is largely unpredictable. Although zero-order release from PLGA matrices is more desired, mono-phasic release pattern is rare [143]. Bi-phasic or even tri-phasic drug release profile is most commonly seen in PLGA polymer matrices. Small particles usually exhibit biphasic release pattern [148].

Phase one is usually described as a burst release [149]. During phase one, drug molecules on the surface of polymer matrix or close to the surface are in more contact with the surrounding medium and as a result prone to hydration [150]. Disintegration of particles and the formation of cracks are considered to be other reasons for burst release [151]. The initial burst is also affected by the loaded drug's physicochemical characteristics, concentration, and even polymer hydrophilicity. During this phase random cleavage of the ester bond contributes to the formation of oligomers and reduction in polymer molecular weight but soluble monomer products are not formed [152].

During phase two, the drug and water diffuse slowly through depleted layers and existing pores while hydration/hydrolysis and polymer degradation is in process [143]. The hydrolysis of PLGA within the matrix of polymer forms more soluble oligomers and monomers and creates pathways for water and drug to diffuse in and out, respectively, until erosion and drug release is complete [153]. Attraction of aqueous phase to the PLGA matrix plays an important role in determining the rate of polymer degradation and drug release [142]. Overall, the second phase is slow and usually the drug is released in a progressive manner.

#### 1.4.3.2.PLGA Nanoparticle Preparation Methods

Several techniques have been developed by researchers to produce polymeric nanoparticles from preformed polymers. In these techniques, two main steps are usually followed: an emulsified system is prepared and nanoparticles are formed from the emulsified system. The first step is usually similar in all nanoparticle fabrication methods, while the second step varies and gives the name to the method. Common nanoparticle fabrication methods are briefly described below.

#### 1.4.3.2.1. Emulsification Solvent Evaporation

Emulsification solvent evaporation method is one of the most common and the oldest technique used for fabrication of PLGA nanoparticles [122]. In this method, the polymer and drug are first dissolved in an organic solvent. The organic solvent is usually volatile and water-immiscible, like chloroform, methylene chloride, and ethyl acetate. The organic phase is then emulsified in an aqueous phase containing a stabilizer such as poly(vinyl alcohol) or vitamin E-TPGS to stabilize the emulsion. The obtained emulsion is then subjected to a source of high-energy shear stress (like a high-pressure homogenizer or an ultrasonic device) to break large emulsion droplets into smaller droplets. The reduction in the size of emulsion droplets in this step is crucial since it directly relates to the final size of obtained nanoparticles [122]. The emulsified system is then exposed to a reduced pressure or vacuum condition that results in the evaporation of the organic solution and ultimately disperses nanoparticles in the aqueous phase [154]. During this evaporation step, the organic solvent first diffuses out of emulsion droplets into the aqueous surrounding medium and then is removed by evaporation [155].

Based on the type of emulsion prepared during the first step (i.e., oil in water (O/W), water in oil in water (W/O/W)), the emulsification solvent evaporation technique can be used to accommodate drugs with different properties in PLGA nanoparticles [122]. W/O/W type obtained from double-emulsion procedure is used to entrap hydrophilic material while O/W emulsion is suitable for hydrophobic drugs [156].

#### 1.4.3.2.2. Emulsification Solvent Diffusion

In the emulsification solvent diffusion method, PLGA polymer and drug are dissolved in an organic solvent that must be partially miscible with water [157]. Suitable organic solvents with partial miscibility with water include benzyl alcohol, propylene carbonate, and

isopropyl acetate. The obtained organic phase is then emulsified in an aqueous phase under vigorous stirring [158]. The aqueous phase should contain a stabilizing agent such as poly (vinyl alcohol) (PVA), sodium dodecyl sulfate (SDS), or didodecyl dimethyl ammonium bromide (DMAB) to stabilize the emulsion. The obtained emulsion is then diluted with large quantities of water. This dilution diffuses the organic solvent (present in emulsion droplets) into the water and ultimately leads to the solidification and precipitation of the nanoparticles [122].

#### 1.4.3.2.3. Emulsification Salting Out

Emulsification salting out is another method widely used to prepare polymeric nanoparticles [159]. In this method, the polymer and drug are dissolved in an organic solvent that must be miscible with water (e.g., acetone, tetrahydrofuran). While exposed to a high-energy shear stress, the organic phase and aqueous phase (containing a stabilizing agent) are mixed together to prepare an emulsion. Compared to the emulsification steps of other fabrication methods, the aqueous phase here contains a high concentration of salts (which are not soluble in the organic solvent) such as calcium chloride, magnesium chloride, and magnesium acetate. The high concentration of salt prevents the organic solvent in the emulsion droplets from diffusing into the surrounding aqueous medium. A sufficient quantity of water is then added to the emulsion under mild stirring condition. This dilutes the salts and promotes the rapid diffusion of organic solvent into the surrounding medium, which solidifies and precipitates PLGA nanoparticles [160]. Compared to emulsification solvent diffusion method (that has similar steps), the salting out technique's use of salts requires final purification procedures [158].

#### 1.4.3.2.4. Nanoprecipitation

Unlike other nanoparticle fabrication techniques, the nanoprecipitation procedure has only one step. The method is usually suitable for hydrophobic materials, but it has been modified to accommodate water-soluble drugs as well [161, 162]. In this method, the polymer, drug, and a lipophilic stabilizing agent are dissolved in a polar organic solvent that is water miscible, such as acetone, acetonitrile, ethanol, or methanol. The organic solution is then added in a controlled way (e.g., pour drop-wise or injected) to an aqueous phase containing a surfactant under continuous stirring [163]. As a result of fast diffusion of the organic solvent into the aqueous phase, nanoparticles are formed and precipitated. The dispersion is then subjected to a reduced-pressure or vacuum condition to evaporate the organic solvent [121].

#### 1.4.3.2.5. Other Preparation Methods

Other PLGA nanoparticle fabrication techniques follow quite different steps.

**Spray-drying**: The spray-drying approach has also been used for fabrication of PLGA nanoparticles [164]. In this method, an emulsion (e.g., W/O) is prepared and sprayed into a stream of air, which leads to instantaneous formation of nanoparticles [165]. This method has few processing steps and therefore is a rapid method of nanoparticle preparation [166].

**Shirasu porous glass-emulsification:** The method is a modified form of emulsion solvent evaporation technique. In this method, an emulsion is made and then subjected to high pressure in the presence of a glass membrane. The emulsion passes through a porous membrane and as a result, emulsion droplets break into smaller homogenous nano-droplets. The nano-emulsion is then exposed to solvent evaporation to promote solidification of nanoparticles [167].

**Particle Replication in Non-wetting Templates (PRINT®):** The method is based on soft-lithography technology [168] and creates a population of PLGA nanoparticles with monodispersed distribution. It provides control over important characteristics such as nanoparticle size, shape, and drug loading. In this method, the drug and PLGA polymer are dissolved in an organic solvent, which is then deposited on a sheet made from poly(ethylene terephthalate) (PET) and spread using a rod. The solvent is then evaporated with heat to obtain a very thin film. The film and PET sheet is placed in contact with a patterned side of a mold and passed through heated nips. Nanoparticles form in the mold. The patterned side of the mold containing the formed nanoparticles is then placed in contact with another PET sheet that has been coated with a stabilizer (e.g., PVA). It is then passed through a hot laminator to transfer particles from the mold to the PET sheet and the mold is then separated. The nanoparticles are released from PET sheets using motorized rollers.

### 1.4.3.3.Nanoparticle surface Modification

PLGA nanoparticles offer advantages in the delivery of a wide spectrum of drugs owing to their unique characteristics, such as nano-meter size range, biocompatibility, biodegradability, and non-toxicity. To be able to meet their therapeutic potential as a controlled or targeted drug delivery system, PLGA nanoparticles must be able to remain in the systemic circulation for a long period of time after injection into the blood stream [169]. Long circulation times increase the chance that the nanoparticles will either reach their target tissue or release the loaded drug in a controlled manner in the blood stream. Despite several favourable attributes, PLGA nanoparticles encounter clearance from circulation by various natural clearing mechanisms in the body [170]. The fate of nanoparticles in the body is determined by nanoparticle’s characteristics. Accordingly, several nanoparticle parameters, such as size, shape, and surface chemistry, have been manipulated to increase the residence

time of nanoparticles in the systemic circulation and reduce non-specific distribution [171]. Modification of nanoparticles' surface properties is one of the most widely used approaches to increase nanoparticles' retention time and their drug-payload in blood [172]. For example, Park and colleagues [173] used PLGA nanoparticles for doxorubicin delivery and found out that surface-modification of nanoparticles was effective in increasing the drug's retention time in the blood compared to un-modified nanoparticles. Approximately 40% of the initial dose of doxorubicin administered as surface-modified nanoparticles was still present in the blood after 24 hours, while the free drug and the drug loaded in un-modified nanoparticles were not detectable after 24 hours.

Long circulating PLGA nanoparticles are usually obtained by coating of nanoparticles with other types of polymers that confer stealth properties to the nanoparticles so they can escape the natural clearing mechanisms of the body [169]. A stealth property is a characteristic that makes nanoparticles invisible to the biological mechanisms involved in the clearance of nanoparticles [169]. The polymers used to endow stealth properties to PLGA nanoparticles are typically highly hydrophilic, flexible, and electrostatically neutral. A few examples include PEG, poloxamers, polysaccharides (e.g., dextran), chitosan, and human serum albumin. PEG has increased blood circulation residence time of different type of nanoparticles, including PLGA nanoparticles [174]. For example, Duan et al. prepared surface-modified PLGA nanoparticles with PEG for mitoxantrone delivery [175] . PEGylated PLGA nanoparticles contributed to up to a 10-fold increase in drug concentration in the blood compared to un-modified PLGA nanoparticles. Murugesan and colleagues [176] found a two-fold increase in blood residence time using PEGylated PLGA nanoparticles delivering docetaxel compared to un-modified PLGA nanoparticles.

### 1.4.3.4. PEGylation of PLGA nanoparticles

PEG is a polymer prepared from repeating units of ethylene oxide (figure 1-6) with various molecular weights and configurations (e.g., linear or branched). The polymer possesses two reactive hydroxyl end groups (-OH) that can be used to covalently attach PEG to other molecules (i.e, PEG derivatization). To prevent unwanted crosslinking of PEG with other molecules, one of the terminal hydroxyl groups is substituted with a chemically inert group (e.g., $OCH_3$) [177]. Therefore, covalent attachment of PEG to another molecule (such as PLGA polymer) is limited to the remaining hydroxyl group, which consequently controls the stoichiometry of PEG derivatization [178]. PEG is a biocompatible, biodegradable, and non-toxic polymer [179].

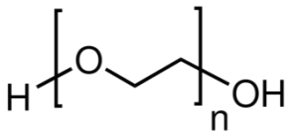


Figure 1-6. Molecular structure of PEG. (n = number of monomers repeated in the chain)

#### 1.4.3.4.1. Particle PEGylation

Surface-decoration of nanoparticles with PEG chains is simply referred to as *PEGylation*. PEG is a flexible, neutral (non-ionic), hydrophilic polymer [180]. Therefore, when stationed on the surface of PLGA nanoparticles, the polymer forms a barrier-like layer that sterically hinders the surface of the original nanoparticle [181]. In addition, it confers a hydrophilic neutral attribute to the surface of nanoparticles. Surface-modification of nanoparticles with PEG chains is usually done by three different methods [174, 182, 183] (figure 1-7):

**i)** Fabrication of nanoparticles with block-copolymer of PLGA and PEG. During preparation, due to PEG's hydrophilicity and PLGA's hydrophobicity, PLGA forms the nanoparticle body while PEG chains interact with the aqueous surrounding media and form the hydrophilic corona on the surface of nanoparticles.

**ii)** Fabrication of PLGA nanoparticles and then chemical coupling (i.e., covalent bonding) of PEG moieties to the surface of the preformed nanoparticles.

**iii)** Fabrication of PLGA nanoparticles and then physically adsorbing PEG copolymers onto the surface of the fabricated nanoparticles.

Various strategies have been considered to determine the optimal PEGylation approach suitable for PLGA nanoparticles [184]. The fabrication of nanoparticles from block-copolymers (first method) and the conjugation of PEG to preformed PLGA nanoparticles (second method) demonstrated higher PEGylation efficiencies [172]. PEGylated PLGA nanoparticles are expected to have a core-shell structure with PLGA as the core and PEG as the shell [174]. However, PEG chains can also be entrapped within the core of nanoparticles [185].

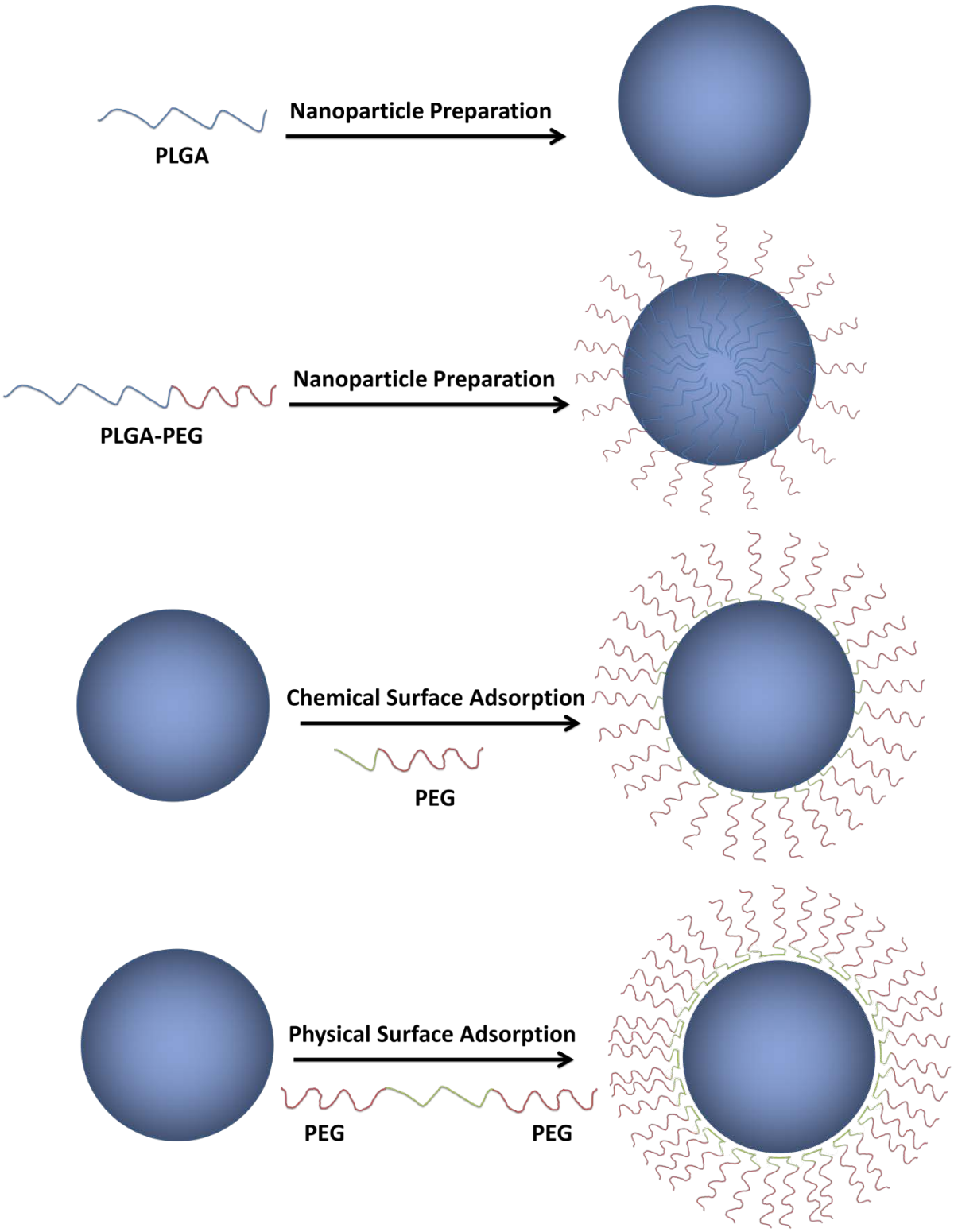


Figure 1-7. Various techniques for preparing PEGylated PLGA nanoparticles.

As mentioned, the PEG coating on the surface of nanoparticles works as a barrier layer opposing the interaction of the nanoparticle surface and other material (e.g., opsonins,

proteins) in the surrounding medium. To provide an efficient protection to nanoparticle surface against such interactions, PEG coating must exceed a minimum level of thickness, which is usually difficult to control in various conditions. The level of PEG layer thickness surrounding the nanoparticle surface is believed to be determined by PEG polymer chain conformation, molecular weight, and surface density (coverage) [183, 186, 187].

#### 1.4.3.4.2. Effect of PEGylation on Fate of PLGA Nanoparticles in the Body

PEGylation of PLGA nanoparticles through adsorption or grafting is the preferred method of surface modification to increase blood residence time of both the loaded drug and nanoparticle itself [188]. PEG polymer creates a protective, hydrophilic, neutral layer that blocks the adsorption of plasma proteins (opsonins) onto the surface of nanoparticles and therefore delays the opsonisation process required for the clearance of nanoparticles from the systemic circulation [189]. Opsonisation is the first step of the mononuclear phagocytic system (MPS) cells' recognition mechanism, which ultimately results in phagocytosis and the removal of nanoparticles from blood. Surface-modification of drug-loaded PLGA nanoparticles can potentially allow nanoparticles to evade the MPS system, elevate plasma half-life, and ultimately result in prolonged exposure of the body to the nanoparticle and loaded drug [190].

## 1.5. PLGA Nanoparticles for Delivery of Docetaxel

As mentioned, docetaxel is considered to be one of the most important and efficient anticancer agents being widely used in the chemotherapy of various cancer types. However, the clinical application of the drug has limitations due to docetaxel's poor water solubility, low selective bio-distribution, fast elimination, and hypersensitivity reactions. With the purpose to overcome such limitations, much attention has been drawn to alternative drug

delivery means [191-193]. The application of polymeric nanoparticles, especially the ones made from PLGA, as docetaxel-delivery systems has demonstrated great promise.

### 1.5.1. Docetaxel-loaded PLGA Nanoparticles

Many researchers have investigated the contribution of PLGA nanoparticles to delivery of docetaxel; their research is briefly discussed below.

Musumeci et al. [194] used low molecular weight PLGA polymer (0.16-0.24 dl/g) with acid end-groups (50:50, L:G molar ratio) to develop docetaxel-loaded nanoparticles using the emulsification solvent diffusion method. Sphere-shape PLGA nanoparticles demonstrated 157 to 172 nm of size, -5 to -10 mV zeta potential, and 16 to 23% drug entrapment efficiency. A biphasic docetaxel release profile was evident from PLGA nanoparticles liberating over 80% of the loaded drug in isotonic Phosphate Buffer Saline (PBS, pH = 7.4) during 14 days.

Murugesan and colleagues [195] prepared docetaxel-loaded PLGA nanoparticles and evaluated the influence of preparation conditions on different characteristics of nanoparticle formulations. They used 50:50 (L:G molar ratio), carboxylic-acid terminated PLGA polymer with molecular weight of 45,500 Da (~0.45-0.6 dl/g) to fabricate docetaxel-loaded nanoparticles using the emulsification solvent evaporation technique. Nanoparticles were prepared in various conditions of polymer concentrations, aqueous to organic phase volume ratios, stabilizing agent concentrations, docetaxel concentrations, and sonication times. Nanoparticles obtained through various preparation conditions were spherical in shape and demonstrated entrapment efficiencies between 25 to 84% while particle size ranged between 69 to 141 nm. They found out that variation in the abovementioned factors directly affected particle characteristics such as drug entrapment efficiency and average particle size.

Nanoparticles had a negative zeta potential equal to -36 mV and released around 40% of the loaded drug (in PBS pH = 7.4) during release test incubation period (30 days).

Later studies evaluated the cytotoxicity of docetaxel-loaded nanoparticles and the cell-uptake. Esmaeili and colleagues [196] prepared, characterized, and evaluated cell cytotoxicity and cell-uptake of docetaxel-loaded PLGA nanoparticles. Acid-terminated PLGA polymer with a 50:50 monomer ratio and 48,000 Da molecular weight (~0.45-0.6 dl/g) was used to prepare docetaxel-loaded nanoparticles using a modified emulsification solvent diffusion technique. The nanoparticles' size, zeta potential, and drug-loading efficiency was 175±13 nm, -12.2±0.6 mV, and 68±2% respectively. Nanoparticles were spherical in shape. The nanoparticles' biphasic release profile (in isotonic PBS pH = 7.4) was characterized by an initial 28% release over the first 24 hours followed by sustained release up to around 80% of the loaded drug. Cytotoxicity of docetaxel loaded in nanoparticles was evaluated using four types of cancer cells (human breast cancer cells MCF7, breast cancer cells T47D, ovary cancer cells SKOV3, and lung cancer cells A549). In all cancer cell lines, docetaxel formulated in PLGA nanoparticles inhibited proliferation more than that obtained from the free solution of the drug (i.e., the PLGA nanoparticles had a higher cytotoxicity at the equivalent dose of docetaxel). The authors attributed this increased cytotoxicity to uptake and retention of nanoparticles by the cells.

In a study by Yu et al. [167], Shirasu porous glass-emulsification technique was used to prepare docetaxel-loaded nanoparticles. The method resulted in around 64% entrapment efficiency and yielded docetaxel-loaded PLGA nanoparticles with a size and zeta potential of 334.1±2.7 nm and -16.4±1.0 mV, respectively. These nanoparticles demonstrated a sustained drug release behavior (in isotonic PBS pH = 7.4). In addition, their effectiveness in inhibiting tumor growth in mice inoculated by murine hepatic carcinoma cell lines (H22) indicated that the nanoparticle formulation decreased tumor size and increased the mean survival rate.

Applying PRINT® technology, Chu and colleagues [197] used PLGA polymer with 85:15 monomer ratio and 0.65 dl/g inherent viscosity to prepare docetaxel-loaded nanoparticles with two different cylinder shapes. One formulation with 200 nm diameter × 200 nm height and another one with 80 nm diameter × 320 nm height. Characterization of these cylinder-shaped nanoparticles indicated these drug loadings for both types of nanoparticles: 33.5% and 45.2% (w/w %) for 80×320 and 200×200 formulations, respectively. The 80×320 and 200×200 nanoparticles had average sizes of 227±10 nm and 263±1.8 nm, respectively, while both formulations had negative zeta potential around -3 mV. Both formulations showed a biphasic sustained release profile. Interestingly, the 200×200 nanoparticle formulation exhibited a lower initial release (38% after 3 hours) and lower overall drug release (i.e., around 72%) after 24 hour of incubation in PBS (37 °C). The 80×320 nanoparticle formulation released around 60% of docetaxel after 3 hours and near 100% of the loaded drug after 24 hours.

In another study, Manoochehri and colleagues [198] used carboxylic-acid terminated PLGA polymer with 48,000 Da molecular weight (~0.45-0.6 dl/g) and 50:50 monomer ratio to prepare docetaxel-loaded nanoparticles. They applied the emulsification solvent evaporation technique and used different ratios of acetone:dichloromethane (i.e., 2.5:97.5, 5:95, 10:90, 20:80, 30:70, and 40:60) and organic:aqueous phase (i.e., 10 % and 20 %) to prepare nanoparticles. The obtained nanoparticles were spherical and had an average size range between 180 nm and 221 nm. The fabrication process had entrapment efficiencies between 3 % and 48 % and yielded nanoparticles with zeta potential around -11 mV. A biphasic pattern was obtained from a study of the drug release (in PBS, pH = 7.4, 37 °C) in which 40% of the loaded drug was initially liberated within 10 hours followed by sustained release of the remainder of the drug over 13 days. Cytotoxicity of docetaxel loaded in PLGA nanoparticle was evaluated on human hepatocellular carcinoma cells (HepG2). At equivalent

concentrations of docetaxel between 0.3 and 20 µg/ml, docetaxel-loaded PLGA nanoparticle demonstrated a higher cytotoxicity. However, at higher concentrations (i.e., 40, 80 and 160 µg/ml), cytotoxicity obtained from free docetaxel and nanoparticle-loaded docetaxel was not different ($IC_{50}$ of docetaxel loaded nanoparticles was three folds lower than free docetaxel).

Recently, Mody and colleagues [199] compared docetaxel delivery potential of four types of nanoparticles including PLGA nanoparticles. In their study, docetaxel-loaded PLGA nanoparticles, dendrimers, liposomes, and carbon nanotubes were prepared and characterized *in vitro* and compared with each other. The prepared PLGA nanoparticles had 178±1.4 nm average size, -11.8±0.8 mV zeta potential, and 62% drug entrapment efficiency. To monitor potential interactions between nanoparticles and red blood cells, a hemolytic toxicity study was also done. The test determined that free docetaxel had the most hemolytic toxicity. In contrast, PLGA nanoparticles were second least toxic nanoparticles to red blood cells after liposomes. They also conducted docetaxel release tests on nanoparticle formulations in PBS (pH = 7.4, 37 °C). The dendrimer formulation released the drug during the first 12 hours. The others demonstrated a biphasic release profile during the 72-hour study period. The PLGA nanoparticles released 23% of the loaded drug during the initial phase and up to around 60% until the end of incubation time (three days), which was lower than that observed from liposome or carbon nanotube formulations. A cytotoxicity test using the human cervical cancer cell line *SiHa* was also conducted, which exhibited the following trend for $IC_{50}$: free docetaxel < carbon nanotubes < dendrimer < liposome < PLGA nanoparticles.

In another recent study, docetaxel was loaded in PLGA nanoparticles and extensively evaluated. Gupta and colleagues [200] used low molecular weight PLGA (0.22 dl/g) with 50:50 monomer ratio and applied an emulsion solvent evaporation technique to prepare the nanoparticles. Docetaxel-loaded nanoparticles had an average size of 167.4±5.1 nm and zeta potential of -23.9±1.6 mV. The nanoparticle fabrication method demonstrated a drug

entrapment efficiency of 74.9±3.9 %. The *in vitro* release study (in PBS, pH = 7.4) demonstrated a biphasic profile: an initial rapid release of docetaxel (within the first 24 hours), followed by a slower rate that ultimately led to liberation of 74.4% of the loaded drug over 10 days of incubation time. They also evaluated the plasma protein adsorption by nanoparticles, since nanoparticles' adsorption of plasma proteins after administration can potentially facilitate phagocytosis and clear the nanoparticles from systemic circulation. Docetaxel-loaded PLGA nanoparticles demonstrated aggregates, increased average size and poly-dispersity index after 24 hour of incubation with bovine serum albumin. Hemolytic toxicity of nanoparticles demonstrated the free solution of docetaxel had a higher hemolysis compared to nanoparticles. Furthermore, the toxicity of docetaxel-loaded nanoparticles was evaluated on two types of cell lines: human umbilical vein endothelial cells (HUVEC) and fibrosarcoma cells (HT-1080). In case of HUVEC cells, the anti-proliferative activity of PLGA nanoparticles (after 48 and 72 hours) was higher than that observed from the free solution of docetaxel. $IC_{50}$ of the nanoparticle formulation was 1.8- and 1.5-fold lower than free docetaxel after 48 and 72 hours respectively. Likewise, the results for the HT-1080 cell line demonstrated pronounced cytotoxicity profiles related to docetaxel loaded in nanoparticles compared to free solution of the drug, particularly after the long incubation times (i.e., 48 and 72 hours). Anti-tumor activity of the docetaxel-loaded nanoparticles was also evaluated *in vivo* on mice bearing HT-1080 tumors (based on tumor volume and weight change). The animal group treated with free docetaxel demonstrated a progressive reduction of body weight and lost 8.8% of their initial body weight. In contrast, the body weight of the animal group treated with docetaxel-loaded PLGA nanoparticles increased by 8.2%. Also, the docetaxel-loaded PLGA nanoparticles' tumor inhibition performance was better than the free solution of the drug. The percentage of tumor volume growth inhibition was 43.5% and

31.1% and the percentage of tumor weight growth inhibition was 27.4% and 18.5% for docetaxel-loaded nanoparticles and free docetaxel, respectively.

Jain and colleagues also used PLGA nanoparticles for docetaxel drug delivery [201]. They used 48,000 Da molecular weight (~0.45-0.6 dl/g), 50:50 (L:G) PLGA polymer and a modified emulsion solvent diffusion/evaporation technique to prepare nanoparticles. Nanoparticles had 207.8±9.5 nm size and -9.7±0.3 mV zeta potential, with a 95.5±2.8 % drug entrapment efficiency. Biphasic release of the drug from the nanoparticles lead to rapid liberation of docetaxel after 24 hours followed by release of 50% (in total) after 5 days (in PBS pH = 7.4). Docetaxel-loaded nanoparticles had a higher cytotoxicity effect after 24 and 48 hours of incubation with MCF7 cells than the free solution of drug (i.e., nanoparticle formulation had lower $IC_{50}$ values). The IV injection of docetaxel-loaded PLGA nanoparticles to tumor-inoculated animals resulted in higher tumor regression compared to that from free docetaxel solution (i.e., up to around 52% for nanoparticles compared to around 36% for the free docetaxel solution).

In another study, docetaxel was loaded in nanoparticles prepared from PLGA polymer with 25,000-35,000 Da (~0.32-0.44 dl/g) molecular weight by Park et al. [202]. A modified emulsification solvent evaporation technique was used to obtain PLGA nanoparticles with 254.5±8.9 nm size, -10.5±0.6 mV zeta potential, and 67.11% entrapment efficiency. Evaluation of the docetaxel release profile from nanoparticles (in isotonic PBS pH = 7.4) demonstrated a rapid release during the first 48 hour of incubation, which was followed by slow release leading to an overall cumulative release around 25 % (up to 10 days).

As exhibited above, PLGA polymer has been widely used in the preparation of docetaxel-loaded nanoparticles. Docetaxel-loaded nanoparticles demonstrated average sizes as small as 69 nm and as large as 334 nm, while zeta potential varied between -36 and -3 mV.

Between studies, entrapment efficiencies of the nanoparticle preparation methods were also different, ranging from 3% to 95%. The various types of docetaxel-loaded PLGA nanoparticles demonstrated different biphasic release profiles in terms of amount and time. However, docetaxel kept its biological activity after loading into PLGA nanoparticles.

In each study, a type of PLGA polymer was used to prepare docetaxel-loaded nanoparticles and nanoparticles were characterized accordingly. However, the approaches and materials used for nanoparticle preparation were different between different studies, which provided nanoparticles with different properties. In other words, the docetaxel-loaded PLGA nanoparticles demonstrate different characteristics because they have been prepared differently during independent studies. Accordingly, it does not seem to be scientifically right to compare these nanoparticles.

In this regards, a systematic study that provides valuable insight into how important properties of PLGA (such as polymer molecular weight, monomer ratio (L:G), and terminal functional group type) influence particle characteristics is simply lacking. In parallel, studies need to be conducted to evaluate how preparation conditions (in a typical nanoparticle fabrication method) determine particle-important characteristics. Establishing the relationship between PLGA polymer properties, nanoparticle fabrication method, and nanoparticle characteristics would allow researchers to prepare docetaxel-loaded PLGA nanoparticles with intended characteristics.

## 1.6.Pharmacokinetics and Bio-distribution of Nanoparticles after IV administration

### 1.6.1. Factors Controlling Nanoparticle Pharmacokinetics

Aside from the fact that nanoparticles offer suitable means for delivery of a wide spectrum of agents, the association between drugs and nanoparticle vehicles can favourably impact the pharmacokinetics of the parent drug, leading to favourable biological responses

[182, 203]. In this regard, a complex set of determinants are considered to be influential on the bio-distribution and fate of nanoparticles after *in vivo* administration [171, 183, 204]. These include the physicochemical properties of nanoparticle, the interaction between the drug and nanoparticle, and the set of events imposed to the nanoparticles by the host body. The nanoparticles' physicochemical factors control the particles' residence time in the blood circulation, tissue distribution pattern, mode of cell internalization and intracellular trafficking, release profile, and toxicity [182, 205]. The most important nanoparticle physicochemical properties are particle size, shape, chemical composition, mechanical properties (e.g., rigidity, deformability, and strength), and surface characteristics [172, 206].

#### 1.6.1.1.Particle Size

Particle size helps determine the bio-fate of nanoparticles upon administration to the body [203, 207]. It is believed that a size range less than 10 nm results in the removal of nanoparticles by renal filtration [208, 209]. On the other hand, nanoparticles with hydrodynamic radii of over 200 nm demonstrate a higher rate of clearance compared to smaller particles [183]. In other words, very small particles can be rapidly cleared from the systemic circulation via renal filtration while very big particles can potentially become trapped inside the RES organs such as the liver, spleen, and bone marrow [203]. However, the latter phenomenon offers advantages for targeting of particles to RES organs when the RES is the treatment target. Nanoparticles with suitable size ranges can evade both renal and RES clearance systems of the body and circulate in the systemic circulation longer [210, 211]. This was demonstrated by Yadav and colleagues [212] who prepared etoposide-loaded PLGA nanoparticles at two sizes (105 and 160 nm) and subjected them to blood clearance and biodistribution studies after IV administration. The 105 nm nanoparticles remained in the blood circulation longer and had lower RES uptake compared to the 160 nm nanoparticles.

This information is essential in designing delivery systems with systemically sustained drug release objectives. In such systems, a circulating drug reservoir is present in the body, which maintains the systemic drug concentration within acceptable therapeutic indices, ultimately leading to less adverse drug reactions and patient discomfort [213].

#### 1.6.1.2. Particle Surface Properties

Particles' surface characteristics can also affect the fate of nanoparticles in the systemic circulation. These properties include hydrophilicity/hydrophobicity, presence and conformation of any kind of adsorbed or grafted polymer/ligand, and electric charge [172, 214]. Positively-charged nanoparticles have a higher rate of cell-uptake and clearance when compared to neutral and negatively-charged formulations [215]. To test this, Yuan et al. [216] designed zwitterionic nanoparticles. They had a neutral surface charge in the blood to maximize systemic circulation time and further tumor accumulation. The surface charge switched to positive in tumor tissue to maximize cellular uptake. Ymamoto and colleagues [217] prepared polymeric micelles with negative (-10.6 mV) and neutral (1.3 mV) surface charges and exhibited their advantage in long circulation. They demonstrated that nanoparticles with negative zeta potential resulted in lower spleen and liver accumulation. This could be attributed to the presence of glycocalix with a negative charge stationed on the cells' surface that contributed to lower electrostatic interactions between nanoparticles and the cell membrane [218]. The presence of negatively-charged serum proteins can cause aggregates to form after IV administration of positively-charged nanoparticles and vice versa [219]. These aggregates can secondarily become trapped inside RES organs or cause an embolism in blood capillaries. In addition, nanoparticles can bind to serum opsonins, be opsonized and become recognized by the scavenging processes of the RES and immune system [220]. In fact, the initial opsonization of nanoparticles is important in determining the

phagocytic events and clearance from systemic circulation. Currently, research is mainly focusing on methods that can help effectively undermine this event [183]. As such, some trends have been proposed. Generally, particles with hydrophilic surface properties tend to opsonize more slowly than hydrophobic particles, which is attributed to the weaker absorbability of blood serum proteins on the hydrophilic particles' surface [183, 221, 222]. Nanoparticles opsonization has been correlated to the surface charge as well. Thus, efforts have been made to station surface-adsorbed or grafted shielding moieties on the surface of nanoparticles to block the particles' hydrophobic/hydrophilic and electrostatic features [183]. Surface engineering of nanoparticles with polymer coatings such as PEG can effectively hinder the surface charge of nanoparticles and reduce particle opsonization, which subsequently decreases nanoparticles' non-specific clearance from the body.

#### 1.6.1.3. Particle Shape

Shape is another important property that determines the bio-fate of nanoparticulate drug-delivery systems in the body [223-227]. Most nanoparticulate systems under extensive *in vitro* and *in vivo* studies are spherical in shape. However, researchers have applied various methods to fabricate nanoparticles with non-spherical shapes [228], such as ellipsoids [229], cubes [230], rods [231], cones [232], cylinders [233], and discs [206, 234]. The diversity in shape has a profound effect on factors like the residence time of nanoparticles in the systemic circulation [235], endocytosis [236-238] and phagocytosis [239], transport through the vasculature [236, 240], and even intracellular transport of nanoparticles [234]. For example, phagocytosis of nanoparticles as a mechanism of nanoparticle clearance from the systemic circulation has been proposed to strongly depend on nanoparticle shape [239, 241, 242]. Spherical nanoparticles are internalized faster than nanoparticles with higher aspect ratios [236]. In fact, phagocytosis is a two-step procedure (i.e., macrophage attachment and then

internalization) and particle shape can influence each step independently [243]. In other words, the local geometry of nanoparticles at contact point (between macrophage and particle) simply determines whether the phagocytic cell internalizes the particle or just spreads around the particle [239]. The event is proposed to be basically dependent on the contact angle (θ) [239, 244] at the site of attachment between particle and phagocytic cell (figure 1-8). In the case of rod-shaped nanoparticles with major axis being perpendicular to the membrane of phagocytic cell, internalization happens fairly quickly. In contrast, when contact between cell membrane and rod-shaped nanoparticle happens on the sides (i.e., more tangential), the rate of uptake decreases [227]. Spherical nanoparticles are internalized more successfully at a rate that is independent of the contact angle [227]. Therefore, non-spherical particles with high aspect ratios are believed to be able to evade the up-take mechanisms of the RES and persist in the systemic circulation longer than their spherical counterparts [206, 235]. Changing particles away from spherical shape could affect circulation time and particle bio-distribution [206, 235].

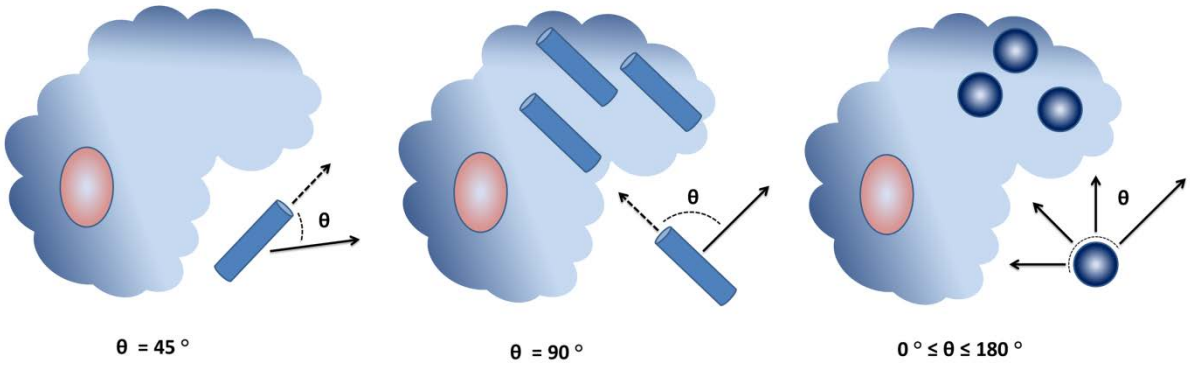


Figure 1-8. Influence of nanoparticle contact angle on rate of uptake by phagocytic cells.

Nanoparticles' shapes also affect their movement in the blood and through the vasculature. Nanoparticles are believed to be exposed to several forces in the systemic circulation (e.g., buoyancy, gravity, van der Waals, and electrostatic interactions) [227]

including the blood flow. Based on the shape, nanoparticles behave differently when subjected to blood flow (figure 1-9). Spherical nanoparticles tend to stay in the streamline of the blood flow they are moving in [240, 245], which makes escaping the blood flow towards vessel wall challenging. Therefore, the movement of spherical nanoparticles to marginal zone of the blood vessel greatly depends on convection and nanoparticle size [207, 246]. In contrast, particles with a high aspect ratio, such as rod-shaped nanoparticles, are subjected to transverse drifts because of the torques and forces exerted to the nanoparticles based on the angle of nanoparticle orientation [247]. Therefore, rod-shaped nanoparticles are believed to drift to the vessel wall more easily and then bind to endothelial cells or extravasate through them [248].

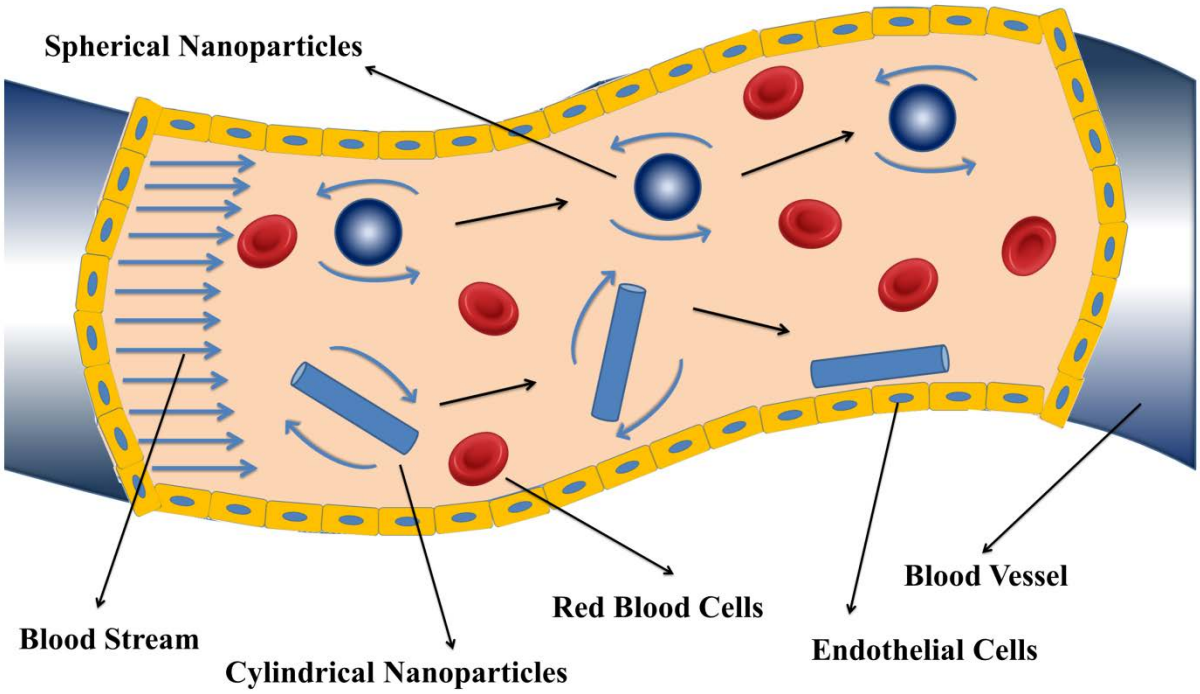


Figure 1-9. Influence of shape on migration behaviour of nanoparticles to the margins of blood vessels.

In general, one or more particle features affect the fate of the drug and result in a different drug-concentration versus time curve and pharmacokinetic profile. Depending on the properties of the drug and nanoparticles, the pattern of drug release from the nanoparticles plays a key role in determining the new kinetics of the drug in the body. In other words, if the drug is rapidly released from the particulate carrier system, the original drug pharmacokinetic governs the final behaviour. However, if the drug is released in a more sustained manner, the outcome pharmacokinetic is more determined by nanoparticle's fate in the body (e.g., erosion, disintegration, clearance) [182].

### 1.6.2. Bio-distribution of Nanoparticles

Upon entrance into the systemic circulation, nanoparticles are carried by the blood flow and are distributed to the tissues and organs of the body [249]. Once the nanoparticles enter the systemic circulation, interaction between nanoparticles and blood constituents can potentially be initiated. These include plasma proteins, coagulation factors, platelets, and red and white blood cells [250-253]. Then, nanoparticles are carried throughout the systemic circulation and distributed to different organs of the body. The accumulation of nanoparticles in different tissues depends on the nanoparticles' properties and the potential interactions with the living system.

Almost immediately after particle entrance to the blood circulation, opsonization occurs [183, 254] and often creates nanoparticle-protein complexes with different characteristics than the original nanoparticles [255, 256]. The protein coating varies considerably in terms of amount and pattern and is dependent on exposure time, physicochemical characteristics, and dose of nanoparticles [257]. Nanoparticle-protein interaction is a major step in the recognition and clearance of nanoparticles from the body [258, 259]. Blood vessels and their varying endothelia can also influence nanoparticle

distribution in the body [260] and contribute to their departure from or retention in the blood circulation. In addition, in cases of changes in the integrity of endothelial structure like what is seen in inflamed tissues, nanoparticles with even higher size ranges can evade the systemic circulation [261]. The distribution of nanoparticles can also potentially be affected by the amount of blood supply to a tissue [262]. In addition, physiological barriers (e.g., blood brain barrier) can lower nanoparticle accumulation in tissues with barriers compared to other parts of the body.

The RES is responsible for rapidly capturing and retaining nanoparticles [262]. In the liver, as the main organ of accumulation (particularly after IV administration), nanoparticles are retained by hepatocytes, kupffer cells, and endothelial cells [263-265]. In addition, open fenestrations of the liver's sinusal endothelia possessing diameters as large as 150 nm can contribute to particle retention in the liver [261]. On the other hand, in the spleen, where blood flows mainly through a pathway with minimal endothelial continuity, nanoparticles come into contact with the reticular meshwork of the marginal zone and red pulp [266]. They can easily get filtered there, particularly when nanoparticles are non-deformable entities with size ranges higher than the width of the cell slits (200-250 nm) [182].

As another RES organ, nanoparticles in the systemic circulation could reach the bone marrow compartment as well. However, they would have to go through transport mechanisms at blood-bone marrow barrier [267], so, although reported, the accumulation of nanoparticles in bone marrow has not been routinely studied [262]. The fate of nanoparticles in the body can also be affected by lymphatic system. Nanoparticles in the systemic circulation can leave the blood vessels through the permeable vascular endothelium present in lymph nodes and enter the lymphatic circulation [262, 268-270]. From the nanoparticle population that have gained access the lymphatic system, a portion accumulates and becomes trapped in lymph nodes, while another portion can get deposited into the blood circulation [271].

### 1.7. Pharmacokinetic Consequences of Docetaxel Loading in PLGA nanoparticles

As mentioned earlier, PLGA nanoparticles have the ability to drastically modify the pharmacokinetics of the loaded drug in the body. Upon administration to the systemic circulation, nanoparticles carry the entrapped drug with them as they circulate in the body and therefore impart a different pharmacokinetic behaviour to the loaded drug. Modification of docetaxel pharmacokinetics using PLGA nanoparticles has been the objective of several studies [272-275], but only a few studies have advanced to *in vivo* experiments on animals to determine pharmacokinetic outcomes.

Esmaeili and colleagues have demonstrated changes in docetaxel's pharmacokinetic characteristics after loading into PLGA nanoparticles [196]. In the experiment, docetaxel-loaded PLGA nanoparticles were prepared and fully characterized *in vitro* before administration to animals. The area under the curve (AUC) calculated for the nanoparticle formulation was markedly higher than that obtained from the free docetaxel solution (approximately 4.5-fold). Nanoparticle formulation also increased docetaxel's mean residence time (MRT) in the systemic circulation by 1.67-fold. In addition, the drug in the PLGA nanoparticle formulation had a longer plasma half-life ($T_{1/2}$) than the free drug alone.

In another study, Yu et al. compared the pharmacokinetic behaviour of docetaxel-loaded nanoparticles to that of the drug's commercial product (Taxoter®) and demonstrated that the formulation of docetaxel in polymeric nanoparticles resulted in superior pharmacokinetic characteristics [167]. The obtained nanoparticle formulation increased docetaxel's AUC by approximately 1.5-fold. Compared to Taxoter, PLGA nanoparticles increased the drug's half-life and MRT by 2.1 and 4.7 times, respectively. Furthermore, the drug's clearance from the body decreased. In general, PLGA nanoparticles exhibited a longer retention time in systemic circulation than the free drug formulation.

In another study, docetaxel-loaded PLGA nanoparticles were prepared using PRINT® technology and the corresponding pharmacokinetic behaviour was evaluated *in vivo* [197]. In the study, two types of PLGA nanoparticles were prepared. One formulation had dimensions equal to d=200 nm × h=200 nm and another to d=80 nm × h=320 nm. The PRINT® nanoparticles demonstrated approximately 20-fold higher plasma drug exposure as calculated by the AUC compared to that of the Taxoter drug formulation. In addition, the volume of distribution ($V_d$) of docetaxel from Taxoter was significantly higher ($p<0.05$) from that obtained from docetaxel in PLGA nanoparticle formulations. Compared to Taxoter, the $V_d$ was respectively 33- and 18-fold lower in the case of both the 200 nm × 200 nm and 80 nm × 320 nm formulations. The difference observed between the $V_d$ of the PLGA nanoparticle formulations was reported to be due to the smaller diameter of the 80 nm × 320 nm formulation and its higher chance to evade clearance mechanisms of the body (e.g., phagocytic cells). Furthermore, docetaxel entrapment in fabricated PLGA nanoparticles reduced the plasma clearance of the drug to approximately 24 times less than that observed from the commercial drug formulation.

In a recent study by Jain and colleagues [201], docetaxel-loaded PLGA nanoparticles were prepared, fully characterized and evaluated in an animal model. Pharmacokinetic characteristics of docetaxel due to PLGA nanoparticles were calculated and compared to those obtained from a free solution of docetaxel (Taxoter). Prepared nanoparticles had 207.8±9.5 nm size and -9.7±0.3 mV zeta potential. Taxoter had a higher plasma concentration after 30 minutes of IV injections, which was declined significantly afterwards, compared to PLGA nanoparticles. The calculation of AUC for both docetaxel formulations demonstrated that PLGA nanoparticles had increased docetaxel exposure by 3.2-fold. Interestingly, the PLGA nanoparticles increased docetaxel's half-life to 18.1 hours from the Taxoter formulation's 2.2 hours (i.e., 8.2-fold increase).

As mentioned, surface-modification of nanoparticles with PEG confers effective characteristics to the nanoparticles to evade clearance mechanisms of the body (e.g., opsonization events) and prolong blood circulation of injected nanoparticles. This in turn can potentially affect the pharmacokinetics of the loaded drug.

Senthilkumar and colleagues [176] evaluated the performance of PLGA and PEGylated PLGA nanoparticles in modifying the pharmacokinetics of docetaxel *in vivo*. They fabricated three formulations: PLGA nanoparticles, surface-modified PLGA nanoparticles with 2kDa PEG, and surface-modified PLGA nanoparticles with 5kDa PEG. *In vitro* characterization steps were also performed on all formulations. PLGA nanoparticles had 102±0.24 nm size and -37±0.6 mV zeta potential while PLGA-PEG (2kDa) and PLGA-PEG (5kDa) nanoparticles had similar size range (103±0.16 and 107±0.25 nm, respectively) and zeta potential (-5.3±0.5 and -5.3±0.7 mV, respectively). The pharmacokinetic profile of docetaxel in Balb/C mice was then evaluated after IV injections with either the free docetaxel solution or nanoparticle formulations. The obtained data exhibited delayed blood clearance of docetaxel by the nanoparticle formulations compared to that from the free drug solution. Although not statistically significant, blood clearance of free docetaxel was approximately 1.5, 2.4, and 2.7 times higher than the PLGA, PLGA-PEG (2kDa), and PLGA-PEG (5kDa) nanoparticle formulations, respectively. The AUC of docetaxel was increased for all nanoparticle formulations compared to the free drug solution, though the PLGA-PEG (5kDa) formulation's increase was statistically significant ($p<0.05$). MRT of the drug increased from 2.3 h (free drug) to 3.6 h (1.5-fold) for the PLGA nanoparticle and to 4.5h (1.9-fold) and 4.9h (2.1-fold) for the PLGA-PEG (2kDa) and PLGA-PEG (5kDa) formulations respectively. Ultimately, docetaxel's half-life increased 1.7, 3.5, 3.7 times when PLGA, PLGA-PEG (2kDa), PLGA-PEG (5kDa) nanoparticle formulations were used (respectively) compared to the free drug solution.

The effect of the PEGylation of PLGA nanoparticle in modifying docetaxel pharmacokinetics was also evaluated by Jain and colleagues [201]. Docetaxel-loaded PEGylated PLGA nanoparticles demonstrated an average size of 224.9±10.8 nm and zeta potential of -5.6±0.3 mV. PEGylation of nanoparticles increased docetaxel half-life by nearly 13-fold and 1.5-fold compared to free solution of docetaxel (Taxoter) and PLGA nanoparticles, respectively (i.e., Taxoter: 2.2 hour; PLGA nanoparticles:18.1 hour; and PEG-PLGA: 28.5 hour). Overall exposure of docetaxel (AUC) was also increased seven times compared to free solution of drug and two times compared to unmodified PLGA nanoparticles.

Docetaxel-loaded nanoparticles act as drug reservoirs that circulate in the blood and provide the systemic circulation with the drug in a sustained manner. In addition, PLGA nanoparticles as docetaxel reservoirs potentially retain the drug in the blood and prevent it from wide distribution to various organs of the body, which includes organs that are involved in clearing docetaxel from the body. Accordingly, PLGA nanoparticles keep docetaxel in the blood longer than when naked docetaxel is used. In other words, docetaxel spends more time in the systemic circulation, and of course, in the body. Consequently, PLGA nanoparticles are expected to prevent wide-distribution of docetaxel, which would decrease docetaxel's apparent volume of distribution as well as its systemic clearance. Similarly, PLGA nanoparticles are expected to increase the total docetaxel exposure (AUC), half-life, and mean residence time of docetaxel in the body.

As noted in the examples above, the pharmacokinetics of docetaxel could be modified using PLGA nanoparticles as drug delivery means. Throughout various studies, AUC (total body exposure) of docetaxel was increased between 1.5- and 20-fold. PLGA nanoparticles also increased docetaxel's mean residence time by as high as 4.7-fold. Due to the application of PLGA nanoparticles, docetaxel's apparent volume of distribution was also

decreased by as low as 30-fold. Generally, the studies provided above also demonstrated an increase in docetaxel's half-life and decrease in its systemic clearance when PLGA nanoparticles were used.

It is worth mentioning that each study used nanoparticles that were uniquely distinct from that nanoparticles used in other studies. In other words, docetaxel-loaded PLGA nanoparticles of various studies had different characteristics, so their contribution to the pharmacokinetic profile of docetaxel has been evaluated independently. Accordingly, comparing the mode and extent of pharmacokinetic consequences of different PLGA nanoparticle formulations does not seem to be scientifically correct.

## 1.8.Bio-distribution Consequences of Docetaxel Loading in PLGA nanoparticles

The fate of nanoparticles in the biologic system after administration determines the extent of various organs' and tissues' exposure to the drug. Highly distributed nanoparticles can carry the drug to a wide range of tissues and make the drug available more universally. Due to physicochemical properties or to targeting features, bio-distribution of some nanoparticle formulations can be limited. Accordingly, the bio-distribution of docetaxel loaded in PLGA nanoparticles to various organs/tissues, including tumour tissues, has been studied extensively.

### 1.8.1. Biodistribution in Healthy Animals

Esmaeili and colleagues [196] demonstrated that the most important difference between docetaxel-loaded PLGA nanoparticles' and Taxoter's *in vivo* bio-distribution behaviour was that the nanoparticles maintained docetaxel's plasma levels, while the free drug solution's plasma levels dropped significantly. In addition, the researchers exhibited that the nanoparticles increased levels of docetaxel in RES organs such as liver, lungs, and spleen

more than Taxoter did and concluded that docetaxel's incorporation in PLGA nanoparticles can be manipulated in the treatment of RES organ carcinomas.

### 1.8.2. Biodistribution in Tumour-Bearing Animals

Senthilkumar and colleagues evaluated the bio-distribution of docetaxel in nanoparticles of PLGA and PEGylated PLGA with two molecular weight PEG moieties (2kDa and 5kDa) [176] in tumour-bearing mice. Different nanoparticle formulations and a free docetaxel solution were subsequently injected to animals and at certain time-points organs/tissues were then collected and analysed. The time-course of docetaxel level in tissues demonstrated that drug distribution to non-tumour organs was more pronounced with the free drug solution. PLGA nanoparticle formulation had no targeting characteristics and therefore was eliminated from the blood circulation quicker than their PEGylated counterparts. The PLGA nanoparticle formulation did decrease docetaxel distribution to non-tumour tissues and increase drug transport to tumour tissue. However, PEGylated PLGA nanoparticles delivered significantly higher concentrations of the drug into the tumour tissue. Interestingly, the docetaxel levels in the blood were markedly higher with the PEGylated PLGA than those of PLGA nanoparticle formulation (at similar time-points), while drug transport to non-tumour tissues was limited. In addition, PEGylation of PLGA nanoparticles with a PEG chain of 5kDa demonstrated a longer blood circulation and therefore resulted in higher levels of drug accumulation in tumour tissue compared to the formulation with the 2kDa PEG chain. The 5kDa chain provided more chances for the particles to extravasate through the leaky vasculature of tumour tissue, which increased the exposure times and drug concentration levels.

The bio-distribution of docetaxel-loaded PRINT nanoparticles at two different sizes/shapes was evaluated by Chu at al. [197]. Compared to the commercial formulation of

the drug (Taxoter), PRINT nanoparticles increased the total tumour exposure of docetaxel by 53% and 76% for of 80 nm × 320 nm and 200 nm × 200 nm formulations, respectively. The 200 nm × 200 nm nanoparticle formulation had a higher docetaxel tumour exposure, although plasma drug exposure for both formulations was similar. Both nanoparticle formulations had higher drug exposure in spleen and liver in contrast to Taxoter, as expected for a nanoparticle formulation. Compared to the 80 nm × 320 nm nanoparticle formulation, the 200 nm × 200 nm formulation demonstrated 4.8 times more docetaxel exposure in spleen and 1.5 times more in the liver and lungs. The observed behaviour from PRINT nanoparticles was attributed to the existing difference in the nanoparticles' aspect ratios, which can affect the nanoparticles' interactions with biological mechanisms.

### 1.9. Conclusion and Summary

Polymeric nanoparticles of PLGA are suitable means of drug delivery since they offer advantages as drug delivery vehicles. Accordingly, PLGA polymer has been extensively used to prepare nanoparticles to deliver a wide range of pharmaceutically active agents including chemotherapeutics. The polymer can assume different physicochemical characteristics based on the type and number of monomers present in the PLGA structure. Therefore, nanoparticles prepared from PLGA polymer can assume variable features and characteristics based on the type of polymer, type of loaded drug, and nanoparticle fabrication method. As mentioned above, several studies have prepared and characterized PLGA nanoparticles for the delivery of docetaxel as a chemotherapeutic agent with wide application in a variety of cancer types. These studies have been conducted independently to prepare PLGA nanoparticles as a new means for docetaxel drug delivery with pharmacokinetic- and biodistribution-modification benefits. In these studies, a variety of PLGA polymers and fabrication methods have been used to prepare docetaxel-loaded PLGA nanoparticles. Consequently, obtained nanoparticles

of these studies demonstrated a variety of characteristics. Therefore, the pharmacokinetic and biodistribution consequences of corresponding nanoparticle formulations cannot be compared between different studies.

Several studies used PLGA polymer to prepare nanoparticles for the delivery of docetaxel following extensive *in vitro* steps to characterize the prepared formulations. However, not all of the studies proceeded to *in vivo* steps. Based on the data from these studies, it is apparent that PLGA nanoparticles could potentially modify the pharmacokinetic and biodistribution of docetaxel. Accordingly, a few general conclusions could be made in this regard:

1) Changes made to docetaxel's pharmacokinetic and biodistribution profile were attributed to the form of the drug delivery system itself, the nanoparticle.
2) The mode of these changes have been attributed to main particle characteristics including average size, surface properties (zeta potential), and shape.
3) Almost all the relevant data from these studies only provide general insight of how "typical" PLGA nanoparticle formulations modified docetaxel's pharmacokinetic and biodistribution profile in animal models.
4) The studies provided above have only reported their data. No comparison was made between *in vitro* characteristics of nanoparticles and also between *in vivo* performances of docetaxel nanoparticle formulations.
5) There has not been enough progress towards clinical application of docetaxel-loaded PLGA nanoparticles in humans (based on United States National Institutes of Health, ClinicalTrials.gov) yet.
6) PLGA nanoparticles' performance in modifying docetaxel's pharmacokinetic and biodistribution profile depends on the nanoparticles' features and characteristics, while the nanoparticles' features and characteristics depend on the type of PLGA

polymer and the nanoparticle preparation conditions. In other words, PLGA polymer properties, nanoparticle fabrication method, and PLGA nanoparticles' contribution to docetaxel's pharmacokinetic and biodistribution profile are linked like the links of a chain. However, so far no systematic study has been conducted in a way to explain this connection.

# CHAPTER 2

## Purpose of the Project

### 2.1.Study Rationale

#### 2.1.1. The need for New Drug Delivery Systems

Today, novel drug delivery systems (NDDS) have demonstrated great promise in improving the delivery of many drugs and active pharmacological agents. NDDS are either used to deliver newly discovered active pharmacological agents (i.e., develop drug formulations) or used to deliver already formulated drugs trying to improve upon the drugs' limitations. Generally, modifications in a drug's delivery are performed ultimately to improve the drug's pharmacodynamic characteristics. However, the drug's pharmacodynamic characteristics and therapeutic outcomes also depend on its own pharmacokinetic characteristics. When components of pharmacokinetics (i.e., absorption, distribution, metabolism, and excretion (ADME)) are desirably modified, therapeutic outcomes are favorably modified as well. NDDS are usually used to modify as many components as possible.

#### 2.1.2. Polymeric Nanoparticles

Among NDDS, nanoparticulate drug carrier systems have great potential to desirably modify the delivery of conventional or newly-discovered drugs. Compared with other types of developed nanoparticle drug carriers, polymeric nanoparticles are one of the most promising drug delivery systems. Polymeric nanoparticles are classified into different categories based on their structure (e.g., nanosphere and nanocapsule) and type of polymer

used for fabrication of the nanoparticle (e.g., synthetic, semi-synthetic, and natural). Various types of polymers are used in the preparation of polymeric nanoparticles.

### 2.1.3. PLGA Nanoparticles

Owing to several favourable characteristics, PLGA is a suitable polymer to prepare polymeric nanoparticles as drug delivery vehicles for various types of drugs. PLGA polymer provides nanoparticles with unique properties that do not have most of the concerns accompanied with other types of polymeric nanoparticles (e.g., polymer toxicity).

PLGA has a variable nature that gives the polymer different physicochemical characteristics. The polymer has different molecular weights based on the number of monomers that participate in the polymer chain. The ratio of monomers in the polymer chain (i.e., lactic acid: glycolic acid) can also vary. The polymer can have different terminal functional groups as well. Other than the polymer itself, several nanoparticle fabrication methods can be used. Therefore, the variability in the type of drugs and pharmacologically active agents to be delivered, the availability of different techniques for nanoparticle preparation, and most importantly, the remarkable variability in PLGA polymer itself results in extreme variability in PLGA nanoparticle features and characteristics. So, any PLGA nanoparticle formulation is uniquely distinct from another formulation prepared differently. This variability brings more attraction to PLGA nanoparticle drug delivery, creates more room for research and development, and provides more areas to explore. Because the fabrication methods create nanoparticles with unique properties, the formulation conditions that lead to nanoparticles with most intended characteristics need to be identified. This is usually done by optimization techniques.

### 2.1.4. PLGA Nanoparticles' Contribution to Pharmacotherapy

PLGA nanoparticles have been used for systemic and targeted drug delivery. PLGA nanoparticles with systemic delivery purposes are used as drug reservoirs that can remain in the blood for prolonged time and release the drug in a sustained manner. Sustainable availability of drug to the systemic circulation potentially reduces the drug concentration fluctuations in the blood and keeps the concentration within the therapeutic window of the medication. Modifications to the nanoparticles' surface can prolong their residence time in the systemic circulation, which further enables PLGA nanoparticles to be used as sustained-releasing, long-circulating drug-delivery systems. Maintaining drug concentration in the blood within the therapeutic window reduces the chances of developing drug toxicity and side effects while presenting the therapeutic outcomes. It also prolongs dosing intervals and reduces the need for frequent dose administrations. Both outcomes benefit pharmacotherapy and patient compliance to the treatment.

### 2.1.5. Anticancer Agent

Docetaxel is a highly potent anticancer agent being used to treat a wide spectrum of cancer types. The drug is insoluble in water, so a combination of co-solvents is used in the commercial formulation to enhance the solubility. Issues such as hypersensitivity reactions, lower level of uptake by tumour tissue, and extensive toxicity/side effects have been associated with the formulation, which may partly be attributed to formulation's ingredients. An alternate drug-delivery system, such as PLGA nanoparticles, may help circumvent these problems with conventional docetaxel pharmacotherapy and improve patient comfort and compliance.

## 2.2. Study Hypothesis

- Taguchi factorial design determines optimum condition for fabrication of PLGA nanoparticles loaded with docetaxel.
- PLGA nanoparticles loaded with docetaxel possess the characteristics of a sustained-release drug-delivery vehicle.
- PLGA nanoparticles increase the blood circulation time for docetaxel by increasing the exposure, elimination half-life, and mean residence time of docetaxel in body.

## 2.3.Study Objectives

### 2.3.1. Objective 1

**Specific aim:** To design an optimized preparation method for PLGA nanoparticles loaded with the anticancer agent docetaxel.

#### 2.3.1.1.Experiments Corresponding with Objective 1

**Design and Optimization of Nanoparticle Preparation:** PLGA polymer was used to prepare nanoparticles as delivery vehicles of the anticancer drug docetaxel. A modified emulsification solvent evaporation technique was used to fabricate nanoparticles. To obtain a suitable PLGA nanoparticle formulation, a factorial experimental design was used to optimize nanoparticle fabrication method. Instead of following the conventional approach towards optimization of a process, in which the effect of one variable is evaluated while other variables are kept constant, a fractional factorial design was used. In fractional factorial designs, a reduced number of experiments (i.e., a fraction of the full factorial combinations) is used to draw out valuable conclusions and establish a relationship between process variables and the outcome of interest. Six factors were of interest, from which two were

evaluated at four levels and four factors were evaluated at two levels. Such combinations of factors and levels require the use of mathematical algorithms with asymmetrical matrices. The Taguchi method is a robust method that allows for fractional design of factorial experiments and asymmetrical mathematical matrices. Therefore, the Taguchi L16 (4**2 2**4) array with 16 different combinations of factors/levels has been used to prepare drug-loaded PLGA nanoparticles. The data obtained was applied to identify preparation factors with the highest magnitude of effectiveness on important nanoparticle characteristics, including size, zeta potential, PDI, and drug-loading efficiency. Models were built to predict important characteristics based on evaluated factors. The statistical significance of each factor in determining the important characteristics was checked as well. Based on the factorial experimental design, an optimized nanoparticle fabrication method was selected.

### 2.3.2. Objective 2

**Specific aim 1:** To prepare docetaxel-loaded PLGA nanoparticle formulations based on the optimized method of fabrication.

**Specific aim 2:** To prepare surface-modified (i.e., PEGylated) docetaxel-loaded PLGA nanoparticle formulations based on the optimized method of fabrication.

**Specific aim 3:** To characterize docetaxel-loaded PLGA nanoparticles in terms of important particle properties.

**Specific aim 4:** To characterize docetaxel-loaded surface-modified (i.e., PEGylated) PLGA nanoparticle in terms of important particle properties.

#### 2.3.2.1.Experiments Corresponding with Objective 2

The selected optimized fabrication method was used to prepare docetaxel-loaded nanoparticles. PLGA nanoparticles were prepared at four different docetaxel concentrations (i.e., low to high concentration) to have four nanoparticle formulations (i.e., low to high drug-loading formulations) to choose from.

PEGylated PLGA nanoparticles were also prepared following the same fabrication method as PLGA nanoparticles. The polymer used was the di-block co-polymer of PLGA (with the same characteristics as parent PLGA) and PEG (with 5000 Da molecular weight).

Both nanoparticle formulations were subjected to extensive *in vitro* characterization including measurement of average size, zeta potential, poly-dispersity index, drug loading, drug-release profile, and cytotoxicity.

### 2.3.3. Objective 3

**Specific aim:** To set up and partially validate analysis methods for the detection and quantification of docetaxel in polymeric and biologic matrices (based on guidelines of the FDA).

#### 2.3.3.1.Experiments Corresponding with Objective 3

To detect and quantify docetaxel in biologic (i.e., mouse tissues) and non-biologic (i.e., PLGA and PLGA-PEG nanoparticles) matrices, an analysis method based on mass spectrometry was developed, partially validated and used throughout the project.

### 2.3.4. Objective 4

**Specific aim 1:** To determine the pharmacokinetic characteristics and bio-distribution (i.e. in the serum, liver, kidney, heart, and lung) of docetaxel (in mice) when used in PLGA nanoparticles, in surface-modified (i.e., PEGylated) PLGA nanoparticles, and in a free solution.

**Specific aim 2:** To establish a relationship between PLGA nanoparticle characteristics and the mode of changes made to docetaxel's pharmacokinetics and bio-distribution profile.

#### 2.3.4.1.Experiments Corresponding with Objective 4

To determine how the loading of docetaxel in nanoparticles contributes to modifications of the drug's pharmacokinetic characteristics and bio-distribution profile, the optimized formulation of docetaxel in PLGA and PLGA-PEG nanoparticles were intravenously injected to mice. An equivalent dose of a free docetaxel solution was also administered to mice. Then, docetaxel concentration versus time profile in serum and tissues under study was established for each formulation. Pharmacokinetic parameters and tissue distribution related to each were evaluated and compared.

# CHAPTER 3

## Experimental Section on Taguchi Design for Formulation and Optimization of Docetaxel-loaded PLGA Nanoparticles

### 3.1. Materials and Chemicals

PLGA polymers of different terminal groups (i.e., acid or ester), lactide:glycolide monomer ratios (i.e., 50:50 and 75:25), and polymer molecular weight (i.e., PLGA inherent viscosity of 0.15-0.25 and 0.55-0.75 dl/g in hexafluoroisopropanol) were purchased from Absorbable Polymers International (Pelham, AL, USA). Docetaxel was purchased from LC laboratories (Woburn, MA, USA). All reagents were analytical grade or above and used as received, unless otherwise stated.

### 3.2. Experimental Factorial Design for Preparation of Docetaxel-loaded PLGA Nanoparticles

#### 3.2.1. Taguchi Experimental Factorial Design

A L16 Taguchi robust design was used to prepare, optimize, and evaluate the effect of different factors on important characteristics of docetaxel-loaded PLGA nanoparticles. Table 3-1 exhibits six factors and their corresponding levels. Two factors—initial drug concentration and organic/aqueous phase ratio—were evaluated at four levels, while polymer molecular weight, polymer terminus, L:G monomer ratio, and PVA concentration were evaluated at two levels. To examine the factors under investigation, 16 combinations of factor and levels were used based on the Taguchi array (table 3-2). To reach the precision required for the ultimate statistical conclusion, all experimental runs were replicated three times.

Table 3-1: Variables (Factors) with their corresponding values and trial levels in the Taguchi experimental design used in the fabrication of docetaxel-loaded PLGA nanoparticles through an emulsification solvent evaporation technique.

| | | **Level** | | | |
|---|---|---|---|---|---|
| **Code** | **Factor** | **1** | **2** | **3** | **4** |
| **A** | Drug Concentration (mg/ml) | 0.25 | 0.5 | 1 | 1.5 |
| **B** | Organic/Aqueous phase ratio | 1:2 | 1:3 | 1:4 | 1:5 |
| **C** | Polymer Molecular weight (dl/g) | 0.15 - 0.25 | 0.55-0.75 | | |
| **D** | Polymer Terminus | Acid | Ester | | |
| **E** | Lactide:Glycolide Ratio | 50:50 | 75:25 | | |
| **F** | PVA Concentration | 2.2% | 9% | | |

Table 3-2. Combination of different factors/levels of Taguchi design studied to prepare the docetaxel-loaded PLGA nanoparticles [L16(4**2 2**4) Array].

| Run # | Drug Conc. (A) | Org./Aq. Ratio (B) | Polymer Mw (C) | Terminus (D) | L:G (E) | PVA Conc. (F) |
|---|---|---|---|---|---|---|
| **1** | 0.25 | 1:2 | 0.15 - 0.25 | Acid | 50:50 | 2.2% |
| **2** | 0.25 | 1:3 | 0.15 - 0.25 | Acid | 50:50 | 9% |
| **3** | 0.25 | 1:4 | 0.55-0.75 | Ester | 75:25 | 2.2% |
| **4** | 0.25 | 1:5 | 0.55-0.75 | Ester | 75:25 | 9% |
| **5** | 0.5 | 1:2 | 0.15 - 0.25 | Ester | 75:25 | 2.2% |
| **6** | 0.5 | 1:3 | 0.15 - 0.25 | Ester | 75:25 | 9% |
| **7** | 0.5 | 1:4 | 0.55-0.75 | Acid | 50:50 | 2.2% |
| **8** | 0.5 | 1:5 | 0.55-0.75 | Acid | 50:50 | 9% |
| **9** | 1 | 1:2 | 0.55-0.75 | Acid | 75:25 | 9% |
| **10** | 1 | 1:3 | 0.55-0.75 | Acid | 75:25 | 2.2% |
| **11** | 1 | 1:4 | 0.15 - 0.25 | Ester | 50:50 | 9% |
| **12** | 1 | 1:5 | 0.15 - 0.25 | Ester | 50:50 | 2.2% |
| **13** | 1.5 | 1:2 | 0.55-0.75 | Ester | 50:50 | 9% |
| **14** | 1.5 | 1:3 | 0.55-0.75 | Ester | 50:50 | 2.2% |
| **15** | 1.5 | 1:4 | 0.15 - 0.25 | Acid | 75:25 | 9% |
| **16** | 1.5 | 1:5 | 0.15 - 0.25 | Acid | 75:25 | 2.2% |

### 3.2.2. PLGA Nanoparticle Preparation For Experimental Design

Drug-loaded nanoparticles were prepared using a modified emulsification solvent evaporation technique as established in our lab. Briefly, PLGA polymer and docetaxel were dissolved in ethyl acetate to give a solution of 10% (w/v) PLGA and either 0.25, 0.5, 1, or 1.5 mg/ml docetaxel, which was then added to a PVA solution of 2.2 or 9 % (w/v) concentration at 1:2, 1:3, 1:4, or 1:5 organic:aqueous phase ratios. The mixture was then subjected to

sonication followed by evaporation. Nanoparticles were ultimately obtained after consecutive washing steps. The freeze-dried nanoparticles were then kept at -20 °C for further use.

### 3.2.3. PLGA Nanoparticle Characterization

#### 3.2.3.1. Determination of Average Size and Zeta Potential

Nanoparticles' mean diameter/size distribution profiles, polydispersity index (PDI) and zeta potential characteristics were measured using a Malvern Zetasizer (Nano-series, Nano ZS, model ZEN3600, Malvern Instruments, Worcestershire, UK). The nanoparticles (at least three replicates) were suspended in water prior to the measurements at 25°C.

#### 3.2.3.2. Determination of Nanoparticle Drug Loading and Encapsulation Efficiency

Embedded docetaxel in PLGA nanoparticles was extracted twice with acetone as follows. Acetone was added to drug-loaded PLGA (0.5 % w/v) nanoparticles to dissolve both the polymer and the drug. The mixture was centrifuged. These steps were repeated twice. Obtained supernatants were mixed and evaporated. Methanol was added to the residue to precipitate the polymer. Docetaxel was then quantified in supernatant using the tandem mass spectrometry method.

Drug loading of nanoparticles and encapsulation efficiency of the preparation method were calculated as follows:

**Equation 3-1:** Drug loading (%) = (weight of drug in particles/weight of particles) ×100

**Equation 3-2:** Encapsulation efficiency (%) = (weight of drug in particles/initial weight of drug added) ×100

### 3.2.4. Experimental Design Data Analysis

The experimental design was used to develop models as means to define the factor(s) in the preparation procedure that significantly affect different characteristics of the obtained nanoparticle formulation. The statistical analysis of the results was performed with MINITAB® statistical software, version 16 (Minitab, State College, PA, USA). The qualities of the fitted models were examined by the coefficient of determination ($R^2$). The data were analysed by analysis of variance (ANOVA) combined with the F test to evaluate whether a given term had a significant effect on the particle characteristic of interest. A *p-value* of <0.05 was considered statistically significant, unless otherwise stated. Particle characteristics included in the analysis comprised of particle size, zeta potential, poly dispersity index, and drug-loading efficiency of the method. A model was fitted for each particle characteristic, and based on ANOVA and F test, factors with statistically significant contributions (*p-value* of <0.05) to the characteristic of interest were determined. Then, based on final models, surface-response graphs were plotted between the particle characteristic of interest (size, zeta potential, poly dispersity index, and drug-loading efficiency), the significant factor, and other factors.

## 3.3. Optimized PLGA Nanoparticle Formulation

Response optimization was applied to identify the combination of nanoparticle preparation factors/levels that jointly optimize nanoparticle characteristics of interest. Response optimization was done for nanoparticle size, zeta potential, PDI, and drug-loading efficiency. Based on the data obtained from the experimental design and response optimization analysis, the below preparation conditions were the optimized fabrication technique for nanoparticle preparation:

**Docetaxel Concentration:** Level 4 (1.5 mg/ml)

**Organic/Aqueous phase ratio:** Level 2 (1:3)

**PLGA Molecular weight:** Level 1 (0.15 - 0.25 dl/g)

**PLGA polymer Terminus:** Level 1 (Acid terminated)

**Polymer lactide/glycolide ratio:** Level 1 (50:50)

**PVA Concentration:** Level 1 (2.2%)

# CHAPTER 4

## Experimental Section on Preparation and Characterization of Optimized PLGA and PLGA-PEG Nanoparticle Formulation

### 4.1. Materials and Chemicals

PLGA polymer with an acid terminal group (COOH), a lactide:glycolide monomer ratio of 50:50, and a low molecular weight (inherent viscosity 0.15-0.25 dl/g in hexafluoroisopropanol) was purchased from Absorbable Polymers International (Pelham, AL, USA). Docetaxel was purchased from LC laboratories (Woburn, MA, USA). PLGA-PEG di-block co-polymer (50:50 PLGA attached to mPEG 5000, 15% wt) was purchased from Evonik Degussa Corp. (Birmingham, AL, USA). All reagents were analytical grade or above and used as received, unless otherwise stated.

### 4.2. Formulation Development of Nanoparticles

The optimized formulation of docetaxel-loaded PLGA nanoparticles was prepared using an emulsification solvent evaporation technique. Briefly, PLGA polymer (10 % w/v) and docetaxel (1.5 mg) were dissolved in ethyl acetate, and added to a 2.2% (w/v) PVA solution (1:3 organic: aqueous phase ratio) to obtain the optimized nanoparticle formulation. The mixture was subjected to high-energy ultrasonication and evaporation. Then the nanoparticles were washed repeatedly to remove the free drug and other materials. The nanoparticles were finally re-suspended in a 1% (w/v) sucrose aqueous solution and freeze-dried. The freeze-dried nanoparticles were then kept at -20°C. To create PLGA nanoparticle formulations with different drug loadings, the optimized preparation method was applied to prepare PLGA nanoparticles with three different docetaxel amounts: 0.25, 0.5, and 1 mg.

Plain PLGA nanoparticles were also fabricated following the same procedure without adding the drug to the organic phase.

Surface-modified docetaxel-loaded PLGA nanoparticles were prepared using PLGA-PEG to obtain PEGylated PLGA nanoparticles (below).

Plain PLGA-PEG nanoparticles and docetaxel-loaded PLGA-PEG nanoparticles were prepared using the same emulsification solvent evaporation technique used to fabricate un-modified PLGA nanoparticles. Briefly, PLGA-PEG di-block co-polymer (10 % w/v) alone or along with docetaxel (1.5 mg) was dissolved in ethyl acetate, and added to a 2.2% (w/v) PVA solution (1:3 organic: aqueous phase ratio) to obtain drug-loaded PEGylated PLGA nanoparticle or drug-free PEGylated PLGA nanoparticle formulations. The mixture was subjected to high-energy ultrasonication and evaporation. Then nanoparticles were repeatedly washed to remove the free drug and other materials. Obtained nanoparticles were finally re-suspended in a 1% (w/v) sucrose aqueous solution and freeze-dried. The freeze-dried nanoparticles were then kept at -20°C. Again, to have PEGylated nanoparticle formulations with different drug loadings, the optimized preparation method was applied to prepare PLGA-PEG nanoparticles with three different docetaxel amounts: 0.25, 0.5, and 1 mg.

### 4.3. Freeze-Drying of Nanoparticles and Cryoprotection

The effectiveness of three cryoprotective agents during the freeze-drying process was determined. After the nanoparticles were prepared, aliquots of nanoparticle suspension (20 mg/ml) were dispensed into glass vials and enough cryoprotectant was added to obtain trehalose and sucrose concentrations of 1, 3, 5 and 10% (w/v) and PVA concentrations of 0.25, 0.5, 1, or 2% (w/v). Samples were then kept at -80°C for 30 minutes and subjected to a freeze-drying procedure at temperature of -84°C and a pressure of 0.12 mBar for 2 days (FreeZone Plus 6 Liter Cascade Freeze Dry System, Labconco Co., Kansas City, MO, USA)

using independent samples from each concentration (n=3). Similar aliquots of nanoparticles were also freeze-dried without using any cryoprotectant to be considered as reference samples. Samples were reconstituted with water, left for five minutes to ensure enough wetting, and then vortexed and subjected to sonication. The reconstituted nanoparticles were evaluated in terms of their average size, polydispersity index (PDI), and zeta potential. The equation below was used to determine the cryoprotective agent's effectiveness in preserving average nanoparticle size:

**Equation 4-1:** $R = (Sf) / (Si)$

Where Sf and Si are the average size of nanoparticles after and before freeze-drying, respectively.

## 4.4. Characterization of Nanoparticle Formulations

### 4.4.1. Determination of Average Size and Zeta Potential

Nanoparticles' mean diameter/size distribution profiles, polydispersity index (PDI) and zeta potential were measured using a Malvern Zetasizer (Nano-series, Nano ZS, model ZEN3600, Malvern Instruments, Worcestershire, UK). At least three replicates of nanoparticles were suspended in water prior to the measurements at 25°C.

### 4.4.2. Determination of Drug Loading and Encapsulation Efficiency

Loaded docetaxel in PEGylated PLGA nanoparticle formulations and un-modified PLGA nanoparticle formulations was determined using a double extraction method with acetone as follows. Acetone was added to drug-loaded nanoparticles (0.5 % w/v) to dissolve both the polymer and the drug. The mixture was centrifuged. These steps were repeated twice. The obtained supernatants were mixed and evaporated. Methanol was added to the

residue to precipitate the polymer. Docetaxel was then quantified in supernatant using the tandem mass spectrometry method.

The yield of the preparation method, drug loading, and encapsulation efficiency of nanoparticles were calculated as follows:

**Equation 4-2:** Yield (%) = (weight of obtained particles/initial weight of polymer and drug added) ×100

**Equation 4-3:** Drug loading (%) = (weight of drug in particles/weight of particles) ×100

**Equation 4-4:** Encapsulation efficiency (%) = (weight of drug in particles/initial weight of drug added) ×100

### 4.4.3. Docetaxel Release profile from Nanoparticle Formulations

To evaluate the rate and pattern of release of docetaxel from PLGA and PEGylated PLGA nanoparticles, *in vitro* drug release tests were performed as described below. Drug-loaded nanoparticles from either PLGA or PEGylated PLGA nanoparticle formulation at the different concentrations (0.25, 0.5, 1, and 1.5 mg/ml) were re-suspended in phosphate-buffered saline (PBS) (0.5 % w/v) and placed at 37 °C in a shaker-incubator (n=3). At designated time-points (1h, 6h, 12h, followed by 1, 2, 3, 4, 5, 6, 7, 8, 9, 10 days for the PLGA nanoparticle formulation, and 1h, 6h, 12h, followed by 1, 2, 3, 4, 5 days for the PEGylated PLGA nanoparticle formulation), samples were collected and fresh PBS was added in the original tube for further incubation. The supernatant was then freeze-dried and the drug was extracted twice from the lyophilized powder using acetone. The acetone extract was then evaporated. Methanol was added to the residue to dissolve the drug. Samples were then centrifuged and the supernatant was subjected to quantitative analysis by mass spectrometer.

## 4.5. Determination of Cytotoxicity of Docetaxel Loaded in Nanoparticles

### 4.5.1. Cell Culture

Hela cell (American Type Culture Collection, Manassas, VA, USA) lines were cultivated in high glucose Dulbecco's modified Eagle's medium (DMEM) culture media supplemented with 10% fetal bovine serum (FBS) and 1% antibiotic (100 unit/ml penicillin, 100 µg/ml streptomycin, and 0.25 µg/ml amphotericin B) at 37°C in a humidified incubator with 5% CO2. The cells were maintained in an exponential growth phase by periodic sub-cultivation.

### 4.5.2. MTT Assay

Hela cells were seeded into 96-well plates at a density of 5000 per well and incubated for 24 hours (humidified 37°C, and 5% CO2). Then, the growth medium was removed from the wells and replaced with 90 µl of fresh medium. Cells were then treated with 10 µl of the following:

1. Free drug solution in culture media at 4, 2, 1, 0.5, and 0.25 µg/ml docetaxel concentrations.
2. PLGA or PEGylated PLGA nanoparticle suspension in phosphate buffer (pH= 7.4) with equivalent docetaxel concentrations of 4, 2, 1, 0.5, and 0.25 µg/ml.
3. Plain PLGA or PEGylated PLGA nanoparticle suspension (control)

Blank wells were also included in the assay to exclude the potential absorbance of culture media and PLGA or PEGylated PLGA nanoparticles. Blank samples were as follows:

1. Wells with culture media without cells.

2. Wells with culture media without cells treated with plain PLGA or PEGylated PLGA nanoparticle suspension.

After cell treatment, plates were incubated for 6, 12, 24, and 48 hours. The percentage of cell viability was assayed by the number of surviving cells after incubation. At each time-point, medium in each well was replaced with 100 µl fresh medium containing 10 µl CellTiter 96® AQueous One Solution Cell Proliferation Assay Reagent (Promega, WI, USA). The compound in the reagent was bio-converted by cells into a coloured product. After incubating the plate for one to four hours, absorbance at each well was measured at 490 nm using a 96-well plate reader. Cell viability was calculated using the following equation:
Cell viability (%) = (Absorbance of treated cells/ Absorbance of untreated cells) × 100

# CHAPTER 5

## Experimental Section on Mass spectrometry Method for Quantification of Docetaxel

### 5.1. Materials and Chemicals

PLGA polymer with acid terminal group (COOH), lactide:glycolide monomer ratio of 50:50, and low molecular weight (inherent viscosity 0.15-0.25 dl/g in hexafluoroisopropanol) was purchased from Absorbable Polymers International (Pelham, AL, USA). Docetaxel was purchased from LC laboratories (Woburn, MA, USA). PLGA-PEG di-block co-polymer (50:50 PLGA attached to mPEG 5000, 15% wt) was purchased from Evonik Degussa Corp. (Birmingham, AL, USA). All reagents were analytical grade or above and used as received, unless otherwise stated.

Mouse serum was purchased from Biocell Laboratories (Rancho Dominguez, CA, USA). Mouse organs, including livers, hearts, lungs, and kidneys were collected from cull mice provided by the Lab Animal Services Unit (LASU) of Health Sciences Building, at the University of Saskatchewan. Mouse serum and organs were used to develop and validate the analytical method. All animals were treated humanely and euthanized according to the protocols approved by the University of Saskatchewan's Animal Research Ethics Board and adhering to the Canadian Council on Animal Care guidelines for humane animal use.

### 5.2. Mass Spectrometry Method for the Quantitation of Docetaxel

Mass spectrometry was used to quantitatively determine the docetaxel present in samples throughout the study. Paclitaxel was used as the internal standard in all the experiments. The structures of both molecules are presented in figure 5-1.

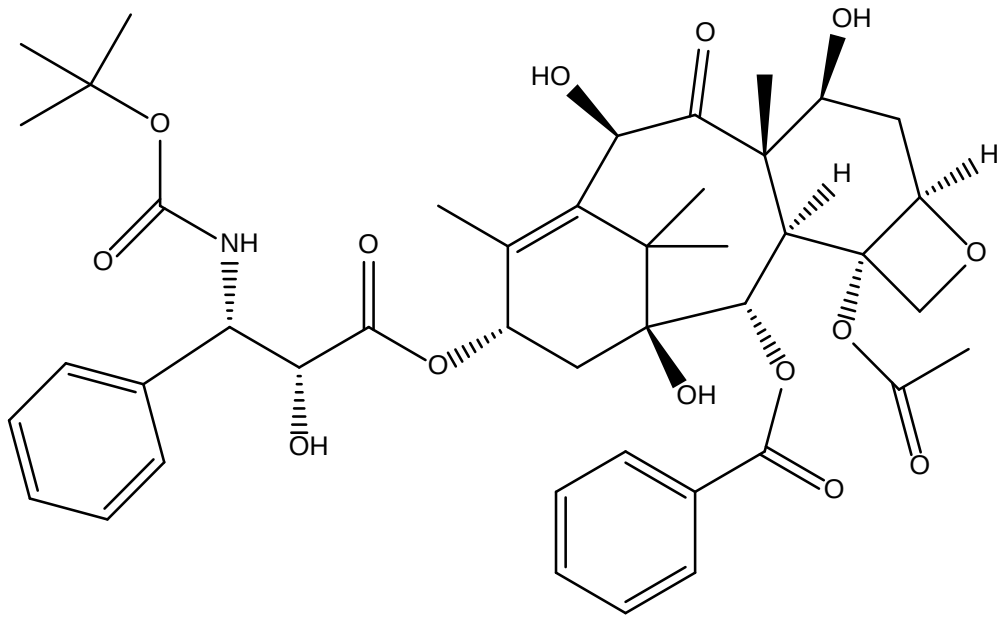


(A)

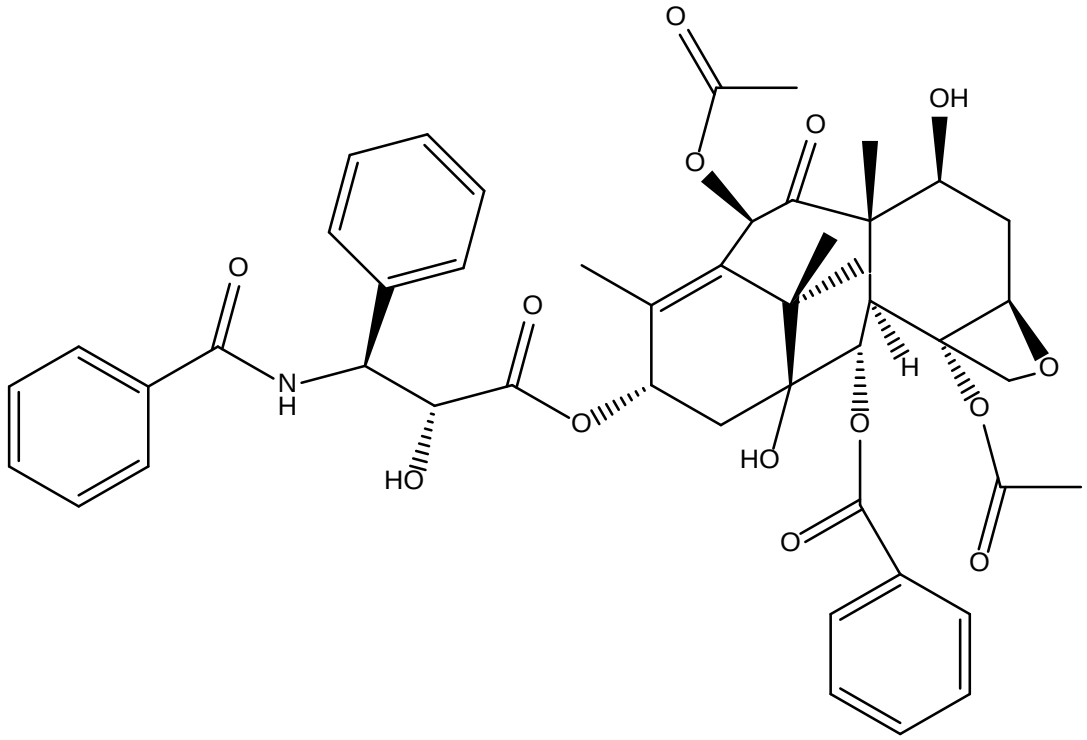


(B)

Figure 5-1: Molecular structure of docetaxel (A) and paclitaxel (B).

### 5.2.1. Determination of Docetaxel and Paclitaxel Fragmentation Patterns

Solution of docetaxel and paclitaxel (10 µg/mL in methanol containing 0.1% (v/v) formic acid) were prepared and directly infused into the ionization source using a model 11 Plus syringe pump (Harvard Apparatus, MA, USA) at a flow rate of 10 µL/min into a Hybrid Triple Quadrupole/Linear Ion trap mass spectrometer (AB Sciex 4000 QTRAP MS/MS system, Framingham, MA, US). The Turbo Ion-spray Source was set to 5500 volts. Curtain gas, nebulizer, and heater gas pressure were 30, 40, and 40 psi respectively. The de-clustering potential (DP) of docetaxel and paclitaxel was 46 and 55 volts respectively. The collision energy of docetaxel and paclitaxel was 21 and 93 respectively. Collision cell exit potential was 18 for both materials. Other instrument parameters were as follows: interface heater = ON (150°C), collisionally activated dissociation (CAD) = 5, and exit potential = 10. Product-ion scans (MS/MS) were performed using positive electrospray ionization (+ESI) with appropriate set mass (parent m/z).

According to the obtained pattern of docetaxel and paclitaxel fragmentation, two fragments of docetaxel (m/z = 226 and 528) were chosen to be used in Multiple Reaction Monitoring (MRM) transitions and docetaxel quantitation. Injection of the samples into the mass spectrometer was done using an Agilent Quaternary pump (1200 series) and Agilent G1329A (1200 series) auto sampler (Santa Clara, CA, USA) through a pre-column guard (Eclipse XDB-Rapid resolution, C18, 2.1×30mm, 3.5µ, Agilent, Santa Clara, CA, USA) with a mobile phase flow rate of 200 µl/min (Methanol, 0.1 % formic acid, isocractic elution). The quantitation procedure was performed on corresponding docetaxel and paclitaxel MRM graphs using Analyst software version 1.6.

### 5.2.2. Partial Analysis Validation Tests for Docetaxel in Non-biological Matrices

To determine the reliability and suitability of the method of analysis for docetaxel in PLGA and PLGA-PEG nanoparticles, partial analysis validation tests were carried out as follows.

#### 5.2.2.1. Sample Preparation

A stock solution of 100 µg/ml docetaxel was prepared by dissolving the drug in methanol and stored at -20°C for further use. Working solution concentrations of 3.9, 7.8, 15.6, 31.2, 62.5, 125, 250, 500, 1000, 2000, 4000, 8000, and 16000 ng/ml were prepared by further diluting the stock solution with methanol. A stock solution of paclitaxel in methanol as the internal standard was also prepared at 100µg/ml.

#### 5.2.2.2. Preparation of Standard and Control Samples

To prepare polymer-free standards (docetaxel in methanol), the internal standard and the working solution (3.9-1000 ng/ml) were transferred into tubes. Polymer-free controls were prepared as such to obtain 100, 200, 400, and 800 ng/ml docetaxel concentrations. To prepare standard samples of nanoparticle formulations, the internal standard and the working solution (125-8000 ng/ml and 125-16000 ng/ml for PLGA-PEG and PLGA nanoparticles, respectively) were transferred into tubes. The solvent was then evaporated and drug-free nanoparticles (0.5 % w/v) were added to the tube. A concentration set of 1250, 2500, 5000, and 10000 ng/ml was used to prepare quality-control samples of PLGA nanoparticles and a concentration set of 625, 1250, 2500, and 5000 ng/ml was used to prepare quality-control samples of PLGA-PEG nanoparticles. Paclitaxel was added to the control samples of PLGA and PLGA-PEG nanoparticles. The solvent was evaporated and drug-free nanoparticles (0.5

% w/v) were added to the tube. Standard and control samples of PLGA and PLGA-PEG nanoparticles were extracted twice with acetone.

#### 5.2.2.3. Docetaxel Extraction Method from Nanoparticles

Docetaxel was extracted from PLGA and PLGA-PEG nanoparticles as follows. Acetone was added to drug-loaded nanoparticles (0.5 % w/v) to dissolve both the polymer and the drug. The mixture was centrifuged and the procedure was repeated. Obtained supernatants were mixed and evaporated. Methanol was added to the residue and centrifuged. Docetaxel was then quantified in supernatant using mass spectrometry.

#### 5.2.2.4. Determination of Limits of Detection and Quantitation

The limit of detection (LOD) of docetaxel in methanol, PLGA nanoparticles, and PLGA-PEG nanoparticles were measured based on a signal-to-noise ratio of 3:1. The limit of quantitation (LOQ) of the method for the mentioned nanoparticle matrices were measured based on a signal-to-noise ratio of 10:1 with acceptable precision and accuracy (within ±20% of the nominal value).

#### 5.2.2.5. Linearity

Standard samples of docetaxel in methanol (3.9-1000 ng/ml), PLGA nanoparticles (125-16000 ng/ml), and PLGA-PEG nanoparticles (125-8000 ng/ml) were prepared as described previously, extracted, and subjected to mass spectrometer for analysis. Linear regression analysis was carried out on known added concentrations of docetaxel (weighted 1/x) against the peak area ratio of docetaxel to paclitaxel. Then, the regression coefficient ($R^2$), slope, intercept, and equation of the resulting standard curves were determined.

#### 5.2.2.6. Method Precision

Quality control samples—limit of quantitation (LOQ), low quality control (LQC), middle quality control (MQC), and high quality control (HQC)—were prepared for the samples of docetaxel in methanol, PLGA nanoparticles, and PLGA-PEG nanoparticles as described and injected into the mass spectrometer (n=6). The coefficient of variations of the corresponding concentrations were determined in each case.

#### 5.2.2.7. Method Accuracy

Quality control samples were prepared for samples of docetaxel in methanol, PLGA nanoparticles, and PLGA-PEG nanoparticles as described and subjected to mass spectrometer analysis (n=6). The method's accuracy was determined as the difference between the measured concentration (based on the standard curve) and the nominal concentration divided by corresponding added (nominal) concentration multiplied by 100.

### 5.2.3. Partial Analysis Validation Tests for Docetaxel in Mouse Tissue

To determine the reliability and suitability of the method of analysis for docetaxel in mouse tissues, partial analysis validation tests were carried out as follows.

#### 5.2.3.1. Sample Preparation for Mouse Serum

A stock solution of 100 µg/ml docetaxel was prepared by dissolving the drug in methanol and kept in -20 °C for further use. A working solution of 2000 ng/ml was prepared by addition of 20 µl stock to 980 µl of mouse serum. A stock solution of paclitaxel in

methanol was also prepared at 100 µg/ml to be used as internal standard. A working solution of 10000 ng/ml paclitaxel in methanol was prepared.

#### 5.2.3.2. Preparation of Standard and Control Samples

A standard concentration set of 1000, 500, 250, 125, 62.5, 31.2, and 15.6 ng/ml and control concentrations of 100, 200, 400, and 800 ng/ml were prepared by further diluting the working solution with mouse serum.

#### 5.2.3.3. Technique for Extraction of Docetaxel from Mouse Serum

Docetaxel and paclitaxel were extracted from the mouse serum as follows. The paclitaxel working solution was added to the tube. The solvent was evaporated and mouse serum containing docetaxel was added to the tube. Then, tert-butyl methyl ether (TBME) was added at the ratio of 1:10. The mixture was centrifuged and transferred to a -80 °C freezer. The supernatant was then evaporated and residue was reconstituted with mobile phase (methanol containing 0.1% formic acid) and injected into the mass spectrometer for analysis.

#### 5.2.3.4. Sample Preparation for Mouse Liver

A stock solution of 100 µg/ml docetaxel was prepared by dissolving the drug in methanol and was kept at -20°C for further use. Working solutions of 5000, 2500, 1250, 625, 312,156, and 78 ng/ml were prepared by further diluting the stock solution with methanol. A stock solution of paclitaxel in methanol was also prepared at 100 µg/ml to be used as the internal standard.

#### 5.2.3.5. Preparation of Standard and Control Samples

Standard and control samples were prepared in mouse liver homogenizate that was obtained as follows. Liver was weighed and enough normal saline was added to it to obtain a 5% (w/v) mixture. The mixture was then homogenized on ice. A standard concentration set of 500, 250, 125, 62.5, 31.2, and 15.6 ng/ml was prepared by further diluting the working solution with liver homogenizate. Control working solutions were prepared in methanol (1000, 2000, and 4000 ng/ml) and used to prepare 100, 200, and 400 ng/ml control concentrations of liver homogenizate following the same approach.

#### 5.2.3.6. Technique for Extraction of Docetaxel from Mouse Liver

Docetaxel and paclitaxel were extracted from mouse liver as follows. Paclitaxel stock solution was added to a tube and the solvent was evaporated. Liver homogenizate containing docetaxel and TBME at 1:2 ratio were added to the tube. The sample was then centrifuged and transferred to a -80°C freezer. Samples were centrifuged again and the supernatant was separated and evaporated. Acetone was added to the residue, which was then transferred to a new tube and evaporated. The mobile phase (methanol containing 0.1% formic acid) was added to the residue. After centrifugation, the supernatant was injected into the mass spectrometer for analysis.

#### 5.2.3.7. Determination of Limits of Detection and Quantitation

Docetaxel's LOD and LOQ in mouse serum and liver were measured based on a signal-to-noise ratio of respectively 3:1 and 10:1 with acceptable precision and accuracy.

#### 5.2.3.8. Linearity

Standard samples of docetaxel in mouse serum (15.6-1000 ng/ml) and liver (15.6-500 ng/ml) were prepared as described previously, extracted, and injected into the mass spectrometer for analysis. Known concentrations of docetaxel were subjected to linear regression analysis (weighted 1/x) against the peak area ratio of docetaxel to paclitaxel. The $R^2$, slope, intercept, and equation of the resulting calibration curves were then determined.

#### 5.2.3.9. Method Precision

Quality control samples (LOQ, LQC, MQC, HQC) were prepared for samples of docetaxel in mouse serum and liver as described and injected into the mass spectrometer (n=6). The coefficients of variations of the corresponding concentrations were determined in each case.

#### 5.2.3.10. Method Accuracy

Quality control samples were prepared for samples of docetaxel in mouse serum and liver as described and injected into the mass spectrometer for analysis (n=6). The method's accuracy was determined as the difference between the measured concentration (based on the standard curve) and the nominal concentration divided by the corresponding added (nominal) concentration multiplied by 100.

#### 5.2.3.11. Extraction of Docetaxel from Mouse Kidney, Heart, and Lung

The drug extraction technique from mouse liver mentioned above was also used for other mouse kidney, heart, and lung tissues. The method's extraction efficacy and linearity were evaluated in these tissues. Extraction efficiency was calculated as follows:

Extraction Efficiency (%) = (Peak area ratio of docetaxel to paclitaxel from extracted samples/ peak area ratio of docetaxel to paclitaxel from spiked blank samples) × 100

# CHAPTER 6

## Experimental Section on Pharmacokinetics and Bio-distribution of Docetaxel

### 6.1.Animals

BALB/c mice were purchased from Charles River Laboratories (Saint Constant, QC, Canada). The animals were housed in the mouse suite located in Lab Animal Services Unit (LASU) in the Health Sciences Building at the University of Saskatchewan under controlled temperature and humidity with a 12-hour light-dark cycle. They were kept in the facility for a period of at least one week to acclimatize and had free access to water and standard laboratory mouse chow. All animals were treated humanely and euthanized according to the protocols approved by the University of Saskatchewan Animal Ethics Board.

### 6.2. Animal Experiments

Animal experiments were conducted using 8-week-old female BALB/c mice after a 7-day period acclimatization in the LASU. The 96 mice were randomly divided into three groups with free access to food and water. Each group received 5 mg/kg of docetaxel either in the form of the docetaxel-loaded PLGA nanoparticles, docetaxel-loaded PLGA-PEG nanoparticles or free-docetaxel solution. Docetaxel formulations were injected through the mouse tail vein (injection volume: 200µl, solvent: 0.9% sodium chloride). At various time-points (0.5, 1, 2, 4, 6, 12, 18, and 24 hour) after dosing, mice were anesthetized and sacrificed by exsanguination. The blood was collected and the lungs, heart, liver, and kidneys were harvested; these were preserved in plastic bags in the -20°C freezer for later docetaxel extraction and analysis. Each time-point was done in four replicates.

### 6.3. Bio-distribution and Pharmacokinetic Analysis

For bio-distribution studies, mouse organs were subjected to the extraction procedure (explained in chapter 5) and underwent mass spectrometric analysis to determine the concentration of docetaxel in each tissue. Then, the relationship between the docetaxel concentration and time was determined by plotting corresponding graphs. Pharmacokinetic analysis was performed using the collected mouse serum at different time-points as follows. Briefly, the obtained blood was centrifuged and the serum was separated from the rest of the blood components and subjected to the extraction procedure and further analysis by the mass spectrometer. Using Graphpad prism software (version 5.04), a plot of docetaxel concentration versus time was prepared. A non-compartmental pharmacokinetic analysis method was used to determine the pharmacokinetic-important parameters in mouse serum and other organs. Then, results from each study group were compared. Pharmacokinetic parameters were calculated as follows:

1. **Elimination half-life ($T_{1/2}$):** Graphical relationship between docetaxel concentration at y axis and time at x axis was established. Docetaxel concentration at y axis was then transformed to a natural logarithm (Ln) to convert the data into a straight-line relationship. Then, data-points from the terminal elimination phase was used in a non-linear regression to plot a straight line ($Y = -K_eX + B$). Half-life was calculated as:

**Equation 6-1:** $$T_{1/2} = 0.693/ K_e$$

In which $K_e$ is the slope of the plotted line from the non-linear regression analysis.

2. **Concentration at time zero ($C_0$):** Residuals were calculated between the plotted line (above) and the data-points at the distribution phase. Using residuals data-points and regression analysis, a second line was plotted ($Y = -\alpha X + A$). $C_0$ was then calculated as:

**Equation 6-2:** $C_0 = A + B$

In which A and B are the intercepts from the residuals line and terminal elimination phase line, respectively.

3. **Area under the serum concentration versus time curve (AUC):** AUC from time zero ($C_0$) until 24 hours was calculated by software. AUC from t = 24 hours to infinity was calculated as:

**Equation 6-3:** $AUC_{(24\ to\ \infty)} = C_{24}/K_e$

Therefore, total AUC was calculated as:

**Equation 6-4:** $AUC_{(0\ to\ \infty)} = AUC_{(0\ to\ 24)} + AUC_{(24\ to\ \infty)}$

4. **Clearance (Cl) :** Docetaxel clearance was calculated as :

**Equation 6-5:** $Cl = Dose/\ AUC_{(0\ to\ \infty)}$

In which dose is the amount of docetaxel injected intravenously and $AUC_{(0\ to\ \infty)}$ is the area under the serum concentration versus time curve from time zero to infinity.

5. **Volume of Distribution ($V_d$)** : Volume of distribution was calculated as:

**Equation 6-6:** $V_d = (Dose)/\ (AUC_{(0\ to\ \infty)}) \times (K_e)$

6. **Area Under the Moment Curve (AUMC):** The product of concentration (including $C_0$) multiplied by time at each time point was calculated (i.e., concentration × time). Then, the graphical relationship between (docetaxel concentration × time) at y axis and time at x axis was established. AUMC from time zero until t = 24 hours was calculated by software. AUMC from 24 hours to infinity was calculated as:

**Equation 6-7:** $AUMC_{(24\ to\ \infty)} = [(C_{24} \times t_{24})/(K_e)] + [(C_{24})/(K_e^2)]$

Therefore, total AUMC was calculated as:

**Equation 6-8:** $AUMC_{(0\ to\ \infty)} = AUMC_{(0\ to24)} + AUMC_{(24\ to\ \infty)}$

7. **Mean Residence Time (MRT)** : The mean residence time of docetaxel was calculated as:

**Equation 6-9:** $$MRT = AUMC_{(0 \text{ to } \infty)} / AUC_{(0 \text{ to } \infty)}$$

# CHAPTER 7*

## Result and Discussion on Taguchi Design for Formulation and Optimization of Docetaxel-loaded PLGA Nanoparticles

***** Chapter 3 (Experimental Section on Taguchi Design for Formulation and Optimization of Docetaxel-loaded PLGA Nanoparticles) along with chapter 7 was submitted as an 'Original Research Article' to '*Artificial Cells, Nanomedicine and Biotechnology: An International Journal*' for publication:

Pedram Rafiei, Azita Haddadi. Taguchi Design for the Preparation and Optimization of Docetaxel-loaded PLGA Nanoparticles for Intravenous Drug Delivery Purpose. *Artificial Cells, Nanomedicine and Biotechnology: An International Journal,* submitted May 2017.

### Background

PLGA polymer has a variable nature. Depending on the number of monomers present in polymer chain, it can assume different molecular weights. The ratio of monomers (lactide and glycolide) in a PLGA chain can vary and provide polymers with different L:G ratios. In addition, PLGA polymer can assume ester or carboxylic acid terminal groups. Therefore, PLGA can possess different physicochemical properties based on its polymeric structure. PLGA nanoparticles are used to deliver different drugs in terms of physicochemical and pharmacological properties.

Therefore, PLGA nanoparticles prepared for the delivery of various compounds can assume different properties depending on

i) The type of PLGA polymer used for nanoparticle preparation,

ii) The method used for nanoparticle preparation, and

iii) The type of drug/compound associated with nanoparticles.

PLGA nanoparticle properties determine nanoparticles' performance when used as drug delivery systems. Therefore, it is crucial to understand how PLGA polymer, the nanoparticle preparation method, and the associated drug contribute to nanoparticles' properties. This knowledge is important because it provides control over nanoparticle properties and over PLGA nanoparticles' performance as drug delivery systems. This knowledge of how PLGA polymer, the nanoparticle preparation method, and the associated drug contribute to nanoparticles' properties is usually obtained by performing factorial experiments.

Factorial experiments are used to understand the effect of independent variables (factors) on a dependent variable (response). The conventional approach to determine the effect of variables on a process, like the development of a drug formulation, has been to evaluate the effect of one variable while keeping the others constant to see if the variable significantly affects the process. Such approaches are usually strenuous and uneconomical, especially if the process is performed in replicates [276, 277]. Meanwhile, a much simpler screening of experimental parameters has been made possible through the application of experimental factorial designs with a reduced number of experiments (i.e., a fraction of the full factorial combinations) to draw out valuable conclusions and establish a relationship between the process variables and the outcome of interest [278]. The Taguchi method has been widely used to analyze many factors with few runs: equally weighted factors are analyzed independently of one another to offer a balanced design [279]. In addition, the estimation of one factor is not influenced by the effect from another factor.

Here, the experimental design based on the Taguchi robust method was used to optimize PLGA nanoparticles loaded with docetaxel and an optimized method was identified. The optimized docetaxel-loaded PLGA nanoparticle formulation was further subjected to *in vitro* characterization and used for pharmacokinetic and biodistribution studies. The L16

Taguchi design used here contributed to the identification of factors that could significantly influence nanoparticle-important characteristics including average size, PDI, zeta potential, and drug-loading efficiency. The design was helpful in ranking factors based on their level of effectiveness on various particle characteristics under study. Furthermore, analysis of the data from the experimental design helped build models that were statistically significant with good robustness. Generally, built models help predict particle characteristics from a combination of factors and various levels.

### 7.1. L16(4**2 2**4) Experimental Design

Table 7-1 demonstrates the combination of sixteen different factors and their corresponding levels based on the L16 Taguchi design. Runs were done in triplicate and the nanoparticles obtained from each run were characterized in terms of their size, PDI, zeta potential, and drug-loading efficiency. Then, statistical analysis was performed on each characteristic individually. Nanoparticles demonstrate average size between 93.5±6.9 nm and 191.4±21.1 nm. The range of zetapotential exhibited by nanoparticles was between -17.8±1.2 mV and -36.5±0.6 mV. Fabricated nanoparticles demonstrated a uni-distributed population having PDI values between 0.095±0.015 and 0.290±0.059. Nanoparticle preparation at 16 different combinations of factors/levels resulted in a range of drug-loading efficiency between 25.2±1.1 % and 96.2±4.0 %.

Table 7-1. Combination of different factor/levels of the Taguchi design studied in the preparation of the docetaxel-loaded PLGA nanoparticles [L16(4**2 2**4) Array] and the corresponding characteristics demonstrated by fabricated nanoparticles.

| Run # | Drug Conc. (A) | Org./Aq. Ratio (B) | Polymer Mw (C) | Terminus (D) | L:G (E) | PVA Conc. (F) | Particle Size (nm) | PDI | Zeta Potential (mV) | Entrapment (%) |
|---|---|---|---|---|---|---|---|---|---|---|
| **1** | 0.25 | 1:2 | 0.15 - 0.25 | Acid | 50:50 | 2.2% | 151.1±19.3 | 0.175±0.080 | -22.8±2.3 | 79.6±2.6 |
| **2** | 0.25 | 1:3 | 0.15 - 0.25 | Acid | 50:50 | 9% | 108.6±1.8 | 0.256±0.014 | -29.8±4.5 | 41.5±3.6 |
| **3** | 0.25 | 1:4 | 0.55-0.75 | Ester | 75:25 | 2.2% | 159.8±11.4 | 0.113±0.019 | -25.3±5.1 | 86.4±4.2 |
| **4** | 0.25 | 1:5 | 0.55-0.75 | Ester | 75:25 | 9% | 105.1±5.5 | 0.130±0.035 | -17.8±1.2 | 43.2±3.3 |
| **5** | 0.5 | 1:2 | 0.15 - 0.25 | Ester | 75:25 | 2.2% | 191.4±21.1 | 0.219±0.070 | -19.3±4.8 | 96.2±4.0 |
| **6** | 0.5 | 1:3 | 0.15 - 0.25 | Ester | 75:25 | 9% | 105.0±2.6 | 0.158±0.022 | -18.9±1.0 | 60.0±3.1 |
| **7** | 0.5 | 1:4 | 0.55-0.75 | Acid | 50:50 | 2.2% | 135.1±1.6 | 0.122±0.004 | -31.1±1.7 | 50.8±6.0 |
| **8** | 0.5 | 1:5 | 0.55-0.75 | Acid | 50:50 | 9% | 93.5±6.9 | 0.154±0.061 | -28.7±3.7 | 35.1±3.4 |
| **9** | 1 | 1:2 | 0.55-0.75 | Acid | 75:25 | 9% | 117.2±8.6 | 0.148±0.019 | -32.8±4.8 | 46.6±3.1 |
| **10** | 1 | 1:3 | 0.55-0.75 | Acid | 75:25 | 2.2% | 171.9±7.1 | 0.118±0.015 | -32.5±0.3 | 49.7±0.8 |
| **11** | 1 | 1:4 | 0.15 - 0.25 | Ester | 50:50 | 9% | 100.2±1.5 | 0.177±0.015 | -18.2±0.3 | 29.9±3.6 |
| **12** | 1 | 1:5 | 0.15 - 0.25 | Ester | 50:50 | 2.2% | 113.4±4.5 | 0.198±0.037 | -26.0±2.7 | 42.9±1.6 |
| **13** | 1.5 | 1:2 | 0.55-0.75 | Ester | 50:50 | 9% | 119.8±2.0 | 0.095±0.015 | -18.4±2.7 | 43.7±4.2 |
| **14** | 1.5 | 1:3 | 0.55-0.75 | Ester | 50:50 | 2.2% | 163.1±8.9 | 0.180±0.033 | -21.1±3.6 | 41.4±4.1 |
| **15** | 1.5 | 1:4 | 0.15 - 0.25 | Acid | 75:25 | 9% | 104.0±8.1 | 0.290±0.059 | -29.8±1.7 | 25.2±1.1 |
| **16** | 1.5 | 1:5 | 0.15 - 0.25 | Acid | 75:25 | 2.2% | 118.4±2.2 | 0.243±0.022 | -36.5±0.6 | 37.8±1.6 |

### 7.1.1. Particle Size

Figure 7-1 demonstrates the main effect plot for the means of particle size due to factors under study at different levels. The difference between the maximum and minimum mean particle sizes is highest in the case of PVA concentration (43.8 nm) followed by organic:aqueous phase ratio (37.3 nm), lactide:glycolide ratio (11.0 nm), polymer Mw (9.2 nm), polymer terminus (7.3 nm), and drug concentration (5.6 nm). The rankings of factors affecting the response (particle size) are exhibited in table 7-2 based on the mean particle size range variation. PVA concentration had the largest effect on particle size, followed by organic:aqueous phase ratio, lactide:glycolide ratio, polymer Mw, polymer terminus, and drug concentration. Figure 7-2 demonstrates the mean of signal/noise ratio (S/N) corresponding to each factor at various levels. S/N was calculated by the software using equation below:

**Equation 7-1:** $S/N = -10*\log(\Sigma(1/Y^2)/n)$

Where Y is responses for the given factor level combination and n is number of responses in the factor level combination.

The magnitude of range between maximum and minimum S/N identifies the factor that leads to most reduced variability. The larger S/N range is preferred to have less variation in response. Accordingly, PVA has the largest S/N range (2.87) followed by organic:aqueous phase ratio (2.39), polymer Mw (0.66), lactide:glycolide ratio (0.64), polymer terminus (0.42), and drug concentration (0.37). Figure 7-3 represents the normal probability plots of residuals for particle size. It demonstrates the normality of particles size variation.

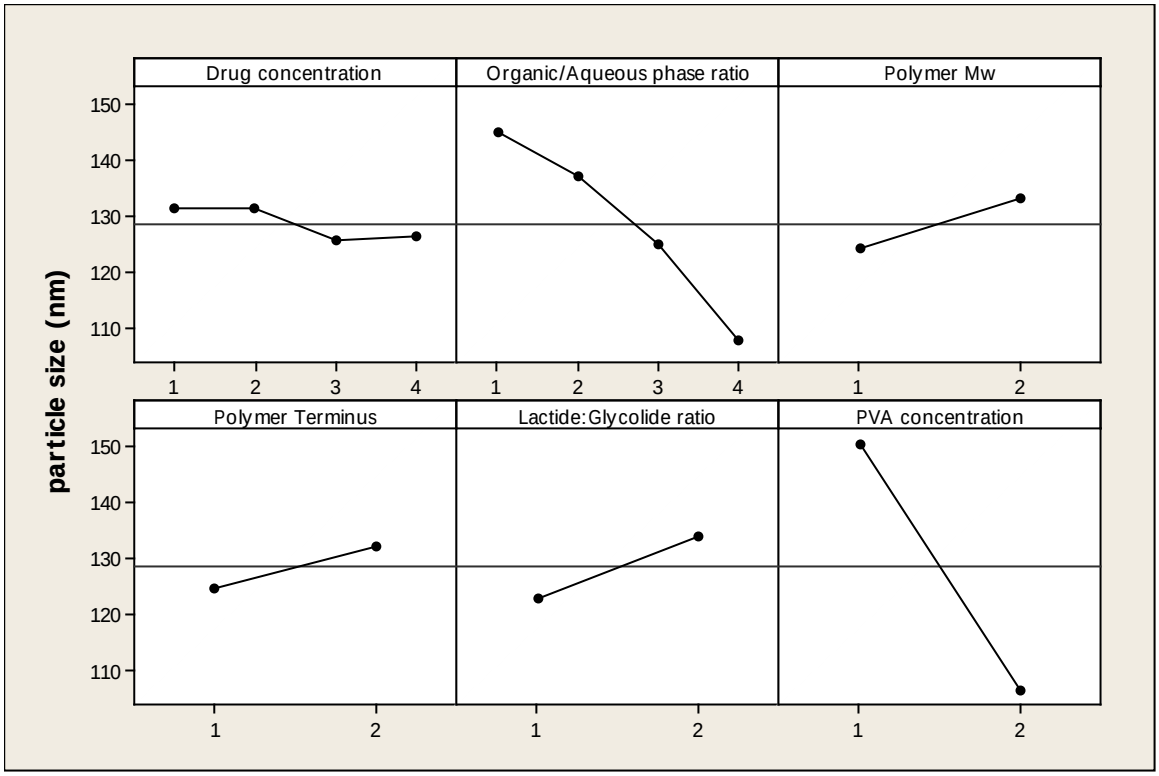


Figure 7-1. Main effect plot for particle size at different factor levels

Table 7-2. Ranking trend of factors affecting the particle size as the response of interest.

| | **Factors** | | | | | |
|---|---|---|---|---|---|---|
| | **Drug Conc.** | **Organic: Aqueous** | **Polymer Mw** | **Polymer Terminus** | **L:G** | **PVA Conc.** |
| **Rank** | 6 | 2 | 4 | 5 | 3 | **1** |

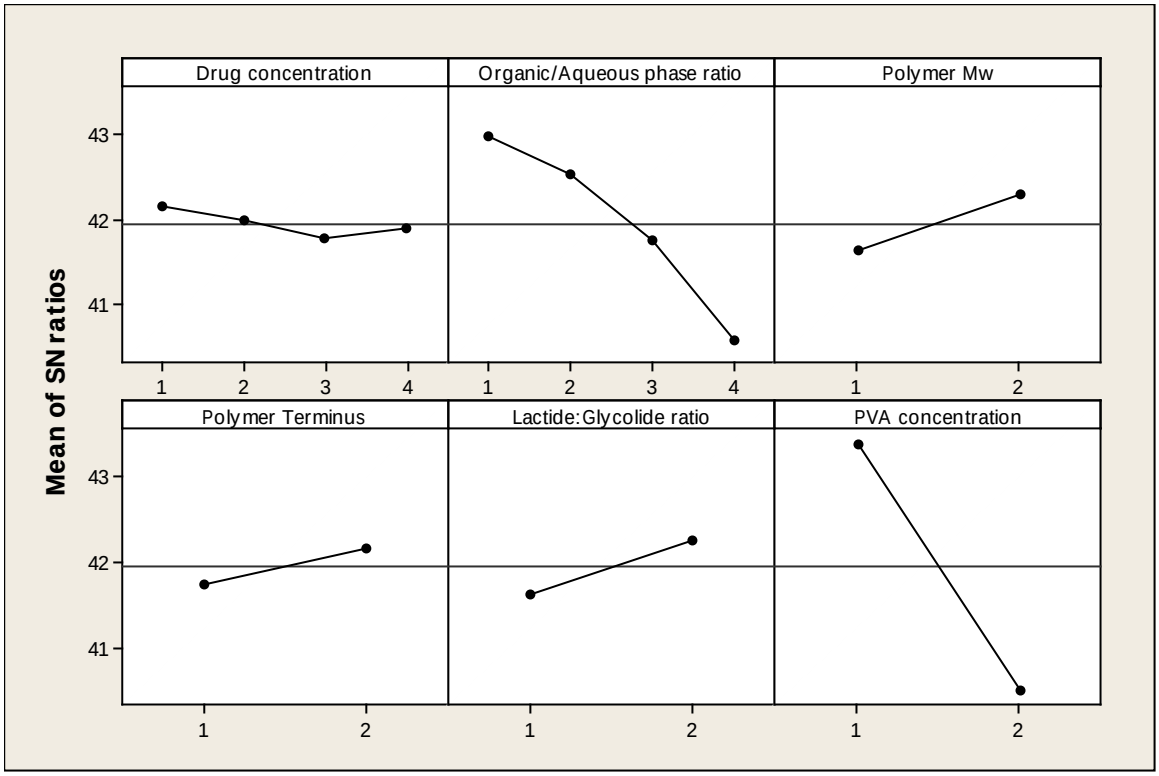


Figure 7-2. Main effect plot for S/N ratio at different factor levels

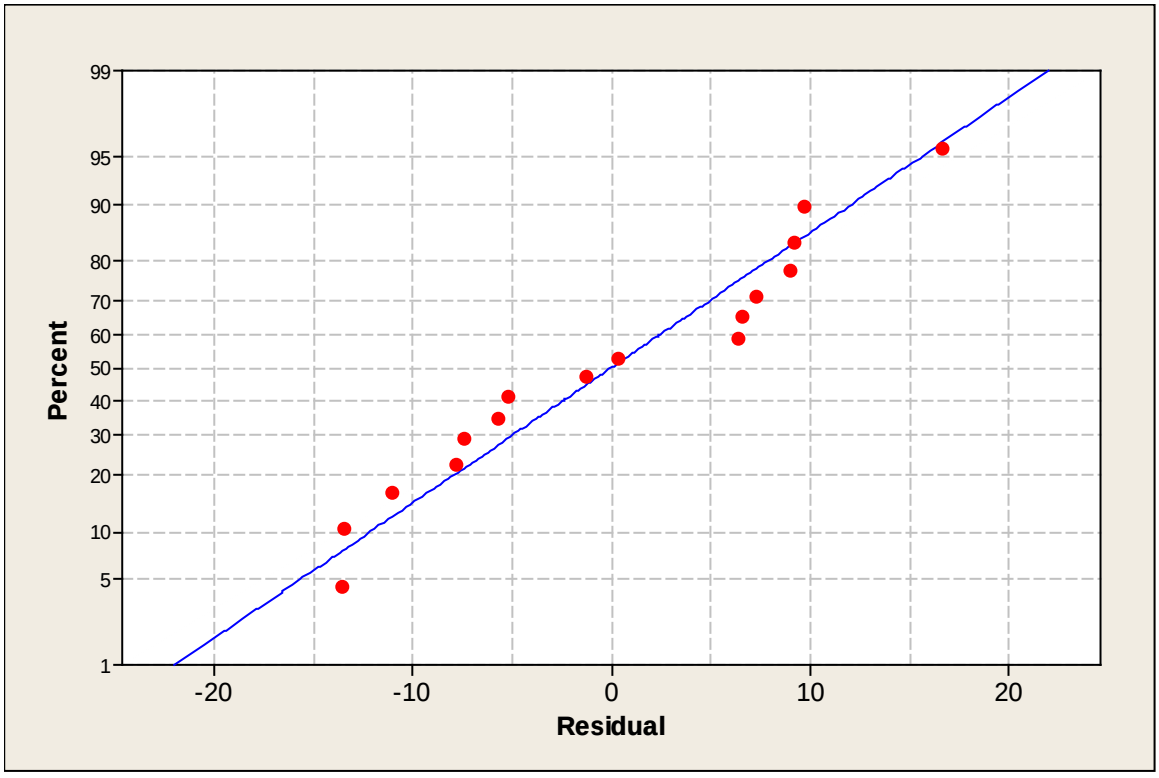


Figure 7-3. Normal probability plot of residuals by the final model for particle size

Linear regression analysis, ANOVA, and F tests were performed on the data to fit a model that best defined the variations in particle size versus the six factors under study. $R^2$ was equal to 0.899 while the regression equation was calculated to be:

**Equation 7-2: Particle Size = 189 - 2.01 (A) - 12.4 (B) + 9.18 (C) + 7.26 (D) + 11.0 (E) - 43.8 (F)**

Tables 7-3 and 7-4 respectively exhibit the result of ANOVA and regression analysis for the fitted model of particle size distribution. The model fitted for particles size explained variations in particle size with statistical significance ($p = 0.001$). Regression analysis determined that PVA concentration and organic:aqueous phase ratio significantly contributed to particles size ($p < 0.05$).

Table 7-3. ANOVA table for fitted model for particle size

| Source | Degree of Freedom | Sum of Squares | Mean Square | F | P |
|---|---|---|---|---|---|
| **Regression** | 6 | 11885.1 | 1980.9 | 13.33 | **0.001** |
| **Residual Error** | 9 | 1337.1 | 148.6 | | |
| **Total** | 15 | 13222.2 | | | |

Table 7-4. Regression analysis of particle size versus nanoparticle preparation variables

| Predictor | Coefficients | SE Coefficients | T | P |
|---|---|---|---|---|
| **Constant** | 189.30 | 20.89 | 9.06 | 0.000 |
| **Drug concentration (A)** | -2.008 | 2.725 | -0.74 | 0.480 |
| **Organic/Aqueous phase ratio (B)** | -12.413 | 2.725 | -4.55 | **0.001** |
| **Polymer Mw (C)** | 9.183 | 6.094 | 1.51 | 0.166 |
| **Polymer Terminus (D)** | 7.258 | 6.094 | 1.19 | 0.264 |
| **Lactide:Glycolide ratio (E)** | 10.992 | 6.094 | 1.80 | 0.105 |
| **PVA concentration (F)** | -43.850 | 6.094 | -7.20 | **0.000** |

To understand the relationship between the response of interest (i.e., particle size) and the factors that significantly affect that response (i.e., Organic/Aqueous phase ratio and PVA

concentration), response surface graphs were plotted and are presented in supplementary figure 1. The figure indicates that the maximum response (i.e., particle size) was obtained at low PVA concentration (level one) and 1:2 organic:aqueous phase ratio (level one) and vice versa.

As exhibited in figure 7-1, increasing the ratio of aqueous phase decreased particle size. Here, the amount of aqueous phase in the suspension played an important role in determining the final size of the nanoparticles. In samples with a high volume of aqueous phase, nano-droplets were distributed throughout a large volume of liquid and therefore had less chance of adhesion. The rate of organic solvent diffusion from nano-droplets to the surrounding aqueous medium and the final evaporation from nano-suspension also decreased particle size. In a nano-suspension with a large volume of aqueous phase, the rate of organic solvent diffusion from nano-droplet to the aqueous medium was higher [280-282]. Therefore, nano-droplets solidified faster and had less chance of adhesion. Consequently, nanoparticles retained their sizes. Our results agree with those of Murugesan and colleagues [195] who demonstrated that the amount of aqueous phase during nanoparticle preparation has an inverse relationship with nanoparticle size.

PVA concentration also had an inverse relationship with nanoparticle size. PVA, a non-ionic surfactant (spatial stabilizer), was stationed on the surface of nano-droplets during preparation, which prevented droplet adhesion and fusion. In case of high PVA concentrations, nano-droplets were surrounded with large numbers of PVA molecules, which stabilize the nano-droplets. This stability in turn resulted in fewer interactions between nano-droplets, so the overall particle size remained unchanged. The study by Murugesan et al. [195] also demonstrated that increasing the concentration of stabilizing agent reduces nanoparticle size.

The ratio of monomers (L:G) also affected the size of nanoparticles. As mentioned in chapter one, lactic acid is chemically more hydrophobic than glycolic acid. Consequently, the 50:50 (L:G) PLGA polymer was less hydrophobic than the 75:25 (L:G) PLGA polymer. Therefore, the organic phase prepared from 50:50 (L:G) PLGA had a lower hydrophobic integrity than the organic phase prepared from 75:25 (L:G) PLGA . During probe-sonication, organic phase droplets with lower hydrophobicity more easily broke into smaller droplets, which lowered nanoparticle average size. On the other hand, because of their lower hydrophobic integrity, the organic solvent escaped nano-droplets prepared from 50:50 (L:G) PLGA faster, which caused the nanoparticles to solidify more rapidly. This decreased the chance of droplet adhesion and fusion during the solvent evaporation period.

Increasing the polymer molecular weight also increased average particle size. The PLGA polymer with low molecular weight resulted in an organic phase with low viscosity. During probe-sonication, organic phase droplets with low viscosity broke into small droplets more easily than droplets with higher viscosity. Therefore, low molecular weight PLGA provided nanoparticles with a lower average size compared to high molecular weight PLGA. Koopaei and colleagues [283] demonstrated that organic phase with higher viscosity leads to nanoparticles with a higher average size, which agrees with our result.

### 7.1.2. Poly-dispersity Index (PDI)

As exhibited in table 7-1, nanoparticle formulations demonstrated PDI values less than 0.3, which indicated a narrow distribution profile among the particle population. Figure 7-4 demonstrates the main effect plot for the means of particle PDI. The figure demonstrates how the average PDI of nanoparticle populations changes at various factors/levels. The difference between maximum and minimum PDI for each factor was determined. Polymer molecular weight had the highest range (0.0819), followed by drug concentration (0.0419),

polymer terminus (0.297), organic:aqueous phase ratio (0.022), lactide:glycolide ratio (0.0076), and PVA concentration (0.0051). Table 7-5 ranks these factors based on the magnitude of effectiveness on particle PDI. Polymer molecular weight had the largest effect, drug concentration had second largest effect on PDI, and so on. Figure 7-5 demonstrates the S/N corresponding to each factor at various levels. S/N was calculated by the software using equation below:

**Equation 7-3:** $S/N = -10*\log(\Sigma(1/Y^2)/n)$

Where Y is responses for the given factor level combination and n is number of responses in the factor level combination.

The range of the S/N of PDI between different levels were as follows: polymer Mw (4.08) > drug concentration (1.77) > organic:aqueous phase ratio (1.58) > polymer terminus (1.27) > lactide:glycolide ratio (0.34) > PVA concentration (0.18). Accordingly, polymer molecular weight led to the most reduced variability. Figure 7-6 represents the normal probability plot of residuals for particle PDI to show the normality of particles PDI variation.

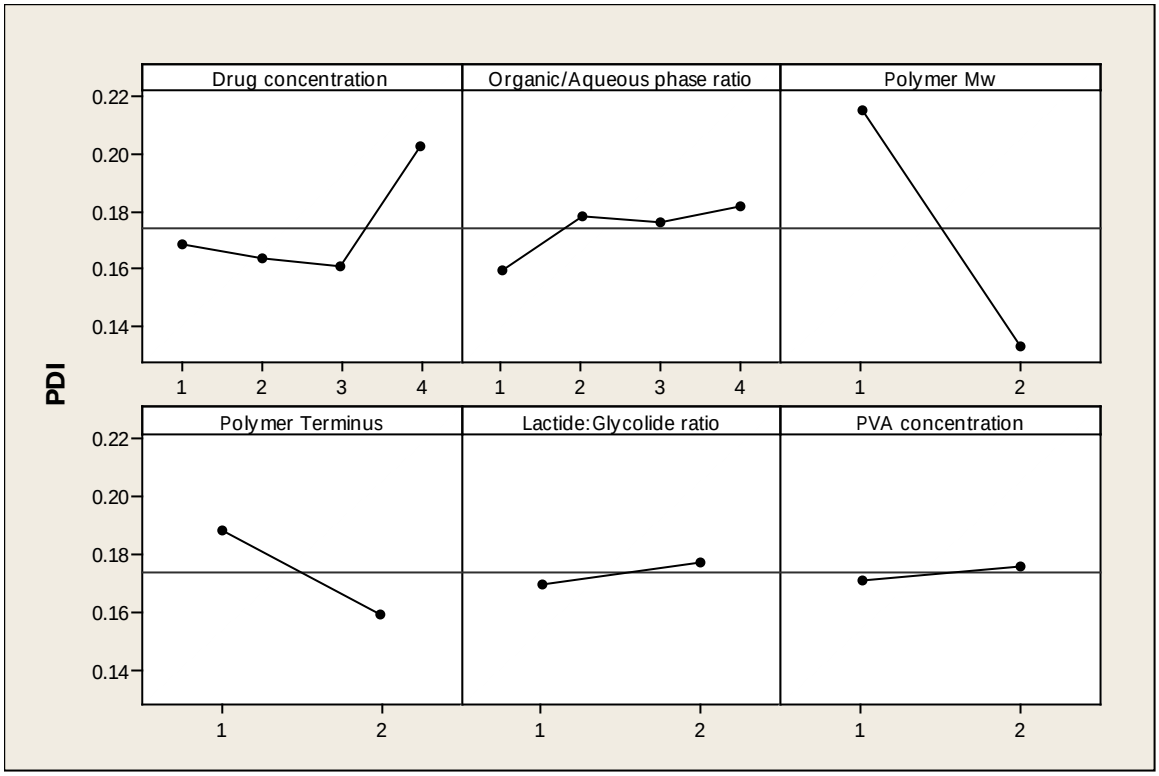


Figure 7-4. Main effect plot for particle PDI at different factor levels

Table 7-5. Ranking trend of factors affecting the PDI as the response of interest.

| | **Factors** | | | | | |
|---|---|---|---|---|---|---|
| | **Drug Conc.** | **Organic: Aqueous** | **Polymer Mw** | **Polymer Terminus** | **L:G** | **PVA Conc.** |
| **Rank** | 2 | 4 | **1** | 3 | 5 | 6 |

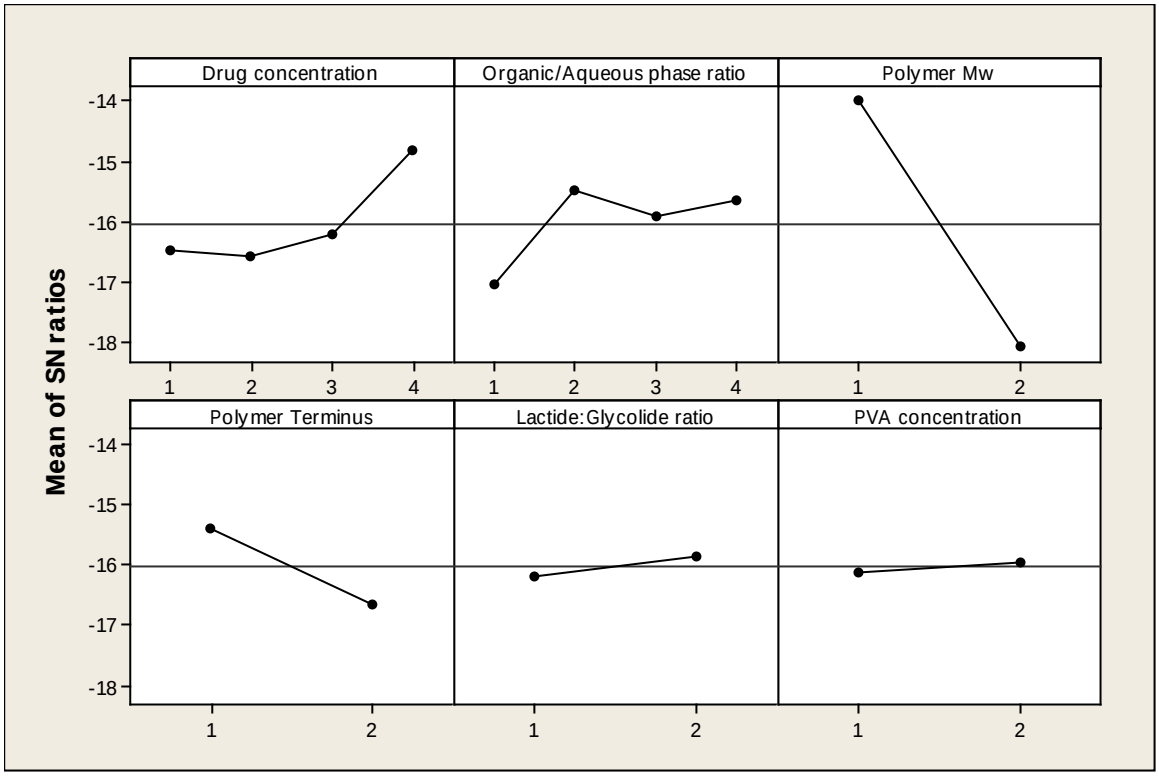


Figure 7-5. Main effect plot for S/N ratio at different factor levels

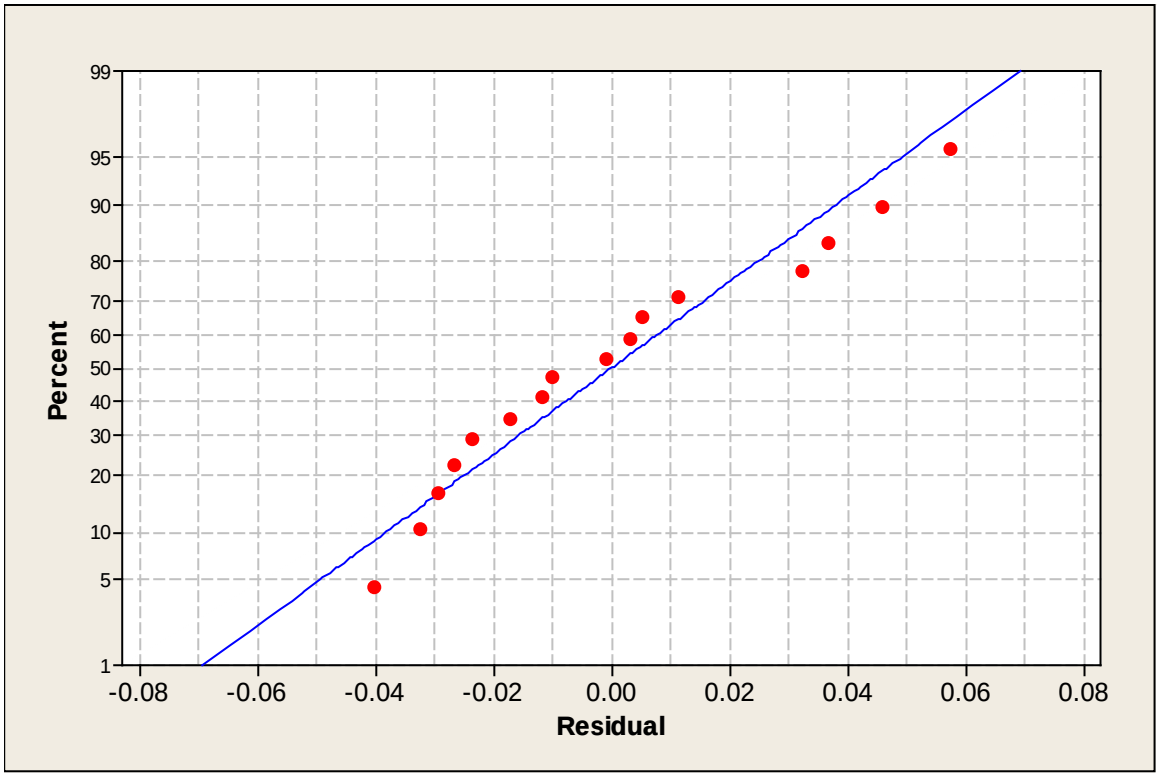


Figure 7-6. Normal probability plot of residuals by the final model for particle PDI

Linear regression analysis, ANOVA, along with F tests, were performed on the data to fit a model that best defined the variations in particle PDI versus the six factors under study. $R^2$ was equal to 0.717 while the regression equation was calculated to be:

**Equation 7-4:** **Particle PDI = 0.282 + 0.00990 (A) + 0.00637 (B) - 0.0819 (C) - 0.0297 (D) + 0.0076 (E) + 0.0051 (F)**

Tables 7-6 and 7-7 respectively exhibit the result of ANOVA and regression analysis for the fitted model of particle PDI. The *p*-value of the fitted model was 0.036 ($p < 0.05$), which indicates that the model is statistically significant to explain variations in PDI. Among the factors studied, polymer molecular weight contributed most significantly to variations in particle PDI ($p = 0.002$).

Table 7-6. ANOVA table for fitted model for PDI

| Source | Degree of Freedom | Sum of Squares | Mean Square | F | P |
|---|---|---|---|---|---|
| **Regression** | 6 | 0.033466 | 0.005578 | 3.79 | **0.036** |
| **Residual Error** | 9 | 0.013236 | 0.001471 | | |
| **Total** | 15 | 0.046702 | | | |

Table 7-7. Regression analysis of PDI versus nanoparticle preparation variables

| Predictor | Coefficients | SE Coefficients | T | P |
|---|---|---|---|---|
| **Constant** | 0.28163 | 0.06573 | 4.28 | 0.002 |
| **Drug concentration (A)** | 0.00990 | 0.00857 | 1.15 | 0.278 |
| **Organic/Aqueous phase ratio (B)** | 0.00636 | 0.00857 | 0.74 | 0.477 |
| **Polymer Mw (C)** | -0.0819 | 0.01917 | -4.27 | **0.002** |
| **Polymer Terminus (D)** | -0.0296 | 0.01917 | -1.55 | 0.156 |
| **Lactide:Glycolide ratio (E)** | 0.00758 | 0.01917 | 0.40 | 0.702 |
| **PVA concentration (F)** | 0.00508 | 0.01917 | 0.27 | 0.797 |

To understand the relationship between the response of interest (i.e., PDI) and factors that significantly affected particle PDI (i.e., polymer molecular weight), response surface

graphs were plotted and are presented in supplementary figure 2. The maximum PDI was obtained when low molecular weight PLGA polymer (level 1) and high docetaxel concentration (level 4) were used for nanoparticle preparation and vice versa. The response surface graph of PDI versus polymer molecular weight and polymer terminus (i.e., factor with second-lowest *p*-value) demonstrates that maximum particle PDI was obtained at low molecular weight (level 1) and acid-terminated (level 1) polymer and vice versa.

Analysis demonstrated that polymer molecular weight affected the particle PDI with statistical significance ($p<0.05$) (table 7-7). Viscosity of organic phase helped determine the average size of nanoparticles. PLGA polymers with higher molecular weight led to more viscose droplets (in the preparation emulsion) that broke into smaller droplets more difficultly. This difficulty kept the size of nano-droplet at a certain range, which decreased the diversity and variability in nanoparticles' size and kept the PDI low. The response surface plot of PDI vs. polymer molecular weight (the significant factor) and factors with the lowest *p*-values following polymer molecular weight (i.e., drug concentration and polymer terminus) were plotted to determine the highest and lowest response (i.e., PDI) in each case (supplementary figure 2). When considering polymer molecular weight and drug concentration as variables, the maximum PDI was obtained at low polymer molecular weight and highest drug concentration, while the minimum PDI was acquired at the opposite condition (supplementary figure 2A). When low molecular weight polymer was used for nanoparticle preparation, organic phase had a lower viscosity than when high molecular weight polymer is used. During probe-sonication, organic-phase droplets with lower viscosity sequentially broke into smaller particles more easily. Consequently, low molecular weight polymer resulted in nanoparticles with smaller average size. The sequential breakdown of droplets resulted in a nano-suspension with nano-droplets possessing a wide range of sizes that increased the PDI. On the other hand, acid terminal functional group and low molecular

weight resulted in maximum PDI response while ester terminus and high molecular weight provided minimum PDI values.

### 7.1.3. Particle Zeta Potential

The zeta potential of nanoparticles was attributed to the role of the polymer terminus on the surface of nanoparticles and the further ionization of carboxylic acid (in the case of acid-terminated polymer) or hydrolysis of ester (in the case of ester-terminated polymer). Figure 7-7 demonstrates the main effect plot for the means of particle zeta potential. The figure exhibits the variation of zeta potential of nanoparticles according to nanoparticle preparation conditions at different factors/levels. The ranges between the minimum and maximum nanoparticle zeta potential were calculated between levels of each factors and were as follows (in decreasing order): polymer terminus (9.85 mV), organic:aqueous phase ratio (3.96 mV), drug concentration (3.43 mV), PVA concentration (2.54 mV), lactide:glycolide ratio (2.10 mV), and polymer Mw (0.81 mV). Table 7-8 exhibits the rankings of factors affecting the response. PLGA polymer terminus had the largest magnitude of effectiveness on particle zeta potential. Organic:aqueous phase ratio had the second largest effect on particles' zeta potential, and so on. This result agrees with the fact that acid terminus can easily become ionized and expose more negative charges to the surface of nanoparticles. Figure 7-8 demonstrates the S/N analysis of the linear model. S/N was calculated by the software using formula below:

**Equation 7-5:** $S/N = -10*\log(s^2)$

Where s is standard deviation of the responses for all noise factors for the given factor level combination.

The range of S/N for each factor at different levels was calculated. The highest range between S/N was demonstrated by drug concentration (8.69) followed by organic:aqueous

phase ratio (7.77), polymer Mw (2.98), lactide:glycolide ratio (2.34), polymer terminus (0.70), and PVA concentration (0.58). Based on analysis of S/N calculations, drug concentration with largest range led to the most reduced variability in particle zeta potential. This, in part, might be because docetaxel and PLGA are hydrophobic molecules. Consequently, non-covalent interactions such as van der waals or hydrogen-bonds between these two molecules (particularly at different docetaxel concentration) can result in constant rearrangement of polymer terminus on the surface of nanoparticles and reduce potential variation in surface electric potential.

Figure 7-9 represents the normal probability plot of residuals for particle zeta potential. It demonstrates the normality of variation observed in particles zeta potential.

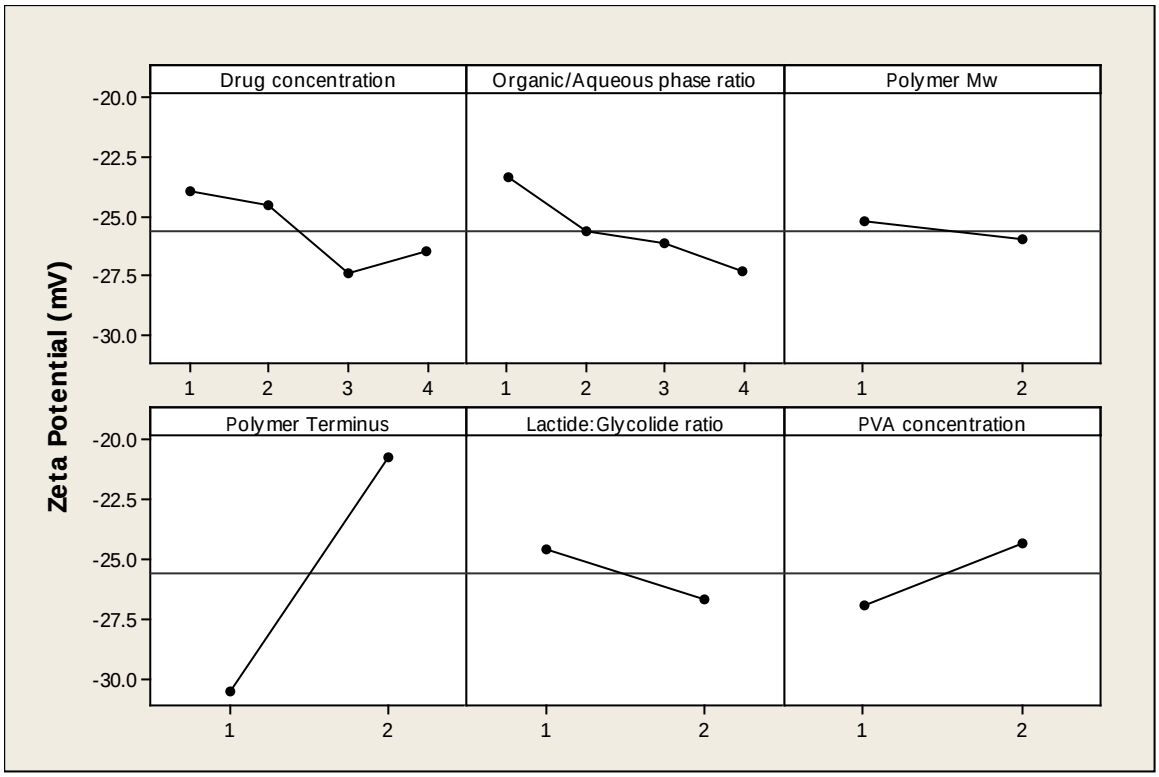


Figure 7-7. Main effect plot for particle zeta potential at different factor levels

Table 7-8. Ranking trend of factors affecting the particle zeta potential as the response of interest.

| | Factors | | | | | |
|---|---|---|---|---|---|---|
| | **Drug Conc.** | **Organic: Aqueous** | **Polymer Mw** | **Polymer Terminus** | **L:G** | **PVA Conc.** |
| **Rank** | 3 | 2 | 6 | **1** | 5 | 4 |

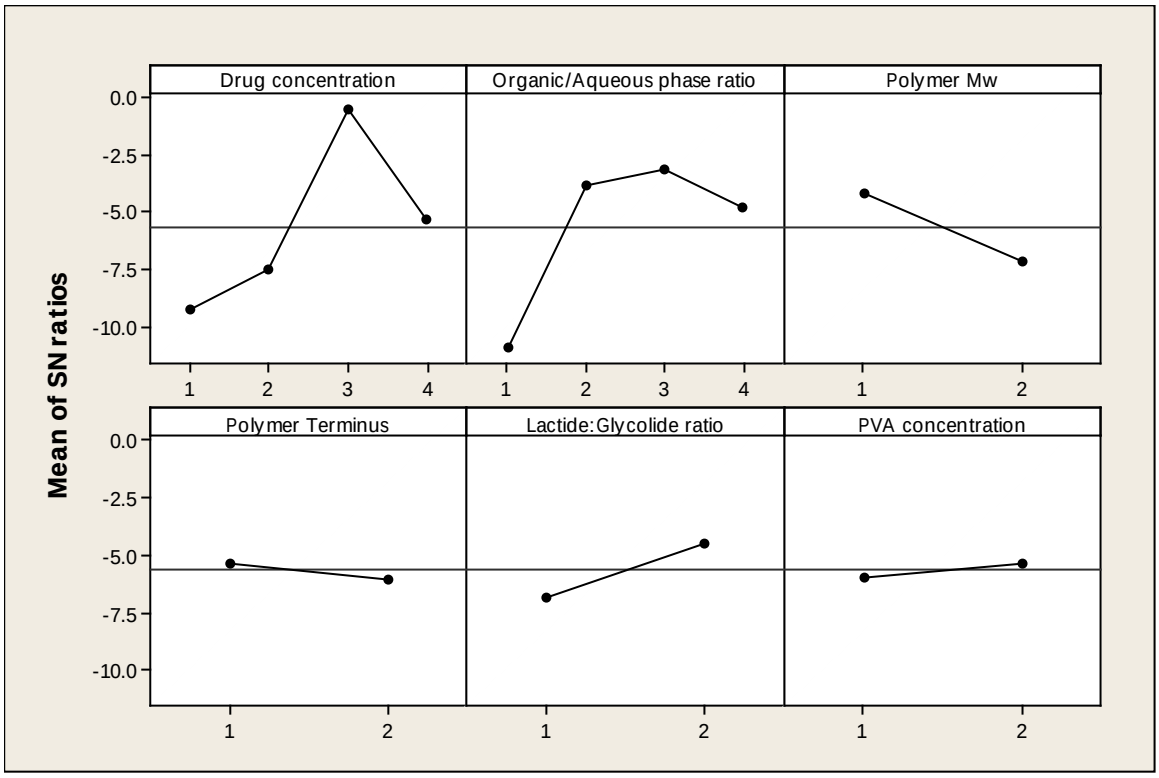


Figure 7-8. Main effect plot for S/N ratio at different factor levels

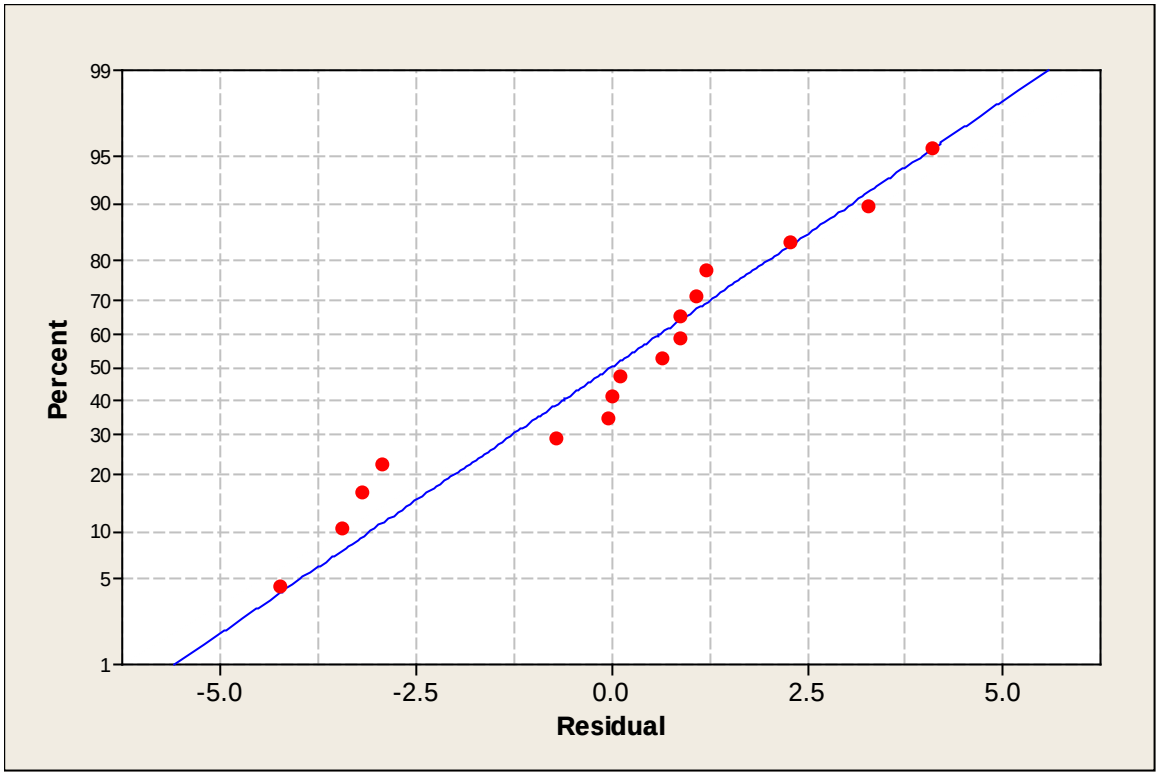


Figure 7-9. Normal probability plot of residuals by the final model for particle zeta potential

Linear regression analysis, ANOVA, along with F tests, were performed on the data to fit a model that best defined the variations in particle zeta potential versus the six factors under study. $R^2$ was equal to 0.849 while the regression equation was calculated to be:

**Equation 7-6:** **Particle Zeta potential = - 34.1 - 1.04 (A) - 1.24 (B) - 0.81 (C) + 9.85 (D) - 2.10 (E) + 2.54 (F)**

Tables 7-9 and 7-10 respectively exhibit the result of ANOVA and regression analysis for the fitted model of particle zeta potential. The fitted model demonstrated a *p*-value equal to 0.003, meaning that the model could be used to define zeta potential of PLGA nanoparticles with statistical significance. Among other factors under study, the *p*-value

calculated for polymer terminus was less than 0.05, showing its statistically significant contribution to zeta potential characteristic of PLGA nanoparticles.

Table 7-9. ANOVA table for fitted model for particle zeta potential

| Source | Degree of Freedom | Sum of Squares | Mean Square | F | P |
|---|---|---|---|---|---|
| **Regression** | 6 | 486.552 | 81.092 | 8.45 | **0.003** |
| **Residual Error** | 9 | 86.332 | 9.592 | | |
| **Total** | 15 | 572.883 | | | |

Table 7-10. Regression analysis of particle zeta potential versus nanoparticle preparation variables

| Predictor | Coefficients | SE Coefficients | T | P |
|---|---|---|---|---|
| **Constant** | -34.103 | 5.308 | -6.42 | 0.000 |
| **Drug concentration (A)** | -1.0446 | 0.6925 | -1.51 | 0.166 |
| **Organic/Aqueous phase ratio (B)** | -1.2404 | 0.6925 | -1.79 | 0.107 |
| **Polymer Mw (C)** | -0.810 | 1.549 | -0.52 | 0.613 |
| **Polymer Terminus (D)** | 9.848 | 1.549 | 6.36 | **0.000** |
| **Lactide:Glycolide ratio (E)** | -2.098 | 1.549 | -1.35 | 0.209 |
| **PVA concentration (F)** | 2.540 | 1.549 | 1.64 | 0.135 |

To understand the relationship between the response of interest (i.e., particle zeta potential) and the factor significantly affecting it (i.e., polymer terminus), response surface graphs were plotted and are presented in supplementary figure 3A and 3B. Supplementary figure 3A demonstrates that the maximum value of particle zeta potential was obtained when ester-terminated polymer (level 2) and a 1:2 ratio of organic:aqueous phase (level 1) were used during the nanoparticle fabrication procedure and that polymers with acid terminus at 1:5 organic:aqueous phase ratio resulted in highest surface negativity. Also, supplementary figure 3B demonstrates that the minimum value of particle zeta potential was obtained when acid-terminated polymer (level 1) and a low PVA concentration (level 1) were used during nanoparticle fabrication and that using a high concentration of PVA and ester-terminated polymer resulted in nanoparticles with less surface negative zeta potential. This result can be

attributed the role of PVA as a spatial stabilizer and to the traces of PVA that remain on the surface of PLGA nanoparticles even after consecutive washing steps.

### 7.1.4. Drug Loading Efficiency

Figure 7-10 demonstrates the main effect plot for the means of drug-loading efficiency at different factors/levels. The range between the maximum and minimum drug-loading efficiency was calculated for each factor and determined organic:aqueous phase ratio had the highest range (26.78%). The ranges for other factors were as follows: drug concentration (25.61%), PVA concentration (19.95%), lactide:glycolide ratio (10.04%), polymer terminus (9.67%), and polymer molecular weight (2.03%). Accordingly, table 7-11 exhibits the rankings of factors affecting the response (drug-loading efficiency). Organic:aqueous phase ratio (rank 1) is considered to be the factor with highest magnitude of effect on drug loading efficiency. Drug concentration (rank 2) has the second largest effect on drug loading efficiency, and so on. Drug-loading efficiency is reduced parallel to the increase in drug concentration. This result is attributed to the fact that polymer matrix (forming the nanoparticles) gets saturated by drug molecules when a higher concentration of the drug is used. Another trend is the decrease in drug-loading efficiency parallel to the increment in the amount of aqueous solution. With the increase in aqueous solution, more drug molecules could escape from organic phase to aqueous phase, which reduced the overall drug-loading efficiency. Murugesan and colleagues [195] also evaluated the effect of initial docetaxel concentration and stabilizer concentration on drug-loading efficiency. They demonstrated that drug-loading efficiency inversely relates to the concentration of docetaxel during preparation. In other words, increasing the concentration of stabilizer or docetaxel reduces the loading efficiency of the PLGA nanoparticles' preparation method. They also demonstrated that increasing the amount of aqueous phase during nanoparticle preparation reduces the drug

entrapment efficiency. Figure 7-11 demonstrates the S/N analysis of the linear model. S/N was calculated by the software using equation below:

**Equation 7-7:** $S/N = -10*\log(\Sigma(1/Y^2)/n)$

Where Y is responses for the given factor level combination and n is number of responses in the factor level combination.

Based on the preferences, the larger S/N is better. Drug concentration demonstrates largest range (4.27) of S/N ratio. The ranges for S/N ratio of other factors are as follows: organic:aqueous phase ratio (4.01) > PVA concentration (3.24) > polymer terminus (1.45) > lactide:glycolide ratio (1.40) > polymer Mw (0.17). Figure 7-12 represents the normal probability plot of residuals for drug-loading efficiency. It demonstrates normality of drug loading efficiency variation.

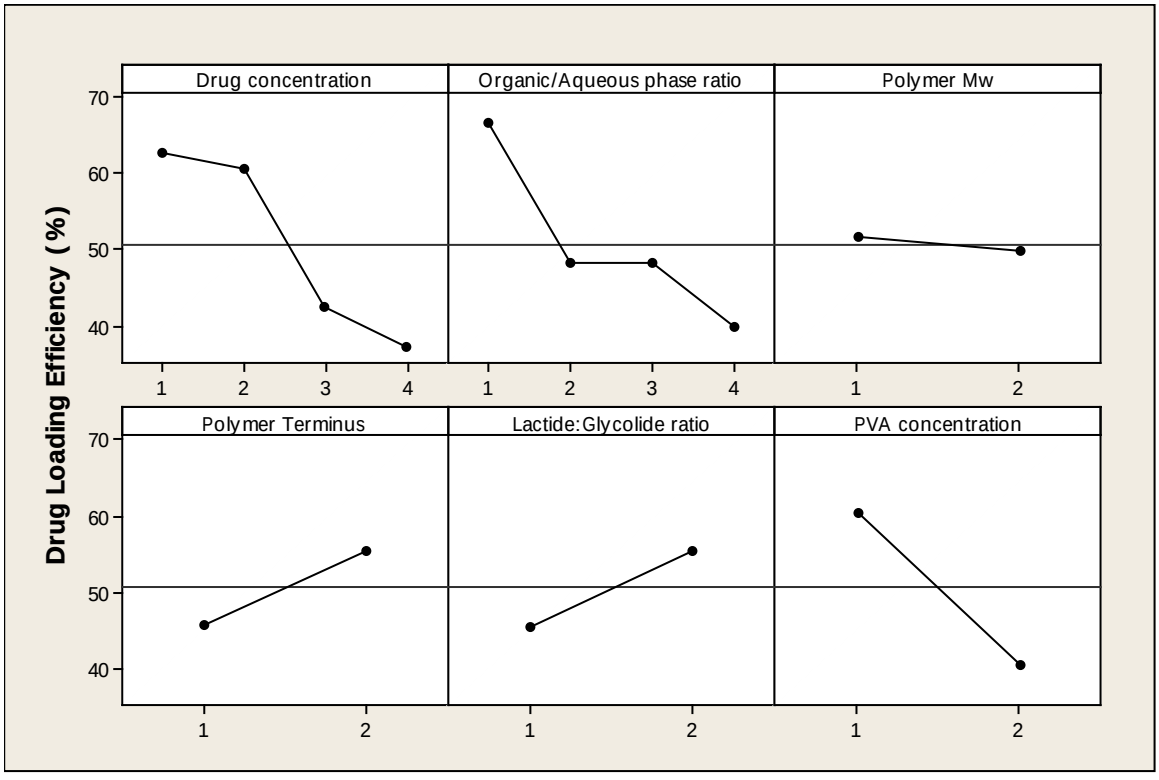


Figure 7-10. Main effect plot for drug-loading efficiency at different factor levels

Table 7-11. Ranking trend of factors affecting the drug-loading efficiency as the response of interest.

| | Factors | | | | | |
|---|---|---|---|---|---|---|
| | **Drug Conc.** | **Organic: Aqueous** | **Polymer Mw** | **Polymer Terminus** | **L:G** | **PVA Conc.** |
| **Rank** | 2 | **1** | 6 | 5 | 4 | 3 |

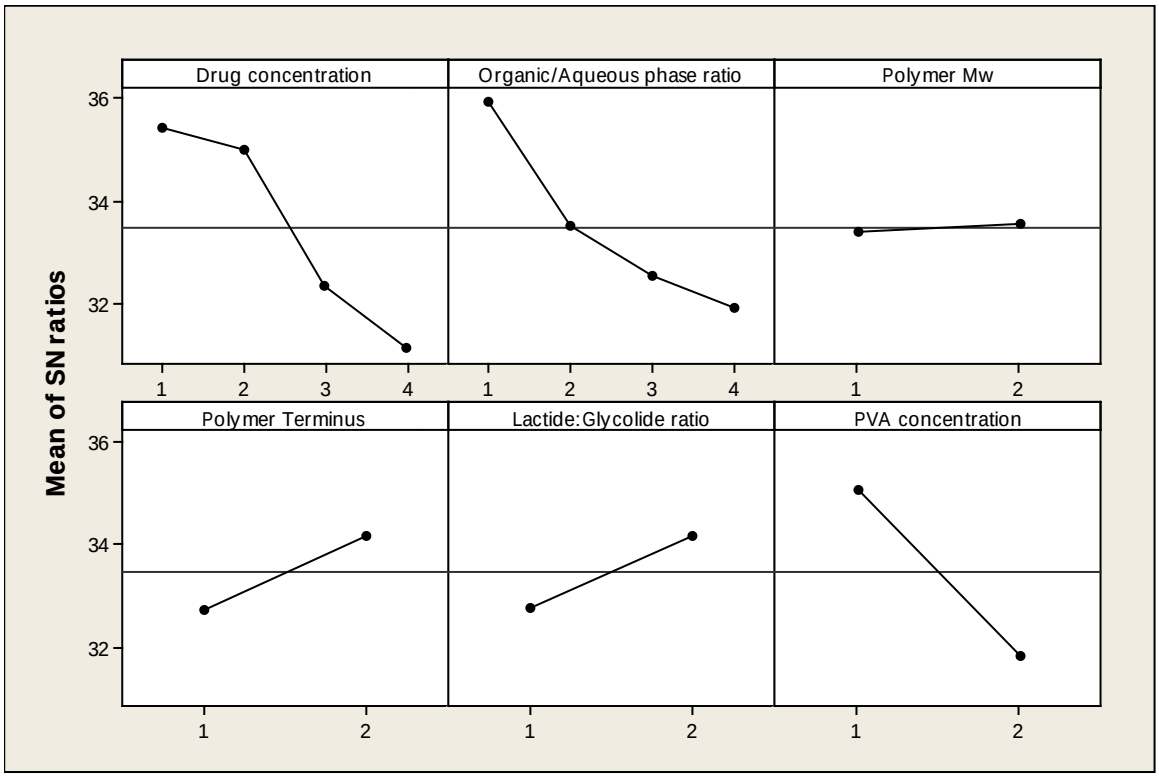


Figure 7-11. Main effect plot for S/N ratio at different factor levels

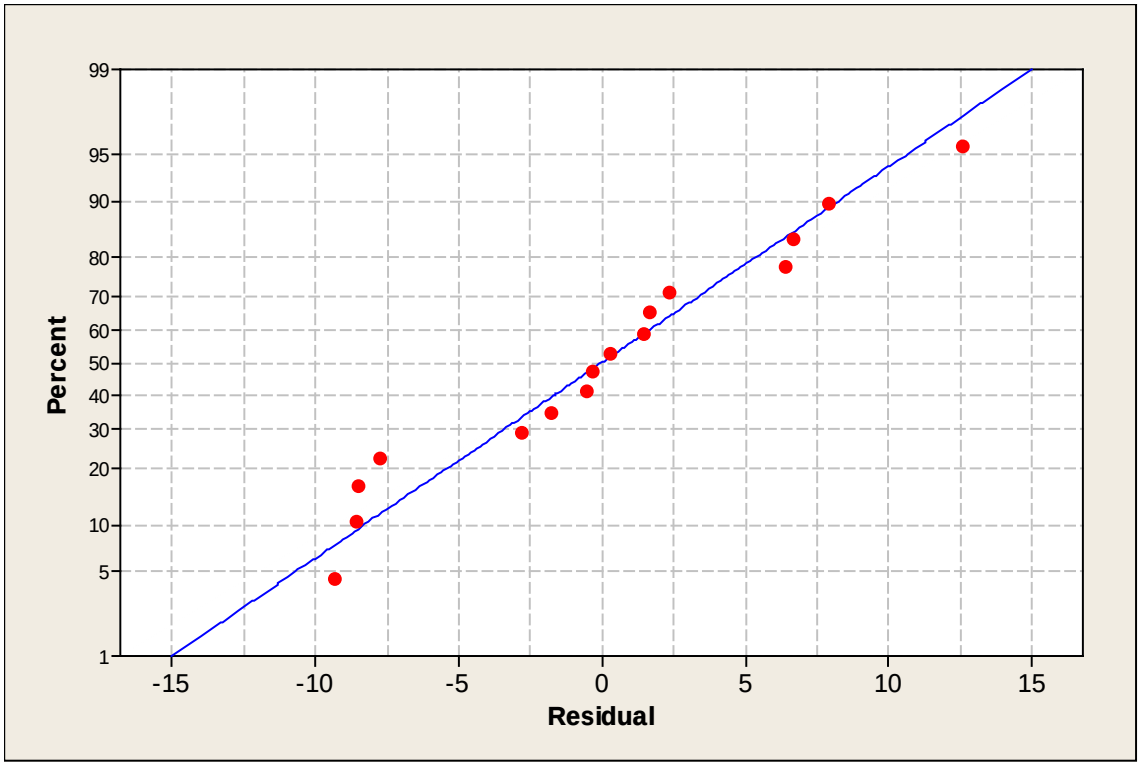


Figure 7-12. Normal probability plot of residuals by the final model for drug-loading efficiency

Linear regression analysis, ANOVA, along with F test have been performed on the data to fit a model that best defines the variations in drug-loading efficiency versus the six factors under study. $R^2$ was equal to 0.898 while the regression equation was calculated to be:

**Equation 7-8:** **Drug Loading Efficiency = 97.9 - 9.51 (A) - 8.04 (B) - 2.03 (C) + 9.67 (D) + 10.0 (E) - 19.9 (F)**

Tables 7-12 and 7-13 respectively exhibit the result of ANOVA and regression analysis for the fitted model of drug-loading efficiency, which demonstrated a *p*-value equal to 0.001. This means that the variations in drug-loading efficiency could be explained by the fitted model with statistical significance. *P*-values related to the following five factors were lower than 0.05: drug concentration, organic:aqueous phase ratio, polymer terminus,

lactide:glycolide ratio, and PVA concentration. This finding provides valuable insight about nanoparticle preparation conditions when drug-loading is the intended characteristic.

Table 7-12. ANOVA table for fitted model for drug-loading efficiency

| Source | Degree of Freedom | Sum of Squares | Mean Square | F | P |
|---|---|---|---|---|---|
| **Regression** | 6 | 5486.88 | 914.48 | 13.22 | **0.001** |
| **Residual Error** | 9 | 622.52 | 69.17 | | |
| **Total** | 15 | 6109.41 | | | |

Table 7-13. Regression analysis of drug-loading efficiency versus nanoparticle preparation variables

| Predictor | Coefficients | SE Coefficients | T | P |
|---|---|---|---|---|
| **Constant** | 97.94 | 14.25 | 6.87 | 0.000 |
| **Drug concentration (A)** | -9.506 | 1.860 | -5.11 | **0.001** |
| **Organic/Aqueous phase ratio (B)** | -8.044 | 1.860 | -4.33 | **0.002** |
| **Polymer Mw (C)** | -2.034 | 4.158 | -0.49 | 0.636 |
| **Polymer Terminus (D)** | 9.672 | 4.158 | 2.33 | **0.045** |
| **Lactide:Glycolide ratio (E)** | 10.037 | 4.158 | 2.41 | **0.039** |
| **PVA concentration (F)** | -19.949 | 4.158 | -4.80 | **0.001** |

To understand the relationship between drug-loading efficiency and the factors significantly affecting it (i.e., drug concentration, organic/aqueous phase ratio, polymer terminus, lactide:glycolide ratio, and PVA concentration), response surface graphs were plotted and are presented in supplementary figures 4 to 7. Supplementary figure 4 demonstrates that minimum drug-loading efficiency was obtained when a 1:5 ratio of organic:aqueous phase (level 4) and the highest drug concentration (level 4) are used. Drug concentration level 4 (the highest concentration) combined with level 1 of polymer terminus (acid-terminated), level 2 PVA concentration (high), or 50:50 lactide:glycolide ratio also resulted in minimum drug loading. Supplementary figure 5 demonstrates that maximum drug-loading efficiency was obtained when 1:2 of organic:aqueous phase ratio (level 1) and ester terminated polymer (level 2), low concentration of PVA (level 1), or 75:25 of

lactide:glycolide ratio (level 2) were used during nanoparticle preparation. Supplementary figure 6 demonstrates that maximum drug-loading efficiency was obtained when ester-terminated polymer (level 2) and 75:25 of lactide:glycolide ratio polymer (level 2) or low concentration PVA (level 1) were used for nanoparticle fabrication. Supplementary figure7 demonstrates that minimum drug-loading efficiency of nanoparticle preparation was obtained when 50:50 lactide:glycolide ratio polymer (level 1) and high PVA concentration (level 2) are used.

### 7.2. Optimization of Nanoparticle Preparation

Response optimization was applied to identify the combination of factors/levels during nanoparticle preparation that jointly optimize the nanoparticle characteristic of interest. Response optimization was performed for nanoparticle size, PDI, zeta potential, and drug-loading efficiency. Figure 7-13 demonstrates optimization plots of nanoparticle characteristics under study. Each plot exhibits how experimental nanoparticle preparation settings influenced the predicted nanoparticle size, PDI, zeta potential, or drug-loading efficiency.

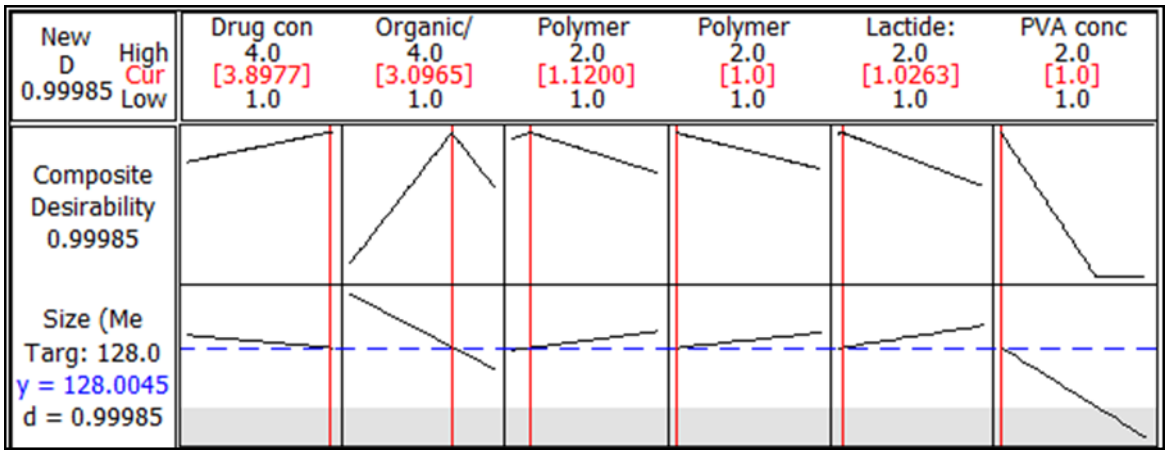


A)

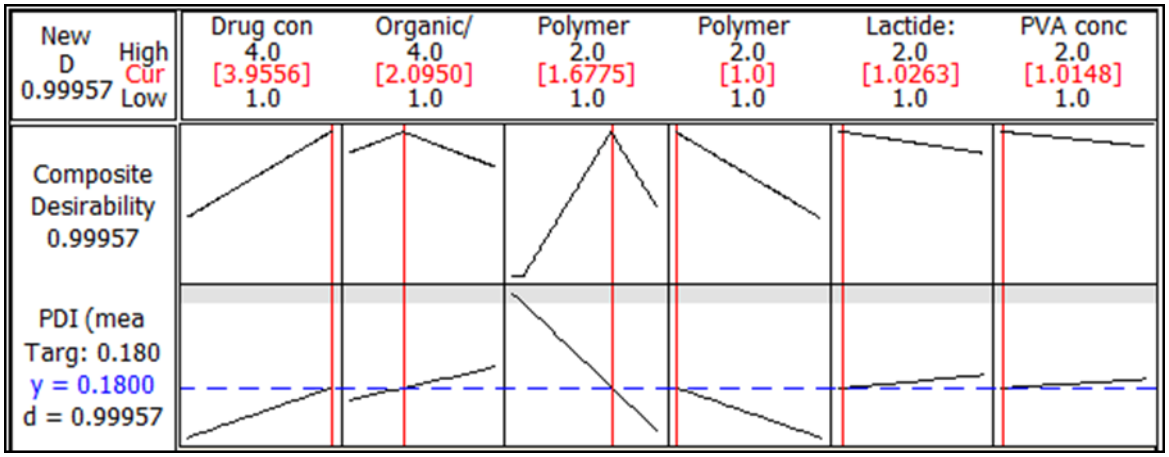


B)

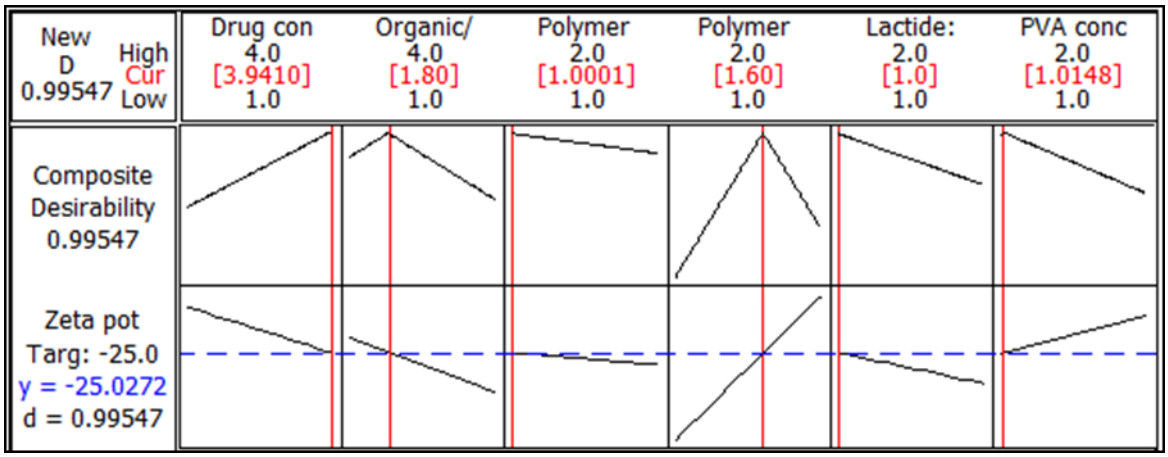


C)

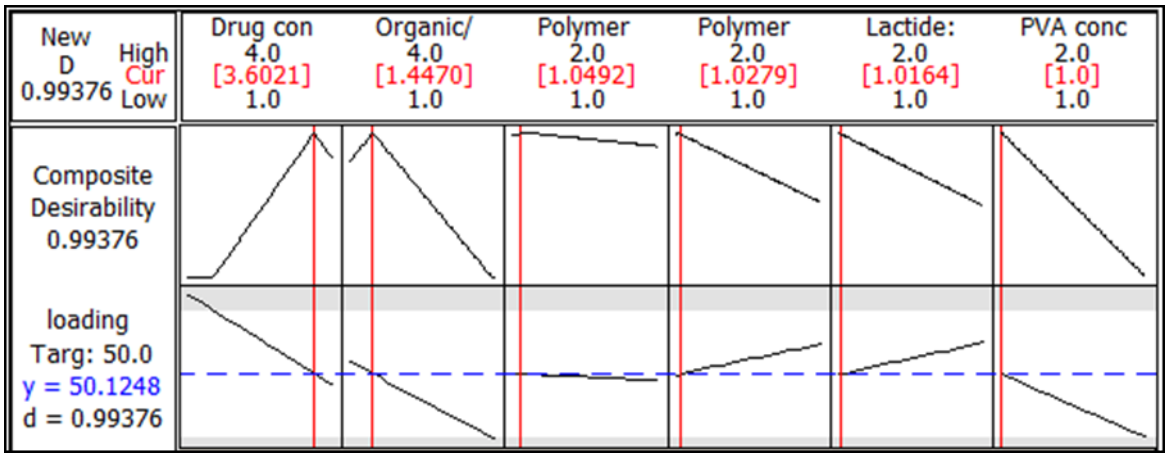


D)

Figure 7-13. Response optimization plot showing the optimized factor/level setting for A) average size, B) PDI, C) zeta potential, and D) drug-loading efficiency.

In each section, the middle row exhibits the composite (first column) and individual (other columns) desirability levels related to the factors under study. Individual desirability is presented schematically as black lines while composite desirability is presented as a number. They assess how the combination of factors satisfies the value defined for a nanoparticle characteristic (response). The desirability range is between 0 and 1. A desirability at 1 means that the ideal response is obtained. Conversely, a desirability of zero indicates that the response is out of the defined limits. The first row exhibits the factors and corresponding levels in the design from high to low levels (in black). The numbers in red represent the level of each factor at which the corresponding desirability is obtained. The third row, first column to the left, exhibits the response of interest and target value. Other columns to the right (third row) schematically demonstrate the target value (blue dashed line) and how moving from one level to another (in each factor) changes the response around target value (black lines in each column). Based on the obtained data from response optimization analysis, optimized PLGA nanoparticle fabrication conditions relating to individual nanoparticle characteristics (size, PDI, zeta potential, drug-loading efficiency) were determined to be as follows:

**Nanoparticle size:** Composite desirability near 1 is obtained at level 3.8977 of drug concentration, 3.0965 of aqueous:organic phase ratio, 1.1200 of polymer molecular weight, 1.0 of polymer terminus, 1.0263 of L:G ratio, and 1.0 of PVA concentration.

**PDI:** Composite desirability near 1 is obtained at level 3.9556 of drug concentration, 2.0950 of aqueous:organic phase ratio, 1.6775 of polymer molecular weight, 1.0 of polymer terminus, 1.0263 of L:G ratio, and 1.0148 of PVA concentration.

**Zeta Potential:** Composite desirability near 1 is obtained at level 3.9410 of drug concentration, 1.80 of aqueous:organic phase ratio, 1.0001 of polymer molecular weight, 1.60 of polymer terminus, 1.0 of L:G ratio, and 1.0148 of PVA concentration.

**Drug Loading Efficiency:** Composite desirability near 1 is obtained at level 3.6021 of drug concentration, 1.4470 of aqueous:organic phase ratio, 1.0492 of polymer molecular weight molecular weight, 1.0279 of polymer terminus, 1.0164 of L:G ratio, and 1.0 of PVA concentration.

Taking the factor/levels at which suitable composite desirability level was obtained (regarding nanoparticle characteristics) collectively, optimized nanoparticle fabrication conditions were determined and used to prepare docetaxel-loaded PLGA nanoparticle formulations, which were then used throughout the research project:

**Docetaxel Concentration:** Level 4 (1.5 mg/ml)

**Organic/Aqueous phase ratio:** Level 2 (1:3)

**PLGA Molecular weight:** Level 1 (0.15 - 0.25 dl/g)

**PLGA polymer Terminus:** Level 1 (Acid terminated)

**Polymer lactide/glycolide ratio:** Level 1 (50:50)

**PVA Concentration:** Level 1 (2.2%)

# CHAPTER 8*

## Result and Discussion on PLGA and PLGA-PEG Nanoparticle Formulation and Characterization

***** Chapter 4 (Experimental Section on Preparation and Characterization of Optimized PLGA and PLGA-PEG Nanoparticle Formulation) along with chapter 8 have been accepted for publication as an 'Original Research Article' in '*Journal of Nanopharmaceutics and Drug Delivery* ':

Pedram Rafiei, Azita Haddadi. Investigation of PLGA and PEG-PLGA nanoparticles loaded with docetaxel as an approach for sustained release intravenous application. *Journal of Nanopharmaceutics and Drug Delivery,* Accepted January 2017.

### Background

Developing PLGA nanoparticle formulations for drug-delivery purposes requires the use of a proper fabrication method that provides nanoparticles with desired properties. After nanoparticle preparation, there is the need to perform rational characterization techniques on nanoparticles to understand their properties because nanoparticle properties contribute to nanoparticles' drug-delivery performance and can help predict their fate after administration [284].

Average diameter and zeta potential provide basic knowledge about nanoparticles. The amount of the drug associated with nanoparticles is also important to evaluate as it provides an assessment of the equivalent dose of the drug in the form of nanoparticles. Other than size, zeta potential, and drug loading, determining the rate and pattern of drug release from nanoparticles is required to understand the mode at which the drug becomes available to the location of interest. Whether the drug molecules' association to nanoparticles affect the drug's biological/pharmacological activity is also important to determine. Therefore, usually

after physicochemical characterization steps, biological activity of nanoparticles is also evaluated using cell culture models.

Here, comparing different cryoprotecting agents led to choosing a proper cryoprotectant for freeze-drying of nanoparticles. The developed optimized nanoparticle fabrication technique was used to prepare docetaxel-loaded PLGA nanoparticles and surface-modified (PEGylated) docetaxel-loaded PLGA nanoparticles. Taking into consideration the need for characterization steps before proceeding to animal experiments, prepared nanoparticle formulations were subjected to extensive characterization techniques. Thus, the average sizes, zeta potentials, drug-loading properties, and drug-release profiles of docetaxel-loaded PLGA and PEGylated PLGA nanoparticle formulations were evaluated. The biologic effect of docetaxel loaded in PLGA and PLGA-PEG nanoparticles was evaluated in Hela cancer cell lines.

### 8.1. Freeze-drying of Nanoparticles and Cryoprotection

The changes in size, PDI, and zeta potential after freeze-drying nanoparticles with various cryoprotectants at different concentrations are exhibited in table 8-1. Nanoparticles' average size before and after freeze-drying with different cryoprotectants is depicted in figure 8-1.

The average size of nanoparticles before freeze-drying was 143.5±12.8 nm. Particles demonstrated around a 500 nm increase (~4.88–fold increase) in average size (701.3±352.0 nm) after freeze-drying when no cryoprotectant was used. In addition, freeze-drying without cryoprotectant increased PDI and zeta potential from 0.279 to 0.762 and -20.5 to -10.5 mV, respectively. In contrast, a 119 to 241 nm, 129 to 239 nm, and 3 to 44 nm increase in size was observed in nanoparticles when 1-10 % (W/V) sucrose, 1-10 % (W/V) trehalose, and 0.25-2% (W/V) PVA were used as cryoprotectants, respectively. For nanoparticles freeze-dried

with sucrose, PDI increased (from 0.279) to values between 0.337 and 0.444. Nanoparticles freeze-dried with trehalose demonstrated PDI values between 0.344 and 0.391. Using PVA for freeze-drying resulted in nanoparticles with PDI values between 0.243 and 0.292. Using sugars as cryoprotectants increased zeta potential to values between -11.9 and -8.6 mV for sucrose and -11.5 and -7.4 mV for trehalose. Zeta potential values of nanoparticles freeze-dried with PVA were not measureable.

The ratio of nanoparticle size after and before freeze-drying (R = (Sf)/(Si)) with different cryoprotectants is exhibited in figure 8-2. The average size of nanoparticles increased 1.89- to 2.66-fold and 1.82- to 2.67-fold when trehalose and sucrose were used as cryoprotectants, respectively. PVA increased average particle size 1.01- to 1.30-fold. One and two percent (W/V) PVA demonstrated lowest R (~1) while 10% (W/V) sucrose exhibited highest R (2.67). PVA appeared to be better preserving nanoparticle size compared to other cryoprotectants used during freeze-drying.

Table 8-1. Characteristics of freeze-dried PLGA nanoparticles in the presence of cryoprotective agents at different concentrations. Data represents mean ± standard deviation (n=3). (PLGA = Poly (lactide-co-glycolide), FD=Freeze-drying, CRP = Cryoprotectant, PDI=polydispersity index, PVA= Poly (vinyl alcohol), nm=nanometers, mV=millivolts, Sf= average diameter after freeze-drying, Si= average diameter before freeze-drying).

| **Formulation** | **Average diameter (nm)** | **PDI** | **Zeta potential (mV)** | **R = (Sf)/(Si)** |
|---|---|---|---|---|
| **PLGA Nanoparticles** | 143.5±12.8 | 0.279±0.052 | -20.5±2.2 | - |
| **After FD without CRP** | 701.3±352.0 | 0.762±0.160 | -10.5±3.0 | 4.88±2.24 |
| **After FD with CRP:** | | | | |
| **Sucrose 1%** | 262.0±7.2 | 0.350±0.013 | -11.9±0.6 | 1.82±0.05 |
| **Sucrose 3%** | 266.1±2.3 | 0.337±0.026 | -10.2±0.6 | 1.85±0.01 |
| **Sucrose 5%** | 289.7±11.5 | 0.343±0.016 | -9.9±0.7 | 2.01±0.08 |
| **Sucrose 10%** | 384.1±26.7 | 0.444±0.54 | -8.6±1.0 | 2.67±0.18 |
| **Trehalose 1%** | 272.1±3.2 | 0.344±0.021 | -11.5±1.1 | 1.89±0.02 |
| **Trehalose 3%** | 344.4±1.1 | 0.386±0.009 | -10.1±2.1 | 2.39±0.01 |
| **Trehalose 5%** | 358.0±28.6 | 0.387±0.029 | -9.5±0.6 | 2.49±0.19 |
| **Trehalose 10%** | 382.7±10.1 | 0.391±0.022 | -7.4±0.5 | 2.66±0.07 |
| **PVA 0.25%** | 187.1±1.3 | 0.271±0.041 | - | 1.30±0.01 |
| **PVA 0.5%** | 162.6±5.7 | 0.243±0.015 | - | 1.13±0.04 |
| **PVA 1%** | 146.1±4.6 | 0.292±0.031 | - | 1.01±0.03 |
| **PVA 2%** | 147.1±4.8 | 0.244±0.029 | - | 1.02±0.03 |

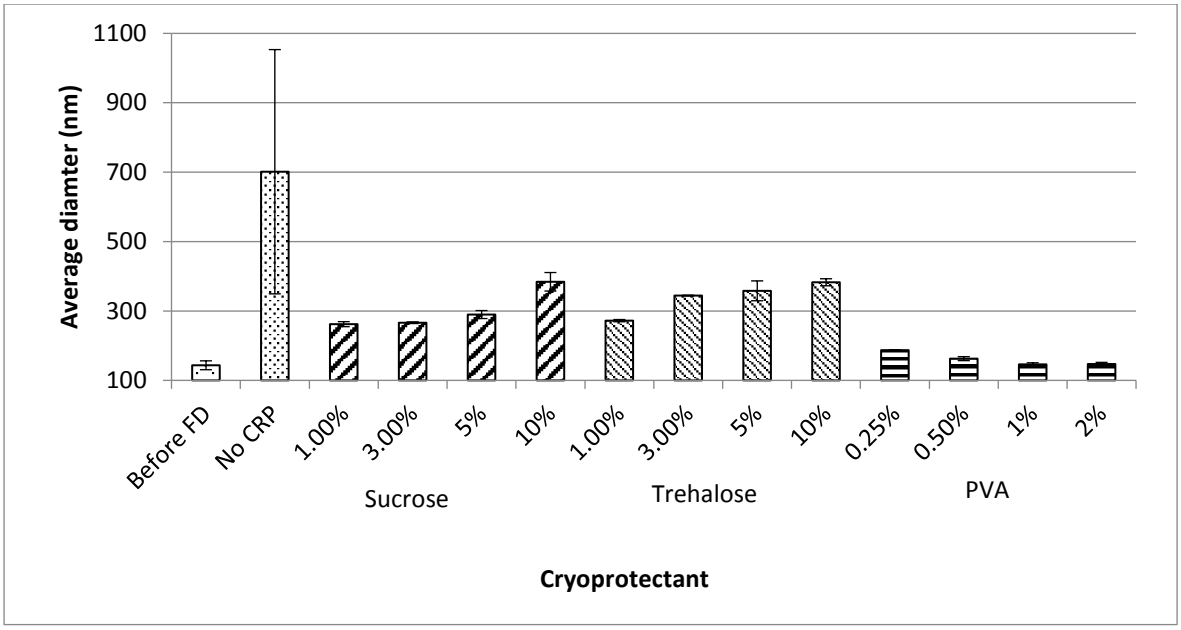


Figure 8-1. Average nanoparticle diameter before and after freeze-drying, and with and without cryoprotection (n=3). Various concentrations of cryoprotectants (nm=nanometers, FD=Freeze-drying, CRP = Cryoprotectant, PVA= Poly (vinyl alcohol)).

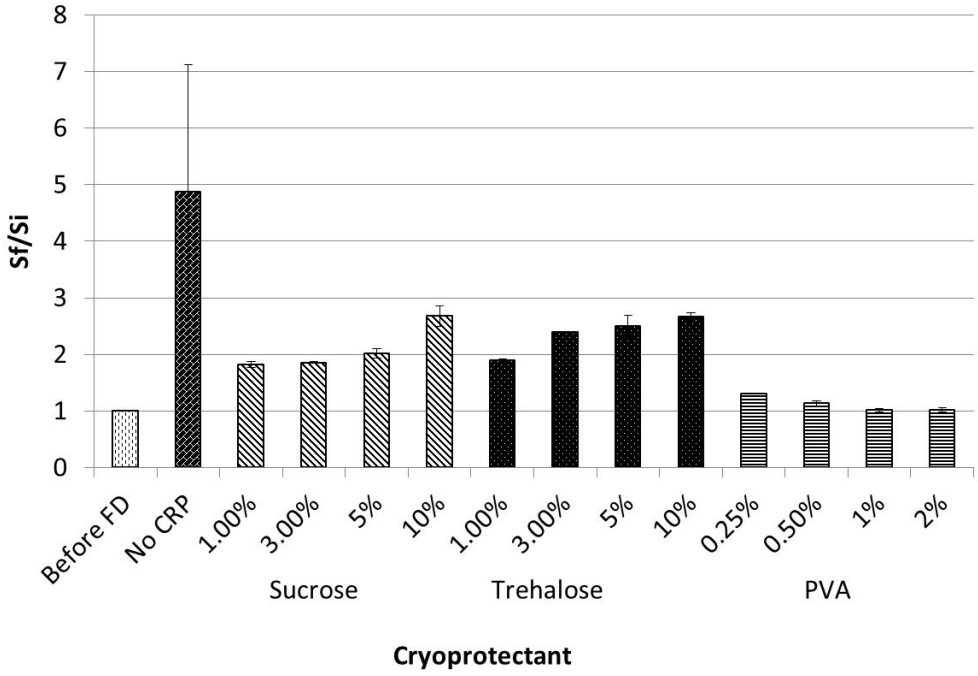


Figure 8-2. Ratios of PLGA nanoparticles size after and before freeze-drying procedure in the presence of various cryoprotective agents at different concentrations (n=3). (nm=nanometers, FD=Freeze-drying, CRP = Cryoprotectant, PVA= Poly (vinyl alcohol)).

Freeze drying polymeric nanoparticles used for drug delivery helps improve their long-term stability [285, 286]. Accordingly, finding a suitable cryoprotective agent and using it at proper concentrations is greatly important. Trehalose demonstrates a similar performance to sucrose with respect to nanoparticles' average size and PDI. Both sugars demonstrate an inverse relationship between the concentration and cryoprotective effectiveness. This could be attributed to more pronounced interactions (possibly hydrogen bonds) at higher concentrations between nanoparticles and cryoprotectant molecules that prevents the entire reconstitution of nanoparticles [287]. In other words, particle aggregation during freeze-drying is increased by higher sugar concentration. The effectiveness of sucrose and trehalose in preserving PLGA nanoparticle properties has been demonstrated by various studies [288-293]. Accordingly, the type of PLGA polymer, type of cryoprotectant, and cryoprotectant concentration are important factors in determining the performance of cryoprotection [287]. Here, cryoprotective performance of PVA was superior to that observed from sugars. In addition, PVA had a better cryoprotective performance when used at a higher concentration. This can be attributed to the pendant hydroxyl groups on the PVA structure that prevents particle aggregation. PVA is usually used as a stabilizer to produce stable nanoparticles with a small size and narrow size distribution [294]. Despite repeated washing steps, a fraction of PVA (used in nanoparticle preparation procedure) remains associated with the surface of nanoparticles [295, 296] and acts as a hydrophilic layer favouring the re-dispersion of the freeze-dried nanoparticles upon rehydration [290, 297]. The presence of PVA on the surface of nanoparticles at high concentrations masks the nanoparticles' surface and makes it difficult to measure the zeta potential.

## 8.2. Nanoparticles Formulation Characterization

### 8.2.1. Determination of Size and Zeta Potential

Table 8-2 demonstrates size, PDI, and zeta potential characteristics of plain and drug-loaded PLGA nanoparticles. Docetaxel-loaded PLGA nanoparticles had an average size of around 120 nm, while plain PLGA nanoparticles showed an average particle size of around 140 nm. Drug-loaded nanoparticles demonstrated PDI values between 0.216 and 0.289. Particle populations in both plain and drug-loaded samples demonstrated a homogenous distribution. PLGA nanoparticles exhibited zeta potential values between -20 and -32.

Table 8-2. Size and zeta potential characteristics of four formulations of drug-loaded PLGA nanoparticles (n=3).

| **Initial Preparation Concentration** | **Average Size (nm)** | **PDI** | **Zeta potential (mV)** |
|---|---|---|---|
| **Plain nanoparticles** | 140±9.0 | 0.299±0.054 | -20.97±2.03 |
| **0.25 mg/ml drug** | 122.2±5.1 | 0.216±0.040 | -25.5±0.75 |
| **0.5 mg/ml drug** | 122±1.4 | 0.229±0.010 | -32.1±2.9 |
| **1 mg/ml drug** | 128.6±9.0 | 0.289±0.051 | -27.6±1.8 |
| **1.5 mg/ml drug** | 123.6±9.5 | 0.245±0.041 | -28.3±1.25 |

Size, PDI, and zeta potential characteristics of plain and drug-loaded PLGA-PEG nanoparticles are exhibited in table 8-3. Plain PLGA-PEG nanoparticles demonstrated an average size range of around 180 nm. Docetaxel-loaded PLGA-PEG nanoparticles demonstrated an average size range between 184 and 188 nm. Plain and drug-loaded nanoparticles demonstrated uni-distributed populations as indicated by their PDI. PDI values of PLGA-PEG nanoparticles were around 0.100. Docetaxel-loaded nanoparticles

demonstrated zeta potentials between -24.7 and -27.0 mV, while plain PLGA-PEG nanoparticles had a zeta potential value of -26.7 mV.

Table 8-3. Size and zeta potential characteristics of four formulations of drug-loaded PLGA-PEG nanoparticles (n=3).

| **Initial Preparation Concentration** | **Average Size (nm)** | **PDI** | **Zeta potential** |
|---|---|---|---|
| **Plain NPS** | 180.8±8.2 | 0.100±0.004 | -26.7±4.9 |
| **0.25 mg/ml** | 188.6±5.9 | 0.096±0.004 | -24.7±2.4 |
| **0.5 mg/ml** | 184.6±4.6 | 0.105±0.003 | -27.0±5.6 |
| **1 mg/ml** | 186±4.3 | 0.100±0.023 | -25.6±4.6 |
| **1.5 mg/ml** | 186.7±2.9 | 0.103±0.10 | -25.9±3.5 |

Docetaxel-loaded PLGA nanoparticles demonstrated lower particle size compared to plain nanoparticles. This is attributed to docetaxel and PLGA polymer molecular structures: they are both highly hydrophobic agents. During formulation processes, both PLGA and docetaxel were dissolved in an organic solvent where they can interact with one another and with solvent molecules through non-covalent interactions. When the organic solution forms nano-droplets in the aqueous phase, hydrophobic forces between the polymer and drug can result in droplets with more condensed structures, due to those non-covalent hydrophobic interactions, compared to when only polymer molecules are present. Consequently, drug-loaded nanoparticles demonstrated a lower size distribution compared to plain nanoparticles [192].

However, it has been reported that loading the drug in nanoparticle formulations can result in an expansion of the polymeric matrix and increase in particle size [194], particularly when the drug concentration is high. To further evaluate this, three PLGA nanoparticle formulations were prepared at high docetaxel concentrations (3, 5, and 10 mg/ml). The

expected increase in size was evident when the preparation concentration was increased from 0.25 to 10 mg/ml (supplementary Table 1).

According to the PDIs of plain and drug-loaded nanoparticles, all formulations exhibit a uni-distribution pattern. Furthermore, a 5 to 12 unit increase in negativity of the zeta potential in drug-loaded nanoparticles is evident. However, it is reported that the association of the drug with the nanoparticles reduces the negativity of zeta potential by masking the effect of the adsorbed drug molecules on the nanoparticles' surface [194]. Again, the increase in negativity of the zeta potential of our nanoparticles is attributed to docetaxel's and PLGA polymer's molecular structures. Non-covalent interactions between the polymer and docetaxel can potentially result in a pronounced arrangement of the polymer's $COO^-$ terminals towards the particles' outer surface [298]. Other reports on docetaxel-loaded PLGA nanoparticles demonstrated similar ranges of particle size and zeta potential to our nanoparticles (i.e., sizes between 100 and 200 nm and negative zeta potential) [176, 194, 196, 299, 300].

Keum et al. [192] demonstrated that the size of the nanoparticles could be influenced by the mixing order of the drug and polymer and by sonicating the organic solvent prior to emulsification. They reported that sonication was likely to decrease the nanoparticle size owing to the increased energy released by emulsification, leading to a smaller particle diameter.

We followed a similar procedure. The mixture of the drug and polymer in ethyl acetate was sonicated prior to emulsification with aqueous phase. Supplementary table 2 summarizes the size, PDI, and zeta potential characteristics of particles obtained after this modification was made to the nanoparticle preparation procedure. Sonication decreased particle size and PDI, while not affecting zeta potential. This 30 to 40 nm reduction in size could be the result of better solvation of the drug and PLGA due to sonication of organic

solution and the reinforce hydrophobic interactions between the drug and polymer giving rise to nano-droplets with higher stability at lower sizes [192].

Plain and docetaxel-loaded PEGylated PLGA nanoparticles demonstrated a size range of around 180 nm. Drug-loaded PLGA-PEG nanoparticles showed a few nanometres of increase in particle size after association with docetaxel, which is attributed to the expansion of the polymer matrix due to the presence of the drug. Compared to docetaxel-loaded PLGA nanoparticles, PEGylated nanoparticles demonstrate larger particle sizes, which are attributed to the PEG moiety on the surface of PLGA-PEG nanoparticles. The PEG structure can protrude on the surface of particles and establish a core-shell structure with PLGA as the core and PEG as the shell [174]. Furthermore, it has been proposed that, in addition to the surface of nanoparticles, PEG structure of the di-block co-polymer can sometimes become entrapped inside nanoparticles matrix [185]. PLGA-PEG nanoparticles demonstrate zeta potentials similar to those of PLGA nanoparticles (around -25), while PEG is expected to mask the surface charge of particles and modify the zeta potential. Surface-modification efficiency of PEG generally dependents on the PEG layer thickness surrounding the nanoparticle, which is believed to be determined by the PEG polymer chain conformation, molecular weight, and surface density (coverage) [183, 186, 187]. Similar zeta potential of PLGA-PEG and PLGA nanoparticles is attributed to low surface coverage of PEG molecules (taking a ‘mushroom’ configuration) contributing to gaps in the protective layer [183] as a result of using PLGA with only 15% PEGylation (weight).

Koopaei and colleagues [301] obtained docetaxel loaded PLGA-PEG nanoparticles with a size of 181±3.5 nm, which is in accordance with the size of nanoparticles obtained in our work. Other studies have reported similar ranges of particles size and zeta potential for docetaxel-loaded PLGA-PEG nanoparticles to those observed from our study [176, 299, 301].

### 8.2.2. Determination of Loading and Encapsulation Efficiency

Table 8-4 demonstrates drug-loading (%), yield, and encapsulation efficiency (%) of the PLGA nanoparticle preparation method. Drug-loading (%) represents the amount of docetaxel (mg) loaded in 100 mg of nanoparticles. Encapsulation efficiency (%) represents the percentage of docetaxel loaded in nanoparticles with respect to the initial drug amount used for nanoparticle preparation. At different formulations, between 1.20 and 5.58 µg docetaxel was loaded into one milligram of nanoparticles. Drug-loading percentages increased parallel to the initial concentrations of the docetaxel used during nanoparticle preparation process. Nanoparticle fabrication at four different initial docetaxel concentrations resulted in a drug encapsulation efficiency maximum of 47.76% and minimum of 37.25%. The nanoparticle preparation method demonstrated yields between 31.66% and 64.88%.

Table 8-4. Drug-loading characteristics of four formulations of docetaxel-loaded PLGA nanoparticles (n=3).

| **Initial Preparation Concentration** | **Drug loading (%)** | **Yield (%)** | **Encapsulation efficiency (%)** |
|---|---|---|---|
| **0.25 mg/ml** | 0.12±0.004 | 39.76±4.56 | 47.76±1.68 |
| **0.5 mg/ml** | 0.21±0.008 | 31.66±4.04 | 41.28±1.6 |
| **1 mg/ml** | 0.45±0.044 | 56.33±11.15 | 45.26±4.4 |
| **1.5 mg/ml** | 0.56±0.025 | 64.88±8.13 | 37.25±1.6 |

Table 8-5 demonstrates various particle characteristics obtained from PLGA-PEG nanoparticles. Drug encapsulation efficiency of the PLGA-PEG nanoparticle preparation method was between 59% and 96%. The percentage of drug loading demonstrated an increasing trend parallel to the increment made in the initial docetaxel preparation

concentration (i.e., from 0.24% to 0.889%). The yield was between 56.2% and 85.7% and between 2.405 and 8.890 µg of docetaxel was loaded in each mg of nanoparticles.

Table 8-5. Drug-loading characteristics of four formulations of drug-loaded PLGA-PEG nanoparticles (n=3).

| **Initial Preparation Concentration** | **Drug loading (%)** | **Yield (%)** | **Encapsulation efficiency (%)** |
|---|---|---|---|
| **0.25 mg/ml** | 0.240±0.008 | 78.1±0.6 | 96.1±3.2 |
| **0.5 mg/ml** | 0.3512±0.031 | 84.5±7.1 | 70.2±6.1 |
| **1 mg/ml** | 0.623±0.008 | 56.2±12.3 | 62.3±0.8 |
| **1.5 mg/ml** | 0.889±0.010 | 85.7±3.6 | 59.3±0.7 |

The drug loading of PLGA nanoparticles demonstrated increases parallel to the increase in initial preparation concentrations of the drug. This finding was expected [176], because with increased drug concentration in the organic solution, more drug molecules can interact with PLGA [192]. However, from the lowest concentration of docetaxel (0.25 mg/ml) to the highest (1.5 mg/ml), the percentage of encapsulation efficiency showed a descending trend from 47.76% to 37.25%. This is attributed to the fact that the PLGA matrix becomes saturated as the initial concentration of docetaxel increases [192]. Different studies have used different settings to fabricate docetaxel-loaded PLGA nanoparticles and thus have reported various drug loading and encapsulation efficiencies (ranging from 16% to 76%) [176, 194, 196, 299, 300].

PLGA-PEG nanoparticles demonstrated similar drug loading and encapsulation efficiency trend. Drug loading increased parallel to the increase in initial preparation concentrations, while the method's encapsulation efficiency demonstrated a converse

relationship to the initial preparation concentration of the drug. In other words, encapsulation efficiency decreased from 96.1% to 59.3% when the initial drug payload increased from 0.25 mg/ml to 1.5 mg/ml. The initial high encapsulation efficiency (e.g., at 0.25 mg/ml) might be due to high interactions of the drug with the polymer relative to the initial drug amount until polymer matrix becomes saturated with drug molecules, such as when a higher concentration is initially used in the preparation procedure [176].

Compared to PLGA nanoparticles of same docetaxel preparation concentration, PLGA-PEG nanoparticles showed a higher drug loading. This could be attributed to the presence of PEG moiety in the infrastructure of PLGA-PEG nanoparticles. A hydrophilic PEG section of di-block copolymer that protrudes on the surface of nano-droplets can influence the hydrophobic interactions inside nano-droplets between the PLGA and drug molecules and ultimately provide more room to accommodate docetaxel molecules in the lipophilic matrix [302]. In addition to the surface of nanoparticles, PEG structure of the di-block co-polymer can sometimes become entrapped inside nanoparticles matrix [185]. This, again, could potentially contribute to the accommodation of more docetaxel molecules in PLGA-PEG nanoparticles.

### 8.2.3. Determination of Drug Release Profile from Nanoparticles

The release profile of docetaxel from different PLGA nanoparticle formulations is exhibited in figure 8-3. As evident, all formulations exhibit a biphasic drug-release profile. Particles demonstrate a burst release during the first 24 hours, followed by a sustained drug release, resulting in cumulative liberation of between 16 and 36 % of the loaded drug. The release profile of docetaxel from different PLGA-PEG nanoparticle formulations is exhibited in figure 8-4. As shown in the figure, docetaxel-loaded PLGA-PEG nanoparticles exhibited a biphasic drug release pattern. The release profile starts at a higher rate in the first 24 hours

followed by a lower pace. After 5 days, 50% to 60% of loaded drug was released from the PLGA-PEG nanoparticles.

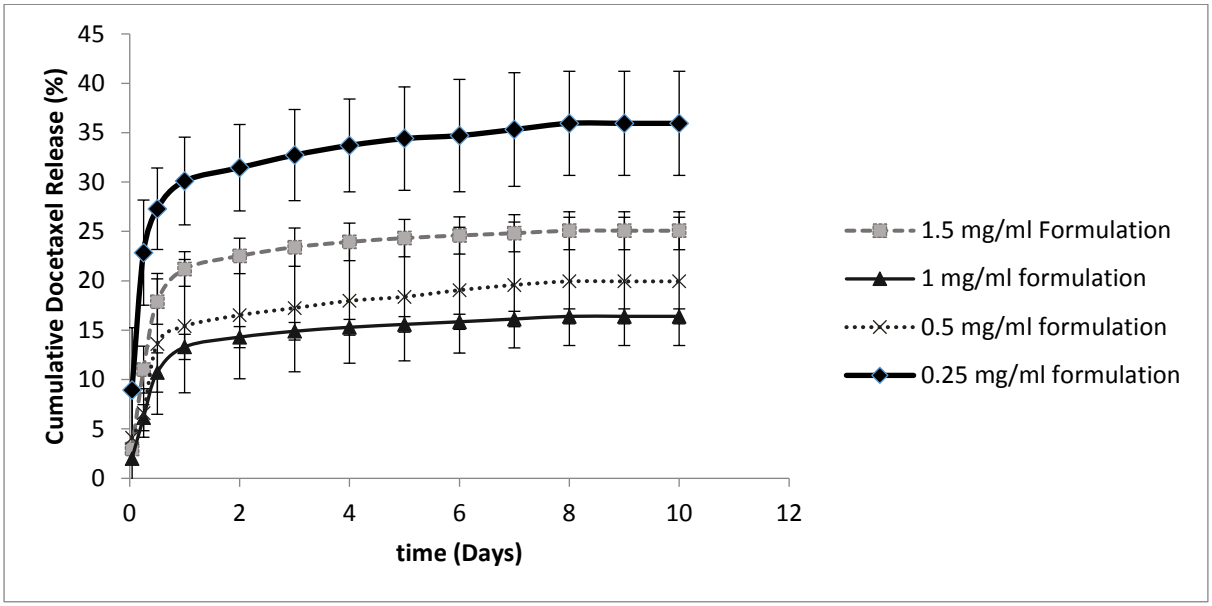


Figure 8-3. Release of docetaxel from four PLGA nanoparticle formulations (n=3).

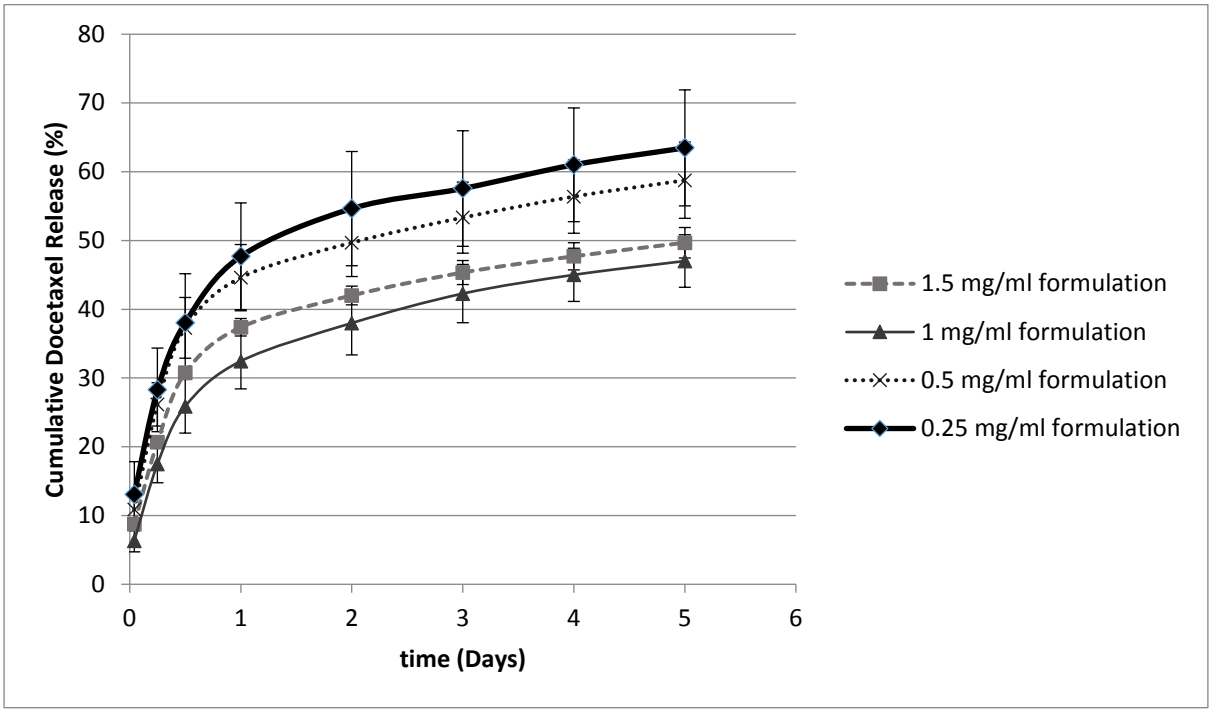


Figure 8-4. Release of docetaxel from four PLGA-PEG nanoparticle formulations (n=3).

Generally, this initial burst can be attributed to the drug molecules embedded at nanoparticle's outermost layers and those adsorbed by the particles' surface. The obtained profile after the initial burst shows a sustained release pattern, giving rise to drug-depletion from various formulations during the incubation period. Diffusion of the drug, erosion and swelling of the polymer matrix, and degradation of the polymer are considered to be the main mechanisms for drug release [192]. This sustained release behaviour can be attributed to the slow degradation rate of PLGA polymer [303]. Therefore, it is believed that the release of docetaxel from the nanoparticles depends mainly on drug diffusion and matrix erosion [304]. Accordingly, particle size, hardness, and porosity can potentially influence the drug release profile [122]. Despite the differences in the total percentages of the liberated drug from the nanoparticles, the biphasic release from PLGA nanoparticles has been reported by other studies [176, 194, 196, 301].

In a similar manner, docetaxel release behaviour observed from PLGA-PEG nanoparticles is also attributed to the liberation of surface-adsorbed/near-surface drug molecules (initial burst release) and further diffusion of the drug from the polymer matrix (sustained release). PLGA-PEG nanoparticles demonstrated a higher percentage of drug release (47% to 63%) compared to that observed from PLGA nanoparticles (16% to 36 %). This difference could be attributed to the role of PEG chain moieties on the surface of PLGA-PEG nanoparticles. PEG molecules can attract water to the surface of nanoparticles and result in more pronounced wetting/hydration of PLGA-PEG nanoparticles [305] and ultimately bring about higher release percentages compared to naked PLGA nanoparticles. In addition, the PEG structure of the di-block co-polymer can sometimes become entrapped inside nanoparticles matrix [185]. This may affect the integrity of PLGA-PEG nanoparticle matrix by making it more hydrophilic, which would contribute to more pronounced hydration of the

nanoparticles. Various experiments reported a similar biphasic docetaxel release pattern from drug-loaded PLGA-PEG nanoparticles [176, 299, 301] to that observed in our formulations.

According to Abouelmagd [306] and colleagues, release profile of poorly water-soluble drugs such as paclitaxel could be different in various media. They studied the release profile of paclitaxel from PLGA nanoparticles in PBS and in PBS/fetal bovine serum (FBS). They observed that the extent of drug release was higher when FBS was present (98%) compared to PBS (34%). They attributed this difference to the role of serum proteins offering solubilizing effect to the drug. They concluded that measuring drug release in PBS could result in under-estimation of the extent of drug release.

### 8.3. Determination of Biological Activity of Docetaxel Loaded in Nanoparticles

Figure 8-5 exhibits the biological activity of docetaxel loaded in PLGA and PLGA-PEG nanoparticles on Hela cancer cells compared to that of the free drug in a set of concentrations (25-400 ng/ml) at various incubation times. Hela cells were also treated and incubated with plain nanoparticles to determine cytotoxicity of empty PLGA and PLGA-PEG. The results showed that plain nanoparticles did not influence cell viability. At six hours of incubation, the free docetaxel solution demonstrated cell viability of 81-94 % (at various concentrations). Cell viability for docetaxel-loaded PLGA and PLGA-PEG nanoparticles (at various concentrations) were 88-107% and 79-99%, respectively. At 12 hours of incubation, the free drug solution demonstrated 34-54% cell viability, while PLGA and PLGA-PEG nanoparticles respectively exhibited 29-62% and 32-74% cell viability. After 24 hours of incubation, the free docetaxel solution, docetaxel-loaded PLGA nanoparticles, and docetaxel-loaded PLGA-PEG nanoparticles resulted in 5-31%, 3-32%, and 3-38% cell viability, respectively. Incubation of cells with the free docetaxel solution, docetaxel-loaded PLGA and

docetaxel-loaded PLGA-PEG nanoparticles for 48 hours resulted in 2-7%, 2-9% and 3-25% cell viability, respectively.

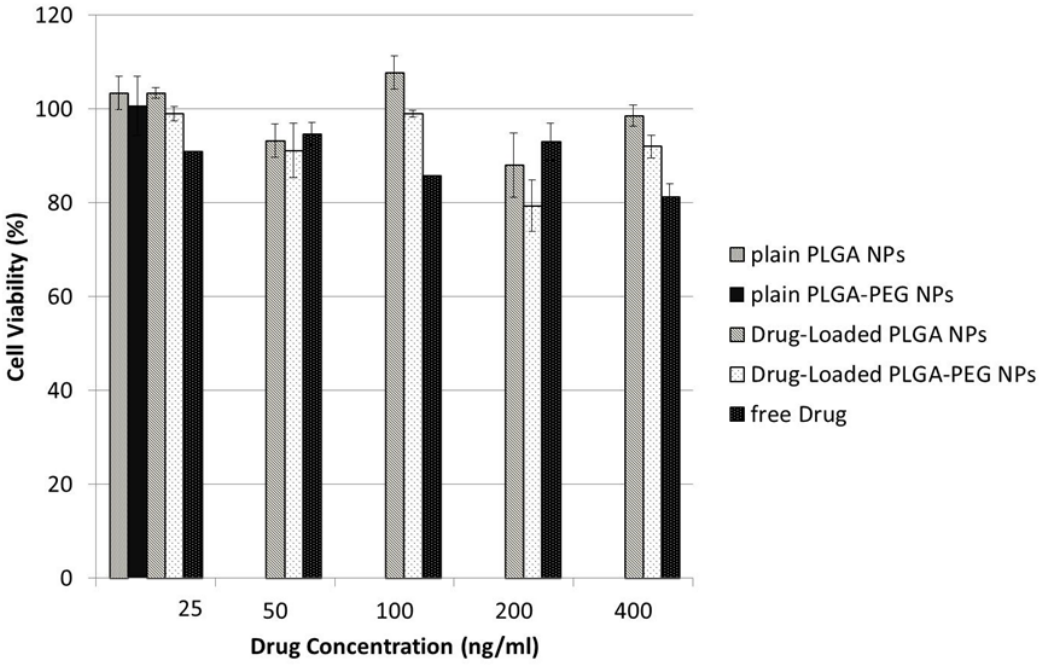


**A)**

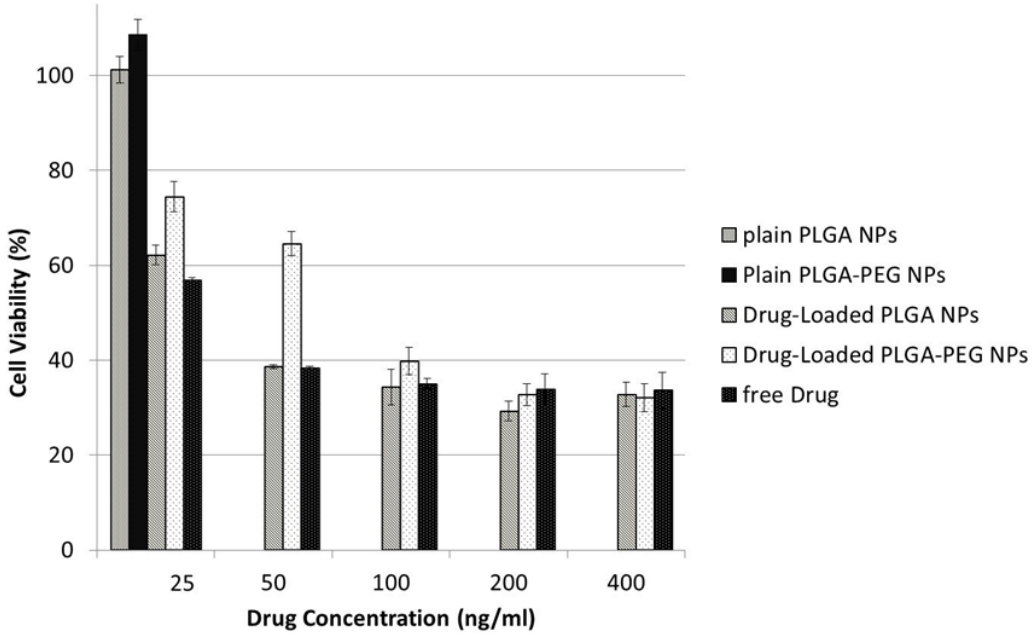


**B)**

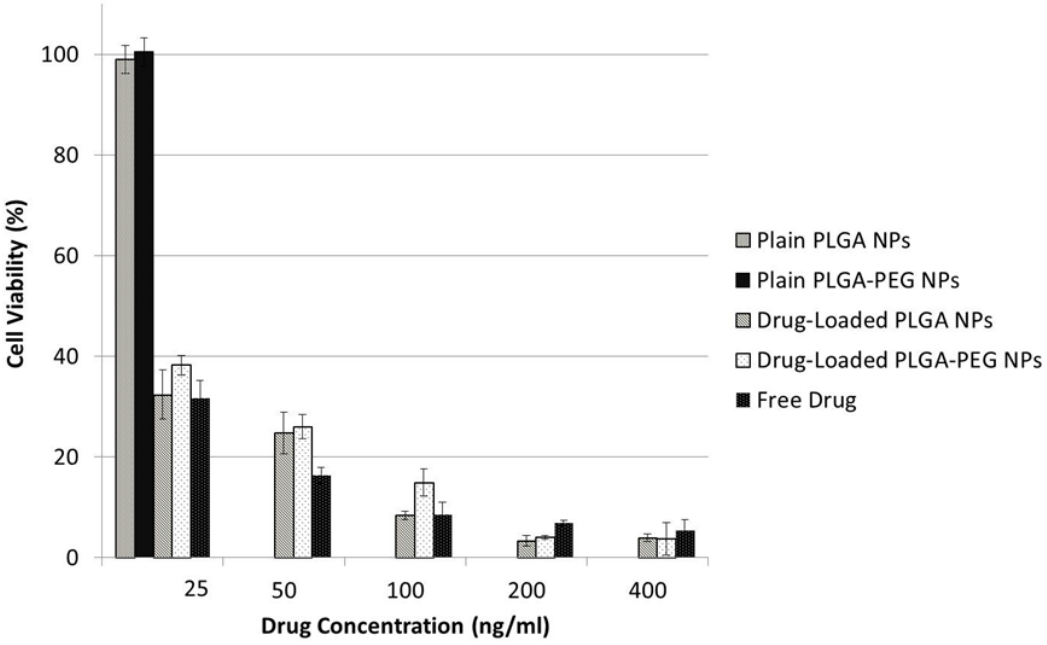


**C)**

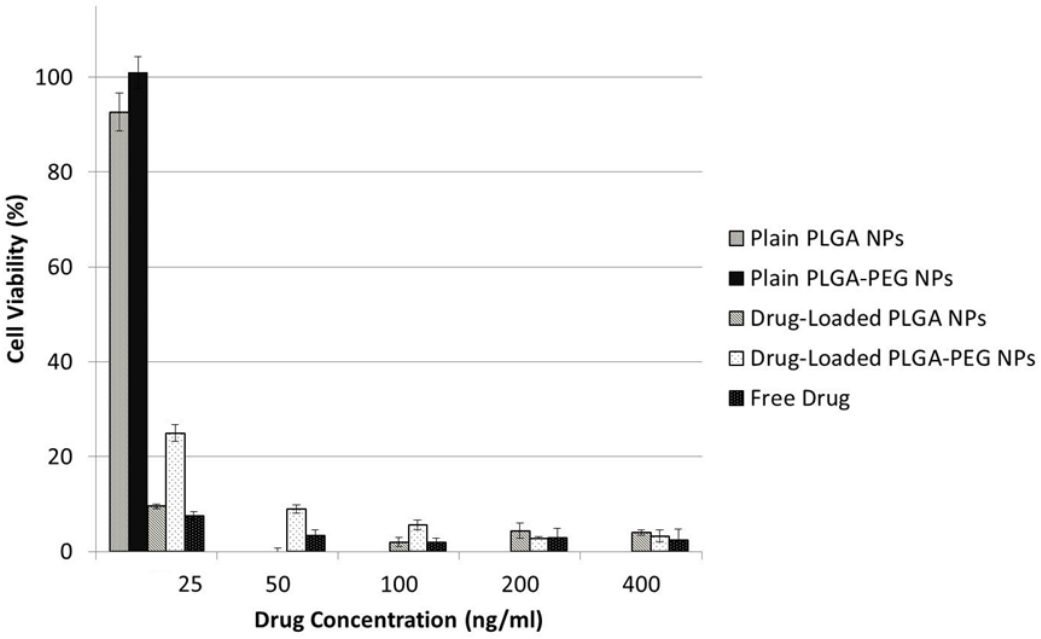


**D)**

Figure 8-5. Effect of plain PLGA and PLGA PEG nanoparticles, free docetaxel, and docetaxel loaded in PLGA and PLGA-PEG nanoparticles on the viability of Hela cells (Human Cervix Carcinoma) after incubation for A) 6 hours, B) 12 hours, C) 24 hours, and D) 48 hours (n=3).

As exhibited in figure 8-5, plain PLGA and PLGA-PEG nanoparticles did not affect viability of Hela cell lines even after 48 hours of incubation. Thus, the observed cytotoxicity from drug-loaded nanoparticles was due to the docetaxel loaded in nanoparticles and not plain nanoparticles [176]. It also demonstrates that biological/pharmacological activity of docetaxel is not affected by its association with the nanoparticles. The proliferation of Hela cancer cell lines was inhibited with even low drug concentration (25 ng/ml) formulas over the 12, 24, and 48 hours of incubation. In contrast to the free drug solution, the cytotoxicity of docetaxel loaded in nanoparticles could be attributed to a series of mechanisms [300] as follows. Nanoparticles can potentially interact with cells and become located near the cell membrane. This could result in the up-holding of an elevated drug concentration adjacent to the cell membrane and result in a concentration gradient that promotes the drug's influx into the cell [307]. It is believed that the efflux transport mechanisms of cancer cells (responsible for multi-drug resistance), such as P-glycoprotein (P-gp) pumps, could contribute to transport out a portion of free drug, which entered the cytoplasm by passive diffusion [308, 309]. Usually, this happens substantially with free drug administration [310]. Considering the possibility that nanoparticles could station near the cells and contribute to elevated drug concentration at the cell membrane, the efflux transport mechanism could become saturated and possibly result in pronounced drug uptake [311, 312]. Another possibility is that drug-loaded nanoparticles could get up taken by cells [313] and ultimately increase the uptake of the entrapped drug [314]. The possibility of cell-internalization could further bypass the effect of P-gp pumps. This potentially contributes to the drug accumulation near the drug's site of action (i.e., cytoplasm) [315]. The release pattern of drug from nanoparticles could be mentioned as another possible contributing factor to the cytotoxicity of docetaxel encapsulated in nanoparticles, [168, 196, 316]. According to the release profile of docetaxel

from PLGA or PLGA-PEG nanoparticles (figures 8-3 and 8-4), only a portion of loaded drug is released and becomes available during the first 12, 24, or 48 hours of incubation. In the study by Abouelmagd [306] and colleagues, they observed that the extent of drug release was higher in the presence of serum proteins (98% in PBS/FBs versus 34% in PBS). They attributed this difference to the role of serum proteins offering solubilizing effect to the drug. They concluded that measuring drug release in PBS could result in under-estimation of the extent of drug release. Therefore, it is probable that nanoparticles release larger amount of docetaxel in culture media than in PBS alone (our release test). In case of the free solution of drug, the whole amount of drug is available to cancer cells extracellularly during the incubation period. In contrast, only a portion of docetaxel is available to cells either extracellularly or intracellularly at a time, which contributes to the observed cytotoxicity. In their study, Sims and colleagues [317] evaluated the uptake and transport of PLGA nanoparticles in Hela cells. Accordingly, they demonstrated that, upon contact (incubation) with PLGA nanoparticles, Hela cells engage in both association and internalization acts. However, the association between the nanoparticles and cells was more pronounced compared to the internalization of nanoparticles.

# CHAPTER 9*

## Result and Discussion on Mass spectrometry Method for Quantification of Docetaxel

***** Chapter 5 (Experimental Section on Mass spectrometry Method for Quantification of Docetaxel) along with chapter 9 have been published as 'Original Research Articles' in '*American Journal of Analytical Chemistry'* and '*Current Pharmaceutical Analysis* ':

Pedram Rafiei, Deborah Michel, Azita Haddadi. Application of a Rapid ESI-MS/MS Method for Quantitative Analysis of Docetaxel in Polymeric Matrices of PLGA and PLGA-PEG Nanoparticles through Direct Injection to Mass Spectrometer. *American Journal of Analytical Chemistry***.** 2015, Volume 6, Number 2, pages 164-175

Pedram Rafiei, Jane Alcorn, Azita Haddadi. Application of a rapid ESI-MS/MS method for quantitative analysis of docetaxel in mouse biological matrices through direct injection to mass spectrometer. *Current Pharmaceutical Analysis***.** 2017, Volume 13.

### Background

Various analytical methods have been developed to quantitatively evaluate docetaxel in polymeric matrices. The majority of studies have benefited from high performance liquid chromatography (HPLC) [176, 194, 196, 300, 318, 319], while a few have applied the UV method [299]. Likewise, several analytical methods have been developed to quantify docetaxel in biological matrices. Available reports have used only HPLC-UV [320, 321] or HPLC coupled to mass spectrometer [322-330]. Due to the inherent specificity and sensitivity, LC-MS/MS is the preferred analytical instrument for quantitative analysis of drugs in various matrices. However, long separation times are usually needed and many resources are required to establish a proper liquid chromatographic (LC) method, particularly if additional techniques (e.g., temperature-programmed or gradient elution) are used.

Therefore, using rapid and simple analysis methods for the fast screening of samples in biologic and non-biologic matrices seems more logical. LC as the limiting step of the quantitative analysis method can be omitted to further speed up the procedure. Many examples of analysis techniques applying mass spectroscopy without LC exist [331-334]. Direct injection into the mass spectrometer can be used as an alternative to LC and MS coupled methods [335, 336].

Here, a method for rapid quantification of docetaxel in PLGA and PLGA-PEG polymer matrices, as well as mouse serum and liver, was developed and partially validated. Simple extraction techniques were used to extract docetaxel from various matrices followed by a positive electrospray ionization-tandem mass spectrometry detection approach. The procedure was performed without the application of a LC column.

### 9.1. Determination of MS/MS Fragmentation Patterns

Figures 9-1 and 9-2 demonstrate electrospray ionization (ESI)-MS/MS (positive ion mode) product-ion spectra of docetaxel (809.4 m/z) and paclitaxel (855.2 m/z). A large abundance of the precursor ion was observed in the MS/MS spectra of both materials as protonated entities ($[M+H]^+$). The proposed fragmentation pattern of each compound is provided in upper-right section of the figures. In addition, the proposed molecular structures of the product ions resulting from the fragmentation of docetaxel and paclitaxel are presented in figure 9-3 and 9-4, respectively. As exhibited in figure 9-1, six product ions of docetaxel demonstrated high intensities: the product ions with an m/z of 226, 91, 105, 182, 528, and 119. The most abundant product ion was used in subsequent MRM transitions. Among those, the product ion with m/z of 226 demonstrated the highest intensity. In the case of paclitaxel (figure 9-2), product ions with m/z of 105, 106, 122, 286, 287, and 570 produced high intensities, and the product ion with m/z of 105 provided the highest intensity.

Depending on the experimental conditions, docetaxel and paclitaxel tend to generate different adducts when ionized through an ESI source. Some studies have reported the alkali-adducts (mainly sodium adduct $[M+Na]^+$) are more intense (up to 5-fold) than the protonated form ($[M+H]^+$) [327, 337, 338]. However, some reports have exploited the protonated adduct MRM transitions [339, 340] with good sensitivity. For instance, in the study by Du and colleagues [341] in which +ESI condition was used, docetaxel and paclitaxel formed the protonated adducts predominantly. Taking into consideration the conditions used in this analysis method (e.g., isocractic elution), we concluded that the protonated adduct could be the prominent ion. In addition, low concentration of formic acid in mobile phase has found to be effective in enhancing the ionization efficiency [342] and improve the signal response. Consequently, in our study, analysis was performed at the chosen MRM transitions in the presence of 0.1 % v/v formic acid in methanol to obtain the protonated adduct for the analyte and internal standard. Total run time of a sample was 2 minutes which was shorter than that used in previous studies [339, 340]. For example, in the study by Yamaguchi and colleagues [339] total analysis run-time was 5 minutes through which retention time of docetaxel and paclitaxel was 3.6 and 4.2 minutes. Du et al. [341] used ultra-high performance liquid chromatography and docetaxel and paclitaxel had a run time of 2.5 minutes (retention time: 1.35 minute). Figure 9-5 demonstrates the typical MRM graphs of docetaxel and paclitaxel in methanol. As shown, the peak response at the selected transitions had same retention times and varied in response. MRM graphs of docetaxel and paclitaxel in extracts of non-biological matrices (PLGA and PLGA-PEG nanoparticles) are demonstrated in supplementary figures 7. MRM graphs of docetaxel and paclitaxel in extracts of biological matrices are exhibited in supplementary figures 11 and 13.

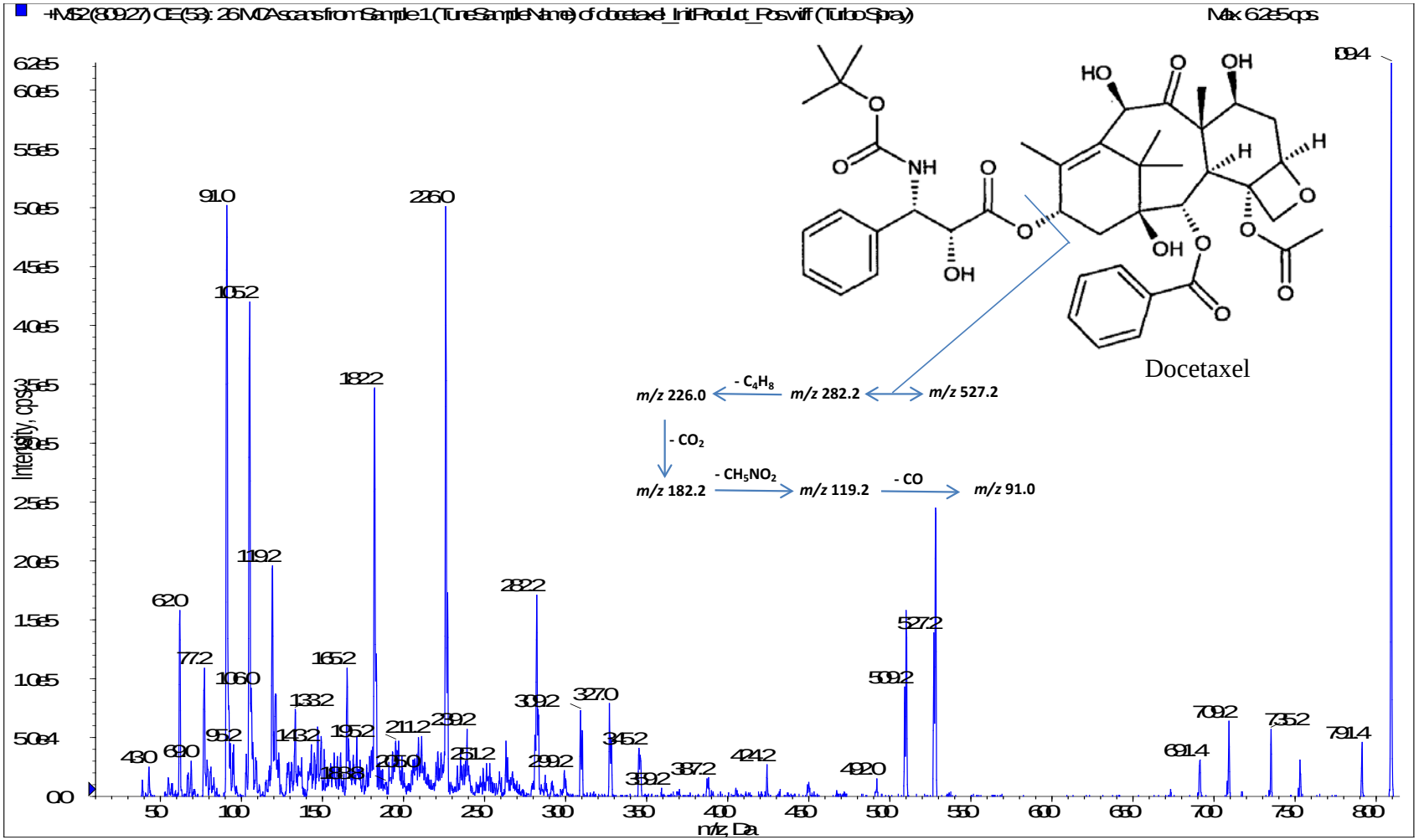


Figure 9-1. Electrospray ionization (ESI)-MS/MS (positive ion mode) product-ion spectrum of docetaxel (10 µg/mL in methanol containing 0.1% (v/v) formic acid).

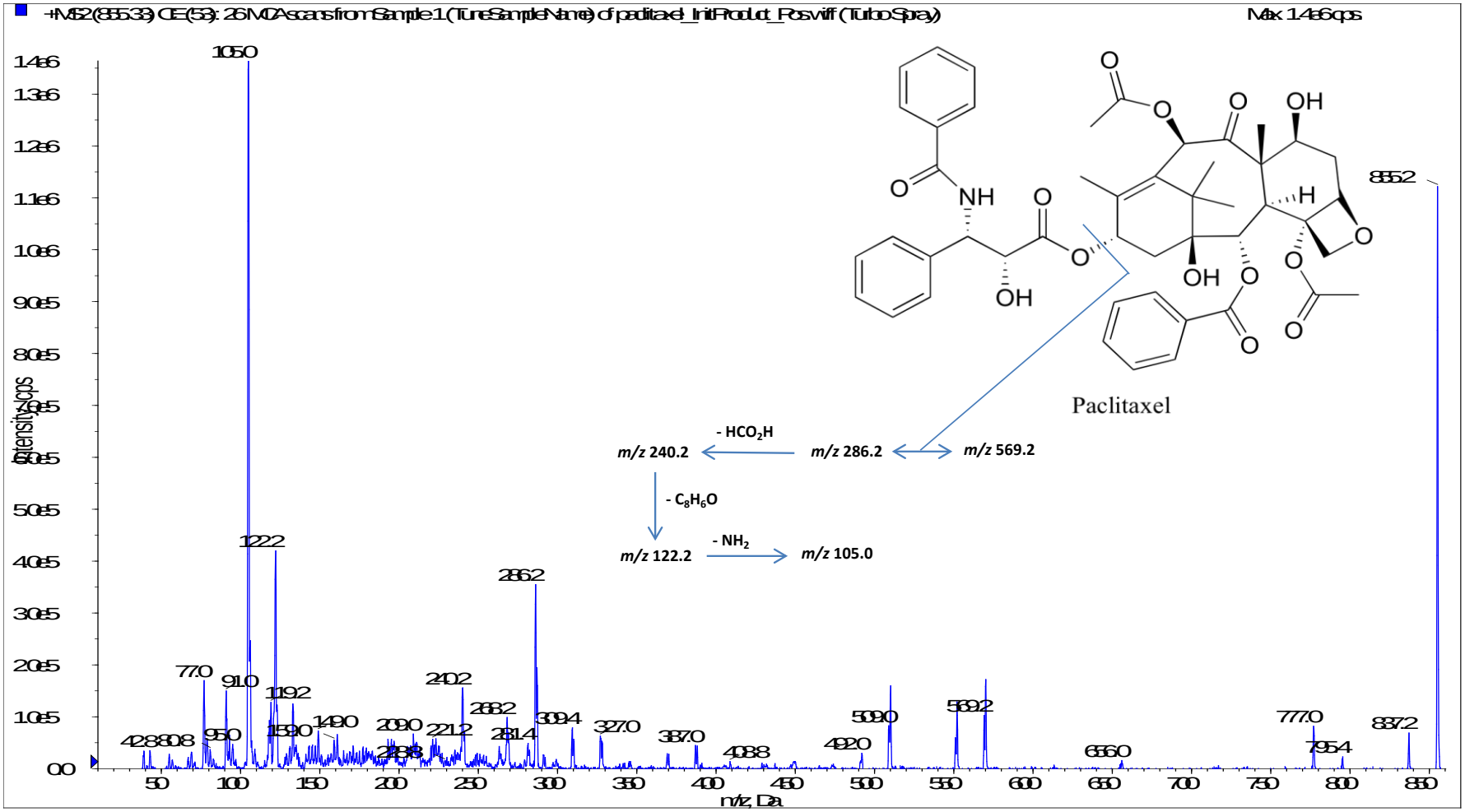


Figure 9-2. Electrospray ionization (ESI)-MS/MS (positive ion mode) product-ion spectrum of paclitaxel (10 µg/mL in methanol containing 0.1% (v/v) formic acid).

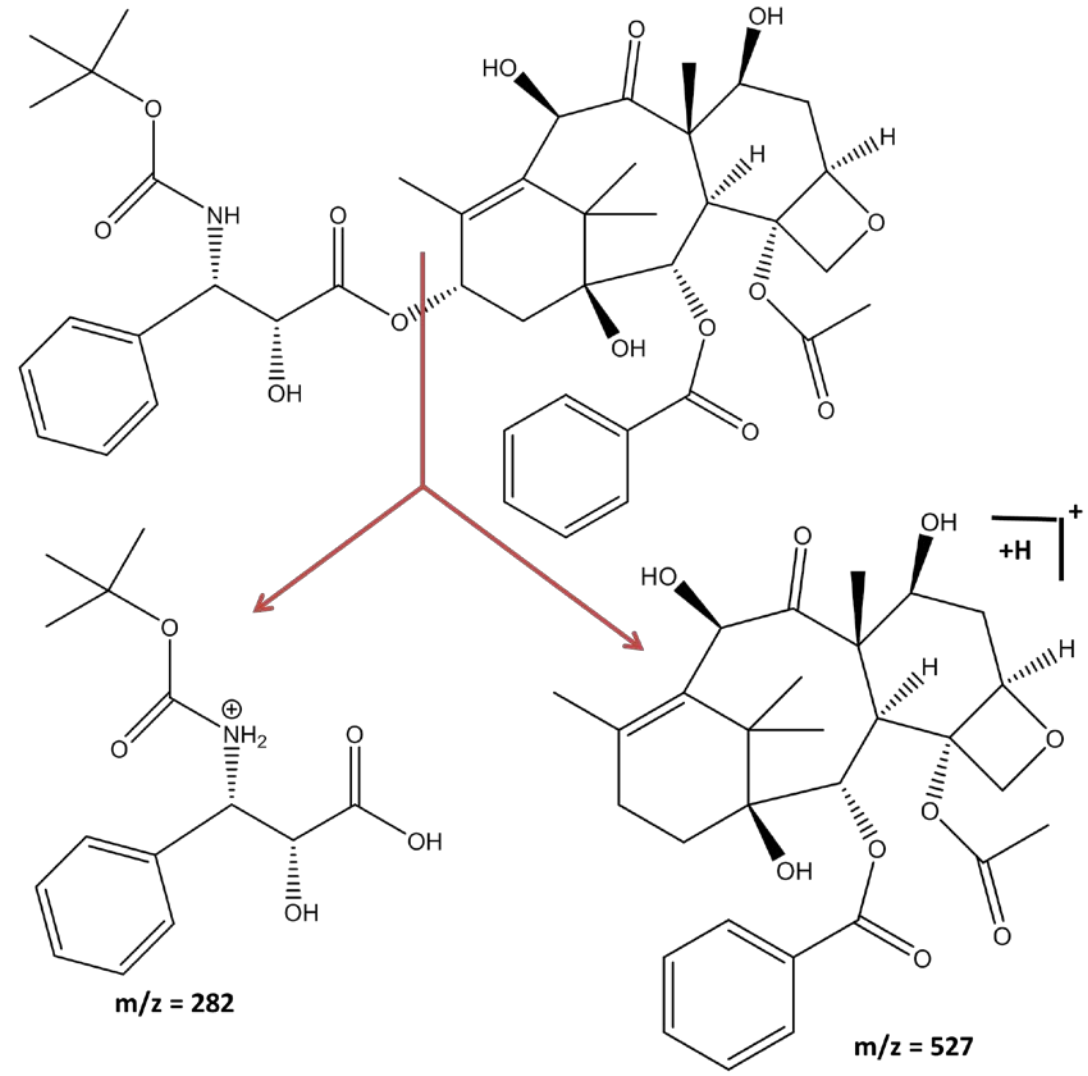
m/z = 282
+H
m/z = 527

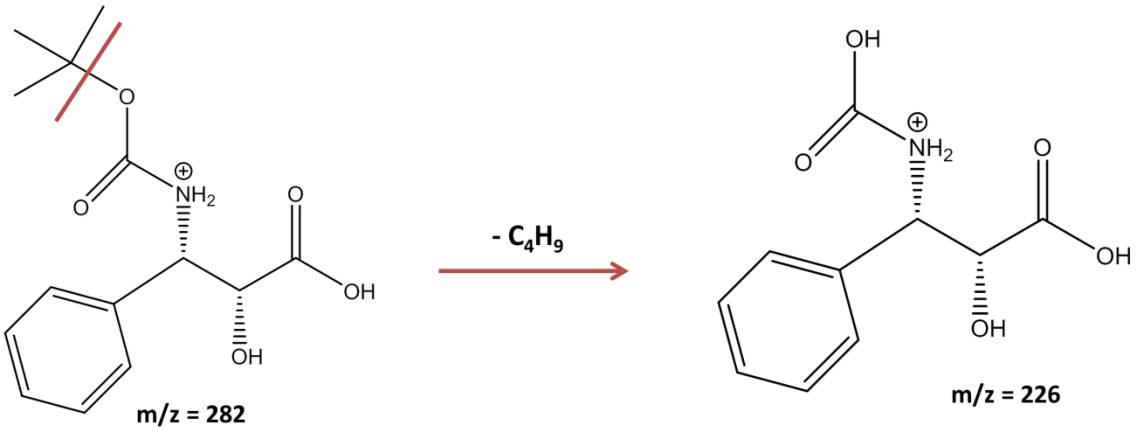
- C4H9
m/z = 282
m/z = 226

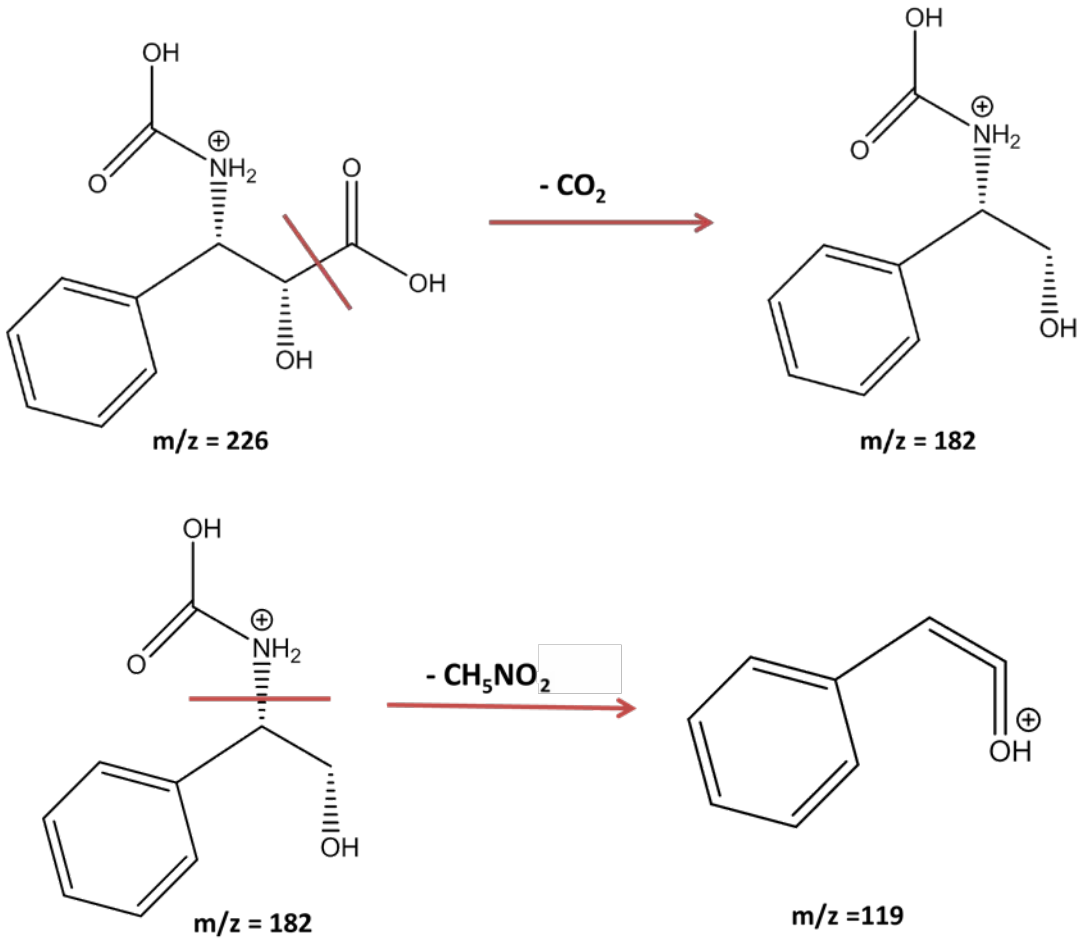


Figure 9-3. Product-ion molecular structures from docetaxel after electrospray ionization (ESI)-MS/MS (positive ion mode) (10 µg/mL in methanol containing 0.1% (v/v) formic acid).

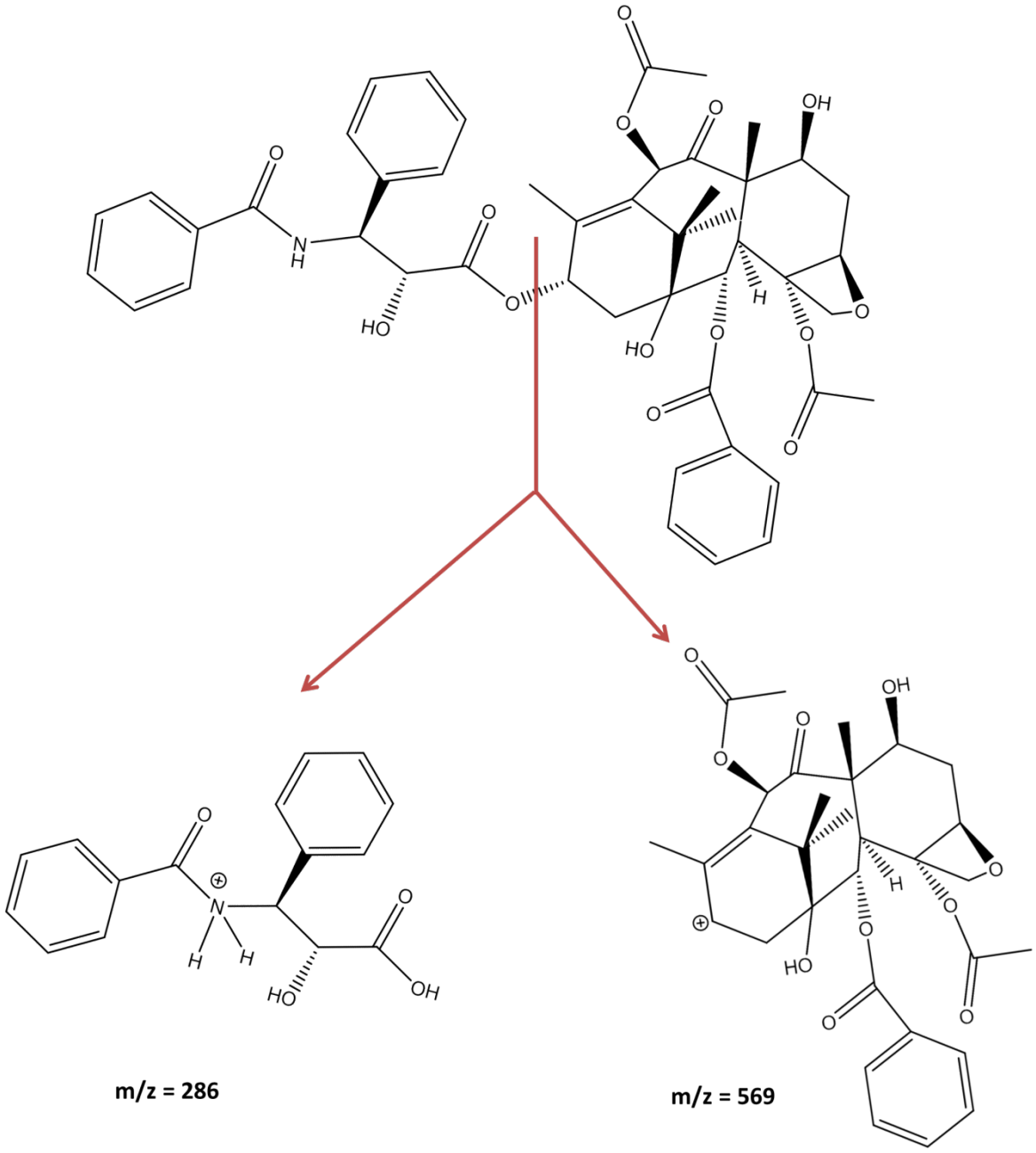
m/z = 286
m/z = 569

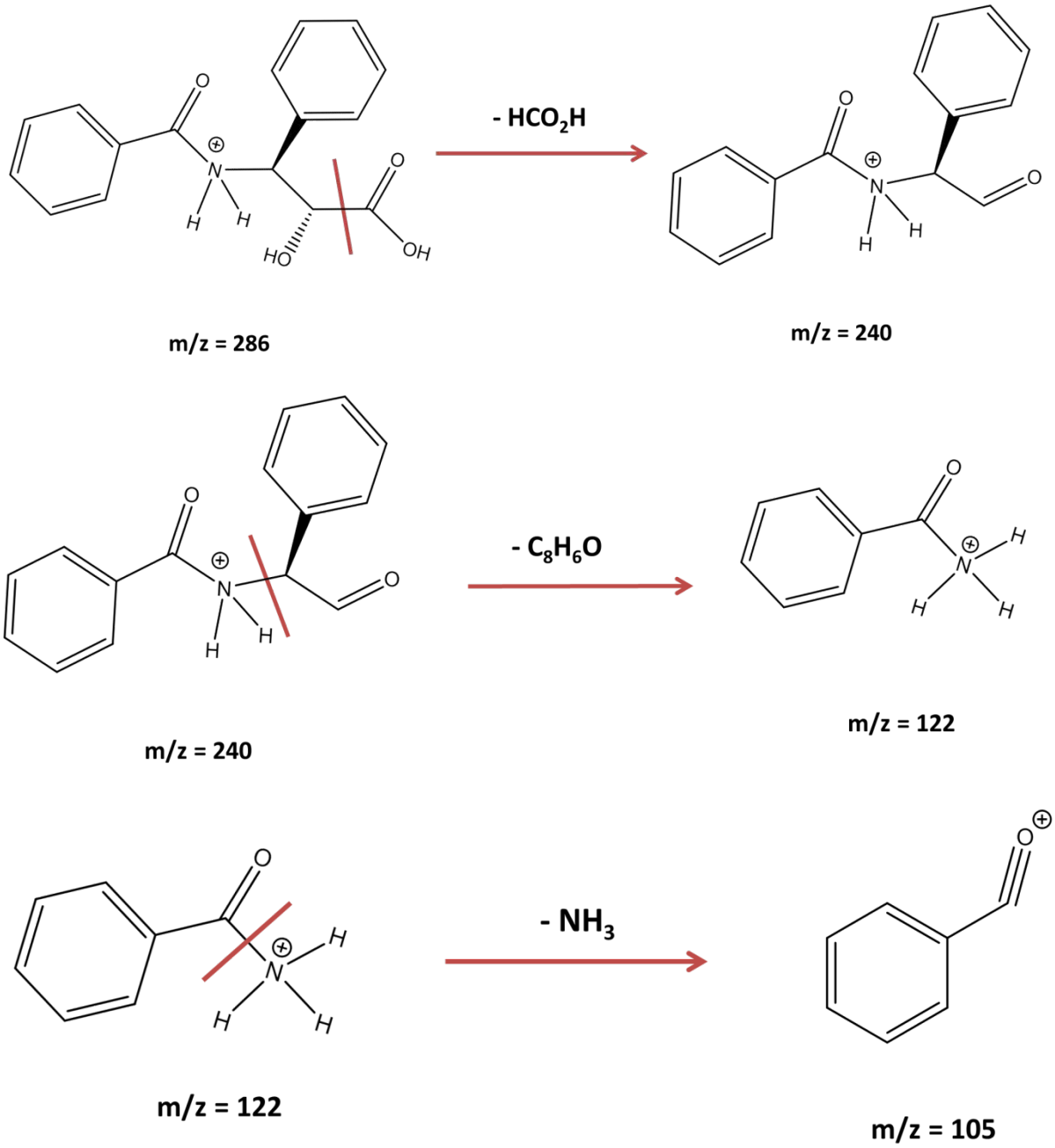


Figure 9-4. Product-ion molecular structures from paclitaxel after electrospray ionization (ESI)-MS/MS (positive ion mode) (10 µg/mL in methanol containing 0.1% (v/v) formic acid).

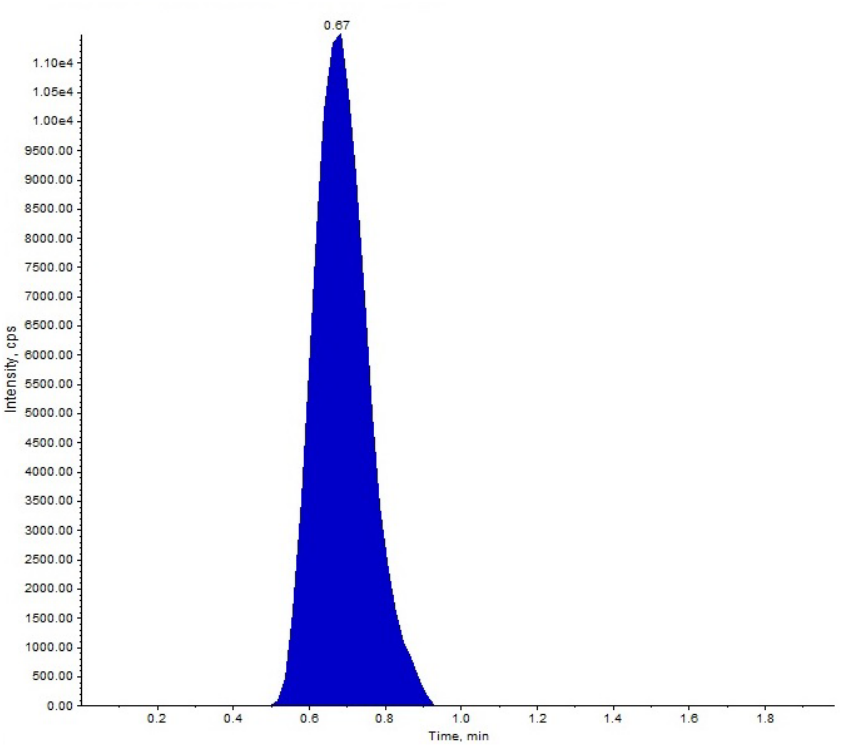


A)

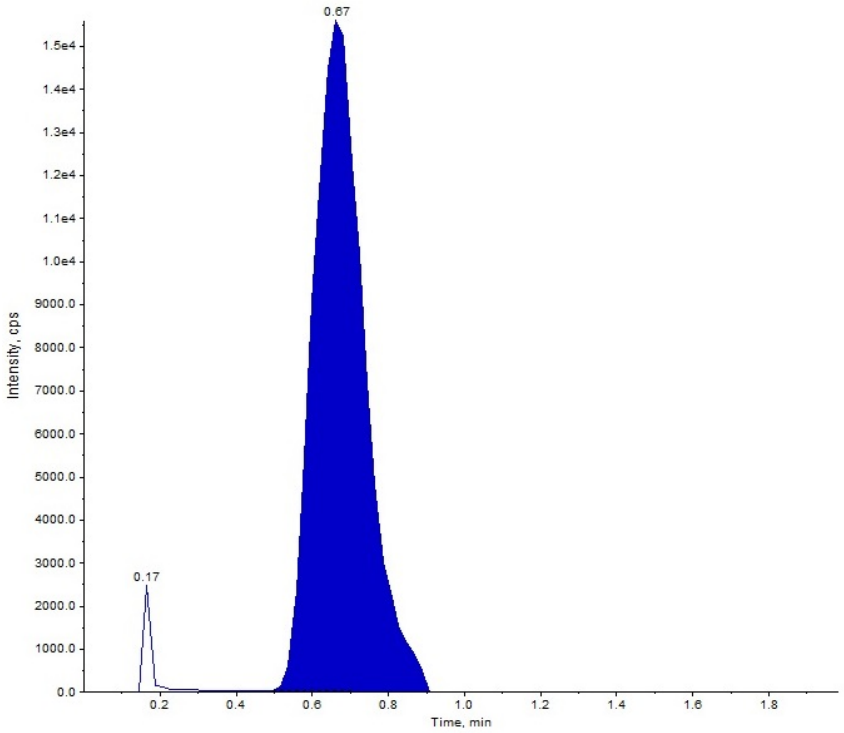


B)

Figure 9-5. Typical MRM graph of A) docetaxel (m/z=226) and B) paclitaxel (internal standard) (m/z= 105) (1000 ng/ml) in methanol.

## 9.2. Docetaxel in Non-biological Matrices

### 9.2.1. Limits of Detection and Quantitation

The LOD and quantitation LOQ of the method used to quantify docetaxel in methanol were found to be 1.95 ng/ml and 3.9 ng/ml, respectively. The LOD and LOQ of the used quantitation method of docetaxel in both nanoparticle types (PLGA and PLGA-PEG nanoparticles) were 62.5 ng/ml and 125 ng/ml, respectively.

### 9.2.2. Linearity

A linear regression analysis was carried out on known added concentrations of docetaxel against the peak area ratio of docetaxel to paclitaxel and weighted 1/x. The analysis produced linear responses throughout the wide range of docetaxel concentrations in methanol from 3.9 to 1000 ng/ml with $R^2$, slope, and intercept values of 0.9966, 0.000789, and 0.00269, respectively, providing the typical equation of y=0.000789x+0.00269 for a set of concentrations (n=3) as shown in supplementary figure 8.

The analysis also produced linear responses throughout the wide range of docetaxel concentration of 125-16000 ng/ml, and 125-8000 ng/ml in PLGA nanoparticles and PLGA-PEG nanoparticles, respectively. $R^2$, slope, and intercept demonstrated values equal to 0.9978, 0.00084, and 0.023 for PLGA nanoparticles and 0.9966, 0.000778, and 0.108, for PLGA-PEG nanoparticles, respectively. The typical equations of the lines for PLGA and PLGA-PEG nanoparticles were respectively y=0.00084x+0.023 and y = 0.000778x + 0.108 for a set of concentrations (n=3). Supplementary figures 9 and 10 demonstrate typical daily calibration curves of the method for PLGA and PLGA-PEG nanoparticles, respectively.

### 9.2.3. Method Precision and Accuracy

Within- and between-run variations (precision) and accuracy of the docetaxel quantitation method in methanol are shown in table 9-1. As evident, quality control samples demonstrated deviations of less than 15% (i.e., ±15%), showing that this method can quantitate docetaxel in methanol with acceptable precision and accuracy. The variation evident in LOQ concentration (3.9 ng/ml) was within an acceptable range (i.e., ±20%) (n=6).

Within- and between-run variations (precision) and accuracy of the docetaxel quantitation method in PLGA and PLGA-PEG nanoparticles are shown in tables 9-2 and 9-3, respectively. The quality control samples demonstrated deviations of less than 15% (i.e., ±15%), showing that the method can quantitate docetaxel in nanoparticle formulations with acceptable precision and accuracy. The variation evident in the LOQ concentration (125 ng/ml) was within acceptable range (i.e., ±20%) (n=6).

Table 9-1. Accuracy and precision of mass spectrometry analysis method for docetaxel quantitation in methanol. Data represents mean ± standard deviation (n=18). (CV% = Coefficient of Variation).

| **Actual concentration** | Within-run variations | | | Between-run variations | | |
|---|---|---|---|---|---|---|
| | **Measured concentration** | **CV%** | **Accuracy (%)** | **Measured concentration** | **CV%** | **Accuracy (%)** |
| **100 ng/ml** | 99.8±8.7 | 8.7 | 99.7±8.8 | 100.6±5.9 | 5.9 | 100.6±5.9 |
| **200 ng/ml** | 197.7±10.5 | 5.3 | 98.8±5.2 | 207.2±9.2 | 4.4 | 103.5±4.7 |
| **400 ng/ml** | 371.2±16.7 | 4.5 | 92.8±4.2 | 370.3±45.5 | 12.3 | 96.8±4.4 |
| **800 ng/ml** | 756.8±70.5 | 9.3 | 94.7±8.9 | 826.2±53.6 | 6.48 | 103.3±6.7 |

Table 9-2. Accuracy and precision of mass spectrometry analysis method for docetaxel quantitation in PLGA nanoparticles. Data represents mean ± standard deviation (n=18). (CV% = Coefficient of Variation).

| **Actual concentration** | Within-run variations | | | Between-run variations | | |
|---|---|---|---|---|---|---|
| | **Measured concentration** | **CV%** | **Accuracy (%)** | **Measured concentration** | **CV%** | **Accuracy (%)** |
| **1250 ng/ml** | 1351.7±81.8 | 6.0 | 107.8 ±6.6 | 1285±135.8 | 10.5 | 102.8±11.0 |
| **2500ng/ml** | 2613.3±117.6 | 4.5 | 104.6±4.6 | 2550±215.4 | 8.4 | 102.1±8.7 |
| **5000 ng/ml** | 5375±258.1 | 4.8 | 107.6±5.2 | 5373.3±294.7 | 5.5 | 107.4±5.8 |
| **10000 ng/ml** | 10323.3±803.5 | 7.8 | 103.2±8.0 | 9811.7±810.1 | 8.3 | 98.1±8.1 |

Table 9-3. Accuracy and precision of mass spectrometry analysis method for docetaxel quantitation in PLGA-PEG nanoparticles. Data represents mean ± standard deviation (n=18). (CV% = Coefficient of Variation).

| **Actual concentration** | Within-run variations | | | Between run variations | | |
|---|---|---|---|---|---|---|
| | **Measured concentration** | **CV%** | **Accuracy (%)** | **Measured concentration** | **CV%** | **Accuracy (%)** |
| **625 ng/ml** | 651.7±51.5 | 7.87 | 104.2±8.2 | 641.8±46.1 | 7.23 | 102.8±7.44 |
| **1250ng/ml** | 1286.7±139.1 | 10.58 | 103.0±10.9 | 1375±85.2 | 6.16 | 110.1±6.78 |
| **2500 ng/ml** | 2596.6±179.2 | 6.84 | 103.8±7.1 | 2588±195.7 | 7.54 | 103.4±7.8 |
| **5000 ng/ml** | 5078.3±563.2 | 10.94 | 101.4±11.1 | 5230±562.9 | 10.75 | 104.5±11.24 |

### 9.2.4. Overall Method Performance

Overall, the applied method covered a linearity range of 3.9-1000 ng/ml, 125-16000 ng/ml, and 125-8000 ng/ml of docetaxel concentration in methanol, PLGA nanoparticles and

PLGA-PEG nanoparticles, respectively. The method was sensitive enough to help evaluate the amount of the drug in the abovementioned matrices. In all cases, the obtained daily standard curves demonstrated $R^2$s higher than 0.996. An analysis of docetaxel in methanol at LOQ concentration (n=6) demonstrated an accuracy and coefficient of variation (CV%) of less than 14.8% and 15.3% respectively. The evaluated within- and between-run variations of the docetaxel quantitation method in methanol (table 9-1) demonstrated CV%s of less than 12.3% between concentration sets (i.e., good precision). An analysis of docetaxel in PLGA nanoparticles at LOQ concentration (n=6) exhibited an accuracy and CV% of less than 10.7 % and 11.6%, respectively. Within- and between-run variation studies of the docetaxel quantitation method in PLGA nanoparticles (table 9-2) demonstrated CV%s of less than 10.5% between various concentrations (i.e., good precision). The CV% for within- and between-run variation studies of docetaxel quantitation method in PLGA-PEG nanoparticles was less than 10.94% (table 9-3). Analysis of docetaxel in PLGA-PEG nanoparticles at LOQ concentration (n=6) demonstrated an accuracy and CV% of less than 13.42 % and 13.07%, respectively. In addition, to check accuracy, back calculation of docetaxel quality control concentrations in methanol, PLGA nanoparticles, and PLGA-PEG nanoparticles were conducted and exhibited values with an acceptable deviation from the actual concentrations (i.e., less than 15% deviation). These results suggested that the present method could accurately and reproducibly measure docetaxel in non-biological matrices including methanol, PLGA nanoparticles, and PLGA-PEG nanoparticles.

## 9.3. Docetaxel in Biological Matrices

### 9.3.1. Limits of Detection and Quantitation

Supplementary figure 11 demonstrates a typical MRM graph of docetaxel and paclitaxel in mouse serum and liver. Both docetaxel and paclitaxel possess a retention time of

around 0.5 minute. The LOD and LOQ of the method used to quantify docetaxel in mouse serum and liver were 7.8 ng/ml and 15.6 ng/ml, respectively.

### 9.3.2. Linearity

The linear regression analysis carried out on known added concentrations of docetaxel against the peak area ratio of docetaxel to paclitaxel (weighted 1/x) produced linear responses throughout the wide range of docetaxel concentration in mouse serum from 15.6 to 1000 ng/ml. $R^2$, slope, and intercept demonstrated values equal to 0.9951, 0.00117, and 0.00125, respectively. The typical equation of the line was y=0.00117x+0.0125 for a set of concentrations (n=3). Supplementary figure 12 shows a typical daily calibration curve of the method.

Known added concentrations of docetaxel against the peak area ratio of docetaxel to paclitaxel (weighted 1/x) in mouse liver were also subjected to linear regression analysis. Linear responses were obtained from the method throughout the wide range of docetaxel concentration (15.6 to 500 ng/ml). $R^2$, slope, and intercept values were 0.9979, 0.00116, and 0.0215, respectively, providing a typical equation of y=0.00116x+0.0215 for a set of concentrations (n=3). Supplementary figure 13 shows a typical daily calibration curve of the method.

### 9.3.3. Method Precision and Accuracy

Within- and between-run variations and accuracy of the docetaxel quantitation method in mouse serum are shown in table 9-4. The quality control samples demonstrated deviations of less than 15% (i.e., ±15%), showing the efficacy of the method to quantitate docetaxel in mouse serum with acceptable precision and accuracy. The variation evident in LOQ concentration (15.6 ng/ml) was within an acceptable range (i.e., ±20%) (n=6).

Within- and between-run variations and accuracy of the docetaxel quantitation method in mouse liver are shown in table 9-5. The quality control samples demonstrated deviations of less than 15% (i.e., ±15%), showing the efficacy of the method to quantitate docetaxel in mouse liver with acceptable precision and accuracy. The variation evident in LOQ concentration (15.6 ng/ml) was within an acceptable range (i.e., ±20%) (n=6).

Table 9-4. Accuracy and precision of mass spectrometry method for docetaxel quantitation in mouse serum. Data represents mean ± standard deviation (n=18). (CV% = Coefficient of Variation).

| **Actual concentration** | Within-run variations | | | Between-run variations | | |
|---|---|---|---|---|---|---|
| | **Measured concentration** | **CV%** | **Accuracy (%)** | **Measured concentration** | **CV%** | **Accuracy (%)** |
| **100 ng/ml** | 98.0±3.1 | 3.2 | 98.0±3.1 | 92.4±7.9 | 8.5 | 92.4±7.9 |
| **200 ng/ml** | 201.8±5.6 | 2.8 | 101.1±2.8 | 193.5±19.6 | 10.1 | 96.7±9.8 |
| **400 ng/ml** | 393.2±25.7 | 6.6 | 98.4±6.5 | 370.7±22.9 | 6.0 | 92.7±5.6 |
| **800 ng/ml** | 834.3±84.1 | 10.1 | 104.2±10.5 | 803.3±74.9 | 9.2 | 100.2±9.2 |

Table 9-5. Accuracy and precision of mass spectrometry method for docetaxel quantitation in mouse liver. Data represents mean ± standard deviation (n=18). (CV% = Coefficient of Variation).

| **Actual concentration** | Within-run variations | | | Between-run variations | | |
|---|---|---|---|---|---|---|
| | **Measured concentration** | **CV%** | **Accuracy (%)** | **Measured concentration** | **CV%** | **Accuracy (%)** |
| **100 ng/ml** | 90.7±4.0 | 4.4 | 90.7±4.0 | 90.9±7.1 | 7.8 | 90.9±7.1 |
| **200 ng/ml** | 196.5±18.5 | 9.1 | 98.1±9.0 | 193.2±17.8 | 9.4 | 96.7±9.1 |
| **400 ng/ml** | 397.8±25.1 | 6.4 | 99.5±6.4 | 377.0±32.9 | 8.7 | 94.2±8.2 |

### 9.3.4. Overall Method Performance

Linear ranges from 15.6 to 1000 ng/ml and 15.6 to 500 ng/ml of docetaxel were covered by the method in mouse serum and mouse liver, respectively. $R^2$ obtained daily from standard curves were higher than 0.995 for biological matrices under study. Analysis of docetaxel in mouse serum at LOQ concentration (n=6) exhibited an accuracy and CV% below 10.0 % and 9.7%, respectively. The docetaxel quantitation method in mouse serum exhibited CV%s below 10.1% (good precision), as obtained from within- and between-run variation studies (table 9-4). However, in the case of mouse liver, CV%s were lower than 9.4% (table 9-5). In addition, docetaxel at LOQ concentration (n=6) in mouse liver demonstrated an accuracy and CV% of less than 11.9 % and 11.8%, respectively. Over all, acceptable deviations (<15%) from actual concentrations were obtained when docetaxel quality control concentrations in both matrices (i.e., mouse serum and mouse liver) under study were analysed and back calculated. Consequently, the analysis method developed and partially validated could measure docetaxel in the biological matrices with acceptable reproducibility, accuracy, and precision.

### 9.4. Docetaxel in Mouse Kidney, Heart, and Lung

Supplementary figure 14 demonstrates typical MRM graphs of docetaxel and paclitaxel in mouse kidney, heart, and lung. A linear response was obtained throughout the wide range of docetaxel concentration (15.6 to 500 ng/ml) in mouse kidney, heart, and lung after linear regression analysis done on known added concentrations of docetaxel against the peak area ratio of docetaxel to paclitaxel (weighted 1/x). Regression parameters of the analysis ($R^2$, slope, intercept, and corresponding typical equation of the line) for a set of concentrations (n=3) in each tissue is demonstrated in table 9-6. Typical daily calibration curves of the method in mouse kidney, heart, and lung are demonstrated in supplementary figures 15 to 17.

Extraction efficiencies of docetaxel from mouse liver, kidney, heart, and lung are exhibited in table 9-7. The efficiency of the extraction was evaluated at three QC concentrations (100, 200, and 400 ng/ml) of docetaxel in homogenized tissues. The linearity response of the analysis method in mouse kidney, heart, and lung indicated the analysis method's adaptability for the analysis of docetaxel in these organs. The method of extraction demonstrated an efficiency percentage of around 80% in mouse tissues except for mouse heart, which showed around 70% extraction efficiency. The reason might be docetaxel's high affinity for microtubules and the fact that heart tissue is a microtubule-rich organ.

Typically, to overcome selectivity/sensitivity-related limitations and to minimize/eliminate the matrix effect usually seen with biological matrices, samples are pre-treated to remove proteins and lipids to ensure proper analysis [343, 344]. Endogenous substances such as proteins, peptides, and phospholipids can potentially result in interference [345] by intervening the process of transfer of charged analyte to gas phase and consequently increase or decrease ionization efficiency [346]. Here, Liquid-Liquid phase extraction

without protein-precipitation has been applied as an effective approach using TBME which appears to provide a cleaner extract compared to other organic solvents such as ethyl acetate, hexane, and diethyl ether [347-349].

Table 9-6. Typical daily standard curve regression parameters for a set of docetaxel concentrations (n=3) in mouse kidney, heart and lung tissues.

| | **Parameter** | | | |
|---|---|---|---|---|
| **Tissue** | **$R^2$** | **Slope** | **Intercept** | **Line Equation** |
| **Kidney** | 0.9977 | 0.00236 | -0.00162 | y=0.00236x-0.00162 |
| **Heart** | 0.9973 | 0.00209 | 0.0107 | y=0.00209x+0.0107 |
| **Lung** | 0.9951 | 0.00174 | 0.0207 | y=0.00174x+0.0207 |

Table 9-7. Efficiency (%) of docetaxel extraction method from mouse tissues at different QC concentrations (n=3).

| | **Individual extraction efficiency (%)** | | | **Overall Efficiency (%)** |
|---|---|---|---|---|
| **Tissue** | **100 (ng/ml)** | **200 (ng/ml)** | **400 (ng/ml)** | |
| **Liver** | 82.15±4.09 | 67.65±1.43 | 89.08±0.63 | 79.63±9.72 |
| **Kidneys** | 86.97±0.94 | 76.97±0.67 | 74.57±4.05 | 79.66±6.09 |
| **Heart** | 73.88±0.37 | 74.08±0.77 | 67.04±1.68 | 71.67±3.68 |
| **Lungs** | 78.13±5.3 | 82.48±1.22 | 83.34±0.21 | 81.31±3.48 |

# CHAPTER 10*

## Result and Discussion on Pharmacokinetics and Bio-distribution of Docetaxel

***** Chapter 6 (Experimental Section on Pharmacokinetics and Bio-distribution of Docetaxel) along with chapter 10 have been published as an 'Original Research Article' in '*International Journal of Nanomedicine':*

Pedram Rafiei, Azita Haddadi. Docetaxel Loaded PLGA and PLGA-PEG Nanoparticles for Intravenous Application: Pharmacokinetics and Bio-distribution Profile. *International Journal of Nanomedicine.* 2017, Volume 12, pages 935-947.

### Background

Once nanoparticle formulations are characterized in terms of physicochemical properties, they are tested in animal models for various purposes. These include tests to evaluate the toxicity, safety, and therapeutic efficacy of nanoparticles. In addition, the contribution of nanoparticles to the associated drug's pharmacokinetics and biodistribution is evaluated. Nanoparticles may enhance a drug's systemic circulation residence time or modify its tissue distribution. They may elevate the drug's delivery to particular organs or decrease the drug's distribution to other organs. Thus, the drug's pharmacokinetics and biodistribution often changes when associated to nanoparticles. Modifications made to drugs' pharmacokinetic and biodistribution by nanoparticles are greatly important because these modifications can reduce effects in one tissue and increase effects in another tissue. Therefore, monitoring the pharmacokinetics and biodistribution of the drug loaded into nanoparticles is important because it helps predict efficacy and side effects. The pharmacokinetics and biodistribution of nanoparticles depend on characteristics such as their average size, surface properties, and zeta potential. Accordingly, a relationship can be

established between nanoparticle characteristics and the mode of change made to the drug's pharmacokinetics and biodistribution profile.

Here, the pharmacokinetics and tissue distribution profiles for docetaxel loaded into PLGA nanoparticles, docetaxel loaded into surface-modified (PEGylated) PLGA nanoparticles, and free docetaxel were evaluated and compared after administration to animal model (mice). The nanoparticle formulations modified the pharmacokinetics and biodistribution of the drug. These modifications are reflected in docetaxel's pharmacokinetic parameter estimates in mouse serum and monitored tissues and are attributed to nanoparticles' sizes and surface characteristics.

## 10.1. Docetaxel in Mouse Serum

Docetaxel serum concentration versus time curve for drug-loaded nanoparticles and for the free drug solution after IV injection to mice is shown in figure 10-1. The concentration of docetaxel in all formulations demonstrates a gradual declining trend. It is evident that the serum concentration of docetaxel provided by PLGA and PLGA-PEG nanoparticles is higher throughout the study compared to that provided by the free docetaxel solution. The observed difference between the treatment groups is statistically significant ($p < 0.05$) at the time-points of 0.5, 1, 4, and 6 hours. The docetaxel concentration provided by nanoparticle formulations remains within a quantifiable range up to 24 hours, while the docetaxel concentration from the free drug solution is quantifiable only up to 12 hours. The docetaxel concentration from PLGA nanoparticles is higher than that of PLGA-PEG nanoparticles up to 4 hours. Conversely, after 4 hours, the docetaxel concentration from PLGA-PEG nanoparticles becomes dominant compared to PLGA nanoparticle.

Table 10-1 demonstrates docetaxel's important pharmacokinetic parameters in mouse serum. Compared to the free docetaxel solution, both types of nanoparticles decreased the

drug's elimination rate constant ($K_e$) from serum ($p$ <0.05), which is reflected in their corresponding half-lives. Interestingly, PLGA-PEG nanoparticles contributed to a 3.7-fold increase in $T_{1/2}$, while PLGA nanoparticles increased it by only 1.4-fold. The level of serum exposure to docetaxel (AUC) increased most with PLGA-PEG nanoparticles (5.4-fold), followed by PLGA nanoparticles (3.9-fold), than with the free drug solution ($p$ <0.05). Compared to the free drug solution, docetaxel systemic clearance significantly decreased when nanoparticle formulations were used (i.e., 3.5- and 4.9-fold for PLGA and PLGA-PEG nanoparticles, respectively) ($p$ <0.05). Both nanoparticle formulations lowered docetaxel's apparent volume of distribution ($V_d$) ($p$ <0.05). $V_d$ of docetaxel was decreased from 383.5 ml in the case of the free drug solution to 150.8 ml and 290.4 ml in the case of PLGA and PLGA-PEG nanoparticles, respectively. Furthermore, MRT of docetaxel demonstrates a statistically significant difference ($p$ <0.05) between treatment groups. MRTs exhibited an approximately 4.8- and 2.4-fold increase in the case of PLGA-PEG (18.46 hour) and PLGA (9.29 hour) nanoparticles, respectively, compared to the free solution of docetaxel (3.81 hour).

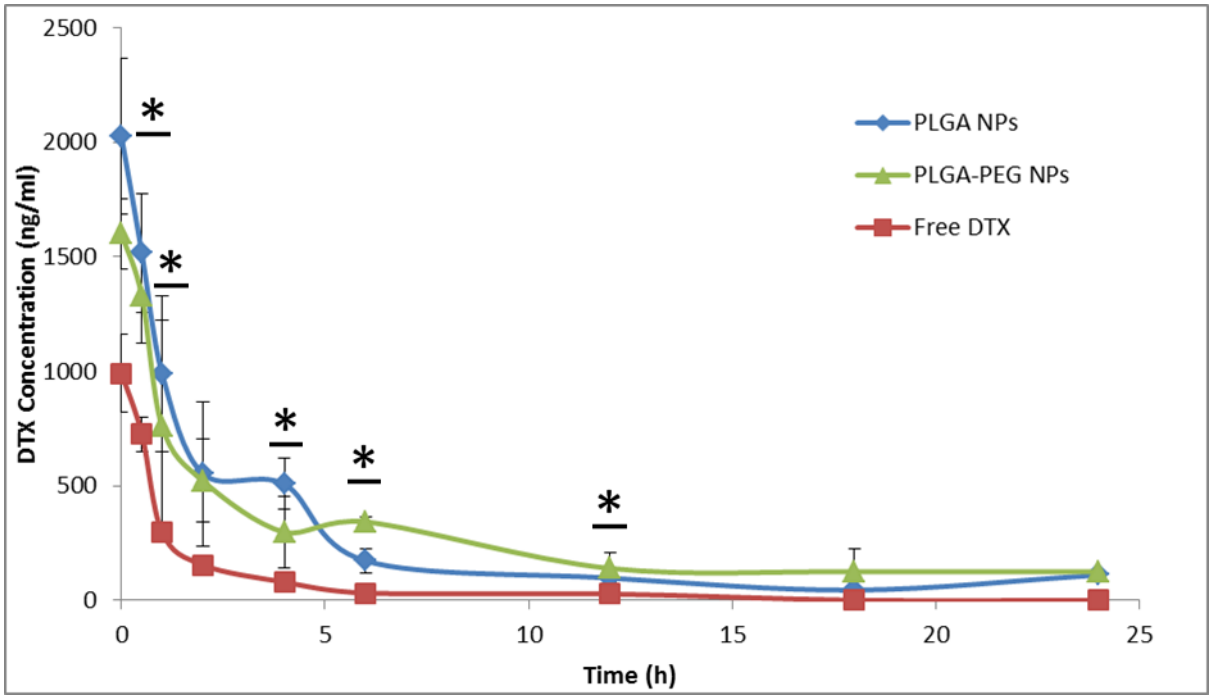


A)

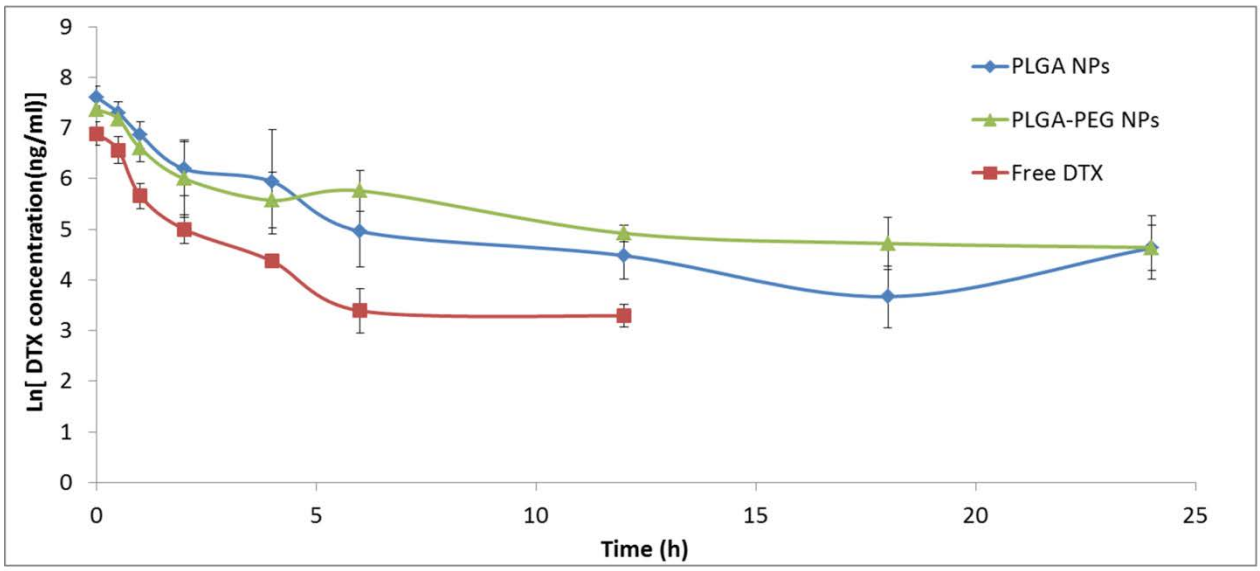


B)

Figure 10-1. Docetaxel serum concentration versus time after IV injection of different drug formulations at a dose of 5 mg/kg (n=4) to Balb/C mice. A) Concentration Vs time, B) Natural logarithm (Ln) of concentration Vs time. * indicates statistically significant difference between treatment groups.

Table 10-1. Docetaxel pharmacokinetic parameters in mouse serum after IV injection of different drug formulations (n=4). ($T_{1/2}$: half-life, $Cl_s$: Systemic Clearance, $V_d$: Apparent Volume of distribution, MRT: Mean Residence Time, AUC: Area Under the Curve). * indicates statistically significant difference between treatment groups.

| **Docetaxel Formulation** | | | | |
|---|---|---|---|---|
| **Tissue** | **PK Parameter** | **DTX Solution** | **PLGA NPs** | **PLGA-PEG NPs** |
| **Serum** | $T_{1/2}$ (h) * | 4.30±0.17 | 6.05±0.78 | 15.87±1.66 |
| | $Cl_s$ (ml/h) * | 61.79±15.61 | 17.23±7.16 | 12.54±4.53 |
| | AUC (ng/ml × h) * | 1,688±373 | 6,601±2,655 | 9,221±4,709 |
| | $V_d$ (ml) * | 383.57±96.44 | 150.81±74.18 | 290.41±116.32 |
| | MRT (h) * | 3.81±0.23 | 9.29±0.45 | 18.46±2.82 |

As exhibited in figure 10-1, drug concentration due to the docetaxel solution was significantly lower than that of the nanoparticle formulations throughout the study period. This is attributed to the large volume of distribution of docetaxel and also its binding affinity to various tissues [16, 17, 22]. In fact, although it is highly bound to plasma proteins such as albumin and acid glycoproteins [350], docetaxel can escape the blood and be distributed to various organs immediately after IV injection of the drug solution [31]. This could be the reason why docetaxel concentrations in serum dropped fairly rapidly compared to the nanoparticle formulations during the first few time-points followed by a rapid elimination phase. On the other hand, docetaxel nanoparticle formulations kept up the drug's serum concentration for up to 24 hours post-injection. This could be attributed to the role of nanoparticles as long-circulating sustained-release drug-delivery vehicles. Obtained results agree with several studies that have demonstrated docetaxel-loaded nanoparticles' ability to maintain docetaxel concentration levels in the blood better than the free solution of drug [167, 196, 197, 200, 201]. Up to four hours after injection, drug concentration due to PLGA

nanoparticles is higher than that due to PLGA-PEG nanoparticles. However, after 4 hours, drug concentration due to PLGA-PEG nanoparticles becomes dominant. This difference is likely due to the differences in size (i.e., larger average size of PLGA-PEG nanoparticles) and surface properties (i.e., hydrophilic surface of PEGylated nanoparticles) that ultimately contribute to different bio-distribution and entrapment levels in other organs.

As exhibited in table 10-1, the half-life of docetaxel in serum increased when nanoparticle formulations were used. This is particularly evident in the case of PEGylated nanoparticles. This increase could be attributed to the presence of PEG moiety on the surface of PLGA nanoparticles and its role in conferring characteristics to nanoparticles to evade the clearance mechanisms of the body [200, 201, 351]. As a result, the level of serum exposure of docetaxel was also increased in the case of PLGA-PEG nanoparticles, followed by PLGA nanoparticles, compared to that obtained from free drug solution ($p < 0.05$). This result agrees with those obtained by other studies evaluating the effect of docetaxel loading in PLGA nanoparticles on docetaxel pharmacokinetics [176, 201]. The nanoparticle formulations significantly reduced the levels of docetaxel systemic clearance from serum. Both nanoparticle formulations also lowered docetaxel's apparent volume of distribution. Apparent volume of distribution due to PLGA-PEG nanoparticles is higher than PLGA nanoparticles. This could be attributed to the larger size of PLGA-PEG nanoparticles and higher possibility of entrapment in RES organs such as liver and spleen. MRT of docetaxel in serum increased when nanoparticle formulations were used, which means that PLGA nanoparticles, particularly PLGA-PEG nanoparticles, increased the average transit-time of docetaxel molecules through the body.

Generally, the mode of modifications made to docetaxel's pharmacokinetic parameters is in agreement with trends reported by other studies. Esmaeili et al. [196] reported that PLGA nanoparticles contributed to increment in the half-life of docetaxel with a

4.5- fold increase in AUC and 1.67-fold increase in MRT when compared to naked formulation of the drug. Yu et al. [167] also reported that AUC (1.5-fold), MRT (4.7-fold), and half-life (2.1-fold) of docetaxel were increased after loading in PLGA nanoparticles. Systemic clearance of docetaxel due to PLGA nanoparticles was decreased in parallel. Jain et al. [201] reported respectively 3.2-fold and 8.2-fold increase in AUC and half-life of docetaxel due to PLGA nanoparticles as compared to free solution of the drug. They also evaluated the effect of PLGA nanoparticle PEGylation. In contrast, PLGA-PEG nanoparticle formulation contributed to 7-fold and 13- fold increase in AUC and half-life of the drug, respectively (compared to free docetaxel). Accordingly, Senthilkumar and colleagues [176] demonstrated respectively 1.7-fold and 1.5-fold increase in docetaxel's half-life and MRT while its systemic clearance was decreased 1.5-fold (when loaded in PLGA nanoparticles). Ratios were higher when PEGylated PLGA nanoparticles were used. Respectively, half-life and MRT were increased by 3.7- and 2.1-fold while systemic clearance was decreased by 2.7 fold.

### 10.2. Docetaxel in Mouse Liver

Figure 10-2 exhibits the concentration versus time profile of docetaxel in mouse liver after IV administration of various drug formulations. Docetaxel from the free drug solution was present in liver only up to 12 hours. However, for the PLGA and PLGA-PEG nanoparticle samples, docetaxel is seen in the liver up to 18 and 24 hours, respectively. Comparing the two nanoparticle types, PLGA formulation contributed to higher docetaxel concentration up to four hours, but the trend is reversed after that. Throughout the study period, the drug concentration from PLGA nanoparticles is higher than that from the free docetaxel solution.

Pharmacokinetic parameters of docetaxel in mouse liver are shown in table 10-2. $T_{1/2}$ of docetaxel in liver increased ($p$ <0.05) from 6.15 hours from the free drug solution to 8.15 and 19.03 hours from the PLGA and PLGA-PEG nanoparticles, respectively. Accordingly, the AUC of docetaxel concentration versus time for different formulations were as follows: PLGA-PEG nanoparticles>PLGA nanoparticles>free docetaxel solution (no statistically significant difference). On the other hand, the MRT of docetaxel increased ($p$ <0.05) from 7.31 hour (free drug solution) to 9.29 and 28.30 hour when PLGA and PLGA-PEG nanoparticles were used, respectively.

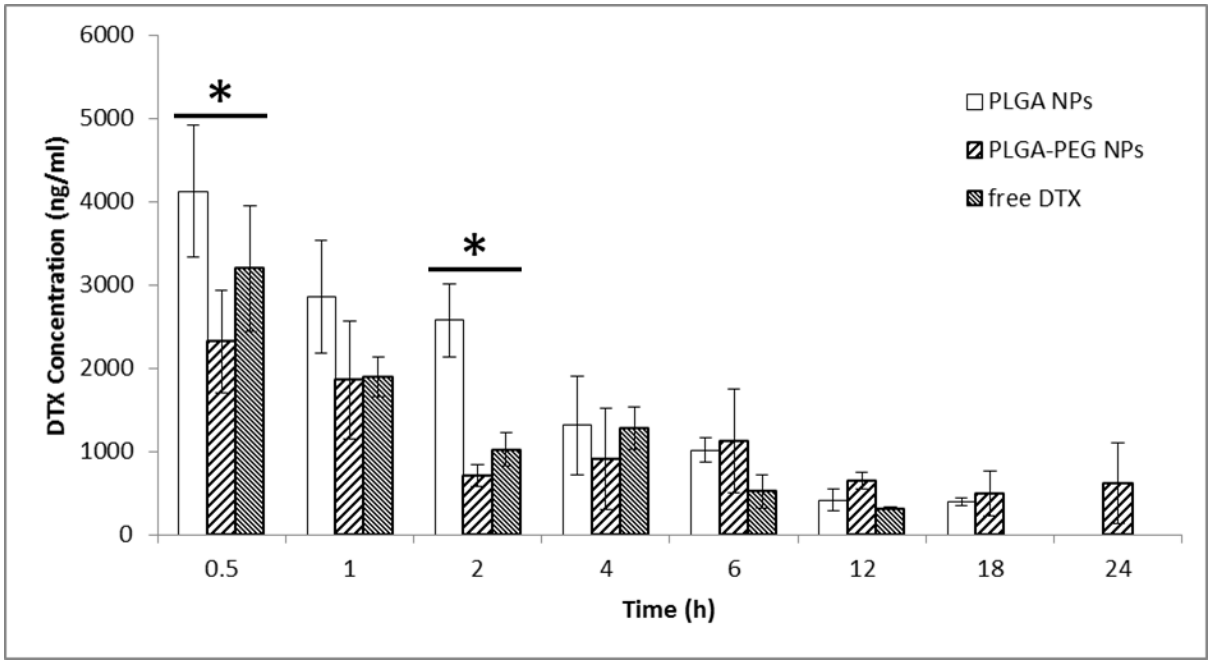


Figure 10-2. Docetaxel concentration in mouse liver versus time after IV injection of different drug formulations at a dose of 5 mg/kg (n=4). * indicates statistically significant difference between treatment groups.

Table 10-2. Docetaxel pharmacokinetic parameters in mouse liver after IV injection of different drug formulations (n=4). ($T_{1/2}$ :half-life, MRT: Mean Residence Time, AUC: Area Under the Curve). * indicates statistically significant difference between treatment groups.

| **Docetaxel Formulation** | | | | |
|---|---|---|---|---|
| **Tissue** | **PK Parameter** | **DTX Solution** | **PLGA NPs** | **PLGA-PEG NPs** |
| **Liver** | $T_{1/2}$ (h) * | 6.15±0.77 | 8.15±0.47 | 19.03±6.42 |
| | AUC (ng/ml × h) | 16,459±4,610 | 24,551±5,373 | 38,981±29,630 |
| | MRT (h) * | 7.31±1.37 | 9.29±0.50 | 28.30±11.30 |

As exhibited in figure 10-2, the gradual declining trend in docetaxel concentration over time is evident for all drug formulations. Accordingly, although docetaxel concentration due to PLGA-PEG nanoparticles was lower than that of the free drug solution and PLGA nanoparticles during the first four time-points (i.e., 0.5, 1, 2, and 4 hour), PLGA-PEG increased docetaxel's concentration over the last four time-points (i.e., 6, 12, 18, and 24 hours). The size distribution of PLGA-PEG nanoparticles contributed to this result. Compared to PLGA nanoparticles, PLGA-PEG nanoparticles possess a higher particle size range and therefore have better contact with the Kupffer cells of the hepatic lobules, as well as liver sinusoidal endothelial cells; thus, they become entrapped easier in liver sinusoids and ultimately remain in the liver for longer [352]. Park and colleagues [353] demonstrated the liver's and hepatic cells' ability to filter nanoparticles from systemic circulation. In their study, nanoparticles were highly localized in sinusoidal area while Kupffer cells largely retained the administered nanoparticles. Therefore, we can conclude that, over time, because of their lower particle size ranges, PLGA nanoparticles had less chance of entrapment in the liver [354, 355]. Consequently, PLGA-PEG nanoparticles remained in the liver for longer. Thus, the elimination half-life of docetaxel in liver due to PLGA-PEG nanoparticles was significantly higher than those due to the free docetaxel solution and PLGA nanoparticles.

The contribution of PLGA-PEG nanoparticles in increasing MRT of docetaxel in liver can potentially be used to target localized cancer tissues in liver [352]. Chu and colleagues [197] demonstrated higher liver exposure of docetaxel due to PLGA nanoparticles compared to that of free docetaxel solution which is in agreement with our result.

### 10.3. Docetaxel in Mouse Kidney

Figure 10-3 demonstrates docetaxel concentration in mouse kidney at various time points after IV injection of three different drug formulations to mice. Here, the gradual declining trend in docetaxel concentration is evident in all formulations. The difference in docetaxel concentration between treatment groups was statistically significant ($p$ <0.05) at all time-points except at four hours. PLGA nanoparticles demonstrated a significant contribution to docetaxel concentration in mouse kidney compared to other formulations ($p$ <0.05).

Table 10-3 exhibits docetaxel's pharmacokinetic parameters in kidney subsequent to IV administration of various drug formulations. Docetaxel's $T_{1/2}$ in kidney tended to decrease ($p$ <0.05) when loaded into PLGA-PEG nanoparticles compared to the free solution of drug (i.e., from 7.54 hours to 4.91 hours). Loading docetaxel into PLGA nanoparticles contributed to a 1.5-fold increase ($p$ <0.05) in docetaxel's $T_{1/2}$. The AUC is highest in the case of PLGA nanoparticles followed by the free docetaxel solution and PLGA-PEG nanoparticles ($p$ <0.05). In addition, the MRT of docetaxel in kidney increased and decreased respectively in the case of PLGA (13.10 hours) and PLGA-PEG nanoparticles (5.72 hours) compared to free docetaxel solution (8.46 hours). The difference between the MRT of the treatment groups was statistically significant.

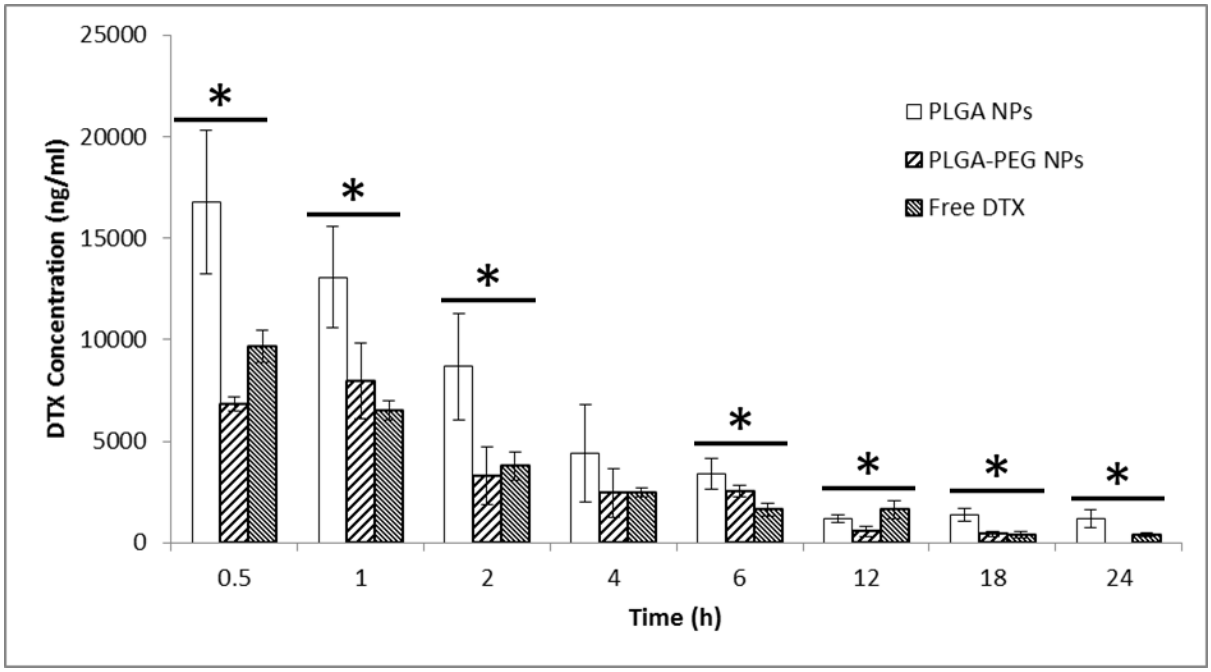


Figure 10-3. Docetaxel concentration in mouse kidney versus time after IV injection of different drug formulations at a dose of 5 mg/kg (n=4). * indicates statistically significant difference between treatment groups.

Table 10-3. Docetaxel pharmacokinetic parameters in mouse kidney after IV injection of different drug formulations (n=4). ($T_{1/2}$ :half-life, MRT: Mean Residence Time, AUC: Area Under the Curve). * indicates statistically significant difference between treatment groups.

| **Docetaxel Formulation** | | | | |
|---|---|---|---|---|
| **Tissue** | **PK Parameter** | **DTX Solution** | **PLGA NPs** | **PLGA-PEG NPs** |
| **Kidney** | $T_{1/2}$ (h) * | 7.54±0.16 | 11.59±1.00 | 4.91±0.42 |
| | AUC (ng/ml × h) * | 47,622±7,473 | 97,937±27,834 | 40,280±8,811 |
| | MRT (h) * | 8.46±0.77 | 13.10±1.82 | 5.72±0.34 |

As exhibited in figure 10-3, docetaxel concentration due to PLGA nanoparticles was higher than those obtained from PLGA-PEG nanoparticles or the free drug solution. The average size of PLGA nanoparticles is around 120 nm, while PLGA-PEG nanoparticles

possessed a larger average size range (i.e., 180 nm). Average size is an important determinant of the fate and bio-distribution of particles [356]. However, it is generally considered that particles with an average size of 10 nm and less are filtered in the kidneys [172, 204]. Therefore, the difference in nanoparticle size does not seem to be responsible for the different bio-distribution behaviour between PLGA and PLGA-PEG nanoparticles. Both types of nanoparticles can potentially get entrapped in kidney capillary bed [171, 207]. However, PLGA nanoparticles with un-modified surfaces were entrapped more. Due to the presence of PEG moiety on the surface of the PLGA-PEG nanoparticles, they tend to remain in the blood circulation longer [357]. Accordingly, compared to the free docetaxel solution, the PLGA nanoparticles increased docetaxel half-life in kidney while PLGA-PEG nanoparticles decreased it. This is again attributed to the difference in surface properties between nanoparticle formulations. PLGA-PEG nanoparticles had a lower AUC for kidney, which meant that PLGA-PEG nanoparticles demonstrated less kidney exposure compared to other formulations.

### 10.4. Docetaxel in Mouse Heart

Changes in docetaxel concentration in mouse heart versus time after IV administration of drug-loaded PLGA nanoparticles, PLGA-PEG nanoparticles, and solution of free drug is demonstrated in figure 10-4. Compared to PLGA-PEG nanoparticles, PLGA-nanoparticles and the free drug solution contribute to higher docetaxel levels in mouse heart, particularly during the first four time-points. The difference in docetaxel concentration between treatment groups is statistically significant ($p$ <0.05) at the time-points of 0.5, 1, and 2 hours. Docetaxel concentration from PLGA-PEG nanoparticles demonstrates minimal variations during the distribution phase.

Loading of docetaxel in nanoparticles modified the pharmacokinetic parameters of the drug in mouse heart (table 10-4). The half-life of docetaxel in heart demonstrates a decrease from 21.74 hours (free drug solution) to 11.34 and 14.00 hours in the case of PLGA and PLGA-PEG nanoparticle formulations, respectively. The reduction evident in half-life is statistically significant ($p$ <0.05). AUC of docetaxel obtained from different formulations demonstrate the following trend ($p$ <0.05): free solution > PLGA nanoparticles > PLGA-PEG nanoparticles. MRT demonstrates decrement in the cases of both nanoparticle formulations (17.36 and 20.71 hours for PLGA and PLGA-PEG nanoparticles, respectively) compared to the free docetaxel solution (28.08 hours) ($p$ <0.05).

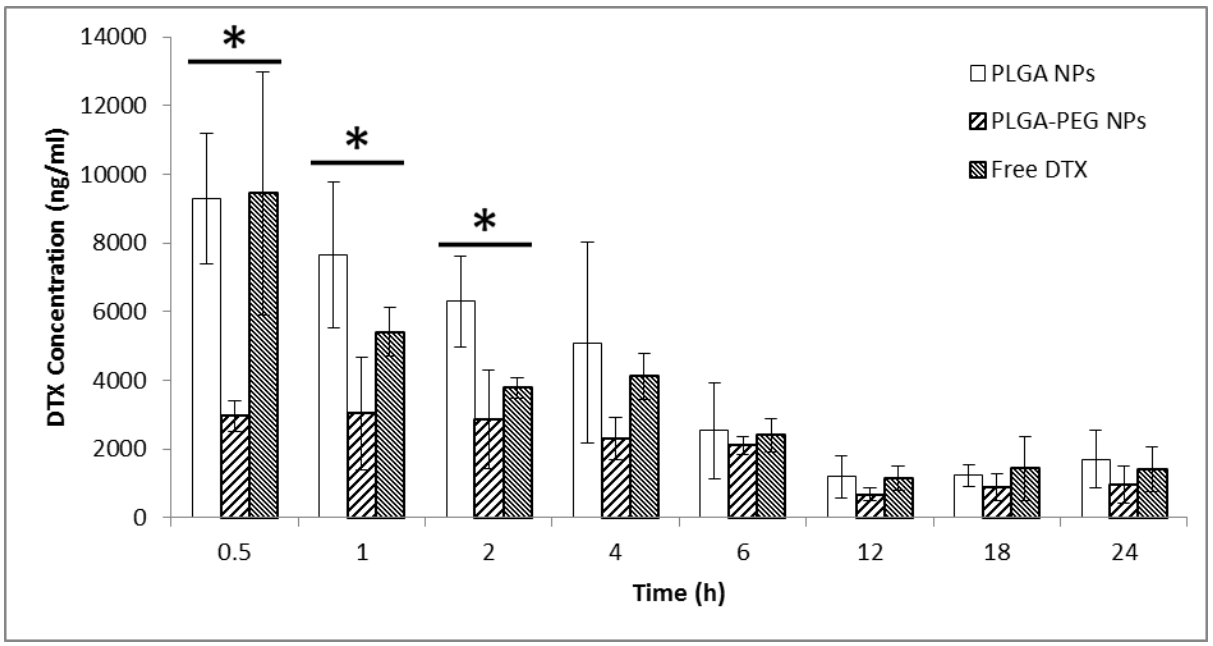


Figure 10-4. Docetaxel concentration in mouse heart versus time after IV injection of different drug formulations at a dose of 5 mg/kg (n=4). * indicates statistically significant difference between treatment groups.

Table 10-4. Docetaxel pharmacokinetic parameters in mouse heart after IV injection of different drug formulations (n=4). ($T_{1/2}$ :half-life, MRT: Mean Residence Time, AUC: Area Under the Curve). * indicates statistically significant difference between treatment groups.

| | | Docetaxel Formulation | | |
|---|---|---|---|---|
| **Tissue** | **PK Parameter** | **DTX Solution** | **PLGA NPs** | **PLGA-PEG NPs** |
| **Heart** | $T_{1/2}$ (h) * | 21.74±3.88 | 11.34±2.25 | 14.00±4.76 |
| | AUC (ng/ml × h) | 100,652±39,953 | 90,445±37,835 | 56,297±27,440 |
| | MRT (h) | 28.08±8.10 | 17.36±2.28 | 20.71±8.73 |

As exhibited in figure 10-4, docetaxel concentration due to PLGA nanoparticles and the free drug solution demonstrate a declining trend throughout the study time, in contrast to PLGA-PEG nanoparticles, which show a relatively constant level of docetaxel in heart during the first few time-points. In addition, the concentration of docetaxel provided by PLGA-PEG nanoparticles is significantly lower than that obtained from other drug formulations particularly during the first four time-points. Generally, after injection of drug formulations into the blood, the formulation are taken to the mouse heart [358]. A high portion of nanoparticles are believed to become trapped there, which results in high levels of docetaxel detected in the heart. In contrast to un-modified PLGA nanoparticles, due to the presence of PEG on the surface of PLGA-PEG nanoparticles, PLGA-PEG nanoparticles are believed to demonstrate less entrapment in the heart. Later, blood flow can wash away trapped nanoparticles from the heart. Microtubules are the major component of the cytoskeleton of myocytes that contribute to structural integrity of cardiac cells [359], and the heart is a microtubule-rich tissue [360]. Docetaxel has a high affinity for microtubules [361]. Docetaxel accumulates in the heart because the docetaxel formulation travels through the heart first and because of docetaxel's affinity for microtubules. This might be the reason the free docetaxel

solution resulted in high concentrations in heart tissue compared to the nanoparticle formulations.

As exhibited in table 10-4, the application of nanoparticle formulations contributed to a lower half-life for docetaxel in heart tissue compared to the free drug solution, likely due to the high levels of docetaxel tissue accumulation in heart after injection of free docetaxel solution. However, surface modification of PEGylated nanoparticles can potentially contribute to less entrapment and therefore less AUC of docetaxel concentration versus time for the PLGA-PEG nanoparticle formulation. On the other hand, PLGA nanoparticles with unmodified surface demonstrated higher entrapment and consequently a higher AUC. Nanoparticle formulations can be gradually washed away from the heart after their initial entrance to heart tissue post-injection, which could have influenced the $T_{1/2}$ of docetaxel due to nanoparticles compared to the free solution of the drug.

### 10.5. Docetaxel in Mouse Lung

Figure 10-5 exhibits the concentration versus time profile of docetaxel in mouse lung after IV administration of various docetaxel formulations. Docetaxel levels in lung was high during the first time-points (i.e., up to 2 hours) particularly for PLGA nanoparticles and the free drug solution ($p$ <0.05 at 0.5 and 2 hour). Afterwards, docetaxel levels significantly decreased from 2 to 24 hours. Docetaxel pharmacokinetic parameters in mouse lung after IV injection of different drug formulations are summarized in table 10-5. PLGA-PEG nanoparticles show the lowest half-life (4.12 hours) for docetaxel in mouse lung compared to other formulations (12.57 and 7.40 hours for the free drug solution and PLGA nanoparticles, respectively). The difference between the half-lives of docetaxel due to treatment groups was statistically significant ($p$ <0.05). The free solution of docetaxel resulted in the highest AUC followed by PLGA and PLGA-PEG nanoparticles, respectively ($p$ <0.05). Nanoparticle

formulations decreased MRT of docetaxel to 5.95 hours (2.88-fold) (PLGA nanoparticles) and to 5.37 hours (3.20-fold) (PLGA-PEG nanoparticles) compared to the free solution of the drug (17.19 hours) ($p$ <0.05).

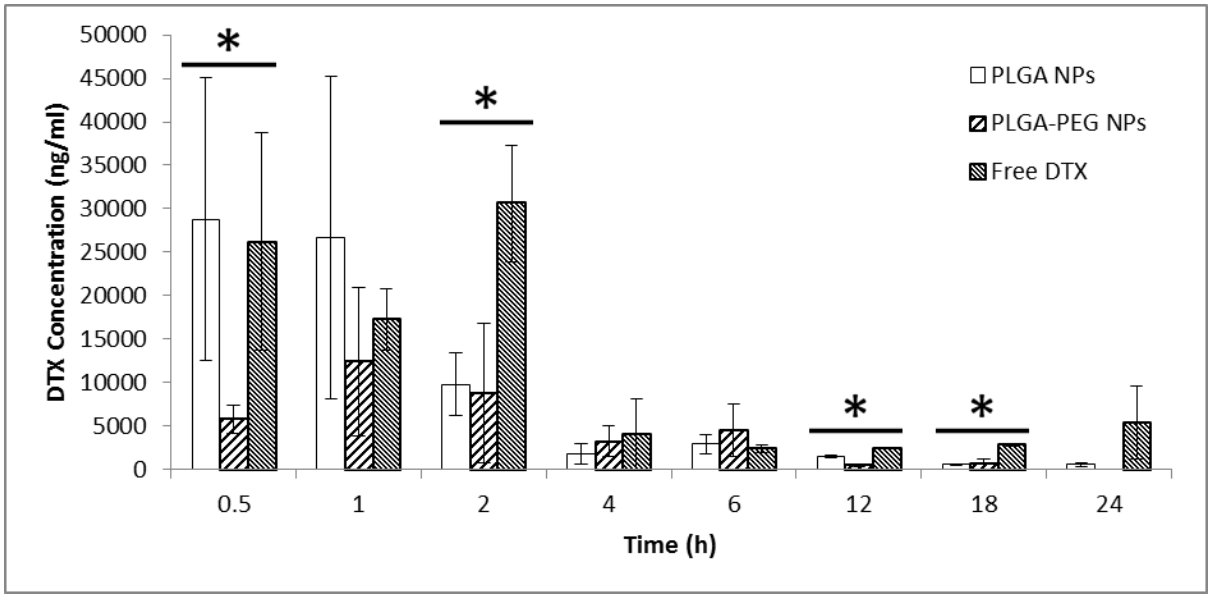


Figure 10-5. Docetaxel concentration in mouse lung versus time after IV injection of different drug formulations at a dose of 5 mg/kg (n=4). * indicates statistically significant difference between treatment groups.

Table 10-5. Docetaxel pharmacokinetic parameters in mouse lung after IV injection of different drug formulations (n=4). ($T_{1/2}$ :half-life, MRT: Mean Residence Time, AUC: Area Under the Curve). * indicates statistically significant difference between treatment groups.

| | | **Docetaxel Formulation** | | |
|---|---|---|---|---|
| **Tissue** | **PK Parameter** | **DTX Solution** | **PLGA NPs** | **PLGA-PEG NPs** |
| **Lung** | $T_{1/2}$ (h) * | 12.57±1.24 | 7.40±0.65 | 4.12±0.66 |
| | AUC (ng/ml × h) * | 190,205±19,402 | 98,826±38,035 | 59,603±40,803 |
| | MRT (h) * | 17.19±4.49 | 5.95±1.69 | 5.37±0.61 |

Generally, drug formulations are considered to enter mouse heart and lung immediately post-injection [358], which is accompanied with the significant influx of a large portion of injected material into the lung. Consequently, there is the chance that docetaxel from free drug solution accumulates in the lung. Afterwards, with further circulation of blood in the lungs, docetaxel concentration tends to decrease gradually. On the other hand, nanoparticles are believed to become trapped in the lung immediately after IV injection, as a result of the lungs' capillary filtration effects [362, 363]. Nanoparticles can become physically entrapped in the lung or become recognized by the lung phagocytic macrophages [364, 365].

PLGA nanoparticles appear to contribute to higher docetaxel concentrations in lung compared to PLGA-PEG nanoparticles (during the first few time-points). Considering their lower size-range (compared to PLGA-PEG nanoparticles), the unmodified surface of PLGA nanoparticles could be the main reason these nanoparticles are retained in the lung. The finding by Esmaeili and colleagues [196] agrees with our results. They reported a significant amount of nanoparticle entrapment in mice lung after IV injection of PLGA nanoparticles. Chu and colleagues [197] demonstrated higher lung exposure of docetaxel due to PLGA nanoparticles compared to that of free docetaxel solution which is in agreement with our result.

Based on docetaxel's concentration-time profile, PLGA-PEG nanoparticles demonstrated less accumulation in lung. Pharmacokinetic analysis shows reductions in the lung half-life of docetaxel when nanoparticle formulations were used. This reduction was more pronounced in the case of PLGA-PEG nanoparticles. PLGA-PEG nanoparticles' tendency to remain in the systemic circulation might be the reason for this. This is also evident by the reduction made in the MRT of docetaxel in lung when nanoparticle formulations were used. All these changes indicate that PLGA and PLGA-PEG nanoparticles

contribute to lower delivery, distribution, retention, and residence of docetaxel in lung. This is potentially helpful in deviating delivery of docetaxel away from lung.

# CHAPTER 11

## Summary, Conclusions, and Perspectives

### 11.1. Summary and Conclusions

#### 11.1.1. Taguchi Experimental Factorial Design

In the present work, an experimental design based on the Taguchi robust method was used to optimize PLGA nanoparticles loaded with docetaxel. As a fractional factorial design, 16 runs of a combination of important factors/levels from a full factorial design were selected and used for nanoparticle fabrication. Docetaxel-loaded PLGA nanoparticles from the design demonstrated an overall uni-distributed population of nanoparticles with a range of size between 93 and 191 nm, zeta potential between -17 and -36 mV, and drug-loading efficiency between 25% and 96%. Among different factors under study, PVA concentration had the highest magnitude of effectiveness on particle size, while organic:aqueous phase ratio contributed most to size with statistical significance. In the case of zeta potential, the type of PLGA polymer terminus was the factor determining zeta potential with statistical significance. It was also the factor with the highest magnitude of effectiveness on zeta potential. Organic:aqueous phase ratio had the highest magnitude of effectiveness on drug-loading efficiency. All factors under study, except PLGA molecular weight contributed to drug-loading efficiency with statistical significance.

The L16 Taguchi design allowed for the fitting of statistically significant models with good robustness as suitable means to predict particle characteristics from the fraction of full combinations of factors/levels. Prediction of particle characteristics based on preparation conditions can help prepare nanoparticle formulations with intended properties. The design also allowed for the optimization of the nanoparticle fabrication method based on surface-

response optimization techniques. This provided the knowledge to determine the fabrication conditions that create nanoparticles with desired characteristics of average size, PDI, zeta potential, and drug loading efficiency. Considering that the nanoparticle's fate in the body is in part determined by its characteristics, having control over those characteristics grants the ability to control nanoparticles' pharmacokinetics.

### 11.1.2. Docetaxel-Loaded Nanoparticles

The optimized method of nanoparticle fabrication, which was suggested by the experimental factorial design, was used to prepare docetaxel-loaded PLGA nanoparticles and PEGylated PLGA nanoparticles. The optimized fabrication method provided nanoparticles with characteristics suitable for an intravenous sustained-release drug-delivery system. Average particle sizes were approximately 120 nm for PLGA and 180 nm for PEGylated PLGA nanoparticles, which, being below 200 nm, were small enough to evade filtration in RES organs and large enough to evade filtration in the kidneys. Nanoparticles had negative surface zeta potential values between -24 and -32 mV, which allow for long circulating times for nanoparticles in the blood. Nanoparticles demonstrated a bi-phasic *in vitro* release profile, which is expected from drug delivery systems (PLGA and PLGA-PEG nanoparticle formulations) meant to provide systemic circulation with sustained drug release. Docetaxel loaded in nanoparticles demonstrated cytotoxicity against Hela cancer cells, which was comparable to that obtained from the free solution of the drug. It confirmed that docetaxel's pharmacological activity is maintained after association with PLGA and PEGylated PLGA nanoparticles.

### 11.1.3. Docetaxel Analysis Method

A simple and rapid mass spectrometric method was developed and partially validated to quantify docetaxel in various biological and non-biological samples throughout the study. Method development was done over 125-16000 ng/ml docetaxel concentration for nanoparticles polymeric matrices and 3.9-1000 ng/ml docetaxel concentration for mouse biological matrices. The method was applied for quantitative analysis of docetaxel with acceptable levels of accuracy/precision.

### 11.1.4. Pharmacokinetics and Biodistribution Profile of Docetaxel

Docetaxel's pharmacokinetic and biodistribution profiles were evaluated and compared in mice after IV administration of free docetaxel and docetaxel-loaded PLGA and surface-modified (PEGylated) PLGA nanoparticles, which were fabricated through the optimized preparation method. Based on the data obtained, the association of docetaxel with PLGA nanoparticles modified docetaxel's pharmacokinetics and bio-distribution. Both nanoparticle formulations increased docetaxel's half-life in serum and decreased its systemic clearance. Overall, they increased docetaxel's MRT as well. Docetaxel's distribution profile to various organs was also different when compared to the free drug solution. For example, PEGylated PLGA nanoparticles contributed to higher MRT in the liver, while surface-unmodified PLGA nanoparticles resulted in higher MRT in the kidneys. Also, docetaxel's exposure to heart tissue was reduced when nanoparticle formulations were used. Nanoparticle formulations were highly entrapped in the liver compared to other organs. Accordingly, the mode of changes made to docetaxel's pharmacokinetics and bio-distribution was attributed to the size and surface properties of nanoparticles. Loading of docetaxel in nanoparticles contributed to increase in blood-residence time of docetaxel, fulfilling the nanoparticles' role as a long-circulating sustained-release drug-delivery system. Surface-modification of

nanoparticles contributed to more pronounced blood concentrations of docetaxel, which confirms PEG's role in helping nanoparticles evade the clearance mechanisms present in the systemic circulation and the body. The role of nanoparticle average size in modifying the bio-distribution was also evident.

## 11.2. Future Perspectives

**Improving Experimental Design:** Valuable information related to PLGA nanoparticle fabrication is provided by the experimental design. The design deals with four of the preparation factors at two levels. Sixteen different combinations of factors/levels have already been completed. It is possible to add two more levels to PLGA Mw and PVA concentration. Consequently, such design would require preparation of nanoparticles at new factor/level combinations and ultimately results in new data points available for analysis. This would potentially increase the precision of analysis outcome. Therefore, as one of the future perspectives, it is recommended to add two more levels to the mentioned factors, and re-run the design.

**Directing Nanoparticles Towards an Organ:** The data from animal experiments demonstrate that the association of the drug to the nanoparticles could modify the pharmacokinetic and bio-distribution profile of docetaxel by a relationship to nanoparticles surface characteristics and average size. The observed trend can be used for directing nanoparticles towards a certain organ by further modifying nanoparticle size or surface properties.

**Example 1:** PLGA-PEG nanoparticles with larger average sizes demonstrate more pronounced residence in liver. Therefore, it is possible to design nanoparticles with average sizes suitable for liver accumulation. This can be manipulated to direct nanoparticles to liver,

possibly for liver-related cancers. Therefore, as a future perspective, it is recommended to use the models built by the Taguchi design to prepare larger PLGA nanoparticles for hepatic drug-delivery purposes.

**Example 2:** Surface-modification of nanoparticles with PEG increases the residence time of the drug in the blood. As a future perspective, it is recommended to use a di-block co-polymer of PLGA-PEG with a higher percentage of PEG. The resulting PEGylated PLGA nanoparticles would have a thicker and denser PEG layer surrounding the nanoparticle. This could cause a more pronounced blood residence time for the nanoparticles. In case of sustained-release nanoparticle formulations, more pronounced blood residence time allows nanoparticles to release the drug in the blood. In case of targeted nanoparticle formulations, it allows nanoparticles to remain in blood until they reach their target tissue.

**Targeted Delivery of Docetaxel:** PLGA nanoparticles offer the possibility of surface-modification with various agents. A well-known modification is to decorate PLGA nanoparticles with the ligands of receptors on cancer cell lines to facilitate specific drug delivery to cancer tissues (i.e., targeting anti-cancer agents).

**Example:** Epidermal growth factor receptor (EGFR) is an example of a receptor being overexpressed on breast cancer cells. Herceptin on the other hand is an EGFR antibody that works as a ligand to block the receptor and inhibit cancer cells' ability to receive growth signals. Decorating docetaxel-loaded PLGA nanoparticles with herceptin could facilitate the delivery of docetaxel specifically to breast cancer cells. At the same time herceptin could block the EGFR. This offers a dual anticancer effect for both solid and metastasized cancer.

**Anti-tumour Efficiency of Docetaxel-loaded Nanoparticles in animal:** This research evaluated the pharmacokinetic and bio-distribution profile of docetaxel loaded in

PLGA nanoparticles. However, it would be informative to evaluate the anti-tumour efficiency of docetaxel loaded in PLGA nanoparticles. Therefore, it is recommended to evaluate how the delivery of docetaxel by PLGA nanoparticles contributes to the anti-cancer effect of the drug in animal models.

**Application of Nanoparticles for *in vivo* Efficacy:** Engineered nanoparticles with long-circulating sustained-release properties would keep systemic drug concentration within its therapeutic window. Also, engineered nanoparticles with targeting purposes would reduce the distribution of chemotherapeutic agent to non-cancer tissues. Either case could potentially reinforce the efficacy of the drug in cancer patients. Therefore, as a future perspective, application of docetaxel-loaded nanoparticle formulations in cancer patients and evaluation of therapeutic efficacy and toxicity is recommended.

The ultimate consequence of nanoparticle application in patients would potentially be better efficacy, fewer side effects, tolerance to the chemotherapy, and having a better quality of life.

## REFERENCES


1. Cooper, G.M., *Chapter 2: classification and development of neoplasms*, in *Elements of Human Cancer*. 1992, Jones and Bartlett Publishers Inc. p. 15-30.
2. *Canadian Cancer Statistics*. 2015, Canadian Cancer Society: Toronto, ON, Canada.
3. Chidambaram, M., R. Manavalan, and K. Kathiresan, *Nanotherapeutics to overcome conventional cancer chemotherapy limitations.* J Pharm Pharm Sci, 2011. **14**(1): p. 67-77.
4. Maeda, H., G.Y. Bharate, and J. Daruwalla, *Polymeric drugs for efficient tumor-targeted drug delivery based on EPR-effect.* Eur J Pharm Biopharm, 2009. **71**(3): p. 409-19.
5. Tzakos, A.G., et al., *Novel oncology therapeutics: targeted drug delivery for cancer.* J Drug Deliv, 2013. **2013**: p. 918304.
6. Ho, M.Y. and J.R. Mackey, *Presentation and management of docetaxel-related adverse effects in patients with breast cancer.* Cancer Manag Res, 2014. **6**: p. 253-9.
7. Feng, S.-S. and S. Chien, *Chemotherapeutic engineering: Application and further development of chemical engineering principles for chemotherapy of cancer and other diseases.* Chem Eng Sci, 2003. **58**(18): p. 4087-4114.
8. Gelderblom, H., et al., *Cremophor EL: the drawbacks and advantages of vehicle selection for drug formulation.* Eur J Cancer, 2001. **37**(13): p. 1590-8.
9. Singla, A.K., A. Garg, and D. Aggarwal, *Paclitaxel and its formulations.* Int J Pharm, 2002. **235**(1-2): p. 179-92.
10. Bergh, M., et al., *Contact allergenic activity of Tween 80 before and after air exposure.* Contact Dermatitis, 1997. **37**(1): p. 9-18.
11. Tiwari, G., et al., *Drug delivery systems: An updated review.* Int J Pharm Investig, 2012. **2**(1): p. 2-11.
12. Jabir, N.R., et al., *Nanotechnology-based approaches in anticancer research.* Int J Nanomedicine, 2012. **7**: p. 4391-408.
13. Markman, J.L., et al., *Nanomedicine therapeutic approaches to overcome cancer drug resistance.* Adv Drug Deliv Rev, 2013. **65**(13-14): p. 1866-79.
14. Alken, S. and C.M. Kelly, *Benefit risk assessment and update on the use of docetaxel in the management of breast cancer.* Cancer Manag Res, 2013. **5**: p. 357-65.
15. Kenmotsu, H. and Y. Tanigawara, *Pharmacokinetics, dynamics and toxicity of docetaxel: Why the Japanese dose differs from the Western dose.* Cancer Sci, 2015. **106**(5): p. 497-504.
16. Vaishampayan, U., et al., *Taxanes: an overview of the pharmacokinetics and pharmacodynamics.* Urology, 1999. **54**(6A Suppl): p. 22-9.
17. Clarke, S.J. and L.P. Rivory, *Clinical pharmacokinetics of docetaxel.* Clin Pharmacokinet, 1999. **36**(2): p. 99-114.
18. Takimoto, C. and M. Beeram, *Microtubule Stabilizing Agents in Clinical Oncology, The Taxanes*, in *The Role of Microtubules in Cell Biology, Neurobiology, and Oncology*, T. Fojo, Editor. 2008, Human Press: Totowa, USA. p. 395-419.
19. Hitt, R. and C. Rodríguez, *Docetaxel*, in *Encyclopedia of Cancer*, M. Schwab, Editor. 2011, Springer-Verlag: Berlin Heidelberg p. 1148-50.
20. Engels, F.K. and J. Verweij, *Docetaxel administration schedule: from fever to tears? A review of randomised studies.* Eur J Cancer, 2005. **41**(8): p. 1117-26.
21. Sweetman, S.C., *chapter:Antineoplastics*, in *Martindale: The Complete Drug Reference*. 2011, Pharmaceutical Press.

22. Baker, S.D., A. Sparreboom, and J. Verweij, *Clinical pharmacokinetics of docetaxel : recent developments.* Clin Pharmacokinet, 2006. **45**(3): p. 235-52.
23. Nagar, S., *Pharmacokinetics of anti-cancer drugs used in breast cancer chemotherapy.* Adv Exp Med Biol, 2010. **678**: p. 124-32.
24. Engels, F.K., R.A. Mathot, and J. Verweij, *Alternative drug formulations of docetaxel: a review.* Anticancer Drugs, 2007. **18**(2): p. 95-103.
25. Trudeau, M.E., et al., *Docetaxel in patients with metastatic breast cancer: a phase II study of the National Cancer Institute of Canada-Clinical Trials Group.* J Clin Oncol, 1996. **14**(2): p. 422-8.
26. Bruno, R., et al., *Population pharmacokinetics/pharmacodynamics of docetaxel in phase II studies in patients with cancer.* J Clin Oncol, 1998. **16**(1): p. 187-96.
27. Piccart, M.J., et al., *Docetaxel: an active new drug for treatment of advanced epithelial ovarian cancer.* J Natl Cancer Inst, 1995. **87**(9): p. 676-81.
28. Drori, S., G.D. Eytan, and Y.G. Assaraf, *Potentiation of anticancer-drug cytotoxicity by multidrug-resistance chemosensitizers involves alterations in membrane fluidity leading to increased membrane permeability.* Eur J Biochem, 1995. **228**(3): p. 1020-9.
29. Behar, A., et al., *The pathophysiological mechanism of fluid retention in advanced cancer patients treated with docetaxel, but not receiving corticosteroid comedication.* Br J Clin Pharmacol, 1997. **43**(6): p. 653-8.
30. Semb, K.A., S. Aamdal, and P. Oian, *Capillary protein leak syndrome appears to explain fluid retention in cancer patients who receive docetaxel treatment.* J Clin Oncol, 1998. **16**(10): p. 3426-32.
31. Loos, W.J., et al., *Clinical pharmacokinetics of unbound docetaxel: role of polysorbate 80 and serum proteins.* Clin Pharmacol Ther, 2003. **74**(4): p. 364-71.
32. Wandel, C., R.B. Kim, and C.M. Stein, *"Inactive" excipients such as Cremophor can affect in vivo drug disposition.* Clin Pharmacol Ther, 2003. **73**(5): p. 394-6.
33. Bravo Gonzalez, R.C., et al., *In vitro investigation on the impact of the surface-active excipients Cremophor EL, Tween 80 and Solutol HS 15 on the metabolism of midazolam.* Biopharm Drug Dispos, 2004. **25**(1): p. 37-49.
34. Irache, J.M., et al., *Nanomedicine: novel approaches in human and veterinary therapeutics.* Vet Parasitol, 2011. **180**(1-2): p. 47-71.
35. Estanqueiro, M., et al., *Nanotechnological carriers for cancer chemotherapy: the state of the art.* Colloids Surf B Biointerfaces, 2015. **126**: p. 631-48.
36. Wicki, A., et al., *Nanomedicine in cancer therapy: challenges, opportunities, and clinical applications.* J Control Release, 2015. **200**: p. 138-57.
37. Drbohlavova, J., et al., *Nanocarriers for anticancer drugs--new trends in nanomedicine.* Curr Drug Metab, 2013. **14**(5): p. 547-64.
38. Prabhu, R.H., V.B. Patravale, and M.D. Joshi, *Polymeric nanoparticles for targeted treatment in oncology: current insights.* Int J Nanomedicine, 2015. **10**: p. 1001-18.
39. Mukherjee, B., *Nanosize drug delivery system.* Curr Pharm Biotechnol, 2013. **14**(15): p. 1221.
40. Mozafari, M.R., *Liposomes: an overview of manufacturing techniques.* Cell Mol Biol Lett, 2005. **10**(4): p. 711-9.
41. Malam, Y., M. Loizidou, and A.M. Seifalian, *Liposomes and nanoparticles: nanosized vehicles for drug delivery in cancer.* Trends Pharmacol Sci, 2009. **30**(11): p. 592-9.
42. Allen, T.M., *Liposomes. Opportunities in drug delivery.* Drugs, 1997. **54 Suppl 4**: p. 8-14.

43. Allen, T.M. and P.R. Cullis, *Liposomal drug delivery systems: from concept to clinical applications.* Adv Drug Deliv Rev, 2013. **65**(1): p. 36-48.
44. Fenske, D.B. and P.R. Cullis, *Liposomal nanomedicines.* Expert Opin Drug Deliv, 2008. **5**(1): p. 25-44.
45. Torchilin, V.P., *Recent advances with liposomes as pharmaceutical carriers.* Nat Rev Drug Discov, 2005. **4**(2): p. 145-60.
46. Çağdaş, M., A.D. Sezer, and S. Bucak, *Liposomes as Potential Drug Carrier Systems for Drug Delivery*, in *Application of Nanotechnology in Drug Delivery*. 2014, InTech: Rijeka.
47. Davis, M.E., Z.G. Chen, and D.M. Shin, *Nanoparticle therapeutics: an emerging treatment modality for cancer.* Nat Rev Drug Discov, 2008. **7**(9): p. 771-82.
48. Huang, S.L., *Liposomes in ultrasonic drug and gene delivery.* Adv Drug Deliv Rev, 2008. **60**(10): p. 1167-76.
49. Yingchoncharoen, P., D.S. Kalinowski, and D.R. Richardson, *Lipid-Based Drug Delivery Systems in Cancer Therapy: What Is Available and What Is Yet to Come.* Pharmacol Rev, 2016. **68**(3): p. 701-87.
50. Akbarzadeh, A., et al., *Liposome: classification, preparation, and applications.* Nanoscale Res Lett, 2013. **8**(1): p. 102.
51. Pattni, B.S., V.V. Chupin, and V.P. Torchilin, *New Developments in Liposomal Drug Delivery.* Chem Rev, 2015. **115**(19): p. 10938-10966.
52. Muller, R.H., K. Mader, and S. Gohla, *Solid lipid nanoparticles (SLN) for controlled drug delivery - a review of the state of the art.* Eur J Pharm Biopharm, 2000. **50**(1): p. 161-77.
53. Buse, J. and A. El-Aneed, *Properties, engineering and applications of lipid-based nanoparticle drug-delivery systems: current research and advances.* Nanomedicine (Lond), 2010. **5**(8): p. 1237-60.
54. Pardeike, J., A. Hommoss, and R.H. Muller, *Lipid nanoparticles (SLN, NLC) in cosmetic and pharmaceutical dermal products.* Int J Pharm, 2009. **366**(1-2): p. 170-84.
55. Pardeshi, C., et al., *Solid lipid based nanocarriers: an overview.* Acta Pharm, 2012. **62**(4): p. 433-72.
56. Joshi, M.D. and R.H. Muller, *Lipid nanoparticles for parenteral delivery of actives.* Eur J Pharm Biopharm, 2009. **71**(2): p. 161-72.
57. Teeranachaideekul, V., et al., *Cetyl palmitate-based NLC for topical delivery of Coenzyme Q(10) - development, physicochemical characterization and in vitro release studies.* Eur J Pharm Biopharm, 2007. **67**(1): p. 141-8.
58. Müller, R.H., et al., *Nanostructured Lipid Carriers (NLC): The Second Generation of Solid Lipid Nanoparticles*, in *Percutaneous Penetration Enhancers Chemical Methods in Penetration Enhancement: Nanocarriers*, N. Dragicevic and H.I. Maibach, Editors. 2016, Springer Berlin Heidelberg: Berlin, Heidelberg. p. 161-185.
59. Muller, R.H., M. Radtke, and S.A. Wissing, *Solid lipid nanoparticles (SLN) and nanostructured lipid carriers (NLC) in cosmetic and dermatological preparations.* Adv Drug Deliv Rev, 2002. **54 Suppl 1**: p. S131-55.
60. Souto, E.B., et al., *Development of a controlled release formulation based on SLN and NLC for topical clotrimazole delivery.* Int J Pharm, 2004. **278**(1): p. 71-7.
61. Pouton, C.W., *Lipid formulations for oral administration of drugs: non-emulsifying, self-emulsifying and 'self-microemulsifying' drug delivery systems.* Eur J Pharm Sci, 2000. **11 Suppl 2**: p. S93-8.
62. Jores, K., et al., *Investigations on the structure of solid lipid nanoparticles (SLN) and oil-loaded solid lipid nanoparticles by photon correlation spectroscopy, field-flow*

*fractionation and transmission electron microscopy.* J Control Release, 2004. **95**(2): p. 217-27.
63. Naseri, N., H. Valizadeh, and P. Zakeri-Milani, *Solid Lipid Nanoparticles and Nanostructured Lipid Carriers: Structure, Preparation and Application.* Adv Pharm Bull, 2015. **5**(3): p. 305-13.
64. Jaiswal, P., B. Gidwani, and A. Vyas, *Nanostructured lipid carriers and their current application in targeted drug delivery.* Artif Cells Nanomed Biotechnol, 2016. **44**(1): p. 27-40.
65. Mukherjee, S., S. Ray, and R.S. Thakur, *Solid lipid nanoparticles: a modern formulation approach in drug delivery system.* Indian J Pharm Sci, 2009. **71**(4): p. 349-58.
66. Geszke-Moritz, M. and M. Moritz, *Solid lipid nanoparticles as attractive drug vehicles: Composition, properties and therapeutic strategies.* Mater Sci Eng C Mater Biol Appl, 2016. **68**: p. 982-994.
67. Haag, R. and F. Kratz, *Polymer therapeutics: concepts and applications.* Angew Chem Int Ed Engl, 2006. **45**(8): p. 1198-215.
68. Duncan, R., *Polymer conjugates as anticancer nanomedicines.* Nat Rev Cancer, 2006. **6**(9): p. 688-701.
69. Greco, F. and M.J. Vicent, *Combination therapy: opportunities and challenges for polymer-drug conjugates as anticancer nanomedicines.* Adv Drug Deliv Rev, 2009. **61**(13): p. 1203-13.
70. Jasbir, S., et al., *Polymer Drug Conjugates: Recent Advancements in Various Diseases.* Curr Pharm Des, 2016. **22**(19): p. 2821-2843.
71. Wadhwa, S. and R.J. Mumper, *Polymer-Drug Conjugates for Anticancer Drug Delivery.* Crit Rev Ther Drug Carrier Syst, 2015. **32**(3): p. 215-45.
72. Larson, N. and H. Ghandehari, *Polymeric conjugates for drug delivery.* Chem Mater, 2012. **24**(5): p. 840-853.
73. Mishra, P., B. Nayak, and R.K. Dey, *PEGylation in anti-cancer therapy: An overview.* Asian J Pharm Sci, 2016. **11**(3): p. 337-348.
74. Duncan, R., *Polymer therapeutics as nanomedicines: new perspectives.* Curr Opin Biotech, 2011. **22**(4): p. 492-501.
75. Rohini, et al., *Polymeric Prodrugs: Recent Achievements and General Strategies.* J Antivir Antiretrovir, 2013. **5**(S15).
76. Duncan, R., *The dawning era of polymer therapeutics.* Nat Rev Drug Discov, 2003. **2**(5): p. 347-360.
77. Paleos, C.M., et al., *Drug delivery using multifunctional dendrimers and hyperbranched polymers.* Expert Opin Drug Deliv, 2010. **7**(12): p. 1387-98.
78. Gillies, E.R. and J.M. Frechet, *Dendrimers and dendritic polymers in drug delivery.* Drug Discov Today, 2005. **10**(1): p. 35-43.
79. Sakthivel, T. and A.T. Florence, *Adsorption of amphipathic dendrons on polystyrene nanoparticles.* Int J Pharm, 2003. **254**(1): p. 23-6.
80. Cheng, Y., et al., *Dendrimers as drug carriers: applications in different routes of drug administration.* J Pharm Sci, 2008. **97**(1): p. 123-43.
81. Cheng, Y., et al., *Pharmaceutical applications of dendrimers: promising nanocarriers for drug delivery.* Front Biosci, 2008. **13**: p. 1447-71.
82. Yiyun, C. and X. Tongwen, *Dendrimers as potential drug carriers. Part I. Solubilization of non-steroidal anti-inflammatory drugs in the presence of polyamidoamine dendrimers.* Eur J Med Chem, 2005. **40**(11): p. 1188-92.
83. Fernandez, L., et al., *Solubilization and Release Properties of Dendrimers. Evaluation as Prospective Drug Delivery Systems.* Supramol Chem, 2006. **18**(8): p. 633-643.

84. D'Emanuele, A. and D. Attwood, *Dendrimer-drug interactions.* Adv Drug Deliv Rev, 2005. **57**(15): p. 2147-62.
85. Hsu, H.J., et al., *Dendrimer-based nanocarriers: a versatile platform for drug delivery.* Wiley Interdiscip Rev Nanomed Nanobiotechnol, 2016.
86. Kesharwani, P., K. Jain, and N.K. Jain, *Dendrimer as nanocarrier for drug delivery.* Prog Polym Sci, 2014. **39**(2): p. 268-307.
87. Svenson, S., *Dendrimers as versatile platform in drug delivery applications.* Eur J Pharm Biopharm, 2009. **71**(3): p. 445-62.
88. Dufès, C., I.F. Uchegbu, and A.G. Schätzlein, *Dendrimers in gene delivery.* Adv Drug Deliv Rev, 2005. **57**(15): p. 2177-2202.
89. Cheng, Y., et al., *Design of biocompatible dendrimers for cancer diagnosis and therapy: current status and future perspectives.* Chem Soc Rev, 2011. **40**(5): p. 2673-703.
90. Gupta, U., et al., *Dendrimers: novel polymeric nanoarchitectures for solubility enhancement.* Biomacromolecules, 2006. **7**(3): p. 649-58.
91. Singh, J., et al., *Dendrimers in anticancer drug delivery: mechanism of interaction of drug and dendrimers.* Artif Cells Nanomed Biotechnol, 2016. **44**(7): p. 1626-34.
92. Sharma, A.K., et al., *Dendrimer nanoarchitectures for cancer diagnosis and anticancer drug delivery.* Drug Discov Today, 2016.
93. Safari, J. and Z. Zarnegar, *Advanced drug delivery systems: Nanotechnology of health design A review.* J Saudi Chem Society, 2014. **18**(2): p. 85-99.
94. Pearson, R.M., et al., *Dendritic nanoparticles: the next generation of nanocarriers?* Ther Deliv, 2012. **3**(8): p. 941-59.
95. Yates, C.R. and W. Hayes, *Synthesis and applications of hyperbranched polymers.* Eur Polym J, 2004. **40**(7): p. 1257-1281.
96. Thatikonda, S., et al., *Dendrimers: a new class of polymers* Int J Pharma Sci Res, 2013. **4**(6): p. 2174-2183.
97. Kataoka, K., A. Harada, and Y. Nagasaki, *Block copolymer micelles for drug delivery: design, characterization and biological significance.* Adv Drug Deliv Rev, 2001. **47**(1): p. 113-131.
98. Torchilin, V.P., *Micellar nanocarriers: pharmaceutical perspectives.* Pharm Res, 2007. **24**(1): p. 1-16.
99. Gaucher, G., et al., *Polymeric micelles for oral drug delivery.* Eur J Pharm Biopharm, 2010. **76**(2): p. 147-58.
100. Lu, Y. and K. Park, *Polymeric micelles and alternative nanonized delivery vehicles for poorly soluble drugs.* Int J Pharm, 2013. **453**(1): p. 198-214.
101. Trivedi, R. and U.B. Kompella, *Nanomicellar formulations for sustained drug delivery: strategies and underlying principles.* Nanomedicine (Lond), 2010. **5**(3): p. 485-505.
102. Hamidi, M., M.A. Shahbazi, and K. Rostamizadeh, *Copolymers: efficient carriers for intelligent nanoparticulate drug targeting and gene therapy.* Macromol Biosci, 2012. **12**(2): p. 144-64.
103. Xiong, X.B., et al., *Engineering of amphiphilic block copolymers for polymeric micellar drug and gene delivery.* J Control Release, 2011. **155**(2): p. 248-61.
104. Zhang, Y., Y. Huang, and S. Li, *Polymeric micelles: nanocarriers for cancer-targeted drug delivery.* AAPS PharmSciTech, 2014. **15**(4): p. 862-71.
105. Cabral, H. and K. Kataoka, *Progress of drug-loaded polymeric micelles into clinical studies.* J Control Release, 2014. **190**: p. 465-76.
106. Kim, S. and K. Park, *Polymer Micelles for Drug Delivery,* in *Targeted Delivery of Small and Macromolecular Drugs*. 2010, CRC Press. p. 513-551.

107. Biswas, S., et al., *Recent advances in polymeric micelles for anti-cancer drug delivery.* Eur J Pharm Sci, 2016. **83**: p. 184-202.
108. Yokoyama, M., *Clinical Applications of Polymeric Micelle Carrier Systems in Chemotherapy and Image Diagnosis of Solid Tumors.* J Exp Clin Med, 2011. **3**(4): p. 151-158.
109. Pridgen, E.M., F. Alexis, and O.C. Farokhzad, *Polymeric nanoparticle drug delivery technologies for oral delivery applications.* Expert Opin Drug Deliv, 2015. **12**(9): p. 1459-1473.
110. Masood, F., *Polymeric nanoparticles for targeted drug delivery system for cancer therapy.* Mater Sci Eng C Mater Biol Appl, 2016. **60**: p. 569-78.
111. Kreuter, J., *Nanoparticles--a historical perspective.* Int J Pharm, 2007. **331**(1): p. 1-10.
112. Cegnar, M., J. Kristl, and J. Kos, *Nanoscale polymer carriers to deliver chemotherapeutic agents to tumours.* Expert Opin Biol Ther, 2005. **5**(12): p. 1557-69.
113. Sinha, V.R. and A. Trehan, *Biodegradable microspheres for protein delivery.* J Control Release, 2003. **90**(3): p. 261-80.
114. Whittlesey, K.J. and L.D. Shea, *Delivery systems for small molecule drugs, proteins, and DNA: the neuroscience/biomaterial interface.* Exp Neurol, 2004. **190**(1): p. 1-16.
115. Hamid Akash, M.S., K. Rehman, and S. Chen, *Natural and Synthetic Polymers as Drug Carriers for Delivery of Therapeutic Proteins.* Polym Rev, 2015. **55**(3): p. 371-406.
116. Park, J.H., M. Ye, and K. Park, *Biodegradable polymers for microencapsulation of drugs.* Molecules, 2005. **10**(1): p. 146-61.
117. Kumari, A., S.K. Yadav, and S.C. Yadav, *Biodegradable polymeric nanoparticles based drug delivery systems.* Colloids Surf B Biointerfaces, 2010. **75**(1): p. 1-18.
118. Jaimes-Aguirre, L., et al., *Polymer-Based Drug Delivery Systems, Development and Pre-Clinical Status.* Curr Pharm Des, 2016. **22**(19): p. 2886-903.
119. Kamaly, N., et al., *Degradable Controlled-Release Polymers and Polymeric Nanoparticles: Mechanisms of Controlling Drug Release.* Chem Rev, 2016. **116**(4): p. 2602-63.
120. Banik, B.L., P. Fattahi, and J.L. Brown, *Polymeric nanoparticles: the future of nanomedicine.* Wiley Interdiscip Rev Nanomed Nanobiotechnol, 2016. **8**(2): p. 271-99.
121. Jain, R.A., *The manufacturing techniques of various drug loaded biodegradable poly(lactide-co-glycolide) (PLGA) devices.* Biomaterials, 2000. **21**(23): p. 2475-90.
122. Astete, C.E. and C.M. Sabliov, *Synthesis and characterization of PLGA nanoparticles.* J Biomater Sci Polym Ed, 2006. **17**(3): p. 247-89.
123. Kapoor, D.N., et al., *PLGA: a unique polymer for drug delivery.* Ther Deliv, 2015. **6**(1): p. 41-58.
124. Nair, L.S. and C.T. Laurencin, *Biodegradable polymers as biomaterials.* Prog Polym Sci, 2007. **32**(8–9): p. 762-798.
125. Shive, M.S. and J.M. Anderson, *Biodegradation and biocompatibility of PLA and PLGA microspheres.* Adv Drug Deliv Rev, 1997. **28**(1): p. 5-24.
126. Jalil, R. and J.R. Nixon, *Biodegradable poly(lactic acid) and poly(lactide-co-glycolide) microcapsules: problems associated with preparative techniques and release properties.* J Microencapsul, 1990. **7**(3): p. 297-325.
127. Gentile, P., et al., *An overview of poly(lactic-co-glycolic) acid (PLGA)-based biomaterials for bone tissue engineering.* Int J Mol Sci, 2014. **15**(3): p. 3640-59.
128. Houchin, M.L. and E.M. Topp, *Physical properties of PLGA films during polymer degradation.* J Appl Polym Sci, 2009. **114**(5): p. 2848-2854.

129. Engineer, C., J. Parikh, and A. Raval, *Review on Hydrolytic Degradation Behavior of Biodegradable Polymers from Controlled Drug Delivery System.* Trends Biomater Artif Organs, 2011. **25**(2): p. 79-85.
130. Wu, X.S. and N. Wang, *Synthesis, characterization, biodegradation, and drug delivery application of biodegradable lactic/glycolic acid polymers. Part II: biodegradation.* J Biomater Sci Polym Ed, 2001. **12**(1): p. 21-34.
131. Makadia, H.K. and S.J. Siegel, *Poly Lactic-co-Glycolic Acid (PLGA) as Biodegradable Controlled Drug Delivery Carrier.* Polymers (Basel), 2011. **3**(3): p. 1377-1397.
132. Lu, L., C.A. Garcia, and A.G. Mikos, *In vitro degradation of thin poly(DL-lactic-co-glycolic acid) films.* J Biomed Mater Res, 1999. **46**(2): p. 236-44.
133. Park, T.G., *Degradation of poly(lactic-co-glycolic acid) microspheres: effect of copolymer composition.* Biomaterials, 1995. **16**(15): p. 1123-30.
134. Lu, L., et al., *In vitro and in vivo degradation of porous poly(DL-lactic-co-glycolic acid) foams.* Biomaterials, 2000. **21**(18): p. 1837-45.
135. Park, T.G., *Degradation of poly(d,l-lactic acid) microspheres: effect of molecular weight.* J Control Release, 1994. **30**(2): p. 161-173.
136. Liggins, R.T. and H.M. Burt, *Paclitaxel loaded poly(L-lactic acid) microspheres: properties of microspheres made with low molecular weight polymers.* Int J Pharm, 2001. **222**(1): p. 19-33.
137. Yoshioka, T., et al., *In vitro evaluation of biodegradation of poly(lactic-co-glycolic acid) sponges.* Biomaterials, 2008. **29**(24-25): p. 3438-43.
138. Xie, Y., J. Park, and S. Kang, *Studies on the Effect of Molecular Weight on Biodegradable Polymer Membrane* Int J Bio-Sci Bio-Tech, 2016. **8**(3): p. 315-322.
139. Tracy, M.A., et al., *Factors affecting the degradation rate of poly(lactide-co-glycolide) microspheres in vivo and in vitro.* Biomaterials, 1999. **20**(11): p. 1057-62.
140. Frank, A., S.K. Rath, and S.S. Venkatraman, *Controlled release from bioerodible polymers: effect of drug type and polymer composition.* J Control Release, 2005. **102**(2): p. 333-344.
141. Siegel, S.J., et al., *Effect of drug type on the degradation rate of PLGA matrices.* Eur J Pharm Biopharm, 2006. **64**(3): p. 287-93.
142. Alexis, F., *Factors affecting the degradation and drug-release mechanism of poly(lactic acid) and poly[(lactic acid)-co-(glycolic acid)]*. Polymer Int, 2005. **54**(1): p. 36-46.
143. Fredenberg, S., et al., *The mechanisms of drug release in poly(lactic-co-glycolic acid)-based drug delivery systems--a review.* Int J Pharm, 2011. **415**(1-2): p. 34-52.
144. Schliecker, G., et al., *Hydrolytic degradation of poly(lactide-co-glycolide) films: effect of oligomers on degradation rate and crystallinity.* Int J Pharm, 2003. **266**(1-2): p. 39-49.
145. Grizzi, I., et al., *Hydrolytic degradation of devices based on poly(DL-lactic acid) size-dependence.* Biomaterials, 1995. **16**(4): p. 305-11.
146. Felix Lanao, R.P., et al., *Physicochemical properties and applications of poly(lactic-co-glycolic acid) for use in bone regeneration.* Tissue Eng Part B Rev, 2013. **19**(4): p. 380-90.
147. Leemhuis, M., et al., *In vitro hydrolytic degradation of hydroxyl-functionalized poly(alpha-hydroxy acid)s.* Biomacromolecules, 2007. **8**(9): p. 2943-9.
148. Berchane, N.S., et al., *Effect of mean diameter and polydispersity of PLG microspheres on drug release: experiment and theory.* Int J Pharm, 2007. **337**(1-2): p. 118-26.

149. Allison, S.D., *Analysis of initial burst in PLGA microparticles.* Expert Opin Drug Deliv, 2008. **5**(6): p. 615-28.
150. Wang, J., B.M. Wang, and S.P. Schwendeman, *Characterization of the initial burst release of a model peptide from poly(D,L-lactide-co-glycolide) microspheres.* J Control Release, 2002. **82**(2-3): p. 289-307.
151. Huang, X. and C.S. Brazel, *On the importance and mechanisms of burst release in matrix-controlled drug delivery systems.* J Control Release, 2001. **73**(2-3): p. 121-36.
152. Kanjickal, D.G. and S.T. Lopina, *Modeling of drug release from polymeric delivery systems--a review.* Crit Rev Ther Drug Carrier Syst, 2004. **21**(5): p. 345-86.
153. Lao, L.L., S.S. Venkatraman, and N.A. Peppas, *Modeling of drug release from biodegradable polymer blends.* Eur J Pharm Biopharm, 2008. **70**(3): p. 796-803.
154. Anton, N., J.P. Benoit, and P. Saulnier, *Design and production of nanoparticles formulated from nano-emulsion templates-a review.* J Control Release, 2008. **128**(3): p. 185-99.
155. Vauthier, C. and K. Bouchemal, *Methods for the preparation and manufacture of polymeric nanoparticles.* Pharm Res, 2009. **26**(5): p. 1025-58.
156. Lamprecht, A., et al., *Influences of process parameters on nanoparticle preparation performed by a double emulsion pressure homogenization technique.* Int J Pharm, 2000. **196**(2): p. 177-82.
157. Moinard-Checot, D., et al., *Nanoparticles for drug delivery: review of the formulation and process difficulties illustrated by the emulsion-diffusion process.* J Nanosci Nanotechnol, 2006. **6**(9-10): p. 2664-81.
158. Bala, I., S. Hariharan, and M.N. Kumar, *PLGA nanoparticles in drug delivery: the state of the art.* Crit Rev Ther Drug Carrier Syst, 2004. **21**(5): p. 387-422.
159. Mendoza-Munoz, N., D. Quintanar-Guerrero, and E. Allemann, *The impact of the salting-out technique on the preparation of colloidal particulate systems for pharmaceutical applications.* Recent Pat Drug Deliv Formul, 2012. **6**(3): p. 236-49.
160. Chorny, M., et al., *Lipophilic drug loaded nanospheres prepared by nanoprecipitation: effect of formulation variables on size, drug recovery and release kinetics.* J Control Release, 2002. **83**(3): p. 389-400.
161. Govender, T., et al., *PLGA nanoparticles prepared by nanoprecipitation: drug loading and release studies of a water soluble drug.* J Control Release, 1999. **57**(2): p. 171-85.
162. Sah, E. and H. Sah, *Recent Trends in Preparation of Poly(lactide-co-glycolide) Nanoparticles by Mixing Polymeric Organic Solution with Antisolvent.* J Nanomater, 2015. **2015**: p. 22.
163. Yadav, K.S. and K.K. Sawant, *Modified Nanoprecipitation Method for Preparation of Cytarabine-Loaded PLGA Nanoparticles.* AAPS PharmSciTech, 2010. **11**(3): p. 1456-1465.
164. Nie, H., et al., *PLGA/chitosan composites from a combination of spray drying and supercritical fluid foaming techniques: new carriers for DNA delivery.* J Control Release, 2008. **129**(3): p. 207-14.
165. Khan, I., et al., *PLGA Nanoparticles and Their Versatile Role in Anticancer Drug Delivery.* Crit Rev Ther Drug Carrier Syst, 2016. **33**(2): p. 159-93.
166. Sharma, S., et al., *PLGA-based nanoparticles: A new paradigm in biomedical applications.* TrAC Trends in Analytical Chemistry, 2016. **80**: p. 30-40.
167. Yu, Y., et al., *Antitumor activity of docetaxel-loaded polymeric nanoparticles fabricated by Shirasu porous glass membrane-emulsification technique.* Int J Nanomedicine, 2013. **8**: p. 2641-52.

168. Enlow, E.M., et al., *Potent engineered PLGA nanoparticles by virtue of exceptionally high chemotherapeutic loadings.* Nano Lett, 2011. **11**(2): p. 808-13.
169. Salmaso, S. and P. Caliceti, *Stealth Properties to Improve Therapeutic Efficacy of Drug Nanocarriers.* J Drug Deliv, 2013. **2013**: p. 19.
170. Moghimi, S.M., A.C. Hunter, and J.C. Murray, *Long-circulating and target-specific nanoparticles: theory to practice.* Pharmacol Rev, 2001. **53**(2): p. 283-318.
171. Alexis, F., et al., *Factors affecting the clearance and biodistribution of polymeric nanoparticles.* Mol Pharm, 2008. **5**(4): p. 505-15.
172. Yoo, J.W., E. Chambers, and S. Mitragotri, *Factors that control the circulation time of nanoparticles in blood: challenges, solutions and future prospects.* Curr Pharm Des, 2010. **16**(21): p. 2298-307.
173. Park, J., et al., *PEGylated PLGA nanoparticles for the improved delivery of doxorubicin.* Nanomedicine: Nanotech Biol Med, 2009. **5**(4): p. 410-418.
174. Avgoustakis, K., *Pegylated poly(lactide) and poly(lactide-co-glycolide) nanoparticles: preparation, properties and possible applications in drug delivery.* Curr Drug Deliv, 2004. **1**(4): p. 321-33.
175. Duan, Y., et al., *Preparation of DHAQ-loaded mPEG-PLGA-mPEG nanoparticles and evaluation of drug release behaviors in vitro/in vivo.* J Mater Sci Mater Med, 2006. **17**(6): p. 509-16.
176. Senthilkumar, M., P. Mishra, and N.K. Jain, *Long circulating PEGylated poly(D,L-lactide-co-glycolide) nanoparticulate delivery of Docetaxel to solid tumors.* J Drug Target, 2008. **16**(5): p. 424-35.
177. Kolate, A., et al., *PEG - a versatile conjugating ligand for drugs and drug delivery systems.* J Control Release, 2014. **192**: p. 67-81.
178. Jain, A. and S.K. Jain, *PEGylation: an approach for drug delivery. A review.* Crit Rev Ther Drug Carrier Syst, 2008. **25**(5): p. 403-47.
179. Knop, K., et al., *Poly(ethylene glycol) in drug delivery: pros and cons as well as potential alternatives.* Angew Chem Int Ed Engl, 2010. **49**(36): p. 6288-308.
180. Hamidi, M., A. Azadi, and P. Rafiei, *Pharmacokinetic consequences of pegylation.* Drug Deliv, 2006. **13**(6): p. 399-409.
181. Patel, B., N. Gupta, and F. Ahsan, *Particle engineering to enhance or lessen particle uptake by alveolar macrophages and to influence the therapeutic outcome.* Eur J Pharm Biopharm, 2015. **89**: p. 163-74.
182. Hamidi, M., et al., *A pharmacokinetic overview of nanotechnology-based drug delivery systems: an ADME-oriented approach.* Crit Rev Ther Drug Carrier Syst, 2013. **30**(5): p. 435-67.
183. Owens Iii, D.E. and N.A. Peppas, *Opsonization, biodistribution, and pharmacokinetics of polymeric nanoparticles.* Int J Pharm, 2006. **307**(1): p. 93-102.
184. Betancourt, T., et al., *PEGylation strategies for active targeting of PLA/PLGA nanoparticles.* J Biomed Mater Res A, 2009. **91**(1): p. 263-76.
185. Riley, T., et al., *Physicochemical Evaluation of Nanoparticles Assembled from Poly(lactic acid)−Poly(ethylene glycol) (PLA−PEG) Block Copolymers as Drug Delivery Vehicles.* Langmuir, 2001. **17**(11): p. 3168-3174.
186. Avgoustakis, K., et al., *Effect of copolymer composition on the physicochemical characteristics, in vitro stability, and biodistribution of PLGA-mPEG nanoparticles.* Int J Pharm, 2003. **259**(1-2): p. 115-27.
187. Mosqueira, V.C., et al., *Biodistribution of long-circulating PEG-grafted nanocapsules in mice: effects of PEG chain length and density.* Pharm Res, 2001. **18**(10): p. 1411-9.
188. Suk, J.S., et al., *PEGylation as a strategy for improving nanoparticle-based drug and gene delivery.* Adv Drug Deliv Rev, 2016. **99**(Pt A): p. 28-51.

189. Beck-Broichsitter, M., J. Nicolas, and P. Couvreur, *Design attributes of long-circulating polymeric drug delivery vehicles.* Eur J Pharm Biopharm, 2015. **97**(Pt B): p. 304-17.
190. Mogosanu, G.D., et al., *Polymeric protective agents for nanoparticles in drug delivery and targeting.* Int J Pharm, 2016.
191. Gaucher, G., R.H. Marchessault, and J.C. Leroux, *Polyester-based micelles and nanoparticles for the parenteral delivery of taxanes.* J Control Release, 2010. **143**(1): p. 2-12.
192. Keum, C.G., et al., *Practical preparation procedures for docetaxel-loaded nanoparticles using polylactic acid-co-glycolic acid.* Int J Nanomedicine, 2011. **6**: p. 2225-34.
193. Chu, K.S., et al., *Nanoparticle drug loading as a design parameter to improve docetaxel pharmacokinetics and efficacy.* Biomaterials, 2013. **34**(33): p. 8424-9.
194. Musumeci, T., et al., *PLA/PLGA nanoparticles for sustained release of docetaxel.* Int J Pharm, 2006. **325**(1-2): p. 172-9.
195. Murugesan, S., et al., *PEGylated Poly(Lactide-co-Glycolide) (PLGA) Nanoparticulate Delivery of Docetaxel: Synthesis of Diblock Copolymers, Optimization of Preparation Variables on Formulation Characteristics and In Vitro Release Studies.* J Biomed Nanotechnol, 2007. **3**(1): p. 52-60.
196. Esmaeili, F., et al., *Cellular cytotoxicity and in-vivo biodistribution of docetaxel poly(lactide-co-glycolide) nanoparticles.* Anticancer Drugs, 2010. **21**(1): p. 43-52.
197. Chu, K.S., et al., *Plasma, tumor and tissue pharmacokinetics of Docetaxel delivered via nanoparticles of different sizes and shapes in mice bearing SKOV-3 human ovarian carcinoma xenograft.* Nanomedicine, 2013. **9**(5): p. 686-93.
198. Manoochehri, S., et al., *Surface modification of PLGA nanoparticles via human serum albumin conjugation for controlled delivery of docetaxel.* Daru, 2013. **21**(1): p. 58.
199. Mody, N., et al., *Dendrimer, liposomes, carbon nanotubes and PLGA nanoparticles: one platform assessment of drug delivery potential.* AAPS PharmSciTech, 2014. **15**(2): p. 388-99.
200. Gupta, M., et al., *Dual Targeted Polymeric Nanoparticles Based on Tumor Endothelium and Tumor Cells for Enhanced Antitumor Drug Delivery.* Mol Pharm, 2014. **11**(3): p. 697-715.
201. Jain, S., et al., *Enhanced Antitumor Efficacy and Reduced Toxicity of Docetaxel Loaded Estradiol Functionalized Stealth Polymeric Nanoparticles.* Mol Pharm, 2015. **12**(11): p. 3871-84.
202. Park, J.H., et al., *Development of poly(lactic-co-glycolic) acid nanoparticles-embedded hyaluronic acid-ceramide-based nanostructure for tumor-targeted drug delivery.* Int J Pharm, 2014. **473**(1-2): p. 426-33.
203. Moghimi, S.M., A.C. Hunter, and T.L. Andresen, *Factors controlling nanoparticle pharmacokinetics: an integrated analysis and perspective.* Annu Rev Pharmacol Toxicol, 2012. **52**: p. 481-503.
204. Ernsting, M.J., et al., *Factors controlling the pharmacokinetics, biodistribution and intratumoral penetration of nanoparticles.* J Control Release, 2013. **172**(3): p. 782-94.
205. Wang, J., et al., *More effective nanomedicines through particle design.* Small, 2011. **7**(14): p. 1919-31.
206. Duan, X. and Y. Li, *Physicochemical characteristics of nanoparticles affect circulation, biodistribution, cellular internalization, and trafficking.* Small, 2013. **9**(9-10): p. 1521-32.
207. Toy, R., et al., *The effects of particle size, density and shape on margination of nanoparticles in microcirculation.* Nanotechnology, 2011. **22**(11): p. 115101.

208. Rao, J., *Shedding light on tumors using nanoparticles.* ACS Nano, 2008. **2**(10): p. 1984-6.
209. Kircher, M.F., et al., *A multimodal nanoparticle for preoperative magnetic resonance imaging and intraoperative optical brain tumor delineation.* Cancer Res, 2003. **63**(23): p. 8122-5.
210. Huynh, N.T., et al., *The rise and rise of stealth nanocarriers for cancer therapy: passive versus active targeting.* Nanomedicine (Lond), 2010. **5**(9): p. 1415-33.
211. Blanco, E., H. Shen, and M. Ferrari, *Principles of nanoparticle design for overcoming biological barriers to drug delivery.* Nat Biotech, 2015. **33**(9): p. 941-951.
212. Yadav, K.S., et al., *Effect of Size on the Biodistribution and Blood Clearance of Etoposide-Loaded PLGA Nanoparticles.* PDA J Pharm Sci Technol, 2011. **65**(2): p. 131-9.
213. Heidel, J.D. and M.E. Davis, *Clinical developments in nanotechnology for cancer therapy.* Pharm Res, 2011. **28**(2): p. 187-99.
214. Nel, A.E., et al., *Understanding biophysicochemical interactions at the nano-bio interface.* Nat Mater, 2009. **8**(7): p. 543-557.
215. Wang, J., M. Sui, and W. Fan, *Nanoparticles for tumor targeted therapies and their pharmacokinetics.* Curr Drug Metab, 2010. **11**(2): p. 129-41.
216. Yuan, Y.-Y., et al., *Surface Charge Switchable Nanoparticles Based on Zwitterionic Polymer for Enhanced Drug Delivery to Tumor.* Adv Mater, 2012. **24**(40): p. 5476-5480.
217. Yamamoto, Y., et al., *Long-circulating poly(ethylene glycol)–poly(d,l-lactide) block copolymer micelles with modulated surface charge.* J Control Release, 2001. **77**(1–2): p. 27-38.
218. Vasir, J.K. and V. Labhasetwar, *Quantification of the force of nanoparticle-cell membrane interactions and its influence on intracellular trafficking of nanoparticles.* Biomaterials, 2008. **29**(31): p. 4244-4252.
219. Zhang, J.S., F. Liu, and L. Huang, *Implications of pharmacokinetic behavior of lipoplex for its inflammatory toxicity.* Adv Drug Deliv Rev, 2005. **57**(5): p. 689-98.
220. Nagayama, S., et al., *Time-dependent changes in opsonin amount associated on nanoparticles alter their hepatic uptake characteristics.* Int J Pharm, 2007. **342**(1-2): p. 215-21.
221. Cedervall, T., et al., *Detailed identification of plasma proteins adsorbed on copolymer nanoparticles.* Angew Chem Int Ed Engl, 2007. **46**(30): p. 5754-6.
222. Gessner, A., et al., *Nanoparticles with decreasing surface hydrophobicities: influence on plasma protein adsorption.* Int J Pharm, 2000. **196**(2): p. 245-9.
223. Petros, R.A. and J.M. DeSimone, *Strategies in the design of nanoparticles for therapeutic applications.* Nat Rev Drug Discov, 2010. **9**(8): p. 615-27.
224. Canelas, D.A., K.P. Herlihy, and J.M. DeSimone, *Top-down particle fabrication: control of size and shape for diagnostic imaging and drug delivery.* Wiley Interdiscip Rev Nanomed Nanobiotechnol, 2009. **1**(4): p. 391-404.
225. Enayati, M., et al., *Preparation of polymeric carriers for drug delivery with different shape and size using an electric jet.* Curr Pharm Biotechnol, 2009. **10**(6): p. 600-8.
226. Tao, L., et al., *Shape-specific polymeric nanomedicine: emerging opportunities and challenges.* Exp Biol Med (Maywood), 2011. **236**(1): p. 20-9.
227. Toy, R., et al., *Shaping cancer nanomedicine: the effect of particle shape on the in vivo journey of nanoparticles.* Nanomedicine (Lond), 2014. **9**(1): p. 121-34.
228. Williford, J.M., et al., *Shape Control in Engineering of Polymeric Nanoparticles for Therapeutic Delivery.* Biomater Sci, 2015. **3**(7): p. 894-907.

229. Yoo, J.W. and S. Mitragotri, *Polymer particles that switch shape in response to a stimulus.* Proc Natl Acad Sci U S A, 2010. **107**(25): p. 11205-10.
230. Perry, J.L., et al., *PRINT: a novel platform toward shape and size specific nanoparticle theranostics.* Acc Chem Res, 2011. **44**(10): p. 990-8.
231. Barua, S., et al., *Particle shape enhances specificity of antibody-displaying nanoparticles.* Proc Natl Acad Sci U S A, 2013. **110**(9): p. 3270-5.
232. Rolland, J.P., et al., *Direct fabrication and harvesting of monodisperse, shape-specific nanobiomaterials.* J Am Chem Soc, 2005. **127**(28): p. 10096-100.
233. Galloway, A.L., et al., *Development of a nanoparticle-based influenza vaccine using the PRINT® technology.* Nanomedicine: Nanotechnol Biol Med, 2013. **9**(4): p. 523-531.
234. Yoo, J.W., N. Doshi, and S. Mitragotri, *Endocytosis and Intracellular Distribution of PLGA Particles in Endothelial Cells: Effect of Particle Geometry.* Macromol Rapid Commun, 2010. **31**(2): p. 142-8.
235. Geng, Y., et al., *Shape effects of filaments versus spherical particles in flow and drug delivery.* Nat Nanotechnol, 2007. **2**(4): p. 249-55.
236. Muro, S., et al., *Control of endothelial targeting and intracellular delivery of therapeutic enzymes by modulating the size and shape of ICAM-1-targeted carriers.* Mol Ther, 2008. **16**(8): p. 1450-8.
237. Hutter, E., et al., *Microglial response to gold nanoparticles.* ACS Nano, 2010. **4**(5): p. 2595-606.
238. Gratton, S.E., et al., *The effect of particle design on cellular internalization pathways.* Proc Natl Acad Sci U S A, 2008. **105**(33): p. 11613-8.
239. Champion, J.A. and S. Mitragotri, *Role of target geometry in phagocytosis.* Proc Natl Acad Sci U S A, 2006. **103**(13): p. 4930-4.
240. Decuzzi, P., et al., *Size and shape effects in the biodistribution of intravascularly injected particles.* J Control Release, 2010. **141**(3): p. 320-7.
241. Champion, J.A. and S. Mitragotri, *Shape induced inhibition of phagocytosis of polymer particles.* Pharm Res, 2009. **26**(1): p. 244-9.
242. Doshi, N. and S. Mitragotri, *Macrophages recognize size and shape of their targets.* PLoS One, 2010. **5**(4): p. e10051.
243. Sharma, G., et al., *Polymer particle shape independently influences binding and internalization by macrophages.* J Control Release, 2010. **147**(3): p. 408-12.
244. Mitragotri, S. and J. Lahann, *Physical approaches to biomaterial design.* Nat Mater, 2009. **8**(1): p. 15-23.
245. Decuzzi, P., et al., *A theoretical model for the margination of particles within blood vessels.* Ann Biomed Eng, 2005. **33**(2): p. 179-90.
246. Gentile, F., et al., *The margination propensity of spherical particles for vascular targeting in the microcirculation.* J Nanobiotechnology, 2008. **6**: p. 9.
247. Park, J. and J.E. Butler, *Analysis of the Migration of Rigid Polymers and Nanorods in a Rotating Viscometric Flow.* Macromolecules, 2010. **43**(5): p. 2535-2543.
248. Carboni, E., et al., *Particle margination and its implications on intravenous anticancer drug delivery.* AAPS PharmSciTech, 2014. **15**(3): p. 762-71.
249. Gatti, A.M., et al., *Detection of micro- and nano-sized biocompatible particles in the blood.* J Mater Sci Mater Med, 2004. **15**(4): p. 469-72.
250. Ilinskaya, A.N. and M.A. Dobrovolskaia, *Nanoparticles and the blood coagulation system. Part I: benefits of nanotechnology.* Nanomedicine (Lond), 2013. **8**(5): p. 773-84.
251. Ilinskaya, A.N. and M.A. Dobrovolskaia, *Nanoparticles and the blood coagulation system. Part II: safety concerns.* Nanomedicine (Lond), 2013. **8**(6): p. 969-81.

252. Rothen-Rutishauser, B.M., et al., *Interaction of fine particles and nanoparticles with red blood cells visualized with advanced microscopic techniques.* Environ Sci Technol, 2006. **40**(14): p. 4353-9.
253. Shah, N.B., et al., *Blood-nanoparticle interactions and in vivo biodistribution: impact of surface PEG and ligand properties.* Mol Pharm, 2012. **9**(8): p. 2146-55.
254. Dutta, D., et al., *Adsorbed proteins influence the biological activity and molecular targeting of nanomaterials.* Toxicol Sci, 2007. **100**(1): p. 303-15.
255. Aggarwal, P., et al., *Nanoparticle interaction with plasma proteins as it relates to particle biodistribution, biocompatibility and therapeutic efficacy.* Adv Drug Deliv Rev, 2009. **61**(6): p. 428-37.
256. Gao, H. and Q. He, *The interaction of nanoparticles with plasma proteins and the consequent influence on nanoparticles behavior.* Expert Opin Drug Deliv, 2014. **11**(3): p. 409-20.
257. Walkey, C.D., et al., *Nanoparticle size and surface chemistry determine serum protein adsorption and macrophage uptake.* J Am Chem Soc, 2012. **134**(4): p. 2139-47.
258. Dobrovolskaia, M.A., et al., *Preclinical studies to understand nanoparticle interaction with the immune system and its potential effects on nanoparticle biodistribution.* Mol Pharm, 2008. **5**(4): p. 487-95.
259. Karmali, P.P. and D. Simberg, *Interactions of nanoparticles with plasma proteins: implication on clearance and toxicity of drug delivery systems.* Expert Opin Drug Deliv, 2011. **8**(3): p. 343-57.
260. Gentile, F., M. Ferrari, and P. Decuzzi, *The transport of nanoparticles in blood vessels: the effect of vessel permeability and blood rheology.* Ann Biomed Eng, 2008. **36**(2): p. 254-61.
261. Romero, E.L., et al., *On the mechanism of hepatic transendothelial passage of large liposomes.* FEBS Lett, 1999. **448**(1): p. 193-6.
262. Li, M., et al., *Physiologically based pharmacokinetic modeling of nanoparticles.* ACS Nano, 2010. **4**(11): p. 6303-17.
263. Longmire, M., P.L. Choyke, and H. Kobayashi, *Clearance properties of nano-sized particles and molecules as imaging agents: considerations and caveats.* Nanomedicine (Lond), 2008. **3**(5): p. 703-17.
264. Sadauskas, E., et al., *Kupffer cells are central in the removal of nanoparticles from the organism.* Part Fibre Toxicol, 2007. **4**: p. 10.
265. Cho, C.S., et al., *Receptor-mediated cell modulator delivery to hepatocyte using nanoparticles coated with carbohydrate-carrying polymers.* Biomaterials, 2001. **22**(1): p. 45-51.
266. Demoy, M., et al., *In vitro evaluation of nanoparticles spleen capture.* Life Sci, 1999. **64**(15): p. 1329-37.
267. Sou, K., et al., *Bone marrow-targeted liposomal carriers.* Expert Opin Drug Deliv, 2011. **8**(3): p. 317-28.
268. Rao, D.A., et al., *Biodegradable PLGA based nanoparticles for sustained regional lymphatic drug delivery.* J Pharm Sci, 2010. **99**(4): p. 2018-31.
269. Khullar, O.V., et al., *Nanoparticle migration and delivery of Paclitaxel to regional lymph nodes in a large animal model.* J Am Coll Surg, 2012. **214**(3): p. 328-37.
270. Cho, H.Y. and Y.B. Lee, *Nano-sized drug delivery systems for lymphatic delivery.* J Nanosci Nanotechnol, 2014. **14**(1): p. 868-80.
271. Yang, R.S., et al., *Pharmacokinetics and physiologically-based pharmacokinetic modeling of nanoparticles.* J Nanosci Nanotechnol, 2010. **10**(12): p. 8482-90.

272. Tao, W., et al., *Docetaxel-loaded nanoparticles based on star-shaped mannitol-core PLGA-TPGS diblock copolymer for breast cancer therapy.* Acta Biomater, 2013. **9**(11): p. 8910-20.
273. Pradhan, R., et al., *Docetaxel-loaded polylactic acid-co-glycolic acid nanoparticles: formulation, physicochemical characterization and cytotoxicity studies.* J Nanosci Nanotechnol, 2013. **13**(8): p. 5948-56.
274. Agrawal, R., et al., *Polyelectrolyte coated polymeric nanoparticles for controlled release of docetaxel.* J Biomed Nanotechnol, 2012. **8**(1): p. 19-28.
275. Shi, W., et al., *Optimization of parameters for preparation of docetaxel-loaded PLGA nanoparticles by nanoprecipitation method.* J Huazhong Univ Sci Technolog Med Sci, 2013. **33**(5): p. 754-8.
276. Singh, B., et al., *Optimizing drug delivery systems using systematic "design of experiments." Part II: retrospect and prospects.* Crit Rev Ther Drug Carrier Syst, 2005. **22**(3): p. 215-94.
277. Singh, B., R. Kumar, and N. Ahuja, *Optimizing drug delivery systems using systematic "design of experiments." Part I: fundamental aspects.* Crit Rev Ther Drug Carrier Syst, 2005. **22**(1): p. 27-105.
278. Saraf, S., *Process optimization for the production of nanoparticles for drug delivery applications.* Expert Opin Drug Deliv, 2009. **6**(2): p. 187-96.
279. Rao, R.S., et al., *The Taguchi methodology as a statistical tool for biotechnological applications: a critical appraisal.* Biotechnol J, 2008. **3**(4): p. 510-23.
280. Song, K.C., et al., *The effect of type of organic phase solvents on the particle size of poly(d,l-lactide-co-glycolide) nanoparticles.* Colloids and Surfaces A: Physicochemical and Engineering Aspects, 2006. **276**(1–3): p. 162-167.
281. Budhian, A., S.J. Siegel, and K.I. Winey, *Haloperidol-loaded PLGA nanoparticles: systematic study of particle size and drug content.* Int J Pharm, 2007. **336**(2): p. 367-75.
282. Sharma, N., P. Madan, and S. Lin, *Effect of process and formulation variables on the preparation of parenteral paclitaxel-loaded biodegradable polymeric nanoparticles: A co-surfactant study.* Asian J Pharm Sci, 2016. **11**(3): p. 404-416.
283. Noori Koopaei, M., et al., *Docetaxel Loaded PEG-PLGA Nanoparticles: Optimized Drug Loading, In-vitro Cytotoxicity and In-vivo Antitumor Effect.* Iran J Pharm Res, 2014. **13**(3): p. 819-33.
284. Cho, E.J., et al., *Nanoparticle characterization: state of the art, challenges, and emerging technologies.* Mol Pharm, 2013. **10**(6): p. 2093-110.
285. Remmele, R.L., S. Krishnan, and W.J. Callahan, *Development of stable lyophilized protein drug products.* Curr Pharm Biotechnol, 2012. **13**(3): p. 471-96.
286. Fonte, P., S. Reis, and B. Sarmento, *Facts and evidences on the lyophilization of polymeric nanoparticles for drug delivery.* J Control Release, 2016. **225**: p. 75-86.
287. Abdelwahed, W., et al., *Freeze-drying of nanoparticles: formulation, process and storage considerations.* Adv Drug Deliv Rev, 2006. **58**(15): p. 1688-713.
288. Chacon, M., et al., *Stability and freeze-drying of cyclosporine loaded poly(D,L lactide-glycolide) carriers.* Eur J Pharm Sci, 1999. **8**(2): p. 99-107.
289. Bozdag, S., et al., *The effect of freeze-drying with different cryoprotectants and gamma-irradiation sterilization on the characteristics of ciprofloxacin HCl-loaded poly(D,L-lactide-glycolide) nanoparticles.* J Pharm Pharmacol, 2005. **57**(6): p. 699-707.
290. Jeong, Y.I., et al., *Effect of cryoprotectants on the reconstitution of surfactant-free nanoparticles of poly(DL-lactide-co-glycolide).* J Microencapsul, 2005. **22**(6): p. 593-601.

291. Holzer, M., et al., *Physico-chemical characterisation of PLGA nanoparticles after freeze-drying and storage.* Eur J Pharm Biopharm, 2009. **72**(2): p. 428-37.
292. Fonte, P., et al., *Effect of cryoprotectants on the porosity and stability of insulin-loaded PLGA nanoparticles after freeze-drying.* Biomatter, 2012. **2**(4): p. 329-39.
293. Tang, K.S., S.M. Hashmi, and E.M. Shapiro, *The effect of cryoprotection on the use of PLGA encapsulated iron oxide nanoparticles for magnetic cell labeling.* Nanotechnology, 2013. **24**(12): p. 125101.
294. Sahoo, S.K., et al., *Residual polyvinyl alcohol associated with poly (D,L-lactide-co-glycolide) nanoparticles affects their physical properties and cellular uptake.* J Control Release, 2002. **82**(1): p. 105-14.
295. Murakami, H., et al., *Preparation of poly(DL-lactide-co-glycolide) nanoparticles by modified spontaneous emulsification solvent diffusion method.* Int J Pharm, 1999. **187**(2): p. 143-52.
296. Murakami, H., et al., *Further application of a modified spontaneous emulsification solvent diffusion method to various types of PLGA and PLA polymers for preparation of nanoparticles.* Powder Technology, 2000. **107**(1-2): p. 137-143.
297. Konan, Y.N., R. Gurny, and E. Allemann, *Preparation and characterization of sterile and freeze-dried sub-200 nm nanoparticles.* Int J Pharm, 2002. **233**(1-2): p. 239-52.
298. Muller, R.H., *Charge determinations,* in *Colloidal carriers for controlled drug delivery and targeting modification, characterization and in vivo distribution*, R.H. Muller, Editor. 1991, CRC Press: Boca Raton, Florida. p. 57–97.
299. Dhankar, R., et al., *HER-2 targeted immunonanoparticles for breast cancer chemotherapy.* J Appl Pharm Sci, 2011. **1**(3): p. 132-9.
300. Sanna, V., et al., *Novel docetaxel-loaded nanoparticles based on poly(lactide-co-caprolactone) and poly(lactide-co-glycolide-co-caprolactone) for prostate cancer treatment: formulation, characterization, and cytotoxicity studies.* Nanoscale Res Lett, 2011. **6**(1): p. 260.
301. Koopaei, M.N., et al., *Docetaxel immunonanocarriers as targeted delivery systems for HER 2-positive tumor cells: preparation, characterization, and cytotoxicity studies.* Int J Nanomedicine, 2011. **6**: p. 1903-12.
302. Locatelli, E. and M. Comes Franchini, *Biodegradable PLGA-b-PEG polymeric nanoparticles: synthesis, properties, and nanomedical applications as drug delivery system.* J Nanopart Res, 2012. **14**(12): p. 1-17.
303. Scholes, P.D., et al., *Detection and determination of surface levels of poloxamer and PVA surfactant on biodegradable nanospheres using SSIMS and XPS.* J Control Release, 1999. **59**(3): p. 261-78.
304. Esmaeili, F., F. Atyabi, and R. Dinarvand, *Preparation and characterization of estradiol-loaded PLGA nanoparticles using homogenization-solvent diffusion method.* Daru, 2008. **16**: p. 196–202.
305. Zhang, H., et al., *Preparation of poly(lactide-co-glycolide-co-caprolactone) nanoparticles and their degradation behaviour in aqueous solution.* Polymer Degradation and Stability, 2006. **91**(9): p. 1929-36.
306. Abouelmagd, S.A., et al., *Release kinetics study of poorly water-soluble drugs from nanoparticles: are we doing it right?* Mol Pharm, 2015. **12**(3): p. 997-1003.
307. Fonseca, C., S. Simoes, and R. Gaspar, *Paclitaxel-loaded PLGA nanoparticles: preparation, physicochemical characterization and in vitro anti-tumoral activity.* J Control Release, 2002. **83**(2): p. 273-286.
308. Katayama, K., K. Noguchi, and Y. Sugimoto, *Regulations of P-Glycoprotein/ABCB1/MDR1 in Human Cancer Cells.* New Journal of Science, 2014. **2014**: p. 10.

309. Abdallah, H.M., et al., *P-glycoprotein inhibitors of natural origin as potential tumor chemo-sensitizers: A review.* J Adv Res, 2015. **6**(1): p. 45-62.
310. Aleman, C., et al., *P-glycoprotein, expressed in multidrug resistant cells, is not responsible for alterations in membrane fluidity or membrane potential.* Cancer Res, 2003. **63**(12): p. 3084-91.
311. Amin, M.L., *P-glycoprotein Inhibition for Optimal Drug Delivery.* Drug Target Insights, 2013. **7**: p. 27-34.
312. Shirasaka, Y., T. Sakane, and S. Yamashita, *Effect of P-glycoprotein expression levels on the concentration-dependent permeability of drugs to the cell membrane.* J Pharm Sci, 2008. **97**(1): p. 553-65.
313. Kou, L., et al., *The endocytosis and intracellular fate of nanomedicines: Implication for rational design.* Asian J Pharm Sci, 2013. **8**(1): p. 1-10.
314. Panyam, J. and V. Labhasetwar, *Dynamics of endocytosis and exocytosis of poly(D,L-lactide-co-glycolide) nanoparticles in vascular smooth muscle cells.* Pharm Res, 2003. **20**(2): p. 212-20.
315. Yoo, H.S. and T.G. Park, *Folate-receptor-targeted delivery of doxorubicin nano-aggregates stabilized by doxorubicin-PEG-folate conjugate.* J Control Release, 2004. **100**(2): p. 247-56.
316. Gan, C.W., S. Chien, and S.S. Feng, *Nanomedicine: enhancement of chemotherapeutical efficacy of docetaxel by using a biodegradable nanoparticle formulation.* Curr Pharm Des, 2010. **16**(21): p. 2308-20.
317. Sims, L.B., et al., *Enhanced uptake and transport of PLGA-modified nanoparticles in cervical cancer.* J Nanobiotechnology, 2016. **14**: p. 33.
318. Danhier, F., et al., *Paclitaxel-loaded PEGylated PLGA-based nanoparticles: in vitro and in vivo evaluation.* J Control Release, 2009. **133**(1): p. 11-7.
319. Cheng, J., et al., *Formulation of functionalized PLGA-PEG nanoparticles for in vivo targeted drug delivery.* Biomaterials, 2007. **28**(5): p. 869-76.
320. Zufia Lopez, L., et al., *Determination of docetaxel and Paclitaxel in human plasma by high-performance liquid chromatography: validation and application to clinical pharmacokinetic studies.* Ther Drug Monit, 2006. **28**(2): p. 199-205.
321. Bermingham, S., et al., *Simultaneous determination of anthracyclines and taxanes in human serum using online sample extraction coupled to high performance liquid chromatography with UV detection.* J Sep Sci, 2010. **33**(11): p. 1571-9.
322. Parise, R.A., et al., *Sensitive liquid chromatography-mass spectrometry assay for quantitation of docetaxel and paclitaxel in human plasma.* J Chromatogr B Analyt Technol Biomed Life Sci, 2003. **783**(1): p. 231-6.
323. Wang, L.Z., et al., *A rapid and sensitive liquid chromatography/tandem mass spectrometry method for determination of docetaxel in human plasma.* Rapid Commun Mass Spectrom, 2003. **17**(14): p. 1548-52.
324. Hou, W., J.W. Watters, and H.L. McLeod, *Simple and rapid docetaxel assay in plasma by protein precipitation and high-performance liquid chromatography-tandem mass spectrometry.* J Chromatogr B Analyt Technol Biomed Life Sci, 2004. **804**(2): p. 263-7.
325. Mortier, K.A., et al., *Development and validation of a liquid chromatography-tandem mass spectrometry assay for the quantification of docetaxel and paclitaxel in human plasma and oral fluid.* Anal Chem, 2005. **77**(14): p. 4677-83.
326. Guitton, J., et al., *Quantification of docetaxel and its main metabolites in human plasma by liquid chromatography/tandem mass spectrometry.* Rapid Commun Mass Spectrom, 2005. **19**(17): p. 2419-26.

327. Huang, Q., et al., *Simultaneous determination of docetaxel and ketoconazole in rat plasma by liquid chromatography/electrospray ionization tandem mass spectrometry.* Rapid Commun Mass Spectrom, 2007. **21**(6): p. 1009-18.
328. Gustafson, D.L., et al., *Analysis of docetaxel pharmacokinetics in humans with the inclusion of later sampling time-points afforded by the use of a sensitive tandem LCMS assay.* Cancer Chemother Pharmacol, 2003. **52**(2): p. 159-66.
329. Kuppens, I.E., et al., *Quantitative analysis of docetaxel in human plasma using liquid chromatography coupled with tandem mass spectrometry.* Biomed Chromatogr, 2005. **19**(5): p. 355-61.
330. Sparreboom, A., et al., *Determination of the docetaxel vehicle, polysorbate 80, in patient samples by liquid chromatography-tandem mass spectrometry.* J Chromatogr B Analyt Technol Biomed Life Sci, 2002. **773**(2): p. 183-90.
331. Ito, Y., et al., *Simple and rapid determination of thiabendazole, imazalil, and o-phenylphenol in citrus fruit using flow-injection electrospray ionization tandem mass spectrometry.* J Agric Food Chem, 2003. **51**(4): p. 861-6.
332. Song, F., et al., *Fast screening of lovastatin in red yeast rice products by flow injection tandem mass spectrometry.* J Pharm Biomed Anal, 2012. **57**: p. 76-81.
333. Zhou, H., et al., *Rapid identification of vinca alkaloids by direct-injection electrospray ionisation tandem mass spectrometry and confirmation by high-performance liquid chromatography-mass spectrometry.* Phytochem Anal, 2005. **16**(5): p. 328-33.
334. Carducci, C., et al., *Quantitative determination of guanidinoacetate and creatine in dried blood spot by flow injection analysis-electrospray tandem mass spectrometry.* Clin Chim Acta, 2006. **364**(1-2): p. 180-7.
335. Peer, C.J., et al., *Direct injection mass spectrometric confirmation of multiple drugs in overdose cases from postmortem blood using electrospray ionization-tandem mass spectrometry and MS(3).* J Anal Toxicol, 2008. **32**(8): p. 709-14.
336. Peer, C.J., et al., *Direct-injection mass spectrometric method for the rapid identification of fentanyl and norfentanyl in postmortem urine of six drug-overdose cases.* J Anal Toxicol, 2007. **31**(8): p. 515-21.
337. Grozav, A.G., et al., *Rapid analysis of docetaxel in human plasma by tandem mass spectrometry with on-line sample extraction.* J Pharm Biomed Anal, 2004. **36**(1): p. 125-31.
338. Hendrikx, J.J.M.A., et al., *A sensitive combined assay for the quantification of paclitaxel, docetaxel and ritonavir in human plasma using liquid chromatography coupled with tandem mass spectrometry.* J Chromatogr B, 2011. **879**(28): p. 2984-2990.
339. Yamaguchi, H., et al., *A rapid and sensitive LC/ESI-MS/MS method for quantitative analysis of docetaxel in human plasma and its application to a pharmacokinetic study.* J Chromatogr B Analyt Technol Biomed Life Sci, 2012. **893-894**: p. 157-61.
340. Corona, G., et al., *High-throughput plasma docetaxel quantification by liquid chromatography-tandem mass spectrometry.* Clin Chim Acta, 2011. **412**(3-4): p. 358-64.
341. Du, P., et al., *Development and validation of a rapid and sensitive UPLC–MS/MS method for determination of total docetaxel from a lipid microsphere formulation in human plasma.* J Chromatogr B, 2013. **926**: p. 101-107.
342. Du, P., et al., *Development and validation of an ultrafiltration-UPLC-MS/MS method for rapid quantification of unbound docetaxel in human plasma.* J Chromatogr B, 2014. **967**: p. 28-35.

343. Annesley, T.M., *Ion suppression in mass spectrometry.* Clin Chem, 2003. **49**(7): p. 1041-4.
344. Taylor, P.J., *Matrix effects: the Achilles heel of quantitative high-performance liquid chromatography-electrospray-tandem mass spectrometry.* Clin Biochem, 2005. **38**(4): p. 328-34.
345. Hall, T.G., et al., *Identifying and Overcoming Matrix Effects in Drug Discovery and Development* in *Tandem Mass Spectrometry - Applications and Principles*, J.K. Prasain, Editor. 2012, InTech.
346. King, R., et al., *Mechanistic investigation of ionization suppression in electrospray ionization.* J Am Soc Mass Spectrom, 2000. **11**(11): p. 942-950.
347. Guo, W., et al., *Paclitaxel quantification in mouse plasma and tissues containing liposome-entrapped paclitaxel by liquid chromatography-tandem mass spectrometry: application to a pharmacokinetics study.* Anal Biochem, 2005. **336**(2): p. 213-20.
348. Tong, X., J. Zhou, and Y. Tan, *Liquid chromatography/tandem triple-quadrupole mass spectrometry for determination of paclitaxel in rat tissues.* Rapid Commun Mass Spectrom, 2006. **20**(12): p. 1905-12.
349. Liu, B., et al., *Simultaneous determination of seven taxoids in rat plasma by UPLC–MS/MS and pharmacokinetic study after oral administration of Taxus yunnanensis extracts.* Journal of Pharmaceutical and Biomedical Analysis, 2015. **107**: p. 346-354.
350. Sparreboom, A., et al., *Preclinical pharmacokinetics of paclitaxel and docetaxel.* Anticancer Drugs, 1998. **9**(1): p. 1-17.
351. Dinarvand, R., et al., *Polylactide-co-glycolide nanoparticles for controlled delivery of anticancer agents.* Int J Nanomedicine, 2011. **6**: p. 877-95.
352. Zhang, Y.N., et al., *Nanoparticle-liver interactions: Cellular uptake and hepatobiliary elimination.* J Control Release, 2016.
353. Park, J.K., et al., *Cellular distribution of injected PLGA-nanoparticles in the liver.* Nanomedicine, 2016. **12**(5): p. 1365-74.
354. Sarin, H., *Physiologic upper limits of pore size of different blood capillary types and another perspective on the dual pore theory of microvascular permeability.* J Angiogenes Res, 2010. **2**: p. 14.
355. Rensen, P.C., et al., *Determination of the upper size limit for uptake and processing of ligands by the asialoglycoprotein receptor on hepatocytes in vitro and in vivo.* J Biol Chem, 2001. **276**(40): p. 37577-84.
356. Kumari, A., et al., *Biodegradable Nanoparticles and Their In Vivo Fate*, in *Nanoscale Materials in Targeted Drug Delivery, Theragnosis and Tissue Regeneration*, K.S. Yadav, Editor. 2016, Springer Singapore: Singapore. p. 21-39.
357. Gref, R., et al., *Long-circulating Drug Delivery SystemsThe controlled intravenous delivery of drugs using PEG-coated sterically stabilized nanospheres.* Adv Drug Deliv Rev, 1995. **16**(2): p. 215-233.
358. E Hoyt Jr, R., et al., *Chapter 2 - Mouse Physiology A2 - Fox, James G*, in *The Mouse in Biomedical Research (Second Edition)*, M.T. Davisson, et al., Editors. 2007, Academic Press: Burlington. p. 23-XVI.
359. White, E., *Mechanical modulation of cardiac microtubules.* Pflugers Arch, 2011. **462**(1): p. 177-84.
360. Aquila-Pastir, L.A., et al., *Quantitation and Distribution of β-tubulin in Human Cardiac Myocytes.* J Mol Cell Cardiol, 2002. **34**(11): p. 1513-1523.
361. Herbst, R.S. and F.R. Khuri, *Mode of action of docetaxel - a basis for combination with novel anticancer agents.* Cancer Treat Rev, 2003. **29**(5): p. 407-15.
362. Jin, C., et al., *Cytotoxicity of paclitaxel incorporated in PLGA nanoparticles on hypoxic human tumor cells.* Pharm Res, 2009. **26**(7): p. 1776-84.

363. Loira-Pastoriza, C., J. Todoroff, and R. Vanbever, *Delivery strategies for sustained drug release in the lungs.* Adv Drug Deliv Rev, 2014. **75**: p. 81-91.
364. Paranjpe, M. and C.C. Muller-Goymann, *Nanoparticle-mediated pulmonary drug delivery: a review.* Int J Mol Sci, 2014. **15**(4): p. 5852-73.
365. Barry Weinberger, et al., *Section II: Airway/Alveolar Surface - Interaction with Lung Macrophages*, in *Nanoparticles in the Lung: Environmental Exposure and Drug Delivery*, Akira Tsuda and P. Gehr, Editors. 2014. p. 85-106.

## APPENDIX A

## SUPPLEMENTARY FIGURES

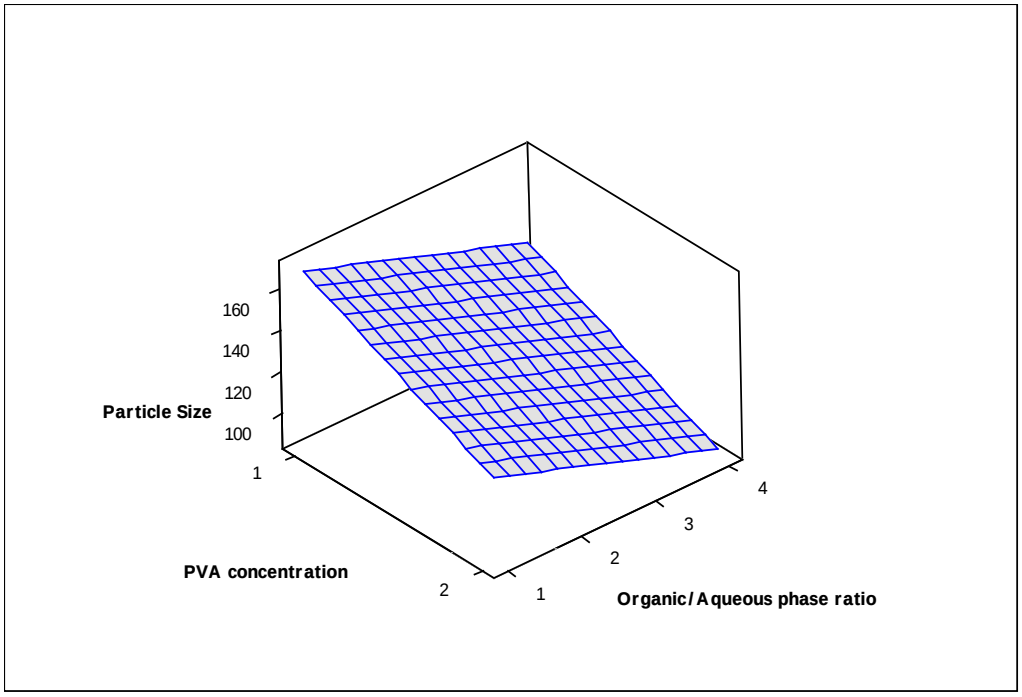


Supplementary figure 1. Response surface plot of particle size Vs organic/aqueous phase ratio and poly (vinyl alcohol) (PVA) concentration

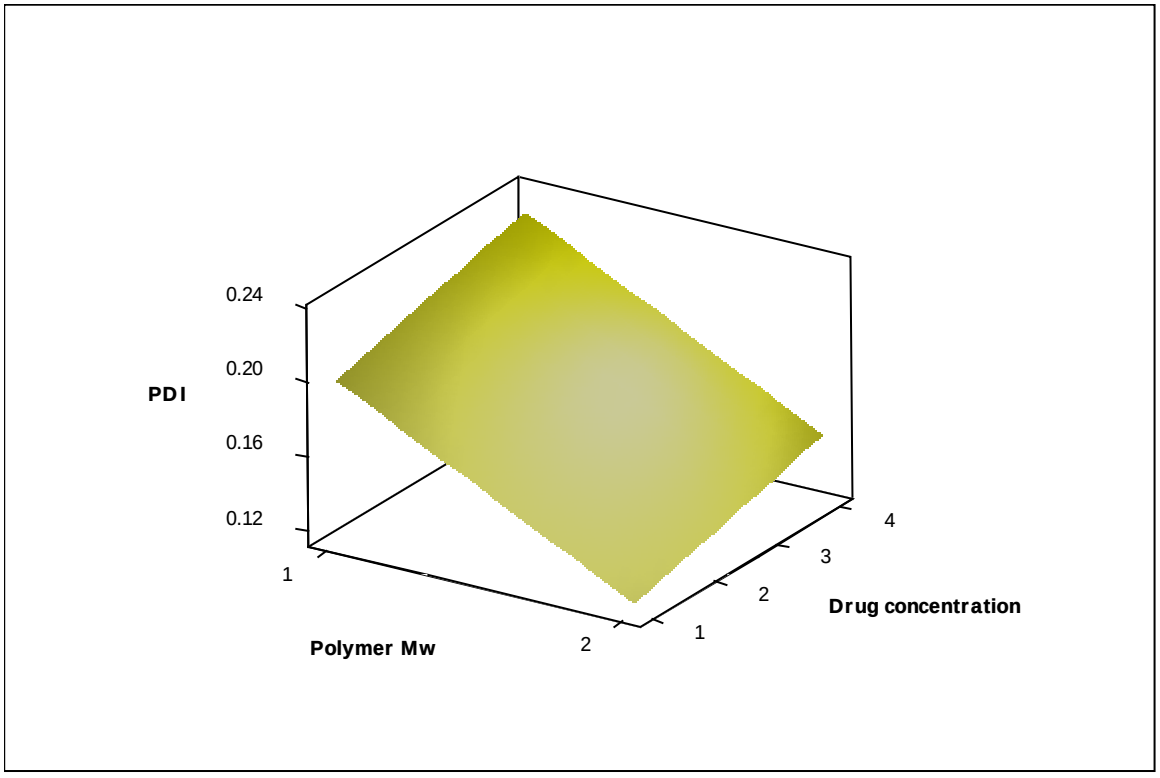

**A**

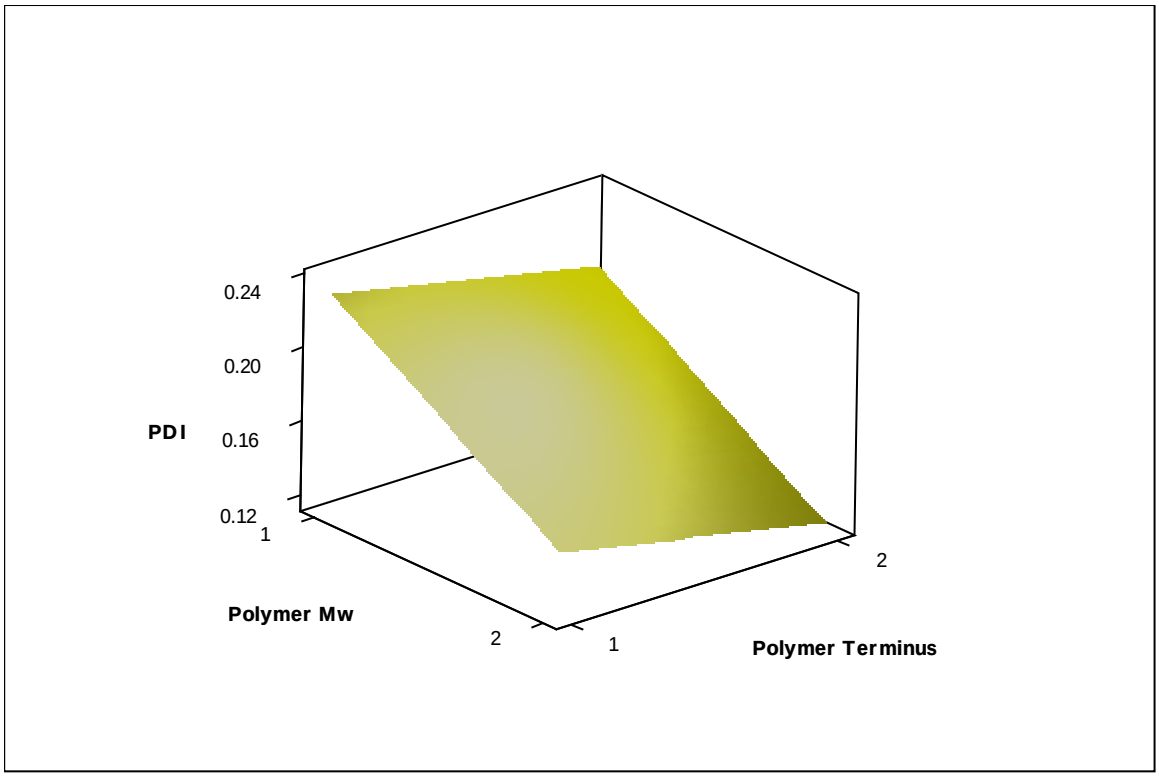


**B**

Supplementary figure 2. Response surface plot of poly dispersity index (PDI) Vs polymer molecular weight (Mw) and A) drug concentration, B) polymer terminus.

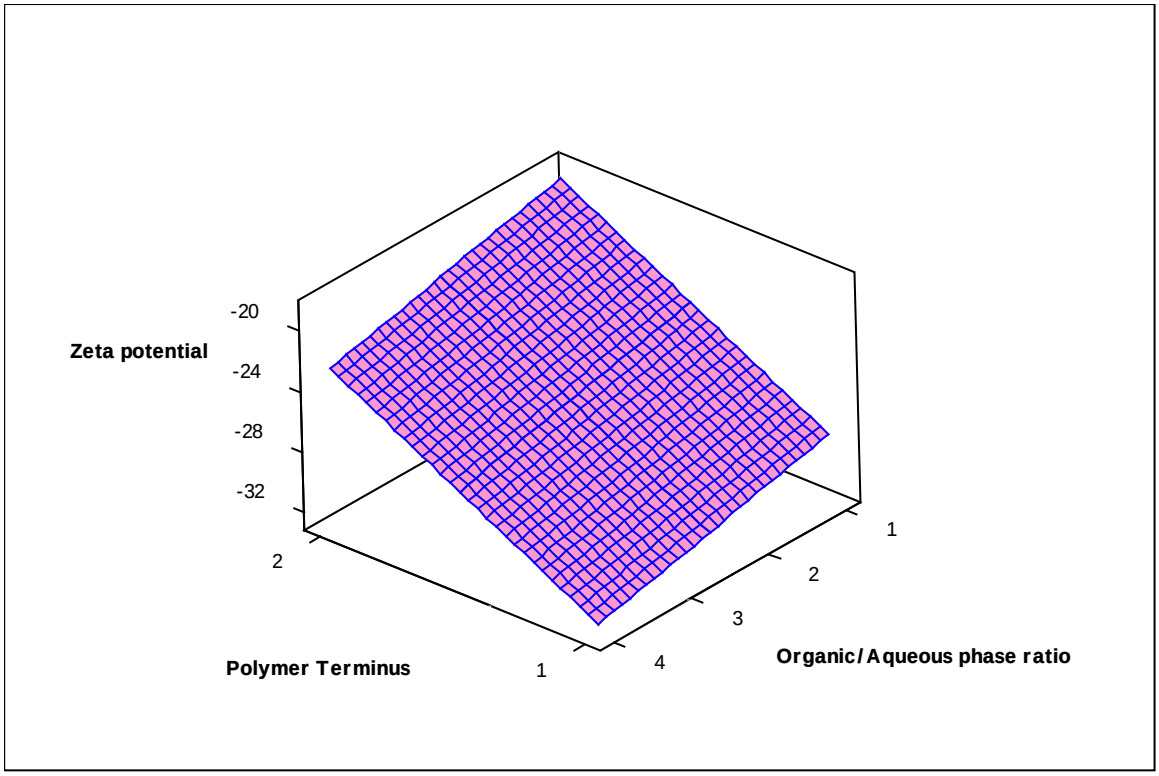

**A**

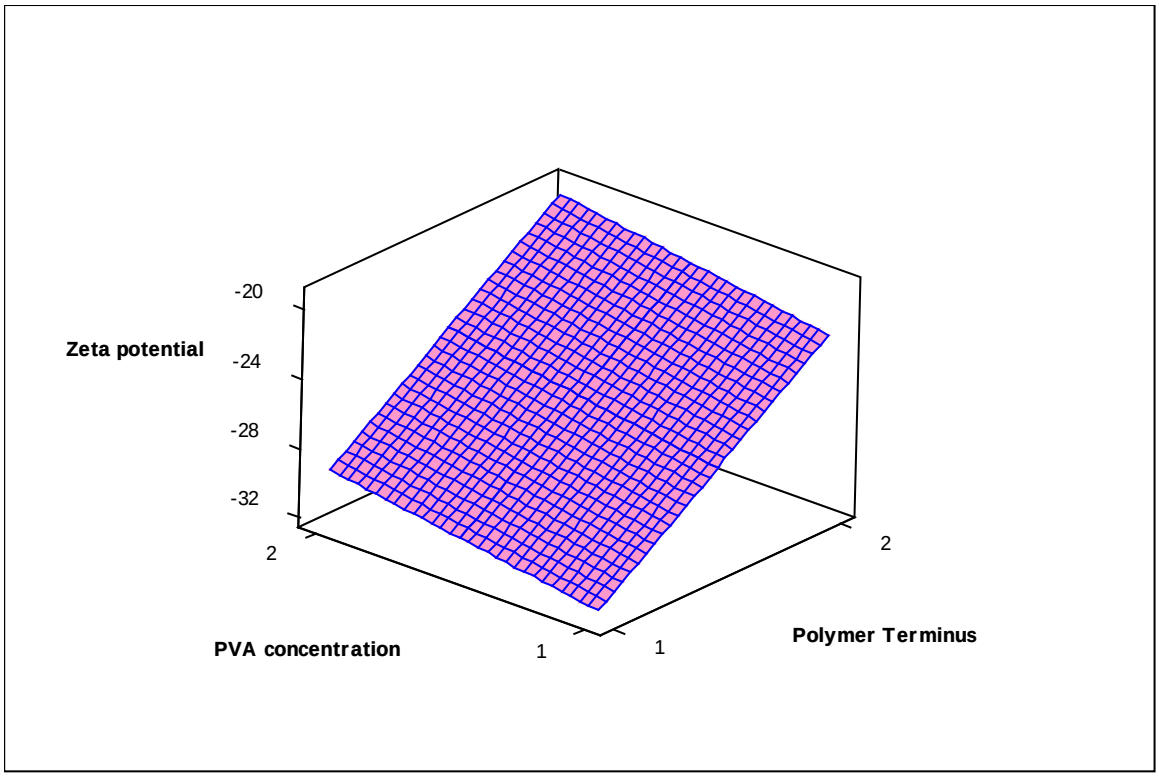


**B**

Supplementary figure 3. Response surface plot of particle zeta potential Vs polymer terminus and A) organic/aqueous phase ratio, B) poly (vinyl alcohol) PVA concentration.

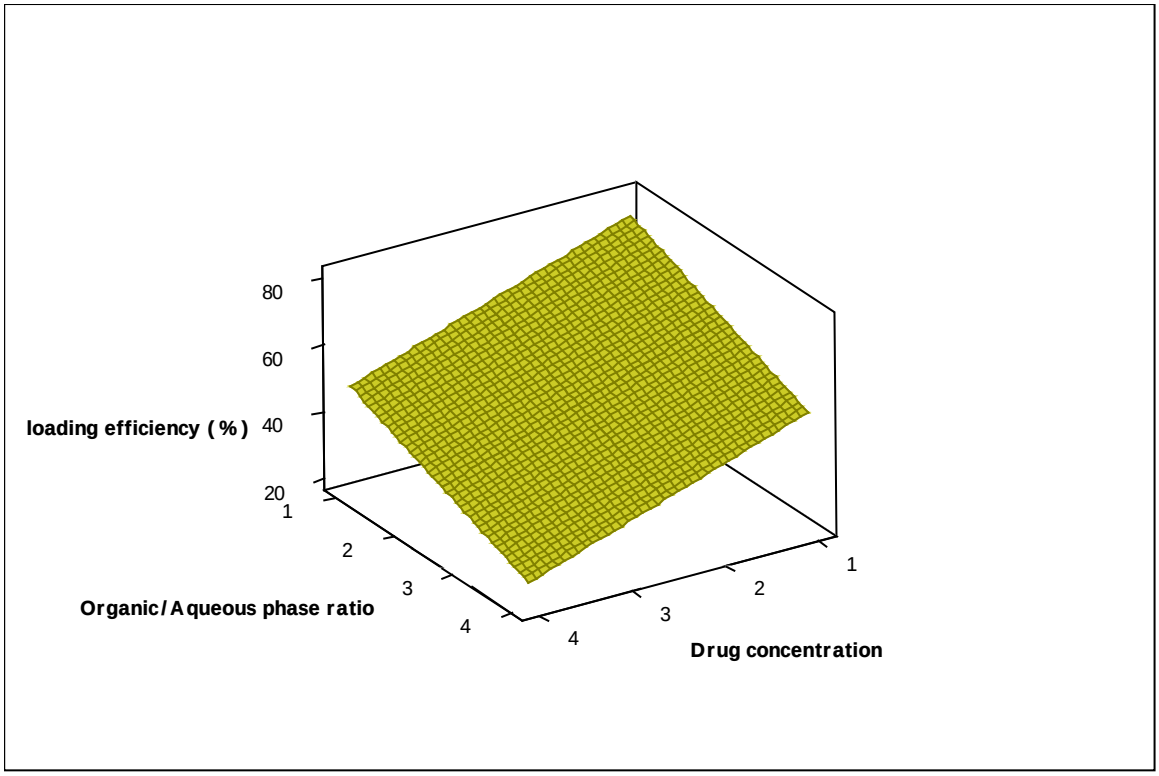

**A**

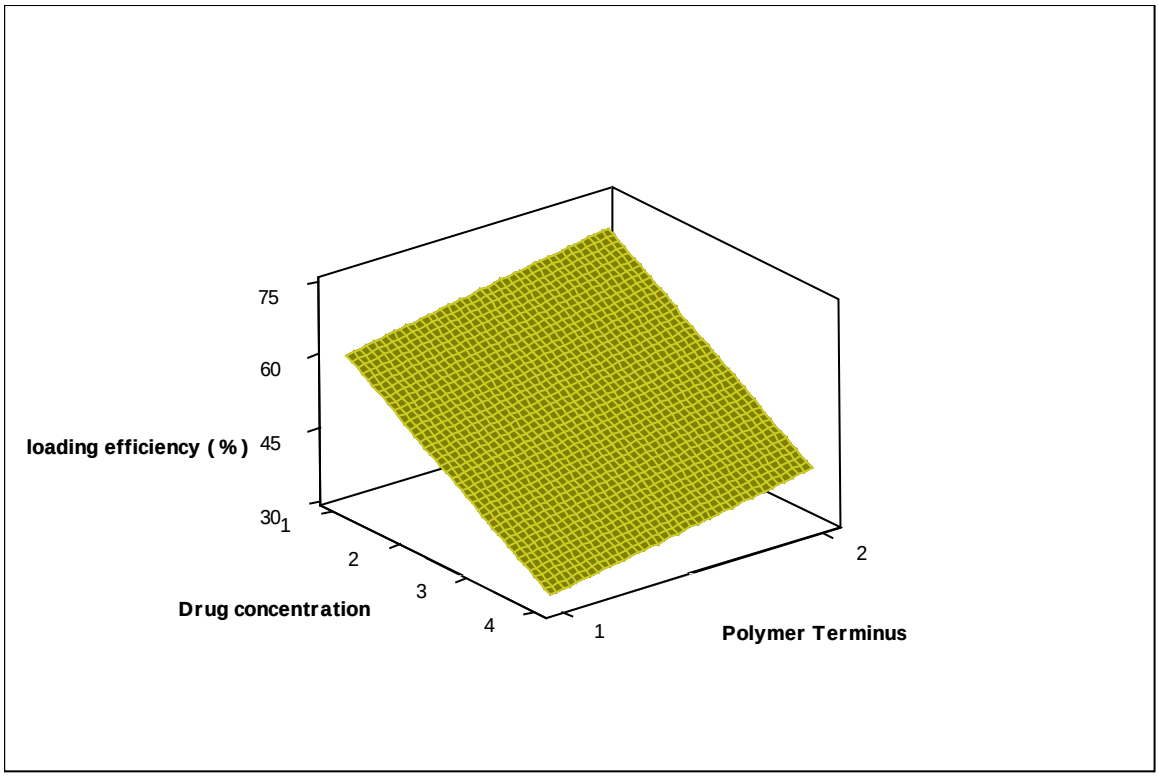
75
60
loading efficiency (%) 45
30
1
2
3
4
Drug concentration
1
2
Polymer Terminus

**B**

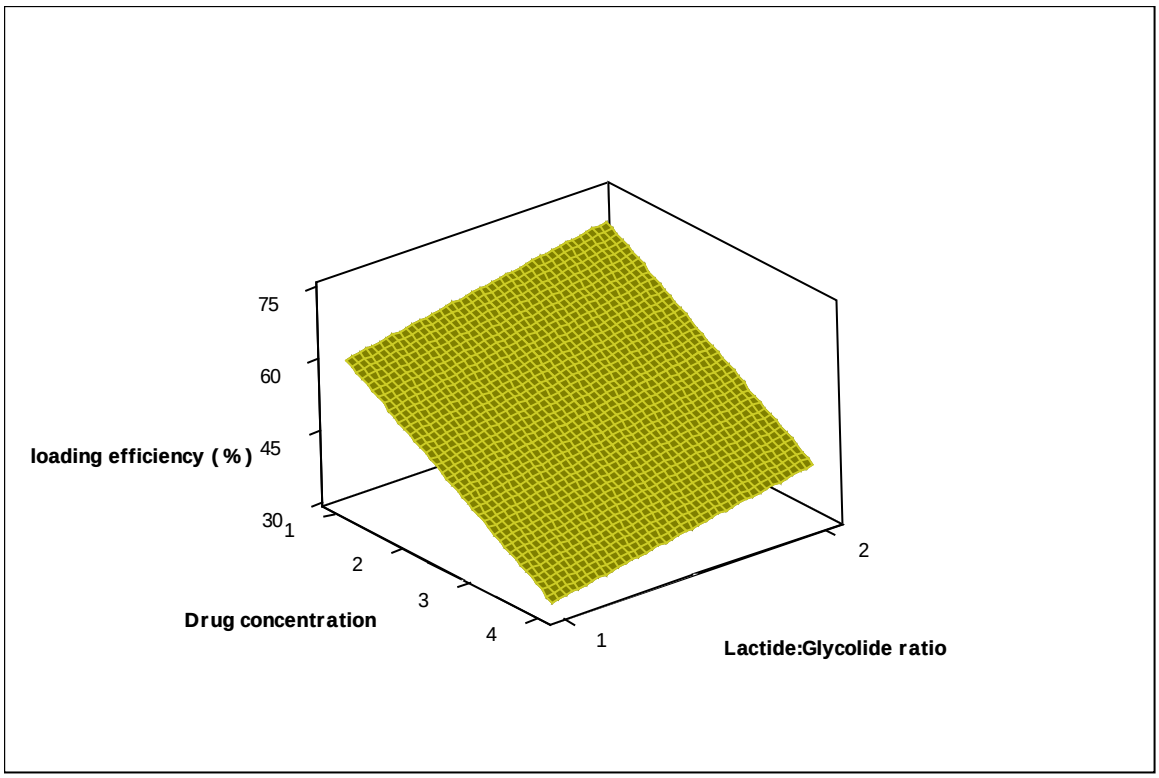
75
60
loading efficiency (%) 45
30
1
2
3
4
Drug concentration
1
2
Lactide:Glycolide ratio

**C**

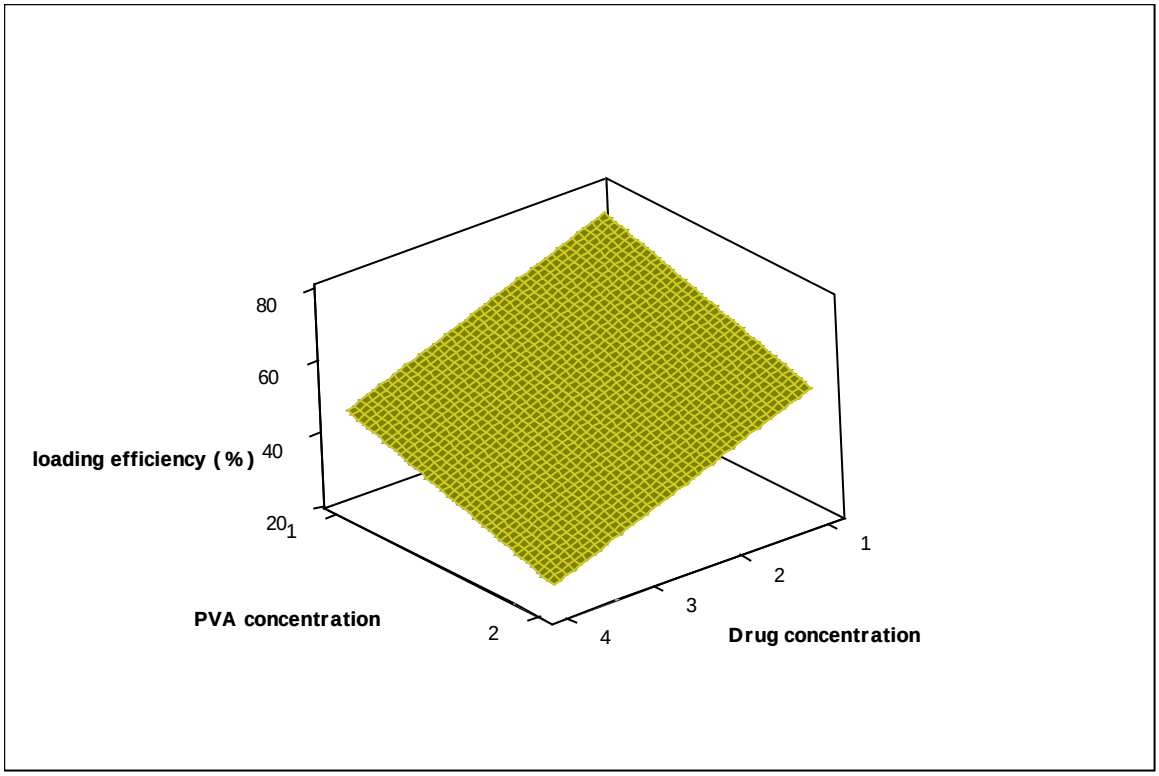


**D**

Supplementary figure 4. Response surface plot of drug-loading efficiency Vs drug concentration and A) organic/aqueous phase ratio, B) polymer terminus, C) lactide:glycolide ratio, D) poly (vinyl alcohol) (PVA) concentration.

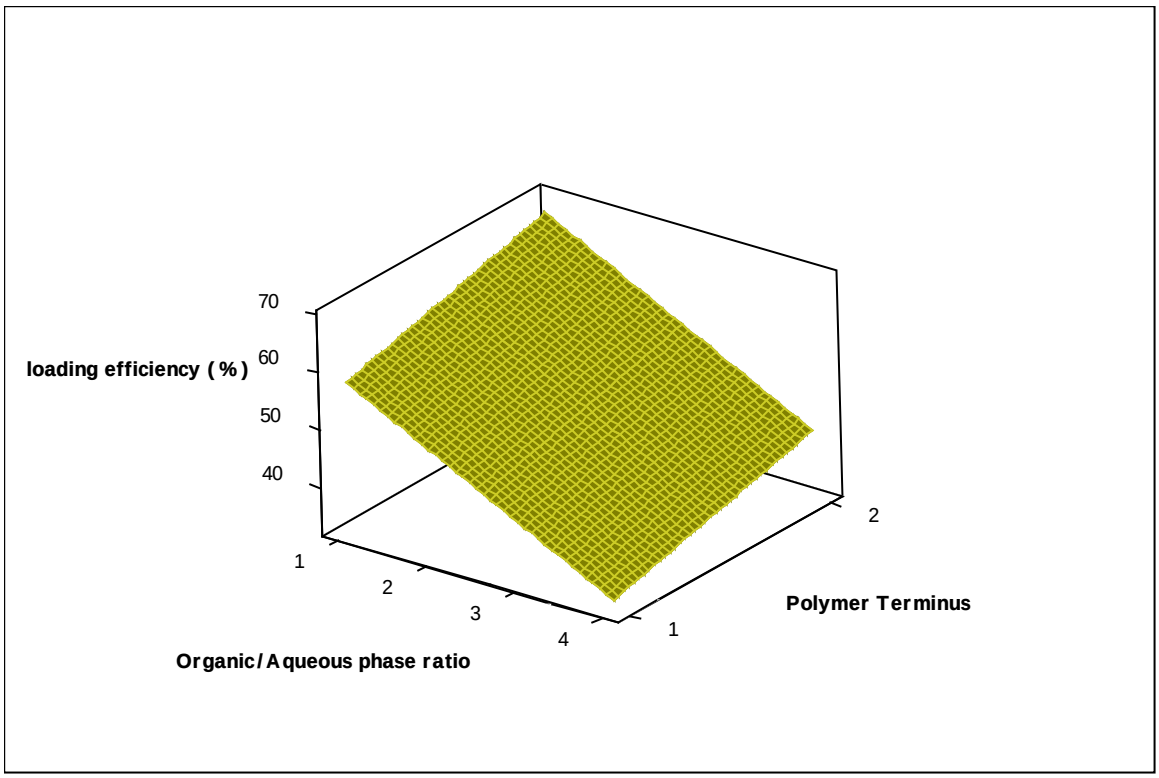


**A**

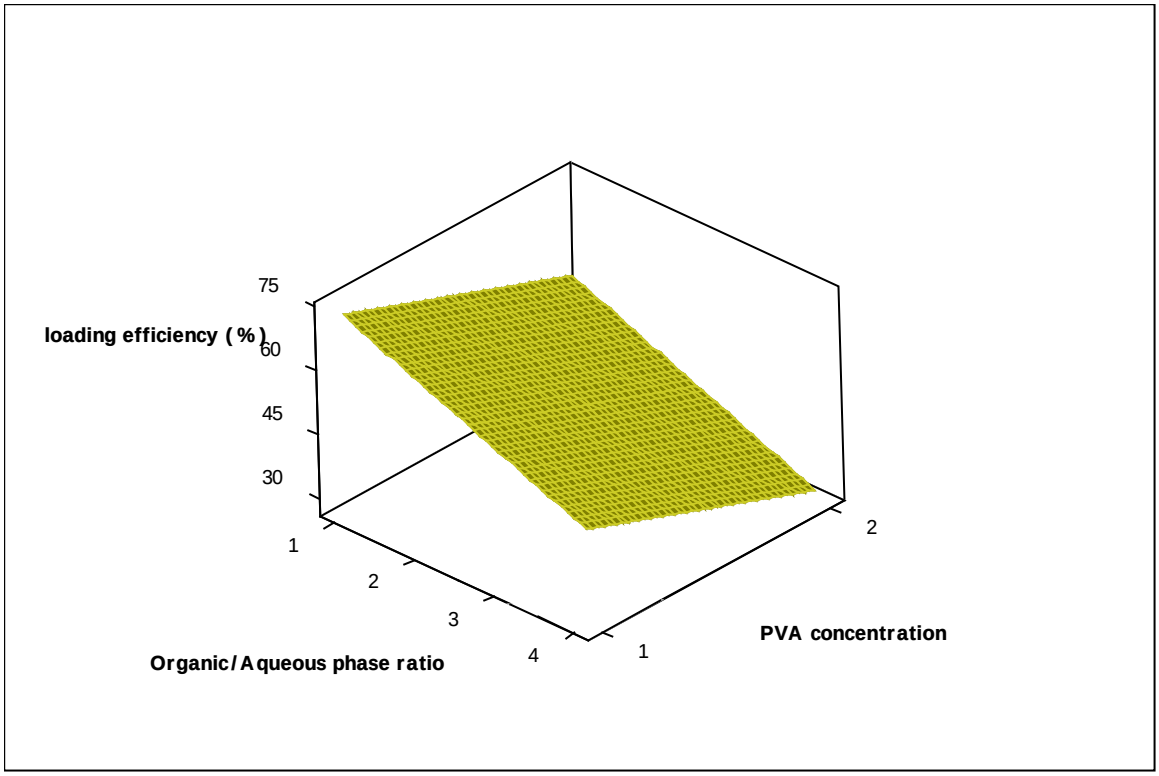


**B**

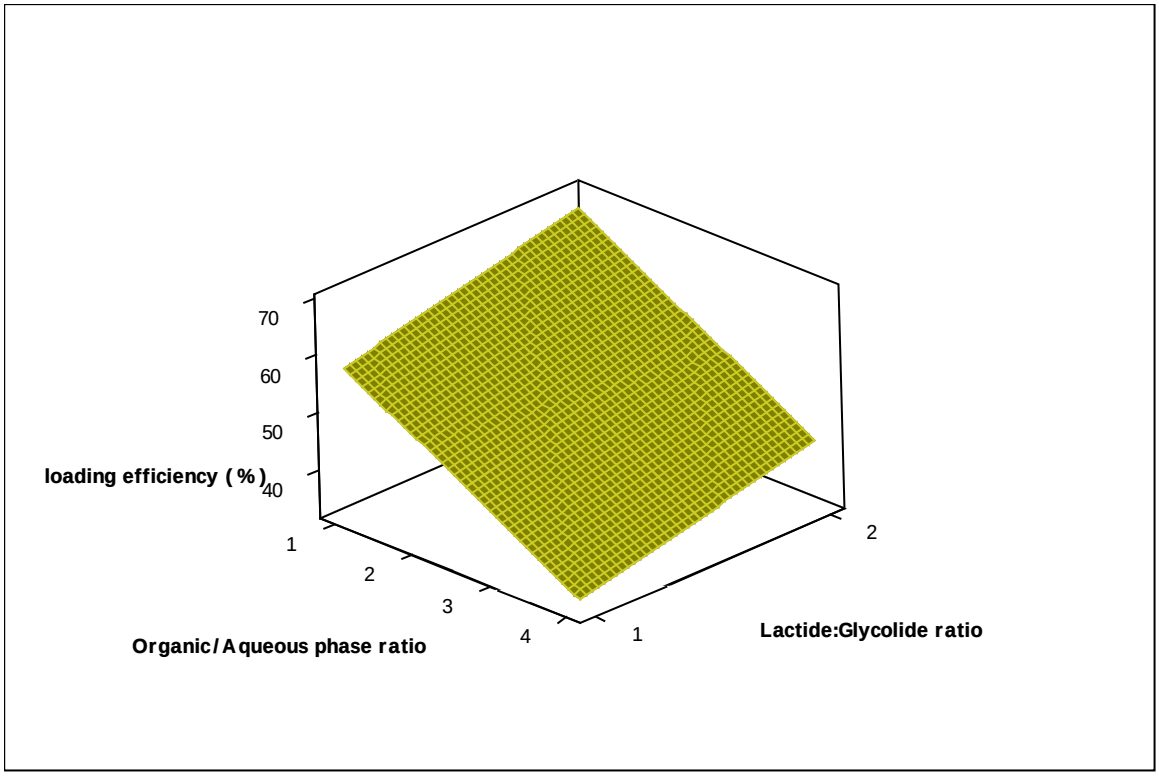


**C**

Supplementary figure 5. Response surface plot of drug-loading efficiency Vs organic/aqueous phase ratio and A) polymer terminus, B) poly (vinyl alcohol) (PVA) concentration, C) lactide:glycolide ratio.

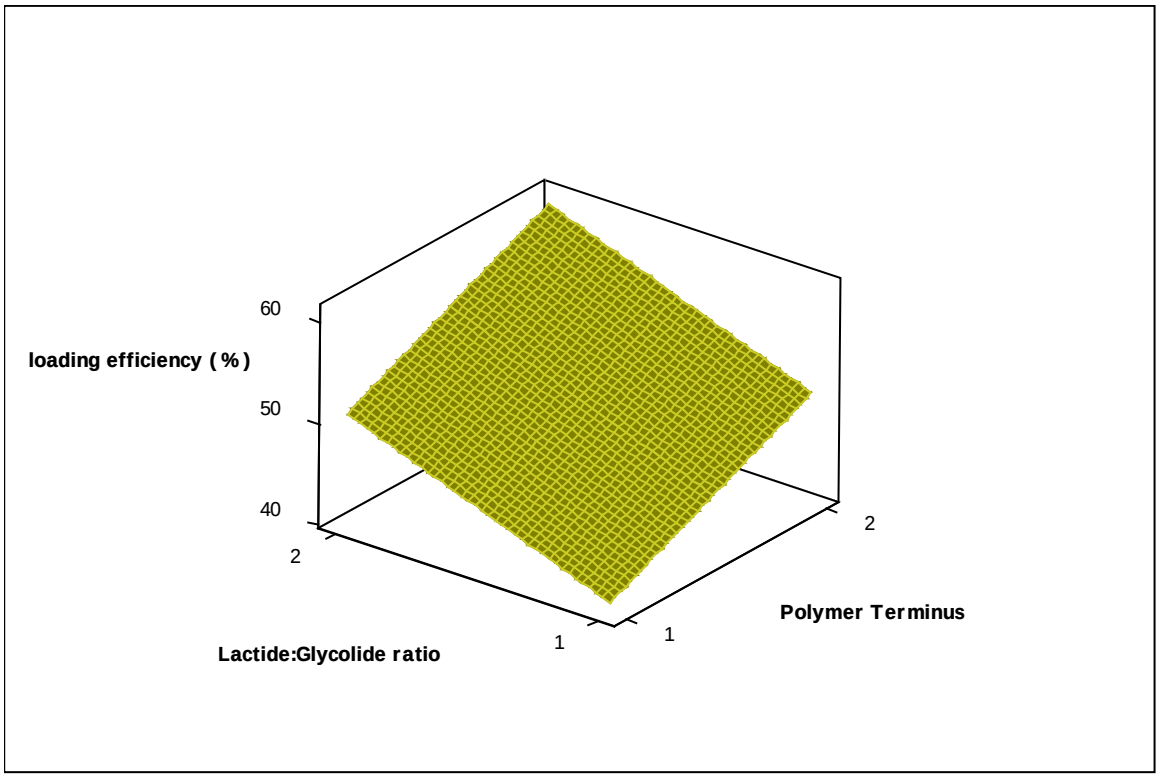
loading efficiency (%)
60
50
40
2
1
Lactide:Glycolide ratio
1
2
Polymer Terminus

**A**

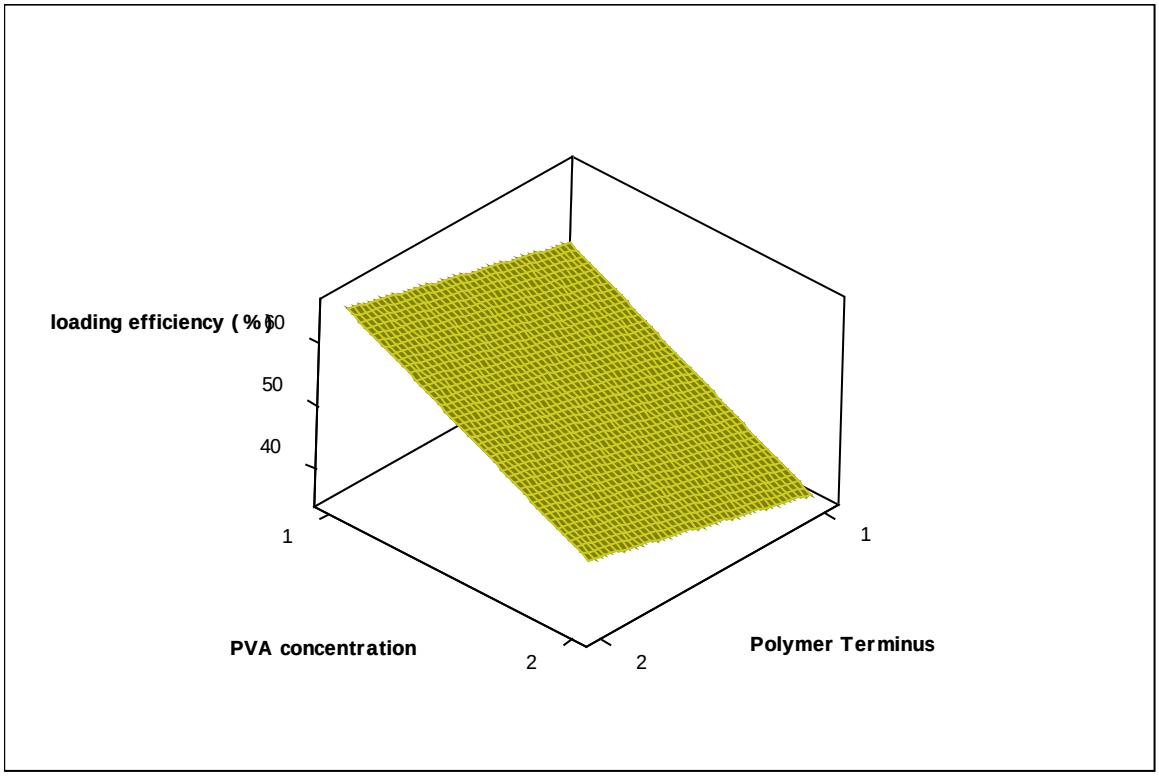
loading efficiency (%)
60
50
40
1
2
PVA concentration
2
1
Polymer Terminus

**B**

Supplementary figure 6. Response surface plot of drug-loading efficiency Vs polymer terminus and A) lactide:glycolide ratio, B) poly (vinyl alcohol) (PVA) concentration.

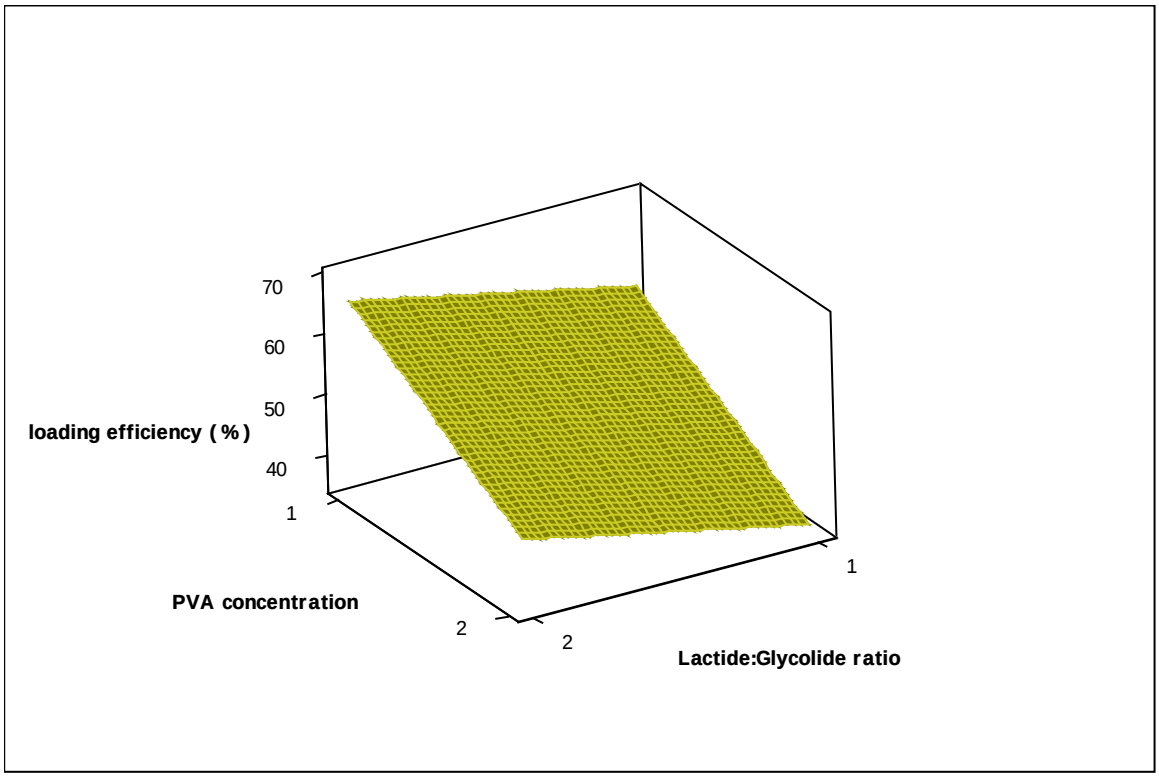


Supplementary figure 7. Response surface plot of drug-loading efficiency Vs lactide:glycolide ratio and poly (vinyl alcohol) (PVA) concentration.

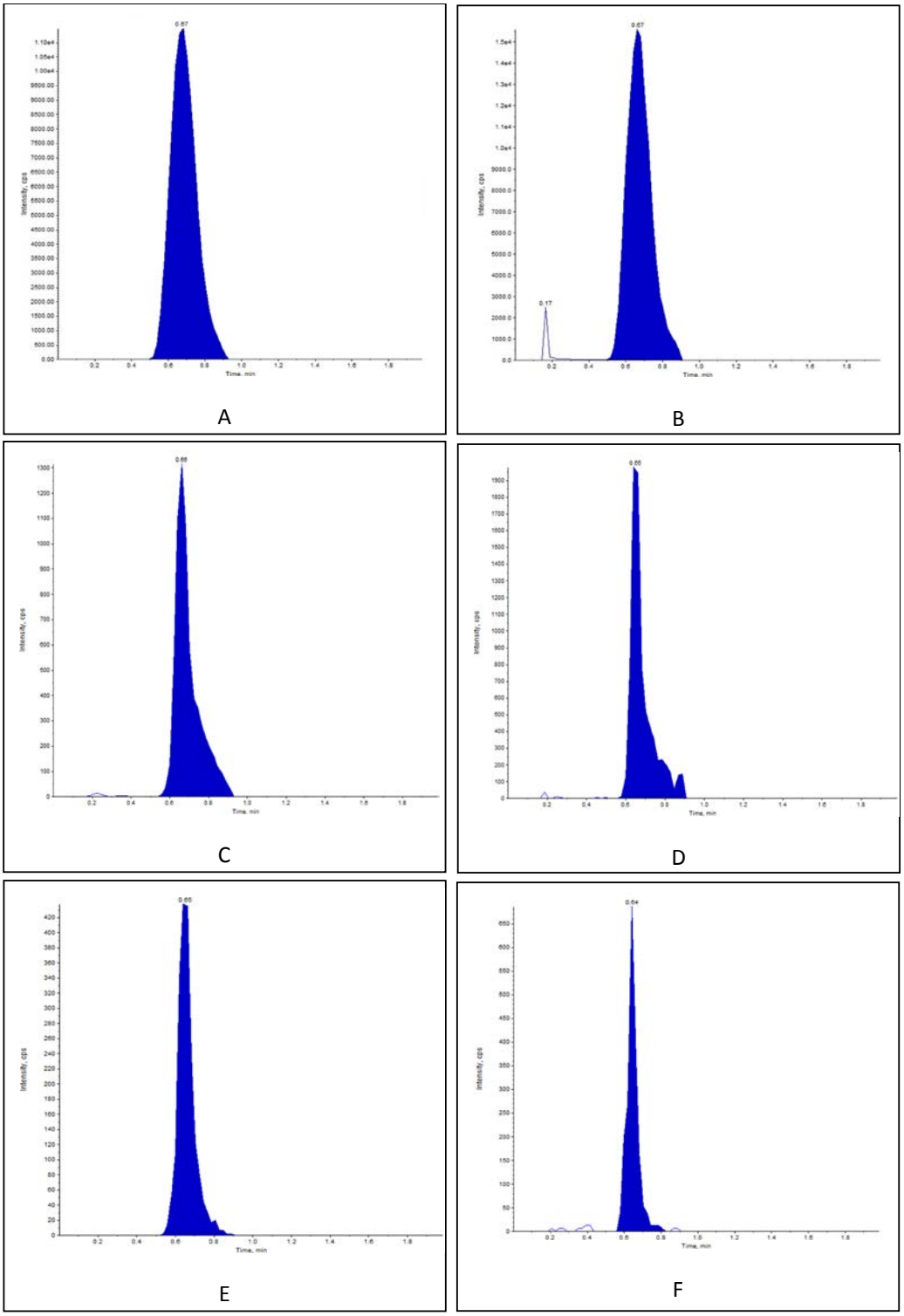


Supplementary figure 7. Typical multiple reaction monitoring (MRM) graph of docetaxel (m/z=226) and internal standard (m/z= 105) (1000 ng/ml). A) docetaxel in methanol B) paclitaxel in methanol, C) docetaxel in PLGA nanoparticles extract D) paclitaxel in PLGA nanoparticles extract, E) docetaxel in PLGA-PEG nanoparticles extract F) paclitaxel in PLGA-PEG nanoparticles extract.

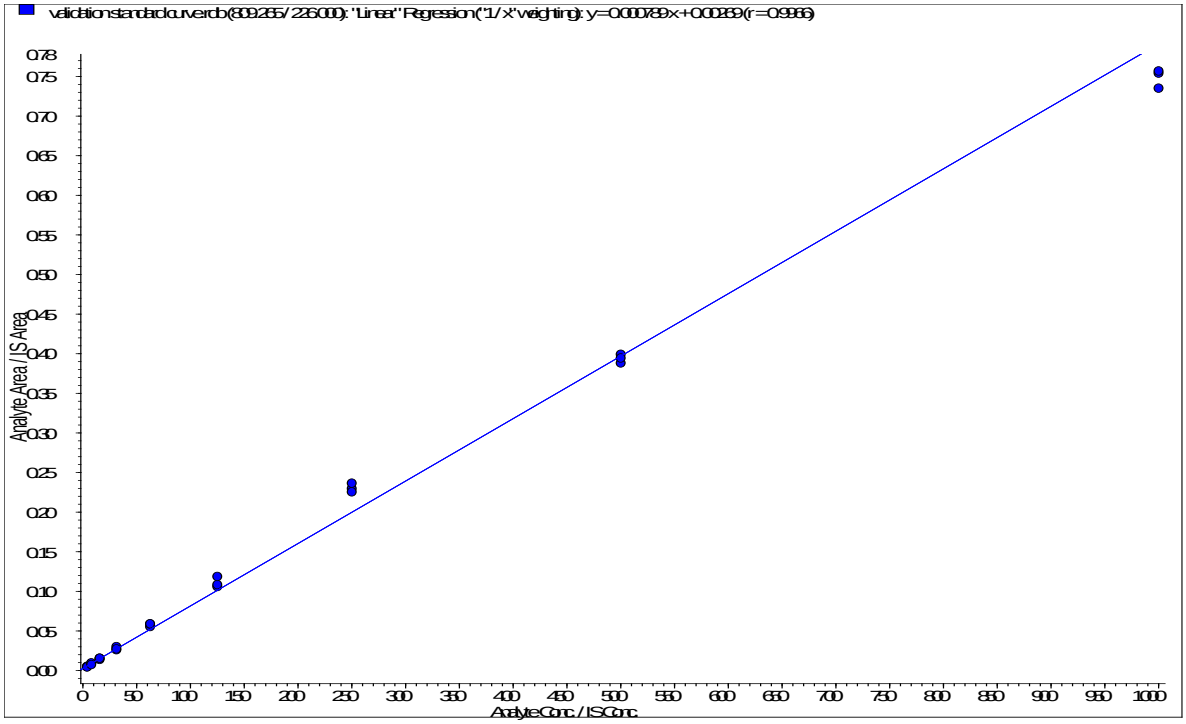


Supplementary figure 8. Typical daily calibration curve of docetaxel in methanol (n=3).

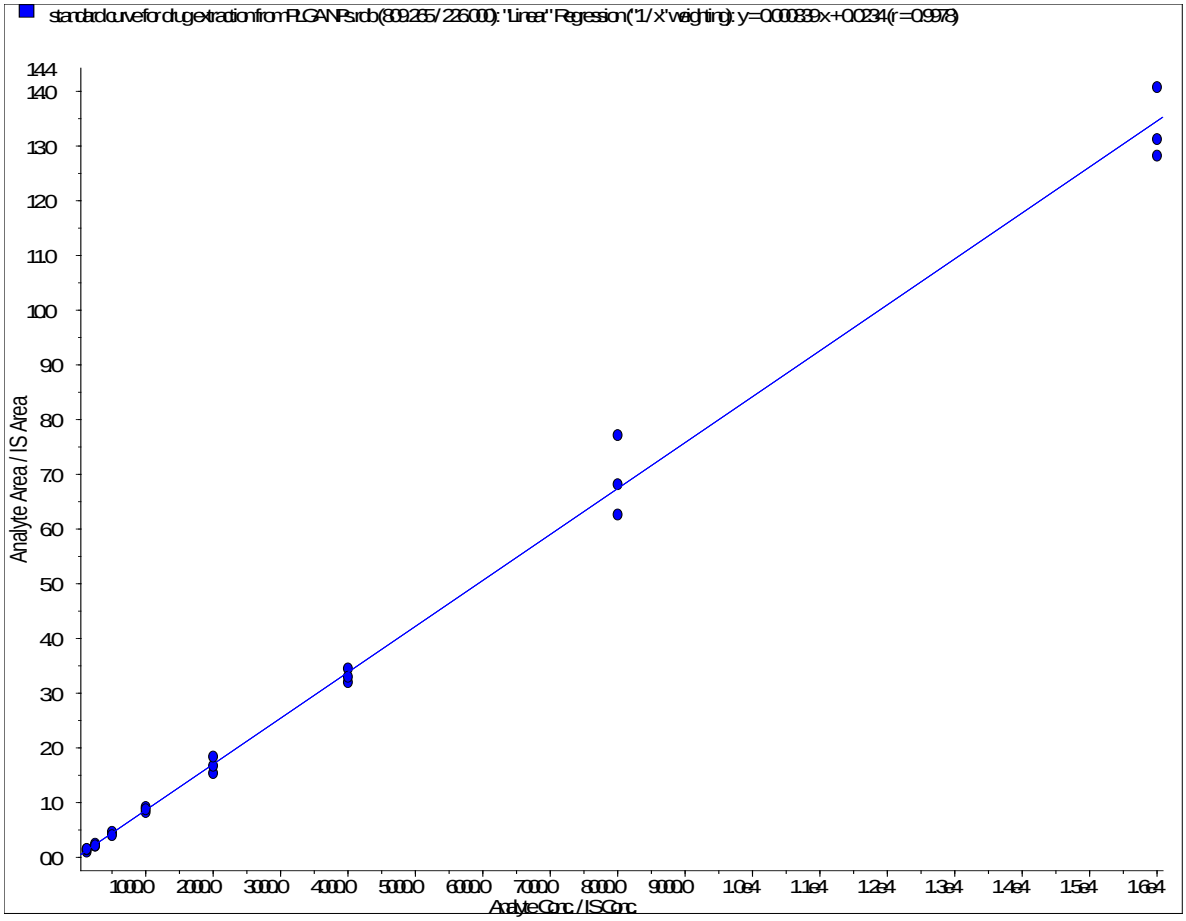


Supplementary figure 9. Typical daily calibration curve of docetaxel in PLGA nanoparticles (n=3).

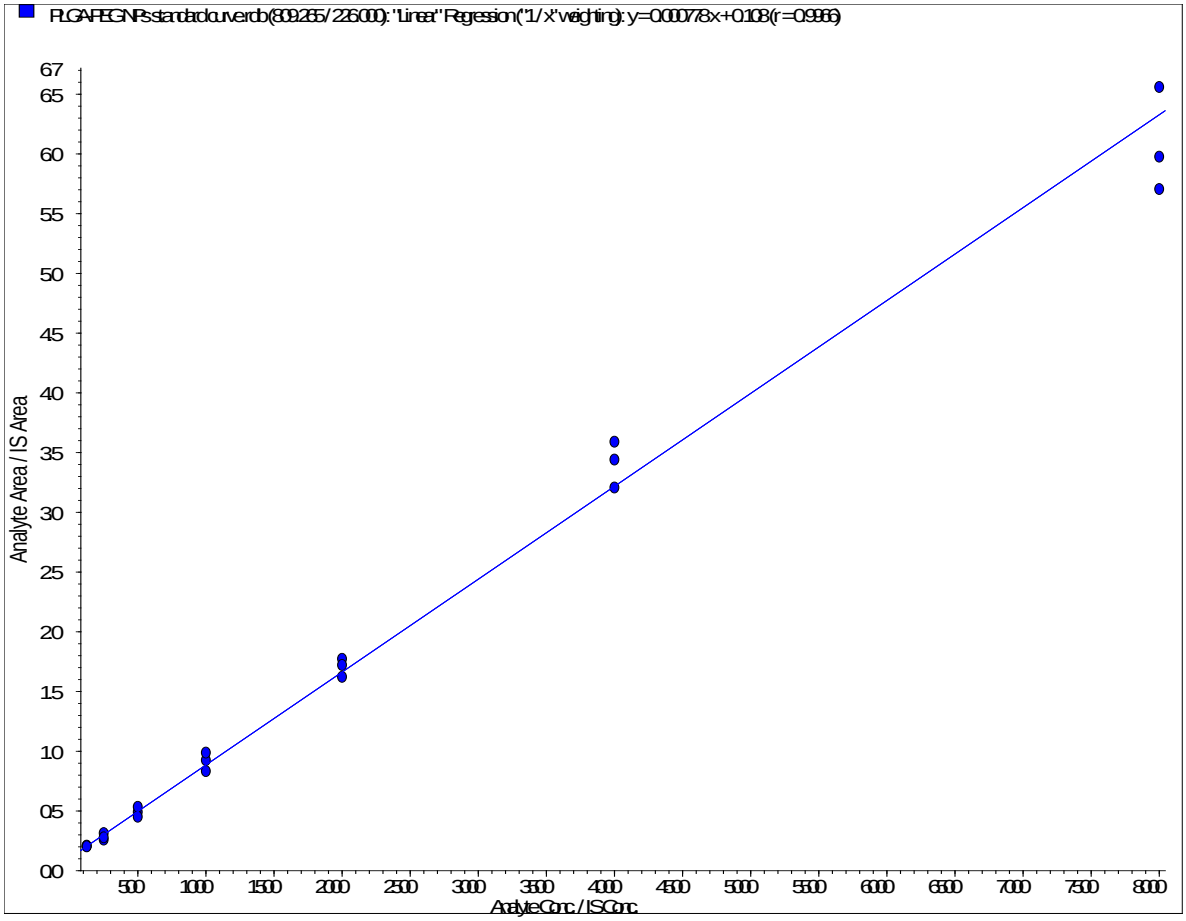


Supplementary figure 10. Typical daily calibration curve of docetaxel in PLGA-PEG nanoparticles (n=3).

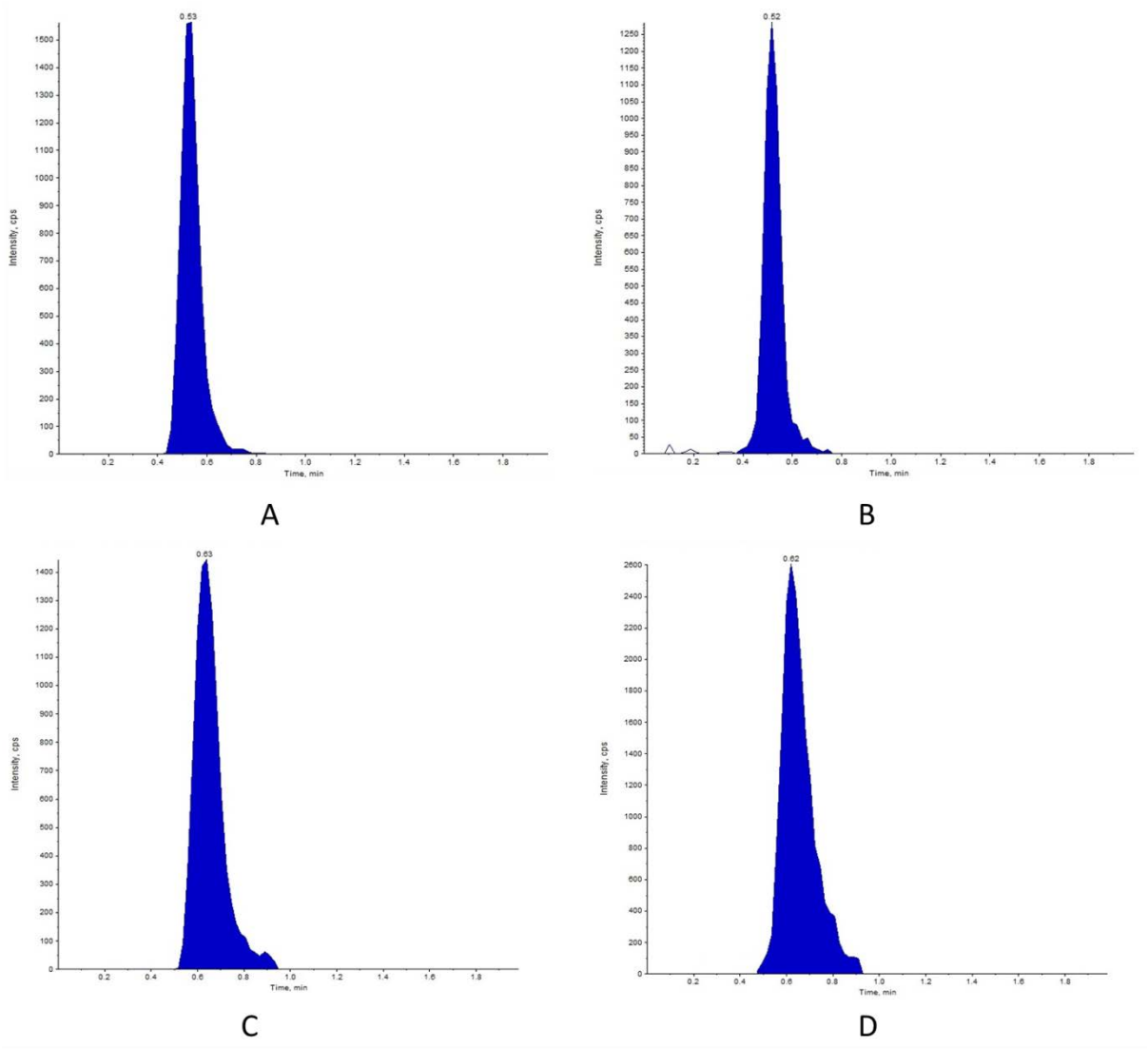


Supplementary figure 11. Typical multiple reaction monitoring (MRM) graph of docetaxel (m/z=528) and internal standard (m/z= 105). A) docetaxel in mouse serum (1000 ng/ml) B) paclitaxel in mouse serum (400 ng/ml), C) docetaxel in mouse liver extract (500ng/ml), and D) paclitaxel in liver extract (400ng/ml).

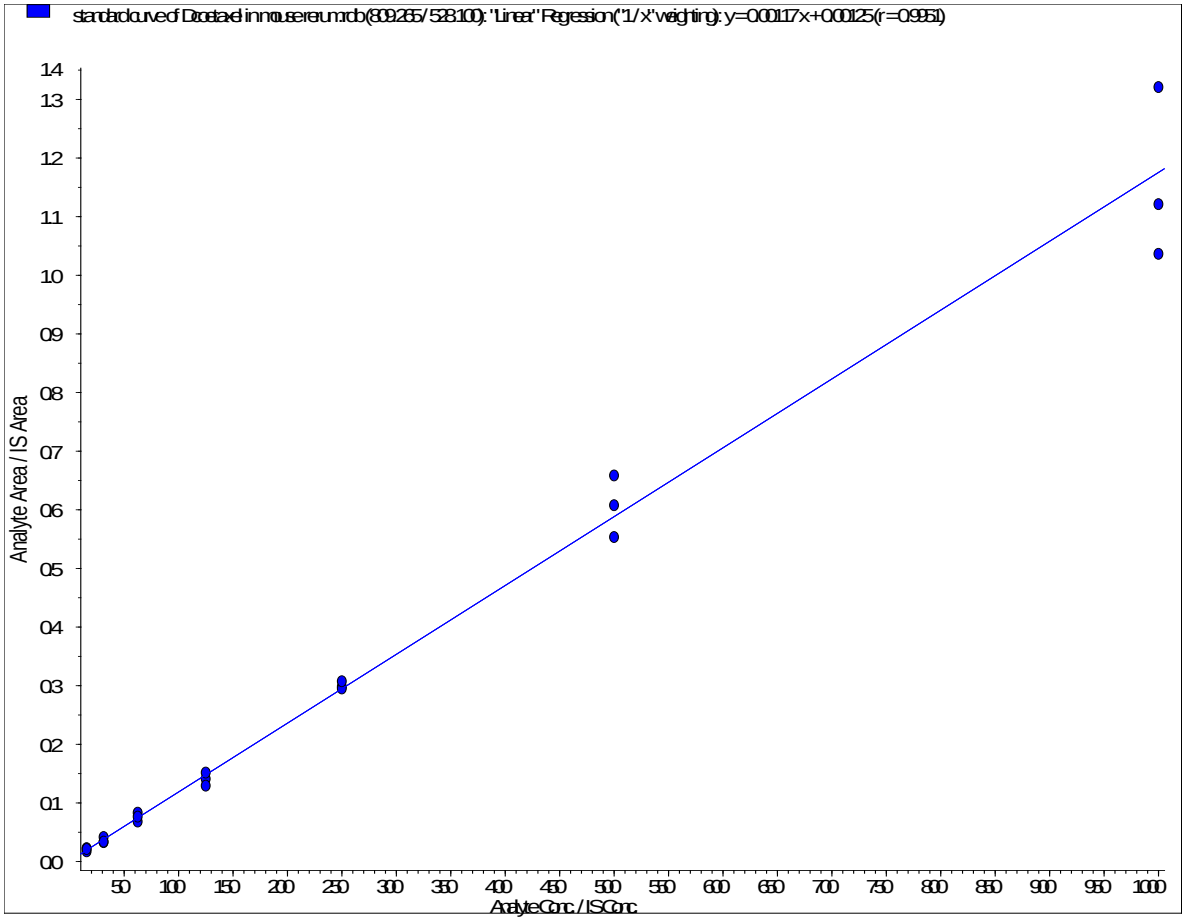


Supplementary figure 12. Typical daily calibration curve of docetaxel in mouse serum (n=3)

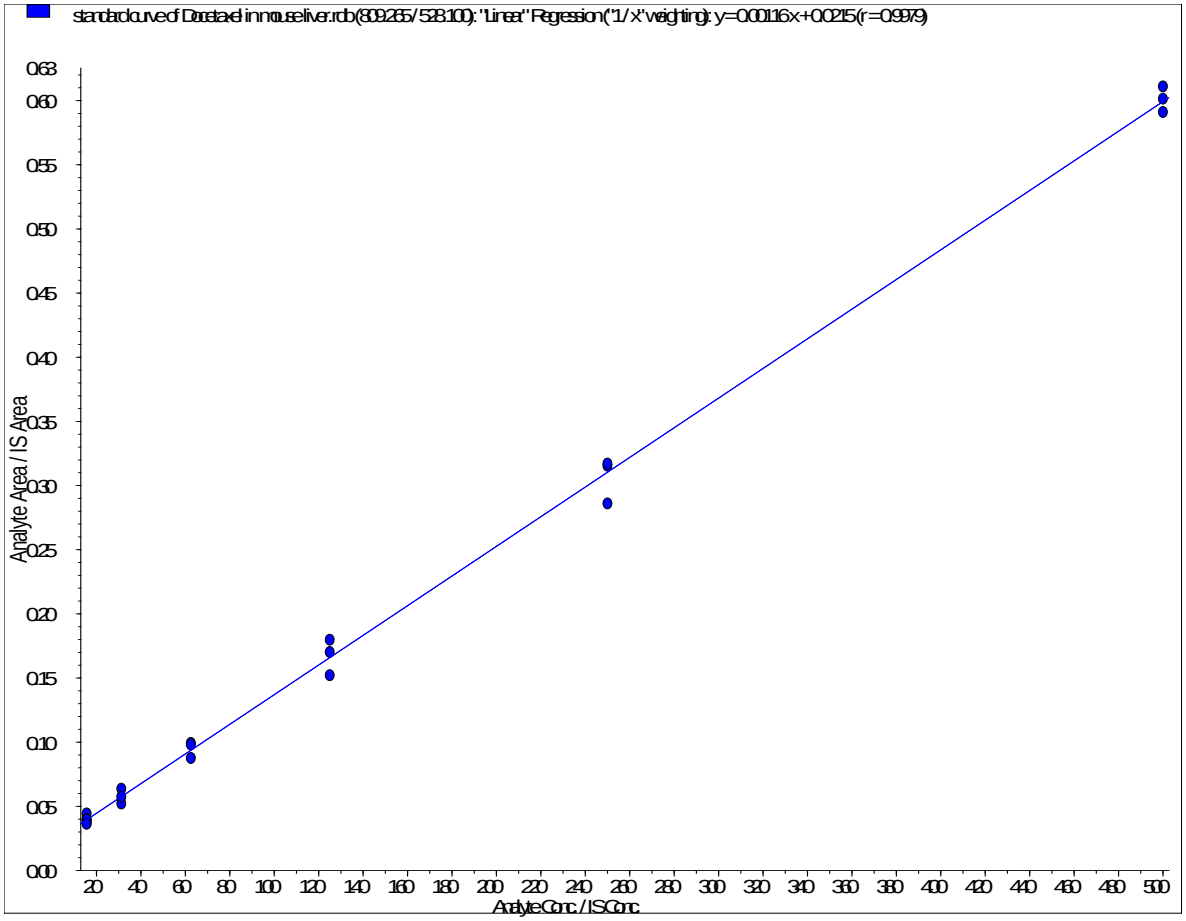


Supplementary figure 13. Typical daily calibration curve of docetaxel in mouse liver (n=3)

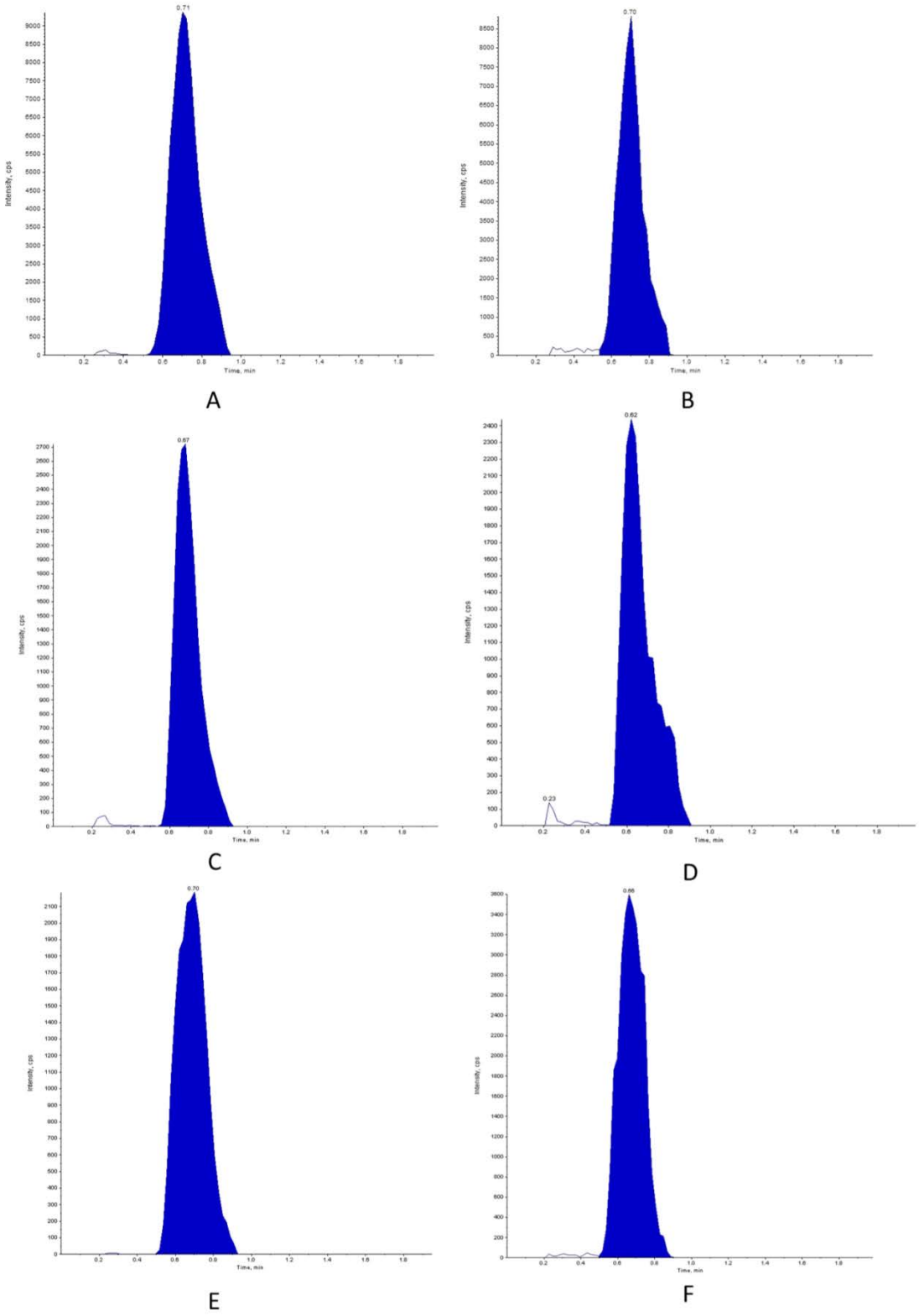


Supplementary figure 14. Typical multiple reaction monitoring (MRM) graph of docetaxel (m/z=528) and internal standard (m/z= 105). A) docetaxel in mouse kidney extract (500 ng/ml) B) paclitaxel in mouse kidney extract (400 ng/ml), C) docetaxel in mouse heart extract

(500ng/ml) D) paclitaxel in heart extract (400ng/ml), E) docetaxel in mouse lung extract (500ng/ml) F) paclitaxel in lung extract (400ng/ml).

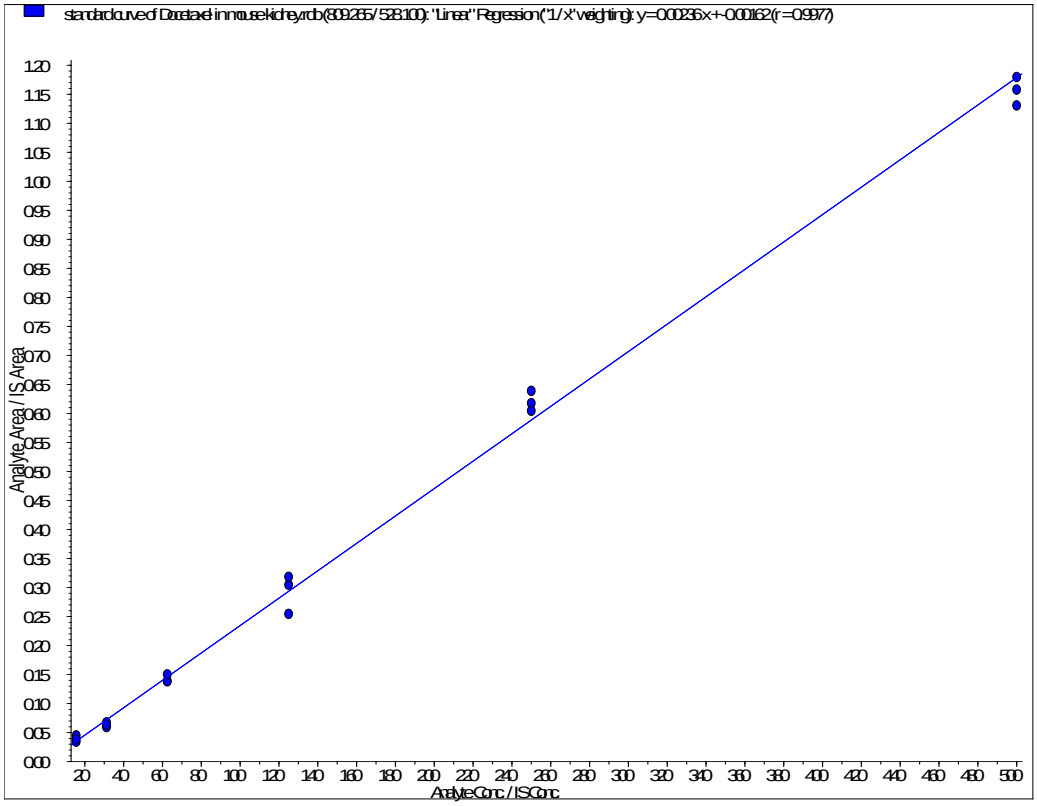


Supplementary figure 15. Typical daily calibration curve of docetaxel in mouse kidneys (n=3)

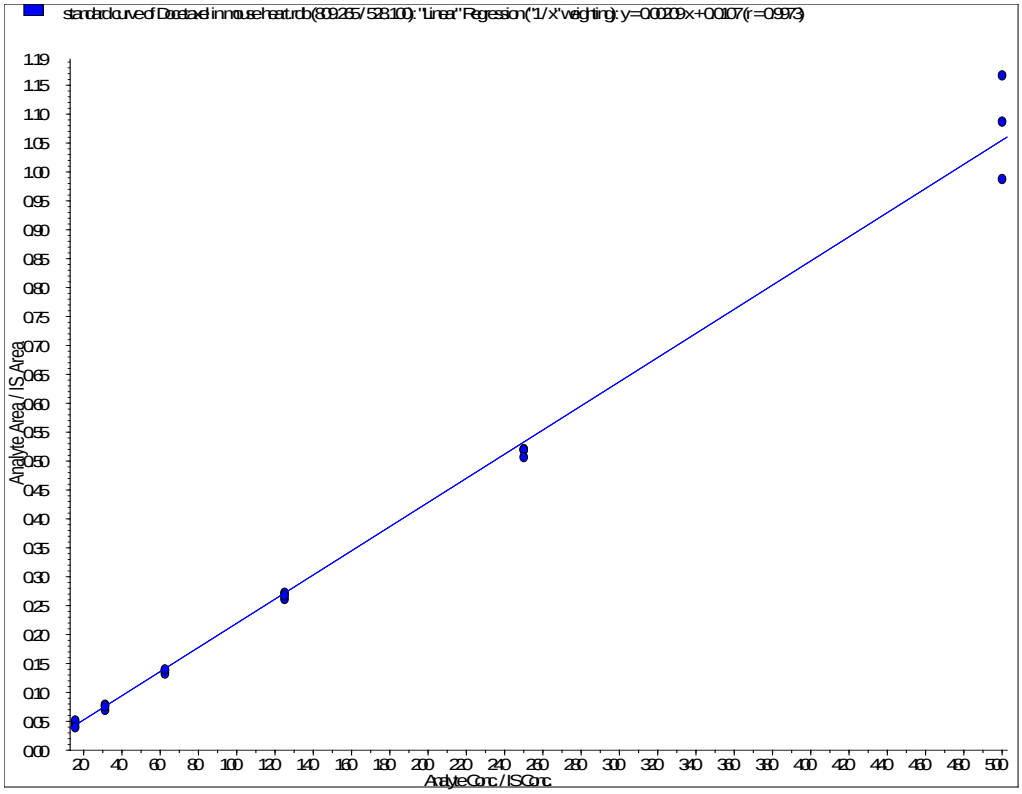


Supplementary figure 16. Typical daily calibration curve of docetaxel in mouse heart (n=3)

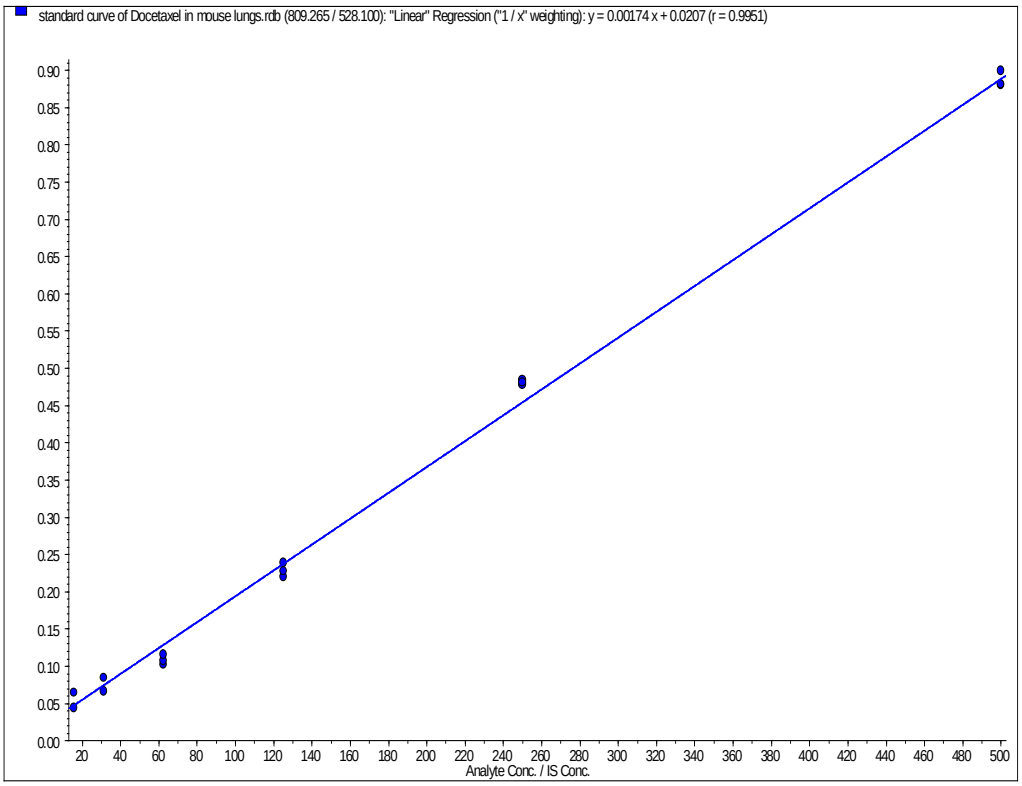


Supplementary figure 17. Typical daily calibration curve of docetaxel in mouse lungs (n=3)

**APPENDIX B**

**SUPPLEMENTARY TABLES**

Supplementary table 1. Size, PDI, and zeta potential characteristics of PLGA nanoparticles formulations prepared at high docetaxel concentration. Data represents mean ± standard deviation (n=3). (PDI=polydispersity index).

| **Docetaxel Preparation Conc.** | **Average Size (nm)** | **PDI** | **Zeta potential (mV)** |
|---|---|---|---|
| **3 mg/ml** | 132.4 ±6.8 | 0.214±0.025 | -29.5±1.3 |
| **5 mg/ml** | 129.5±8.0 | 0.215±0.046 | -29.9±2.4 |
| **10 mg/ml** | 143.9±9.5 | 0.241±0.048 | -25.1±0.7 |

Supplementary table 2. Size, PDI, and zeta potential characteristics of PLGA nanoparticles obtained by modified preparation technique (i.e., sonicated organic phase prior to emulsification with aqueous phase). Data represents mean ± standard deviation (n=3). (PDI=polydispersity index)

| **Docetaxel Preparation Conc.** | **Average Size (nm)** | **PDI** | **Zeta potential (mV)** |
|---|---|---|---|
| **0.25 mg/ml** | 102.1±2.3 | 0.199±0.027 | -25.8±13.4 |
| **0.5 mg/ml** | 108.3±6.6 | 0.207±0.012 | -30.4±0.2 |
| **1 mg/ml** | 107.1±2.0 | 0.213±0.006 | -20.0±0.5 |
| **1.5 mg/ml** | 107.7±2.4 | 0.222±0.010 | -25.1±1.0 |